MECHANICS OF
KINEMATICALLY INDETERMINATE STRUCTURES

Dissertation submitted to the University of Cambridge
for the Degree of Doctor of Philosophy

by

Sergio Pellegrino

Corpus Christi College

April, 1986

Preface

The work described in the present dissertation was carried out by the author in the Department of Engineering, Cambridge University, between October 1982 and March 1986.

I wish to thank Professor J. Heyman for invaluable advice and encouragement from the earliest stages of this work, and Dr. C.R. Calladine, F.R.S., for his guidance and interest, and for his insisting on clear and rigorous ways of tackling any problem of Structural Mechanics.

I am also grateful to Professor W.T. Koiter for pointing out some of the problems connected with a special class of non-rigid structures, to Dr. T. Tarnai for helpful comments on this matter, and to Dr. J.M. Prentis for providing some examples that I could study.

For advice and help during the experiments and the construction of small-scale physical models I wish to thank Mr. R. Denston. The careful tests of cable nets were performed by Messrs. D.M. Steer and P.St.J.L. Yates during their final-year undergraduate project. The finite element computer program, referred to in the text, was developed by Mr. I.M. Kani and Dr. T. See.

Many friends have discussed with me the theoretical, computational and experimental problems connected with this work: I am grateful to all of them and apologise for not mentioning them by name.

I am particularly indebted to Peterhouse, my former college, for financial support in the form of a Research Studentship and conference grants. I am also indebted to the Cambridge Philosophical Society for assistance in translating some German papers.

The contents of this dissertation are original except where specific reference is made to the work of others; the material of Chapter 4 has been presented at a conference and published in collaboration with C.R. Calladine, but none of the remainder is the outcome of work done in collaboration.

This work has not been submitted in part or in whole to any other University.

S. Pellegrino

Summary

The dissertation is concerned with the structural mechanics of assemblies of pin-jointed bars, and in particular with their rigidity and performance under any load system.

A detailed review of the past developments and present knowledge is conducted, which brings back to light some long-forgotten contributions and traces the line for further study. The present investigation starts from an analysis of the rigidity of a class of triangulated hyperbolic-paraboloidal surfaces, which are found to be either rigid and statically determinate, or not, according to the number of sides. In a more general context, the introduction for any assembly of the four linear-algebraic vector subspaces associated with its equilibrium matrix leads to the systematic evaluation of the degrees of statical and kinematical indeterminacy, and of all the states of selfstress and inextensional mechanisms. These are readily computed following a computational scheme described in detail. Criteria for the distinction of rigid-body mechanisms, infinitesimal mechanisms of first and higher order, and finite mechanisms are established and tested by means of several examples; computer-drawn pictures of these examples are enclosed.

The linear and non-linear responses of kinematically indeterminate assemblies are analysed by decomposing any applied load into its extensional and inextensional components, and by evaluating the bar tensions and nodal displacements due to them, respectively. A third-order algebraic equation is introduced for correcting large inextensional displacements. This way of proceeding leads to two efficient computer programs for the structural analysis of cable structures, in which the total external load is applied in only one step. The answers given by this method are compared to the results of some careful experiments on cable structures, and to various data available in the literature. By-products of the investigation are a novel formulation of the force method, in which the analyst does not have to select the 'redundancies', a simple and general numerical technique for finding the nodal coordinates of an unloaded tensegrity structure, and a new instrument for measuring the tension in a steel wire very accurately.

Keywords: Cable structures. Formfinding. Ill-conditioned frameworks. Kinematical indeterminacy. Mechanisms. Non-linear response. Stiff structures. Structural mechanics. Tensegrity.

Contents

1. Introduction

This dissertation is concerned with the structural mechanics of assemblies of bars connected by frictionless, spherical hinges - a structural type which has been investigated extensively since the last century. Strictly speaking the above hypotheses about the connections are almost never satisfied by structures built in practice, and so much interest in them would seem unjustified. Yet many existing structures have been analysed only 'by hand' as pin-jointed, before the advent of the digital computer; and in spite of the sophisticated analyses that can be performed today, the pin-jointed idealization of a framework is often still a meaningful point of reference.

Previous work in this field has left a cloud of unanswered questions, exceptions to the rules commonly used for design, and anomalies in the expected behaviour. The first aim of the present work is to develop a comprehensive framework of ideas which includes all structural assemblies and explains their fundamental patterns of behaviour. Quantitative estimates of the response to arbitrary systems of loads will also be made, and the techniques introduced will be verified in several ways.

An important further reason for the present investigation is that, in the past, many of the concepts and techniques first developed for pin-jointed assemblies have been subsequently extended to more complicated structural systems (e.g. framed structures and continua); with luck, this will happen in the present case as well.

1.1 Basic concepts

The study of pin-jointed assemblies (also called frameworks or trusses) usually occupies the initial chapters of any traditional textbook of Structural Analysis. Its reader is introduced to the concepts of statical and kinematical determinacy, which are central to an understanding of the structural mechanics of any assembly, by means of an example such as that shown in Fig. 1.1a. This framework is clearly statically determinate, since the tension in every bar can be determined by means of the equations of equilibrium of the joint, for any given set of components of external force applied to the joint: there are 3 (linear) equations in 3 unknowns, the matrix of the system of equations is non-singular, and the solution for the set of

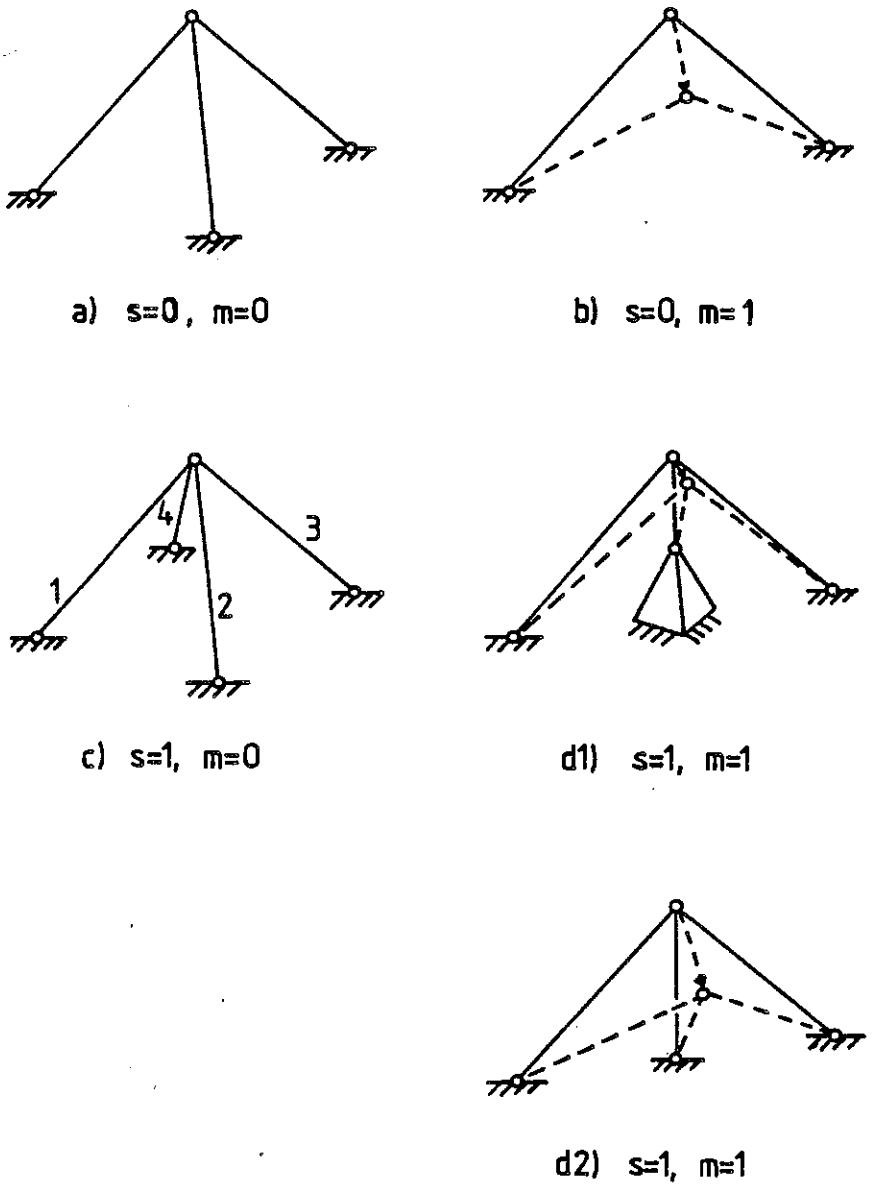

Fig. 1.1 Perspective sketches of three-dimensional assemblies to illustrate statical and kinematical determinacy and indeterminacy. a) The three foundation joints lie at the corners of a square. b) One bar has now been removed, and the assembly has a mode of inextensional displacement, in which the central node moves towards the reader. c) The fourth bar makes the assembly statically indeterminate. d1) A third bar added to b) makes the assembly both statically and kinematically indeterminate, but only small displacements of the 'inextensional' mechanism are possible. d2) As d1), except that the three foundation joints are collinear, and the inextensional mechanism can move freely, as in b).

bar tensions is unique. This framework is also kinematically determinate, since any displacement of the joint from its position causes a change of length of the bars.

If now any one bar of the framework is removed, as in Fig. 1.1b, the resulting assembly is no longer rigid. It is a mechanism having one degree of freedom: it is kinematically indeterminate, since the joint displacement indicated in broken line in the figure causes no change of length of the bars.

But if an extra bar is added to the assembly of Fig. 1.1a, as shown in Fig. 1.1c, it becomes statically indeterminate: there are now 3 equations of equilibrium and 4 unknowns, and the solution for the set of bar tensions is not unique. Such an assembly may be described as having one redundant bar; but the statical indeterminacy is best described by saying that the assembly can sustain one state of selfstress, i.e. a set of bar tensions which are in equilibrium with zero external forces. If the legs of the tetrapod of Fig. 1.1c have equal length, the state of selfstress consists of tensions equal in absolute value and, say, tensile in bars 1,3 and compressive in bars 2,4.[1]

More generally, the textbook would conclude, if the number of bars in a framework is equal to three times the number of joints, the framework is both statically determinate and kinematically determinate. But if the number of bars is smaller (larger), the framework is kinematically (statically) indeterminate.

A discussion along these lines of the general theory of structural frameworks would be adequate at an elementary level, but it has been known for many years - as will be shown in Chapter 2 - that there are exceptions to it. Two such exceptions are the assemblies of Fig. 1.1d: although the above rule would classify each of them as both statically determinate and kinematically determinate, it is plain that this is wrong. In fact, both assemblies are statically indeterminate, their state of selfstress consisting of - say - a compressive force in the vertical bar, and tensile forces elsewhere; but they are also kinematically indeterminate, and their mechanisms are shown in the figure. The main difference in their behaviour is that the first assembly,

[1] It is easiest to visualise this by imagining that the new bar, 4, is a little longer than the distance which it is to connect; and hence the other bars have to provide a compressive axial force that shortens bar 4 and makes it fit.

Fig. 1.1d1, is an infinitesimal mechanism, which tightens up when mobilized in a way which depends quantitatively on the elastic properties of the bars. The second assembly, Fig. 1.1d2, is a finite mechanism which is free to undergo large displacements.

For the sake of brevity, assemblies which are statically determinate and kinematically determinate will be referred to simply as statically and kinematically determinate from now on. And similarly, in the indeterminate case, they will be referred to as statically and kinematically indeterminate.

Lastly, a method of analysis which will be used in Chapter 3 and elsewhere is the method of Tension Coefficients, first introduced in Britain by Southwell (1920). The tension coefficient of a pin-jointed bar is defined as the ratio between the tension in the member and its length. When one considers the equilibrium equation in direction x, say, of one of the joints of the bar, the contribution of the bar is $\pm(l_x/l)t$, where l and l_x denote the bar length and its component along x, respectively, and t is the bar tension. Note that, by introducing the tension coefficient (t/l), one can transform the previous expression into $\pm l_x(t/l)$; thus one needs to consider only the components of the length of each bar, in order to write down the nodal equations of equilibrium. Furthermore, in some circumstances the use of tension coefficients allows complicated states of tension to be expressed by integer numbers.[2]

1.2 Origins of the subject and its aims

It should be clear from Section 1.1 (see Figs 1.1b and 1.1d) that, when starting the analysis of a given framework, one of the first questions to be answered is: is it a rigid structure? Chapters 2-5 of this dissertation will discuss the analytical and numerical techniques that may be used to find out; in particular, Chapter 2 will summarize several contributions by well- and less well-known authors in the field of structural engineering and applied

[2] In one of the initial stages of the research described in this dissertation, the author exploited some of the simplifications introduced by the use of tension coefficients to write a Fortran program for the evaluation of the states of selfstress and inextensional mechanisms of simple frameworks, which performed computations only with integer numbers (Pellegrino,1983). The advantage of this way of proceeding is that one can obtain correct answers, because no numerical approximations are made; its obvious disadvantage is that the class of problems that one can tackle is very limited. This work will not be described here.

mathematics. Yet it is interesting to note that the earliest 'theorem' of structural rigidity, which can be applied to complex three-dimensional frameworks, is due to Euclid about 300 B.C.

Cauchy (1813) aimed at "demonstrating the theorem hidden behind definition no. 9 ih the second volume of the Elements, by Euclid" and indeed he elegantly proved that: the angles formed by the rigid faces of a convex polyhedron are invariable. Or, in simpler terms, any convex polyhedron is rigid if its faces are rigid.

The rigidity of all convex triangulated surfaces built out of pin-jointed bars, such as any geodesic dome, follows from the above theorem. Some more theorems, which cover different structural layouts, will be given in Section 2.2.

Yet the present work aims at a more general approach. For any given assembly, a set of initial transformations of its equilibrium matrix will classify it according to the notions introduced in Section 1.1; will indicate its degree of statical and kinematical indeterminacy; and will provide the statical details of all of its states of selfstress and the kinematical details of all of its inextensional mechanisms. These calculations find their most natural application in the study of the response of a cable net or of a tensegrity[3] structure to a system of applied loads.

It can be concluded that, although the subject of this dissertation originates from one of the most eminent Greek geometers, Euclid, its applications are certainly well into the future.

1.3 General hypotheses

Various points need to be mentioned before the investigation can start. First, it will be assumed without further discussion that the idealization of a physical framework or cable structure as a 'pin-jointed' assembly is appropriate. If a member of the physical framework happens to be a wire, then this idealization is only satisfactory, of course, as long as the wire is in a state of tension; if a prestress has been imposed, it is necessary to check that any subsequent, compressive change of tension (due to applied loads, temperature changes,...) is smaller, or at most equal to the pretension.

---

[3] 'Tensegrity' is a term which was introduced by R. Buckminster Fuller: see Marks (1960) and Fuller (1975).

Furthermore, it will be assumed - with the only exception of the rigid-plastic analyses of Section 6.1.2 - that the response of a member to a change of its axial force is linear-elastic, and hence the possibility of yielding or buckling of any member is excluded.

Second, the equilibrium and compatibility matrices, from which the degrees of statical and kinematical indeterminacy are determined, will be set up in the context of 'small deflection theory'. That is, the equilibrium and compatibility equations will refer to the original, undistorted configuration of the assembly. This is, of course, a well-known procedure in structural mechanics which produces a set of linear-algebraic equations, and its limitations are well known. For kinematically indeterminate assemblies which are finite mechanisms the original configuration is not unique; but all the equations can still be set up in the given configuration.

Third, the final parts of the present investigation, in which the possibility of rather large 'inextensional' displacements will be considered, will assume without discussion that a solution exists and it is unique, which is a known result (see, e.g., Buchholdt, Davies & Hussey (1968), and Møllmann (1974)).

1.4 Outline of the dissertation

Following the introduction, Chapter 2 reviews the development - during the last century - of the standard rules for designing a rigid framework; the early workers were aware of the existence of some exceptional structures, which satisfied the general rules and yet did not behave accordingly. The exceptional cases were the subject of extensive studies, rather on the theoretical side. A loss of interest in these problems seems to have occurred before the turn of this century; and only the recent construction of spectacular cable nets and tensegrity structures has brought fresh interest and some new results.

Chapter 3 examines the rigidity of a class of triangulated hyperbolic paraboloids, and although its initial aim is merely to test some of the techniques available, it is found that the behaviour of these hyperbolic paraboloids may be strongly affected by a change of the number of sides.

Chapter 4 sets up a conceptual framework which can include all frameworks and can explain their behaviour: the crucial point is the introduction for

any assembly of the four vector subspaces associated with the equilibrium matrix. The dimensions of two of these subspaces are equal to the degrees of statical and kinematical indeterminacy of the assembly, and can be readily determined. The same computation provides also details of the states of selfstress and inextensional mechanisms. Some of the inextensional mechanisms of a kinematically indeterminate assembly can in some cases correspond to motions in which the whole structure rigidly moves in space; and these 'rigid-body' mechanisms will be distinguished from the internal ones. And then the small-displacement internal mechanisms will be separated from the 'free' mechanisms. The remainder of Chapter 4 presents applications of these procedures.

A rigorous classification of an infinitesimal mechanism, based on the magnitude of the bar elongations it involves, is introduced in the first part of Chapter 5. Finding the (prestressable) shape of a tensegrity structure by simple means concludes the chapter.

In Chapter 6, the ideas developed in Chapter 4 are applied to the linear-elastic and rigid-plastic analyses of a rigid framework. They are also applied to the analysis of the 'linear' response of prestressed mechanisms such as cable structures; comparisons to results published by previous researchers demonstrate the validity of the approach proposed.

Chapter 7 reports on a set of careful experiments conducted on three hanging wires and two cable nets. Also included in this chapter are the results of the numerical analyses based on Chapter 6.

Chapter 8 concludes with a brief summary of the main results and suggestions for further work.

2. Review of previous work

The first contributions to the analysis of the mechanics of kinematically indeterminate structures, the starting point of this chapter, were made in the second half of the 19th century. In the 1950's and 60's the construction of spectacular cable nets and tensegrity systems showed the first practical realizations of such structures but, by that time, a lot of the basic knowledge accumulated in scientific papers and textbooks had been forgotten or could no longer be understood: these new structures were therefore analysed by means of powerful numerical techniques that left no room for basic understanding. Sections 2.1 and 2.2 deal with the earlier developments of the theory; but, although a chronological arrangement is followed, the description is by no means exhaustive. For the sake of consistency, several of the symbols used are different from those of the original papers; and in particular nodal coordinates will be always denoted by capital letters. The following sections aim at presenting an account of the state of knowledge at present.

The name of Buckminster Fuller is usually associated with tensegrity but, although some of his structures are discussed in great detail in the following chapters, his own published work is not suitable for discussion here.

2.1 Early developments (1837-1900)

Timoshenko (1953) and Charlton (1982) agree in attributing what might be called the earliest work on the subject of this dissertation to Möbius, a German professor of Astronomy. In his Treatise on Statics, Möbius (1837) analysed for the first time the mechanics of pin-jointed assemblies: a general plane framework consisting of n frictionless hinges has to have at least 2n-3 bars in order to be rigid, while a space framework needs 3n-6. Möbius was aware of exceptions to this theorem, such as special plane frameworks with 2n-3 bars that can admit small relative displacements of their nodes; and he observed that this happens when the determinant of the equilibrium equations of the nodes vanishes. As a practical way of detecting whether or not this is the case Möbius suggested a method called the zero-load test by Timoshenko & Young (1965): a system which contains,

according to the rules above, the required number of connecting rods is rigid if there is a unique set of bar tensions in equilibrium with a given load. This is most easily checked by showing that all bar tensions have to vanish if no external loads are applied. Möbius also observed that the removal of one bar from a framework which contains only the minimum number of bars to make it rigid, in general has the consequence of transforming it into a mechanism that allows relative displacements of the nodes, in which the distance between the end nodes of the removed bar changes by finite amounts. But he pointed out that the removal of a bar the length of which is either maximum or minimum, hence a bar the end nodes of which can move by small amounts in prescribed directions without causing significant alteration of its length, does not introduce any further degree of internal mobility. Möbius' work remained unknown to engineers for a long time, his approach being too general and its presentation too abstract to be understood.

The second episode in these brief historical notes is a paper by Maxwell (1864) which also failed to have a great impact at the time of its publication: Maxwell's objective was to introduce a method for evaluating bar tensions and nodal deflections of frameworks "in the least complicated manner ... especially in cases in which the framework is not simply stiff but is strengthened ... by additional connecting pieces". The introductory section of the paper is for present purposes the most interesting; it contains a relationship widely known in framework design as Maxwell's rule: "a framework of n points in space requires in general 3n-6 connecting lines to render it stiff". Two qualifying statements deal with exceptions to it:

(i) if a smaller number of rods is sufficient to obtain a rigid assembly, one or more of the connecting lines must have either maximum or minimum length.

(ii) the stiffness of frameworks like the ones envisaged in (i) is "of an inferior order" in the sense that infinitesimal applied forces may produce finite displacements; in Maxwell's words: "a small disturbing force may produce a displacement infinite in comparison to itself".

These statements entirely agree with Möbius' analysis; it is to be noticed that (ii) is a fairly explicit warning against using frameworks of this sort. Apart from a reference to Clapeyron's Principle of Conservation of Energy as the basis of the new method proposed, Maxwell's paper is entirely

self-contained.

A third author whose contribution to the theory of indeterminate structures was very significant is Mohr (Timoshenko, 1953, Charlton, 1982); indeed his way of using virtual work to obtain the compatibility equations of a redundant framework (Mohr, 1874) is a guideline for the analysis of the 'fitted' components of load which will be introduced in Chapter 6. In a following paper, in a section on "the relationship between rod lengths of a framework" which is not connected to a foundation, Mohr (1885) proved that the following condition has to be satisfied by any system of bar tensions in equilibrium without external loads:

$$\sum_{p=1}^{b} t_p l_p = 0 \qquad (2.1)$$

where t_p is the tension in bar p, l_p is the length of bar p and b is the total number of bars in the framework. This is proved by considering any self-equilibrated system of bar tensions, a set of bar elongations in which the ratio between bar elongations and lengths is constant for all bars, and using virtual work. Equations like (2.1) and an equal number of compatibility equations have to be satisfied by the bar lengths and elongations of a redundant framework, but in 'simple' frameworks - with no redundant members - both lengths and elongations are independent of each other. The effects of altering the length of one particular rod of a framework, while all the remaining bar lengths are kept constant, are then analysed in the two cases:

$b=2n-3$ The elongation of one particular bar of a 'simple' framework is clearly not unlimited; its bounds depend on the length and arrangement of the remaining rods. When the chosen bar has reached its maximum (or minimum) length the other $b-1$ bars, the lengths of which are kept constant, resist any further extension (shortening): the given framework is then able to accept a self-equilibrated system of bar tensions. A consequence of the length of one bar being maximum (or minimum) is that the chosen bar does not change its length if an infinitesimal deformation of the framework is considered in which the remaining bars keep their length constant. The framework is therefore not stiff: it is an infinitesimal mechanism, although it contains the required number of bars. Mohr used virtual work also to show that any load condition that does work for the infinitesimal displacement in which no bar

elongation occurs will produce infinitely large rod tensions. This result is not to be taken literally: rods of real assemblies are not infinitely rigid, so the assembly would deform a little bit when loaded and then require only finite rod tensions to carry an arbitrary load. Hence, he concluded, such frameworks are "not capable of resistance and obviously unsuitable for practical applications". An example of this is the framework in Fig. 2.1, which has n=6 and b=9, hence 2n-3=b and this structure has in general no redundant bars; the exceptional case is obtained if bars 2,5,9 meet in one point, in which case bar 9 - say - is redundant.

b<2n-3 Frameworks of this type can in general take arbitrary shapes, yet the procedure described above can be repeated in order to obtain assemblies which, apart from infinitesimal mechanisms, possess a unique configuration and can sustain a self-equilibrated system of rod tensions. The simplest class of examples is given by any closed chain of b sides: here b=n<2n-3 for b>3; if any bar of the chain is given a length equal to the sum of the lengths of the remaining bars, its length is obviously maximum. A more interesting example is shown in Fig. 2.2, i.e. Fig. 3 of Mohr (1885). Here b=12<2n-3=13; therefore the framework is in general a mechanism with one degree of freedom and no redundancies. But self-equilibrated bar tensions can be assigned if the three intersection points of the rods (1,3),(5,7),(9,10) and (2,4),(6,8),(10,11) respectively lie on straight lines. These conditions ensure that, once the tension in bar 9 - say - has been prescribed and those in bars 1,2,3,4,5,10,11,12 have been evaluated from nodal equilibrium, the remaining part of the framework is in equilibrium. Notice that the number of conditions to be prescribed is given by (2n-3)-(b-1)=2.

The last contributions to be discussed in this section are by Föppl. His books (Föppl, 1892, 1912) were in their day much used in the teaching of structural mechanics to young engineers all over Europe. In his classical treatise Föppl (1912) presented a wide range of problems together with available methods of analysis; two of its sections dealt with the problems of statical and kinematical indeterminacy. The first one, Section 39, is part of a chapter on plane frameworks and is entitled "Analytical investigation of an exceptional case".

The equilibrium equations of node i, see Fig. 4.1, are written in the form:

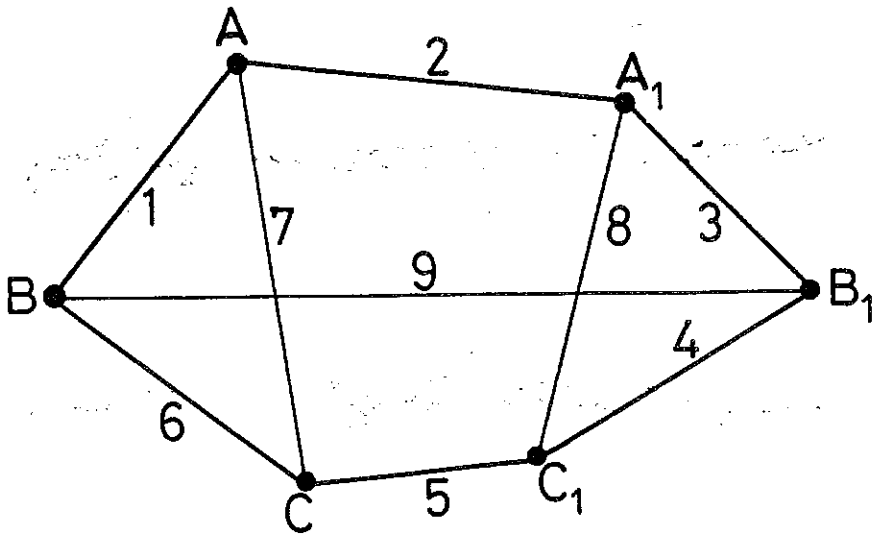

Fig. 2.1 Plane assembly with n=6, b=9. Mohr (1885) showed that it is statically and kinematically indeterminate if the bars joining the triangles ABC and $A_1B_1C_1$ meet in one point.

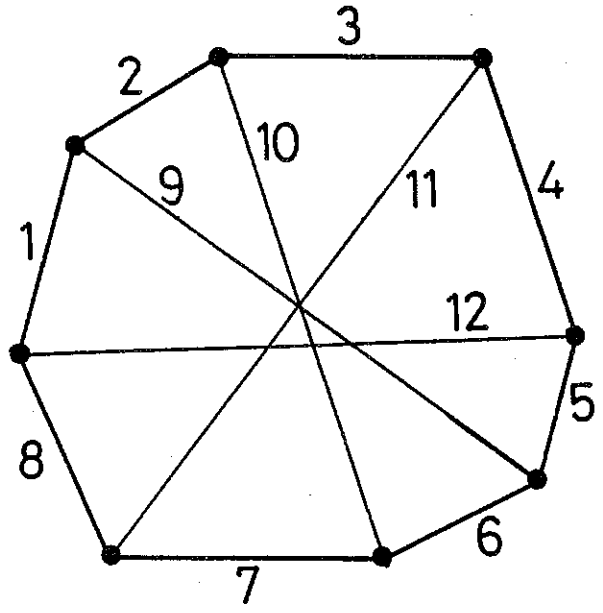

Fig. 2.2 This plane assembly, although it is a statically determinate structure with 1 mechanism in most of its configurations, can sustain a state of self-equilibrated tensions and has 2 mechanisms in the geometry shown. From Mohr (1885).

$$\sum_{p,q} (\partial F_p/\partial X_i)\times(t_p/2l_p)=f_{ix}$$
$$\sum_{p,q} (\partial F_p/\partial Y_i)\times(t_p/2l_p)=f_{iy} \qquad (2.2)$$

where the function F_p has been introduced for bar p, connecting nodes i and j of the framework:

$$F_p=(X_i-X_j)^2+(Y_i-Y_j)^2-l_p^2=0 \qquad (2.3)$$

As the partial derivatives of F_p with respect to nodal coordinates other than X_i, Y_i, X_j, Y_j vanish "of their own accord", equations (2.2) can be easily converted to the more usual expressions such as those in Section 4.1.

By writing equations like (2.2) for each node of the framework, but missing altogether the one which coincides with the origin and writing only the second equation for a node lying on the x axis, a system of 2n-3(=b) equilibrium equations in the b unknown bar tensions is obtained. The analysis of the determinant of the system can indicate whether or not a unique set of bar tensions can be obtained from arbitrary given components of external force:

$$\Delta=\begin{bmatrix} \partial F_1/\partial \xi_1 \cdots\cdots\cdots \partial F_b/\partial \xi_1 \\ \cdots\cdots\cdots\cdots\cdots\cdots \\ \cdots\cdots\cdots\cdots\cdots\cdots \\ \partial F_1/\partial \xi_{2n-3} \cdots\cdots \partial F_b/\partial \xi_{2n-3} \end{bmatrix} \qquad (2.4)$$

here ξ denotes an arbitrary nodal coordinate. The effects of arbitrary bar elongations on the geometry of the structure are also analysed. Differentiation of (2.3) provides the compatibility relationship:

$$(X_i-X_j)\delta X_i+(X_j-X_i)\delta X_j+(Y_i-Y_j)\delta Y_i+(Y_j-Y_i)\delta Y_j= l_p\delta l_p \qquad (2.5)$$

where δX_i,... are 'small' changes of nodal coordinates and δl_p is the corresponding elongation of bar p. The compatibility equation above can be also written in the form:

$$\sum_{i} (\partial F_p/\partial \xi_i)\delta\xi_i = 2l_p\delta l_p \qquad (2.6)$$

The complete system of b(=2n-3) compatibility equations in the 2n-3 unknown displacements has a unique solution for any set of bar elongations if the determinant Δ' of the system does not vanish

$$\Delta' = \begin{bmatrix} \partial F_1/\partial \xi_1 \ldots\ldots\ldots \partial F_1/\partial \xi_{2n-3} \\ \ldots\ldots\ldots\ldots\ldots\ldots \\ \ldots\ldots\ldots\ldots\ldots\ldots \\ \partial F_b/\partial \xi_1 \ldots\ldots\ldots \partial F_b/\partial \xi_{2n-3} \end{bmatrix} \qquad (2.7)$$

In particular, if all δl's are set equal to 0 and $\Delta' \neq 0$, all nodal displacements have to vanish, hence "no infinitesimal displacements are possible without bar elongations of the same order, i.e. the framework is stiff". Having then noticed that $\Delta' = \Delta$, the coefficient matrices being the transpose of each other, Föppl states the theorem: "A framework which contains only the necessary number of bars and is stiff, is also statically determinate. And vice versa, it is stiff if it is statically determinate".

Section 45 of Föppl (1912) makes use of the above theorem, but not of the analytical method just described; it deals with an exceptional type of Schwedler's cupola. According to Timoshenko (1953), Schwedler first suggested in 1866 the layout shown in Fig. 2.3 for a reticulated dome. This layout was successfully modified by Föppl to cover a large market hall in Leipzig; an extensive description of this type of construction is available in Föppl (1892, 1912). The exceptional reticulated dome that Föppl described in 1912 is discussed in detail elsewhere in this thesis; here it is enough to say that the framework in Fig. 2.4a is not of the type envisaged in the theorem above. Although it "contains the necessary number of bars", it is a statically indeterminate mechanism. On the other hand, the framework shown in Fig. 2.4b is stiff and statically determinate. Föppl knew that only an <u>even</u> number of sides would lead to the unexpected features described above.

Finally, Fig. 2.5 shows the chronological relationship between the works described above and several major contributions to the theory of redundant structures, in which the former are embedded. The list is derived from Oravas & McLean (1966) and modified according to remarks by Charlton (1982).

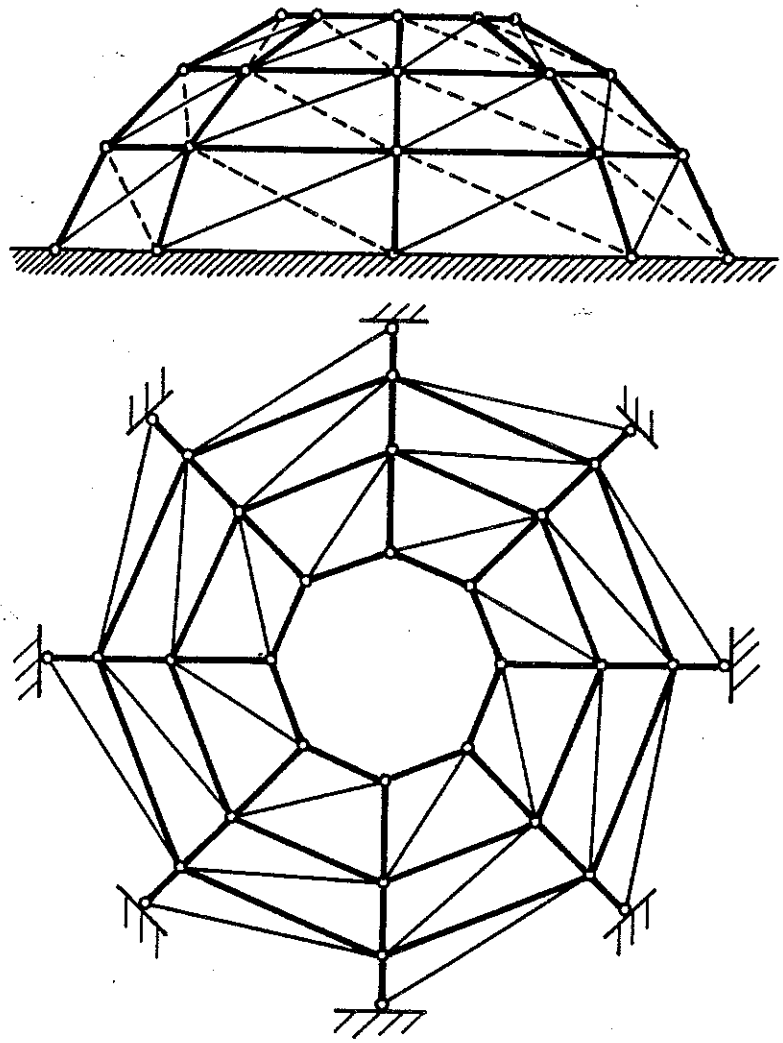

Fig. 2.3 Elevation and plan view of Schwedler's cupola. From Föppl (1912).

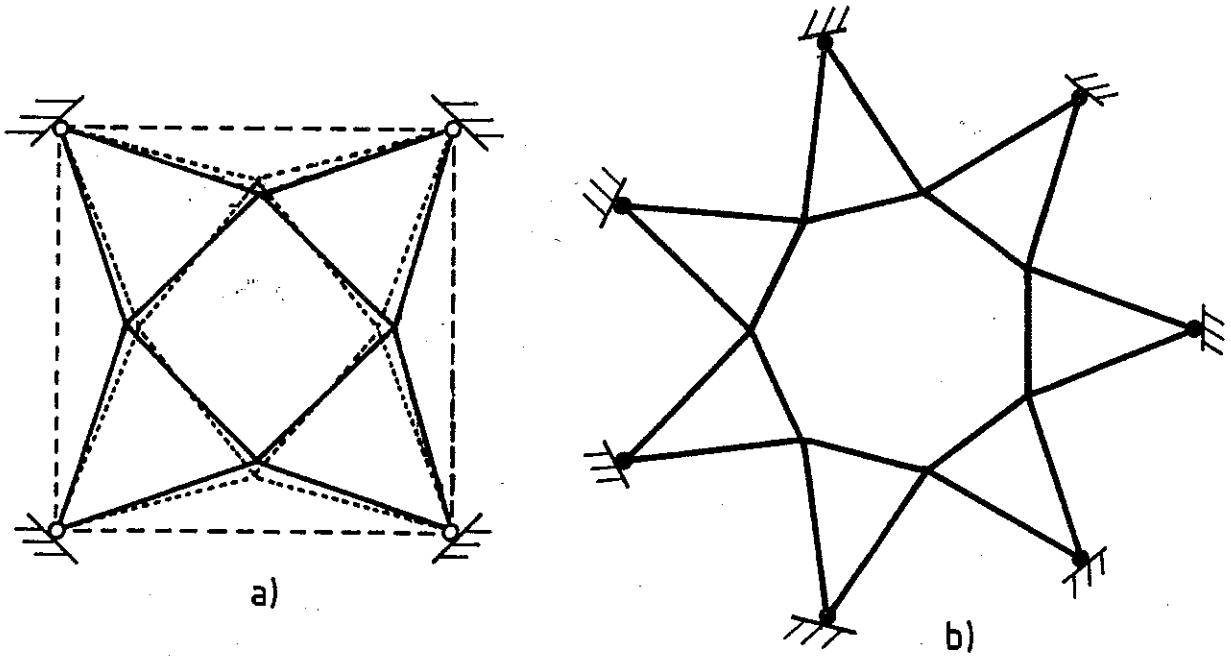

Fig. 2.4 Plan views of modified Schwedler's cupolas which have some rather special properties. This version of the cupola is a statically indeterminate mechanism if it has an even number of sides, see a). Otherwise it is statically determinate and rigid, see b).

(1)	(2)	
	Bossut (1771)	pointed out the statical indeterminacy of beams on more than 2 supports.
	Euler (1774)	solution of a rigid table on 4 legs, supported by an elastic foundation.
	Navier (1826)	analysis of continuous and encastre beams under point loads. Analysis of a pin-jointed framework consisting of n (n>2) elastic bars connected to a rigid foundation at one end, and to the only node of the framework at the other: the nodal displacements were taken as the unknowns of the problem.
Möbius (1837)		
	Menabrea (1857)	solution of statically indeterminate problems by using the principle of least work. In the following years Menabrea gave several derivations of his principle, but all of them were only partly correct.
	Clebsch (1862)	general method for analysing any truss by taking the hinge displacements as unknown variables. Thus the number of equations and of unknowns are always equal.
Maxwell (1864)		
	Castigliano (1873)	gave a correct and general proof of Menabrea's principle. Castigliano also formulated his first and second theorems.
	Mohr (1874)	used virtual work to obtain equations of compatibility.
Mohr (1885)		
Föppl (1892)		
Föppl (1912)		

Fig. 2.5 Column (1): chronological arrangement of work described in Section 2.1. Column (2): more general contemporary developments in the theory of redundant structures. Detailed references for column (2) are available in Oravas & McLean (1966) and Charlton (1982).

2.2 A fundamental paper by E.Kötter and some related work (1900-1940)

The first paper entirely concerned with the statical and kinematical indeterminacy of pin-jointed frameworks was published, to the author's knowledge, in a book in honour of Müller-Breslau (Kötter, 1912). The present interest in this paper is not merely historical: apart from the general theorems on polygonal frameworks that will be described immediately, Kötter introduced an analytical way of evaluating whether or not a plane assembly with $b<2n-3$ is rigid. Kötter's paper "On the possibility of connecting rigidly n points lying in a plane, or in space, by fewer than 2n-3, or 3n-6, inextensible rods" starts from a kinematical investigation of frameworks like the ones in Fig. 2.6, made of inextensible rods, and proves that a 2k-sided polygon braced by diagonal members which connect opposite vertices[1] is rigid if opposite sides are parallel. A similar condition holds for assemblies consisting of two k-sided polygons connected by bracing members, Fig. 2.7; an ad hoc sign count has to be devised in order to deal with such special cases as Fig. 2.8. Removing the hypothesis that opposite sides should be parallel Kötter was able to use the theory of funicular polygons to demonstrate (for $k>2$) the theorems:

"Any framework consisting of the sides of a 2k-sided polygon $A_1A_2 \dots A_{2k}$ and of its main diagonals $A_1A_{k+1}, A_2A_{k+2}, \dots, A_kA_{2k}$, see Fig. 2.6, is selfstressable if and only if the points in which opposite sides of the polygon meet lie on a straight line". A proof of this based on a direct equilibrium argument is given in the caption to Fig. 2.6. And:

"Any framework consisting of the sides of two k-sided polygons $A_1A_2 \dots A_k$; $A_{k+1}A_{k+2} \dots A_{2k}$ and the connecting members A_1A_{k+1}, $A_2A_{k+2}, \dots, A_kA_{2k}$, see Fig. 2.7, can be selfstressed if and only if the points in which two corresponding sides of the two k-sided polygons meet lie on a straight line". Note that the theorems just stated are not as powerful as the ones mentioned above because a framework of n nodes and b rods, with $b<2n-3$, which is selfstressable may be rigid, apart from at least $2n-b-4$ infinitesimal mechanisms, as will be shown later on.

With the aim of extending the treatment by Föppl described in Section 2.1 to the more general case in which $b \leq 2n-3$, and following Mohr's remarks - which he extensively quoted - on the rigidity or lack of it in frameworks, Kötter

---

[1] Two opposite vertices are i and i+k, e.g. A_1 and A_{1+3} in Fig. 2.6.

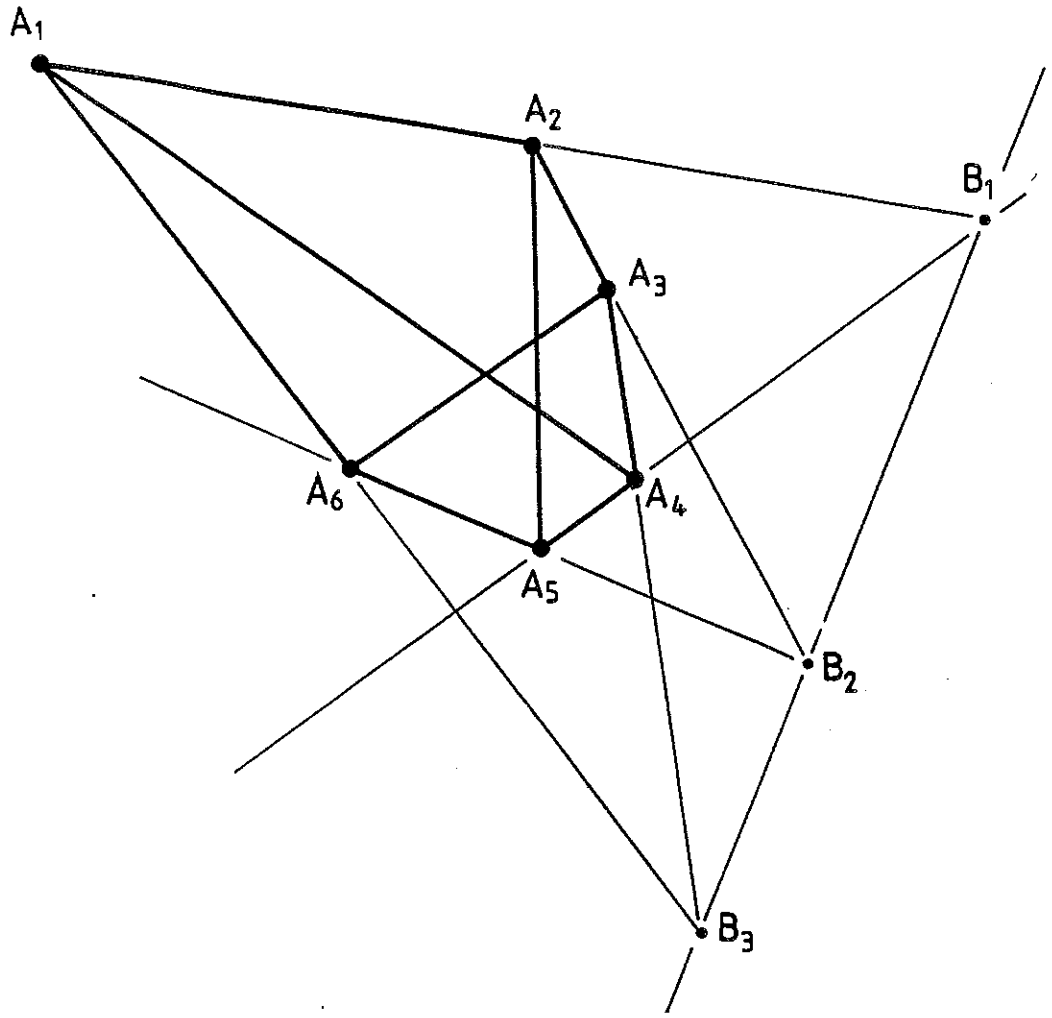

Equilibrium of bar A_1A_4 requires that

$$t_{A_1A_2}+t_{A_1A_6}+t_{A_4A_3}+t_{A_4A_5}=0$$

this condition can be written also as:

$$t_{A_1A_2}+t_{A_4A_5}=-(t_{A_1A_6}+t_{A_4A_3}) \qquad \text{(i)}$$

Similarly, the conditions of equilibrium of the other diagonal bars A_2A_5 and A_3A_6 are:

$$t_{A_2A_3}+t_{A_5A_6}=-(t_{A_2A_1}+t_{A_5A_4}) \qquad \text{(ii)}$$
$$t_{A_3A_4}+t_{A_6A_1}=-(t_{A_3A_2}+t_{A_6A_5}) \qquad \text{(iii)}$$

As all the resultants on the right-hand- and left-hand-sides pass through B_1, B_2, B_3 respectively, they have also to lie on $B_1B_2B_3$ if the 3 conditions are to be satisfied.
The equilibrium conditions of the sides of the hexagon are also satisfied if the resultant forces on the right-hand and left-hand-sides of (i), (ii) and (iii) lie on $B_1B_2B_3$ and are equal in magnitude to a common value t. The magnitude and sign of t is the only way of altering the selfstress in the framework.

Fig. 2.6 The plane structure shown is selfstressable according to the first of Kötter's theorems. In the demonstration above $t_{A_1A_2}$,... indicate the actions of the bars A_1A_2,... upon the nodes A_1,...

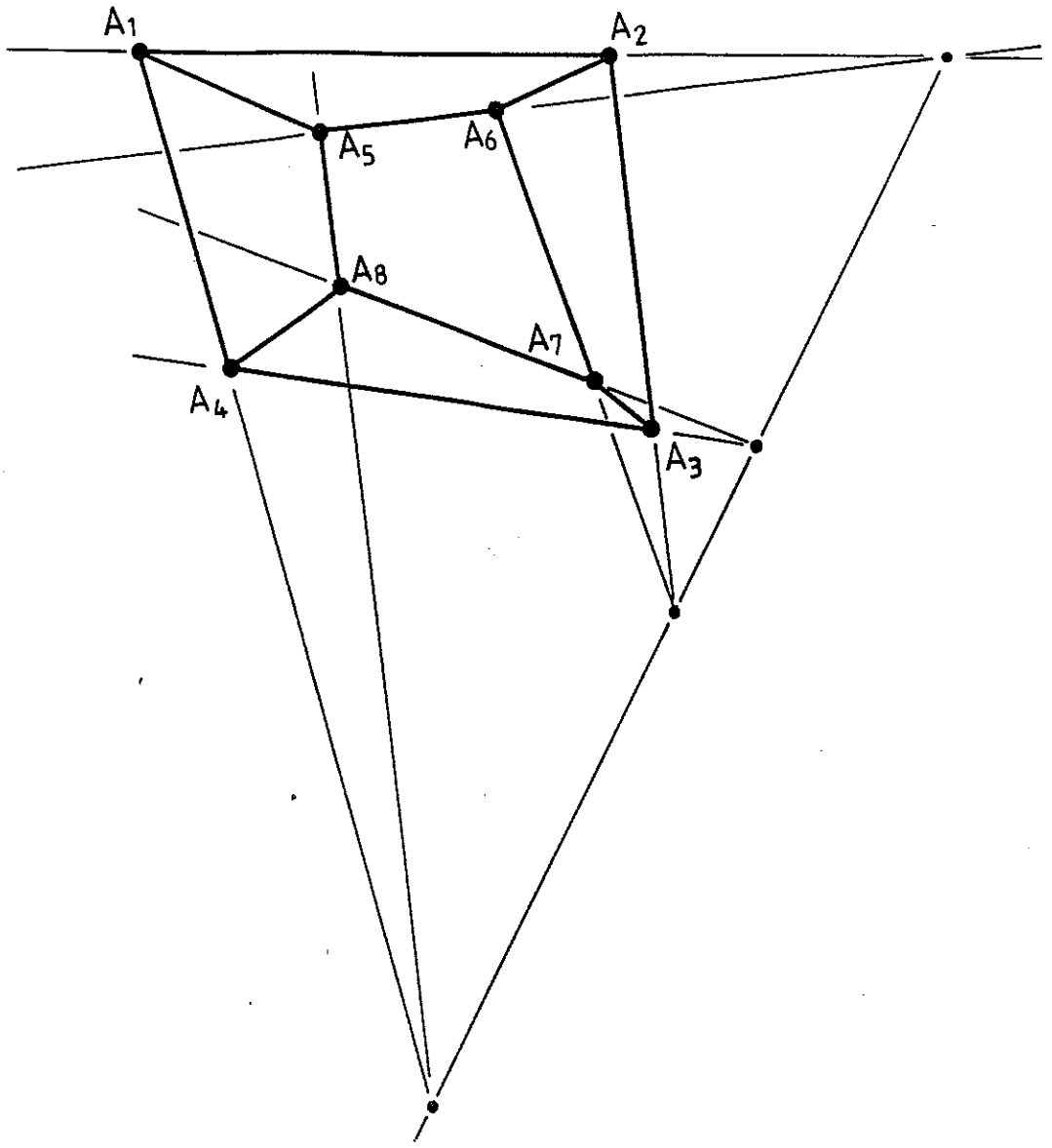

Fig. 2.7 Plane framework consisting of two quadrangles (k-sided polygons with k=4) connected by the diagonal members A_1A_5,... According to the second of Kötter's theorems, assemblies made out of two k-sided polygons are selfstressable if they satisfy the condition shown in the figure.

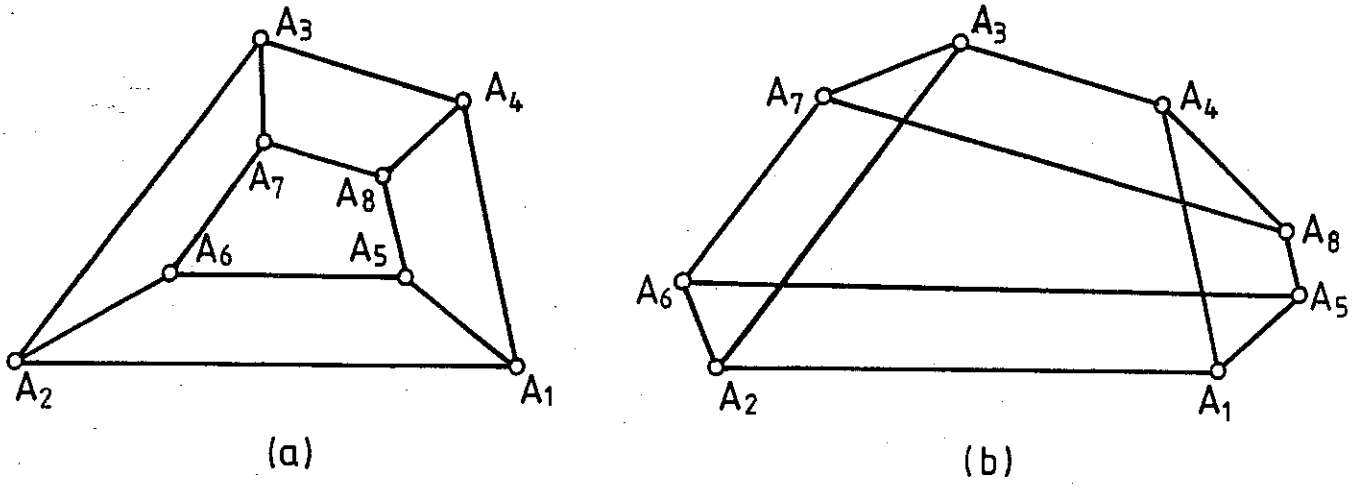

Fig. 2.8 Plane assemblies consisting of two 4-sided polygons; their rigidity was shown by Kötter (1912). This author introduced an ad hoc sign count which allows to extend to (b) the theorems, described in Section 2.2, that apply to (a).

introduced for each bar p connecting nodes i and j of the framework (coordinates X_i, Y_i and X_j, Y_j respectively) a function

$$F_p = \frac{1}{2}[(X_i - X_j)^2 + (Y_i - Y_j)^2 - l_p^2] \tag{2.8}$$

Note the small discrepancy with Föppl's definition (2.3). Kötter also defined the function

$$\Phi = \sigma_1 F_1 + \ldots + \sigma_b F_b \tag{2.9}$$

where the coefficients $\sigma_1, \ldots, \sigma_b$ do not vanish simultaneously. If the length of one bar of the framework - bar b, say - is to be either maximum or minimum, the lengths of the remaining members being assigned, the following $(b-1)+2n$ equations have to be satisfied:

$$\begin{cases} F_p = 0 \quad p = (1, \ldots, b-1) & (2.10a) \\ \partial\Phi/\partial\xi_i = 0 \quad i = (1, \ldots, n), \ \xi = x, y & (2.10b) \end{cases}$$

The first group of equations expresses the condition that the lengths of the first b-1 bars are fixed; the remaining 2n equations ensure that the length of bar b of the framework is stationary for any infinitesimal change of configuration; this condition is necessary for it to be either maximum or minimum. Equations (2.10a) are self-evident. An easily understandable explanation of (2.10b) is obtained by observing that (Maxwell, 1864, Mohr, 1885) the geometrical condition of bar b having maximum or minimum length, in which case the assembly resists any further elongation of that bar, is equivalent to the statical condition that the assembly is selfstressable, i.e. a set of non-vanishing bar tensions in equilibrium without external forces can be prescribed. Equations (2.10b) are in fact the 2n equilibrium equations of the structure when no external loads are applied:

$$\partial\Phi/\partial\xi_i = \sum_{p=1}^{b} \sigma_p (\partial F_p/\partial\xi_i) = \sum_{p,q} \sigma_p (\xi_i - \xi_j) = 0 \ .$$

here σ_p=(tension coefficient of bar p)=t_p/l_p and the last summation is only extended to rods connected to node i. Notice that the function Φ defined in (2.9) can be given a more physical interpretation if each rod of the assembly is pretensioned to a certain level; any small deformation of such a framework, described by the nodal coordinates $X_1,\ldots,Y_n$ of the displaced assembly, involves a change of Total Potential Energy equal to the change in strain energy because there are no applied loads. This is equal to the value assumed by Φ in the new configuration if terms of order higher than 1 are neglected:

$$\Phi(X_1,\ldots,Y_n)=\sum_{p=1}^{b}\sigma_p F_p=\frac{1}{2}\sum_{p=1}^{b}(t_p/l_p)[(X_i-X_j)^2+(Y_i-Y_j)^2-l_p^2]=$$
$$=\frac{1}{2}\sum_{p=1}^{b}(t_p/l_p)[(l_p+\delta l_p)^2-l_p^2]\approx\sum_{p=1}^{b}t_p\delta l_p \qquad (2.11)$$

where δl_p indicates the change of length of rod p in consequence of the imposed deformation. Therefore (2.10b), equivalent to the condition $\delta\Phi=0$, impose the condition that the Total Potential Energy of the prestressed assembly is stationary in its initial configuration. Having noted the difficulty of solving (2.10), Kötter differentiated F_p in (2.8) in a way similar to Föppl's, see Section 2.1, and obtained the b compatibility equations constraining any infinitesimal displacement of the framework which is to preserve the bar lengths:

$$\delta F_p=(X_i-X_j)(\delta X_i-\delta X_j)+(Y_i-Y_j)(\delta Y_i-\delta Y_j)=0,\ p=(1,..b) \qquad (2.12)$$

These equations can admit a non-trivial solution if "each determinant of order b obtained from the matrix

$$\begin{bmatrix}\partial F_1/\partial X_1 & \ldots\ldots & \partial F_1/\partial Y_n\\ \ldots\ldots & & \ldots\ldots\\ \ldots\ldots & & \ldots\ldots\\ \partial F_b/\partial X_1 & \ldots\ldots & \partial F_b/\partial Y_n\end{bmatrix} \qquad (2.13)$$

vanishes". This coincides with a theorem by Föppl in the case b=2n-3.

From the above considerations, and following an intricate procedure, Kötter demonstrated the theorem: "if a framework of n nodes and b (<2n-3) inextensional rods is rigid, then it is selfstressable and it has 2n-b-2 infinitesimal internal mechanisms; whilst in general it would have 2n-b-3 infinitesimal (and in fact finite) internal motions".

The last theoretical development was the following method to check whether or not a framework of the type described above is rigid "according to the rules of the calculus of variations": the second-order differential of Φ is to be computed for all possible displacements of the framework which satisfy (2.12) but are not rigid movements of the whole framework in the plane. This is equivalent to the Total Potential Energy being minimum (or maximum, but in this case the sign of the prestressing tensions would have to be changed). Here:

$$\delta^2\Phi=\sigma_1\delta^2F_1+\ldots+\sigma_b\delta^2F_b=\frac{1}{2}\sum_{p=1}^{b}\sigma_p[(\delta X_i-\delta X_j)^2+(\delta Y_i-\delta Y_j)^2] \qquad (2.14)$$

If $\delta^2\Phi$ assumes only positive values then the framework is rigid. This is because if one displaces the assembly obtained by removing rod b, the distance between the end points of that rod always increases if σ_b agrees in sign with $\delta^2\Phi$; it always decreases in the opposite case. Any other case can be treated in a similar way, and if $\delta^2\Phi$ is positive for some displacements from the original configuration but negative for others, then "a more detailed investigation would show that there must be displacements in which the distance remains unchanged". In short the following cases may be obtained:

$$\begin{aligned}
&\delta^2\Phi>0 \quad \Longrightarrow \text{ the framework is rigid}\\
&\text{" } <0 \qquad\quad \text{"} \qquad\quad \text{"}\\
&\delta^2\Phi\neq0 \quad \Longrightarrow \text{ the framework is not rigid} \qquad (2.15)\\
&\delta^2\Phi=0 \quad \Longrightarrow \text{ "the question remains unsolved"}
\end{aligned}$$

Similar results will be obtained in Chapter 4 following a more physically intuitive approach. The analytical method described above, although known to some of Kötter's contemporaries in Germany and Italy, has been never applied - to the writer's knowledge - to any other structure than the parallelepiped of Fig. 2.9 which was studied by Kötter in the last section of his paper.

Pollaczek-Geiringer followed the steps of Föppl and Kötter to classify a wide range of plane (Pollaczek-Geiringer, 1927) and space frameworks (Pollaczek-Geiringer, 1932), but she obtained the coefficients of (2.13) from straightforward equations of equilibrium. In a section containing various examples she noted the curious behaviour of the mast structure of Fig. 2.10 which has recently been investigated by Tarnai (1980a).

Having come across Kötter's work, Levi-Civita and Amaldi added to the 2nd edition (1949) of their Treatise on Rational Mechanics first published in 1929 a new section which presented the "analytical circumstances in which singular frameworks may be obtained"; the authors themselves referred to this as the most relevant addition to that new edition. Levi-Civita & Amaldi (1949) briefly discussed the algebrical condition $b=2n-3$ that has to be satisfied in general by stiff plane frameworks but they also observed that any polygon in which the length of one bar is equal to the sum of the lengths of the others cannot be deformed irrespectively of the above rule. These authors suggested, as a simple analogy for this, the one equation $x^2+y^2=0$ which determines the values of two parameters, because its only real solution is $x=y=0$. Similarly a system of b equations of compatibility $F_p=0$, $p=(1,\ldots,b)$ may be able to determine uniquely $2n-3$ node coordinates of a plane framework, which is therefore 'stiff'. This happens if the initial configuration of the framework corresponds to a point of either maximum or minimum in the linear combination of the F_p's such that its Taylor expansion has no first order term. In spite of their correct mathematical formulation of the problem, these authors failed to recognize that the polygons with $k=3$ (see the beginning of this section for a definition of k) are also covered by Kötter's theorems.

In the same period the geometers Bricard (1897) and Bennet (1912) developed Cauchy's work on the rigidity of polyhedra: see Bricard's paper for a list of references to earlier workers. Bricard showed by means of elegant kinematical arguments that there exist concave octahedra of three different types which have one finite motion; Bennet's paper contains a classification of the kinematical properties of all possible octahedral mechanisms, but the terminology and techniques used by Bennet lie beyond the boundaries of the present work.

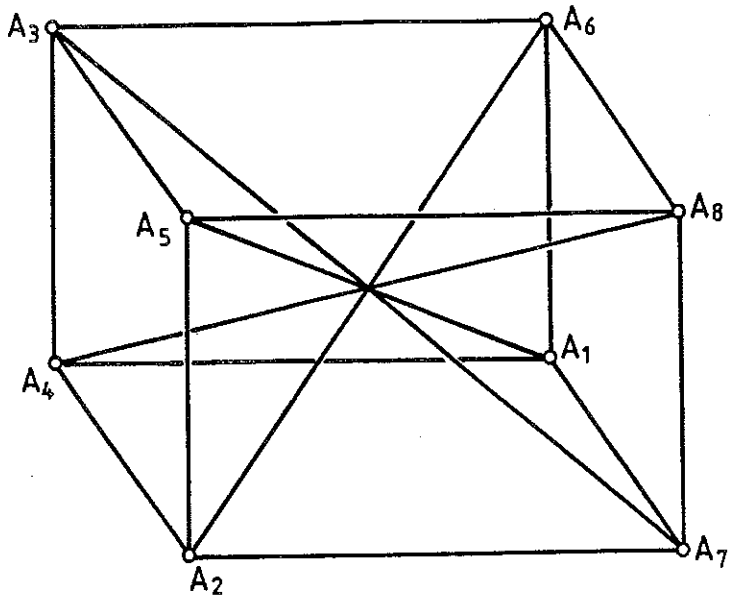

Fig. 2.9 Three-dimensional framework consisting of a parallelepiped with its body diagonals. Kötter (1912) showed that the above structure is statically indeterminate by evaluating the determinant of its equilibrium matrix.

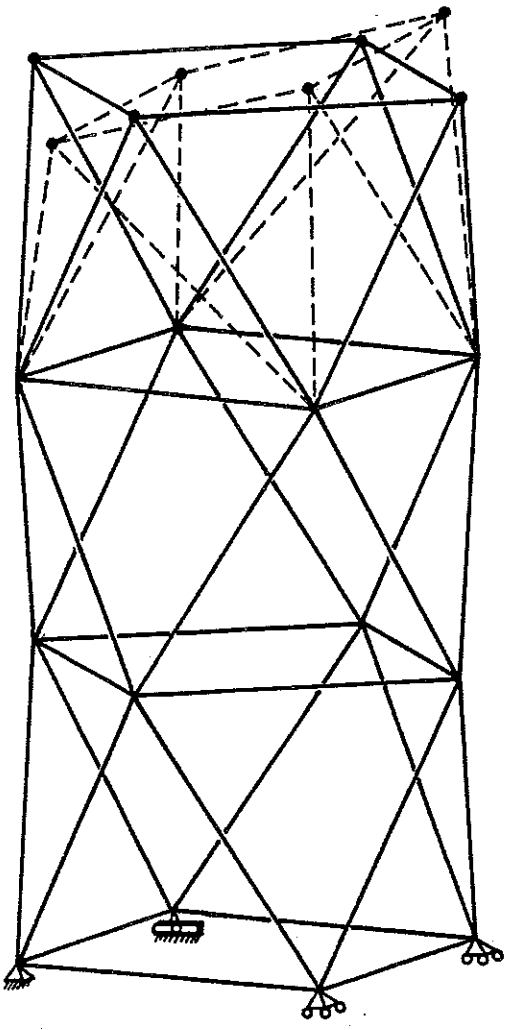

Fig. 2.10 Three-dimensional mast structure first analysed by Pollaczek-Geiringer (1932), who noted that the top part can freely distort as Schwedler's cupola of Fig. 2.4a.

2.3 Instantaneously-rigid and quasi-unstable assemblies

During the 1960's several cable structures were built in Russia (Rabinovich, 1962). At first sight this structural type may seem unrelated to the assemblies of pin-ended rods discussed so far, but Rabinovich (1962) recognized that most cable structures are "kinematic chains with many degrees of freedom which, as a result of a careful selection of the geometrical parameters, behave like systems which are only able to undergo infinitesimal movements". This stimulated new interest in the recognition/analysis of statically and kinematically indeterminate structures. It is clear that Rabinovich did not regard these peculiar structural configurations as in any way awkward, and he took a fresh view of the problems posed by them. This is possibly the reason why some new definitions were introduced. Thus an assembly is instantaneously rigid if it has a positive number of internal mechanisms but nevertheless can only undergo infinitesimal configuration changes if its bar lengths are to be preserved. How does one check whether or not a given assembly with m internal mechanisms is instantaneously rigid, according to Rabinovich? Starting from the framework of Fig. 2.11a, which has four finite mechanisms, move node F the maximum distance away from A: the linkage ABCDEF now lies on a straight line (Fig. 2.11b) but still has four finite mechanisms. Now fix node F to remain in its present position (Fig. 2.11c): this assembly is instantaneously rigid with four infinitesimal mechanisms. The number of mechanisms of an assembly can be obtained in general, i.e. not in special cases, by using the formula:

$$m=2n-b-c \qquad (2.16)$$

where n, b have the usual meanings of number of nodes and bars, and c is the number of external constraints. For the structures of Fig. 2.11 this formula gives $m=2\times6-5-3=4$ for cases a) and b), and $m=2\times6-5-4=3$ for case c). From examination of these examples and of similar ones Rabinovich concluded that an instantaneously rigid assembly has to have at least one more mechanism than the corresponding non-singular assembly. Hence he enunciated the following empirical criterion of instantaneous rigidity: a pin-jointed assembly which has m mechanisms according to (2.16) is instantaneously rigid

if all the structures obtained by 'freezing' m hinges of the original structure have at least one mechanism. Clearly this criterion is only suitable for demonstration purposes because of the sheer amount of work and the difficulty of finding out the number of mechanisms of all the configurations to be considered. Rabinovich was aware of the work by Mohr described in Section 2.1, and indeed he reproduced and discussed Fig. 2.2 from Mohr (1885); he also observed that Mohr had not discussed the problem of instantaneous rigidity and that, although all instantaneously rigid assemblies are selfstressable so that one may think of using this property as a criterion to characterise them, this condition is not sufficient as the structures of Fig. 2.12 demonstrate. Still following Mohr's ideas, Rabinovich proposed two methods of creating instantaneously rigid assemblies: either by choosing any two unconnected nodes of an existing structure, moving them to the maximum distance allowed by the existing links and finally connecting them with a rod; or by building assemblies in which all the instantaneous centres of rotation lie on a straight line. This method leads to frameworks that behave like closed polygons with the length of one side equal to the sum of the lengths of the others.

In the end the paper does not give a rigorous answer to the question posed at the beginning of this section, apart from rather general statements on the appropriateness of having "a preponderance of tensile bar tensions". This kind of remark is rather typical of this paper, which constitutes an 'early' attempt to tackle a class of structures with exceptional configurations; Rabinovich developed his own ideas intuitively when he found that the existing literature was not helpful.

Rabinovich's work was followed by a series of papers by Kuznetsov (1973, 1975, 1979) which laid down general schemes for classifying space structures and analysing the response of kinematically (but not statically) indeterminate frameworks to applied loads. Kuznetsov (1975, 1979) aimed at a completely formalized statical-kinematical analysis of an arbitrary spatial structure that could be performed by a computer; he also extended his analytical method to systems containing unilateral constraints (i.e elements which can only carry tensions of one sign, e.g. cable segments). Kuznetsov (1975) introduced the following structural categories:

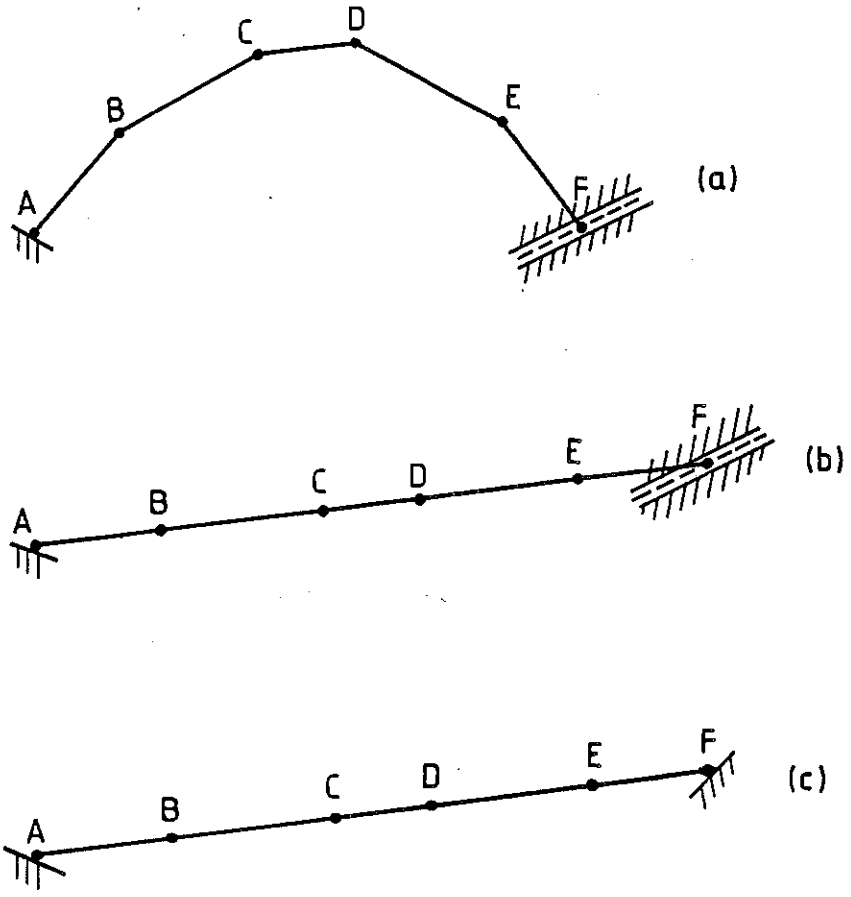

Fig. 2.11 Plane linkages discussed in Section 2.3. From Rabinovich (1962).

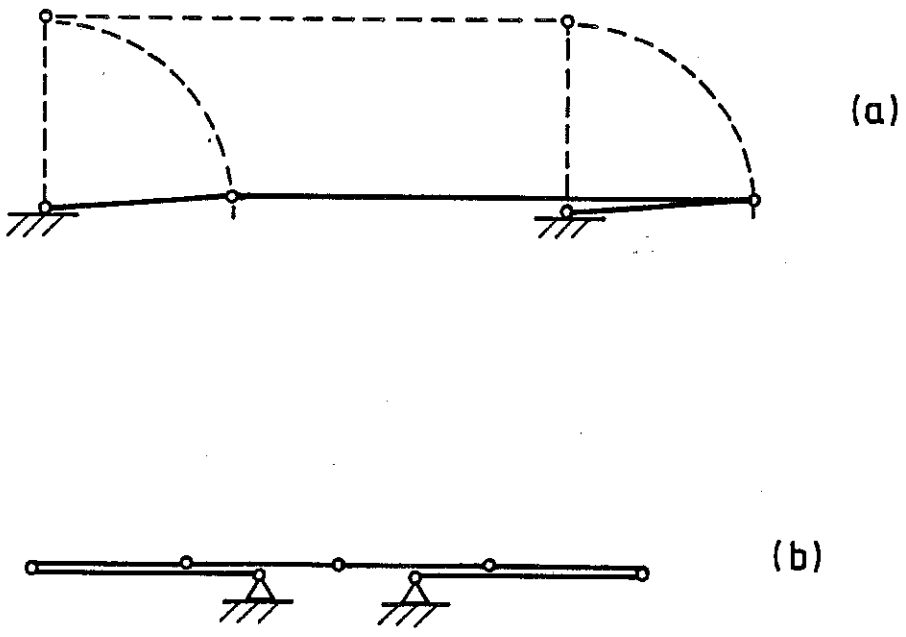

Fig. 2.12 In the Theory of Machines both configurations in solid lines would be called dead points of the plane mechanisms displayed. It is obvious that neither of them satisfies a condition of maximum/minimum length and that they are not instantaneously rigid structures, see Section 2.3.

(i) Stable, assemblies which possess a unique configuration and therefore can equilibrate any load applied to them by means of finite tensions. These would be referred to as kinematically determinate in the terminology adopted in this dissertation.

(ii) Quasi-stable, assemblies which possess a unique configuration if their bars are regarded as infinitely rigid and are unable to equilibrate arbitrary applied loads unless a small distortion is allowed; in which case they become stable. These assemblies are kinematically indeterminate (with only infinitesimal mechanisms). A (small) distortion of the initial geometry of an assembly belonging to this class is usually sufficient to make it stable.

(iii) Quasi-unstable, assemblies satisfying all the conditions of (ii) but which do not become stable after a small distortion. In fact they become unstable (see (iv), below) on distortion. The only substantial difference between this group and the previous one is that (2.16) would give $m>0$ for structures belonging to (iii); they are similar in all other respects and are also kinematically indeterminate (with infinitesimal mechanisms).

(iv) Unstable, structures which do not possess a unique configuration. These are also kinematically indeterminate, but at least one of their mechanisms is finite.

The examples shown in Fig. 2.13 clarify the above classification.

It will be shown in later chapters that structures from the groups (ii) and (iii) are rather similar in their response to applied loads: in fact they all require finite bar elongations in order to displace from their original configuration by a finite amount (as if they were kinematically determinate). Yet Kuznetsov's scheme regards them as substantially different: quasi-stable structures are entirely acceptable because only a small deformation is required to make them stable, which is not the case for the quasi-unstable ones.

Kuznetsov (1979) then followed Föppl and Kötter in the derivation of the compatibility conditions of a given assembly, see (2.8) and (2.10a), and linearized them by using Taylor's expansion to end up with (2.13). According to the number of elements two situations are possible:

A three-dimensional assembly has "sufficient constraints" if $3n-6 \leq b$. It belongs to groups (i), (ii) if a sufficient number of them are independent,

i.e. if either the rank of (2.13), modified to include z-coordinates as well, equals 3n-6 (i) or the number of independent compatibility conditions, now considered in full instead of their linearized versions accounted for by (2.13), (ii); otherwise it belongs to group (iv). The difference between these conditions will be clarified in Chapter 5 when approximations of different orders of the conditions of geometrical compatibility will be used in the study of some examples.

An assembly has "insufficient constraints" if 3n-6>b. It belongs to group (iii) if the rank of (2.13) is smaller than b and a quadratic form equivalent to (2.14) is either positive or negative definite. In all other cases the assembly belongs to group (iv). Unlike Kötter, who first considered this quadratic form, Kuznetsov recognized that this is the "energy increment (accurate to terms of second order) of the system", equal to the work done by the prestressing forces over the corresponding displacement, and understood that the test proposed was just a way of checking the stability of the equilibrium in the initial configuration.

With reference to assemblies containing unilateral members, Kuznetsov (1975, 1979) first looked at the substructure made out of 'bilateral' elements only in order to work out which displacements need to be prevented by the unilateral elements. As the only effective elements are those ones for which the corresponding compatibility condition is satisfied as an equality, a stable system is obtained if the only possible solution of the system of linear inequalities associated with the unilateral members is trivial; hence no nodal displacements are allowed. Kuznetsov (1979) developed an effective but rather lengthy procedure to perform this calculation, the details of which will not be given here. From the developments of Chapter 4 it will be clear that a much more efficient algorithm can be devised. In an earlier paper Kuznetsov (1973) described the response of assemblies belonging to group (iv) to arbitrary applied loads which, he argued in a way analogous to Chapter 6 of the present work, can be uniquely decomposed into an "equilibrium load" which does not produce any change of configuration of the structure but only changes the internal forces, and a "supplementary load" that is responsible for small changes of configuration. He also described a method of doing this which requires "one or two iterations" provided the supplementary part of the applied load is relatively small; otherwise the method would not work. No

applications of these ideas were proposed, and indeed it is unclear whether they were tested at all; nevertheless this work has to be regarded as the first step in the approach followed in Chapter 6.

2.4 Development of a comprehensive classification

Calladine (1978) went back to the paper by Maxwell (1864) discussed in Section 2.1 for an explanation of the mechanics of one of Fuller's tensegrity assemblies and, in so doing, he introduced a novel way of looking at prestressable systems. The crucial point is the introduction of a new version of Maxwell's rule, which includes all possible special cases. For spatial frameworks not connected to a foundation the rule is:

$$3n-b-6=m-s \qquad (2.17)$$

with: n=number of nodes
b= " bars
m= " independent infinitesimal internal mechanisms
s= " states of selfstress.

A relationship like (2.17) should have been formulated at the time of the earlier developments described in this chapter; but only Buchholdt, Davies & Hussey (1968) had previously derived it. These authors introduced it in the context of a study of the behaviour of cable nets, but they did not use it for any practical purpose. Rigorous derivations of (2.17) are given by Calladine (1978) and in the above paper by Buchholdt et al.; it will also follow from a rather obvious dimensional relationship between the four vector subspaces of the equilibrium matrix that will be introduced in Chapter 4.

Formula (2.17) does not in itself solve the problem of correctly classifying any pin-jointed framework according to its statical and kinematical properties, expressed by the numbers s and m, respectively, but it introduces, so to speak, a correct and clear framework within which one has to operate. As an example, Calladine studied one of Fuller's tensegrity structures (see Fig. 2.14). This assembly is obtained by intersecting a tetrahedron with four planes perpendicular to its axes of three-fold symmetry; the truncated tetrahedron obtained in this way had all its edges

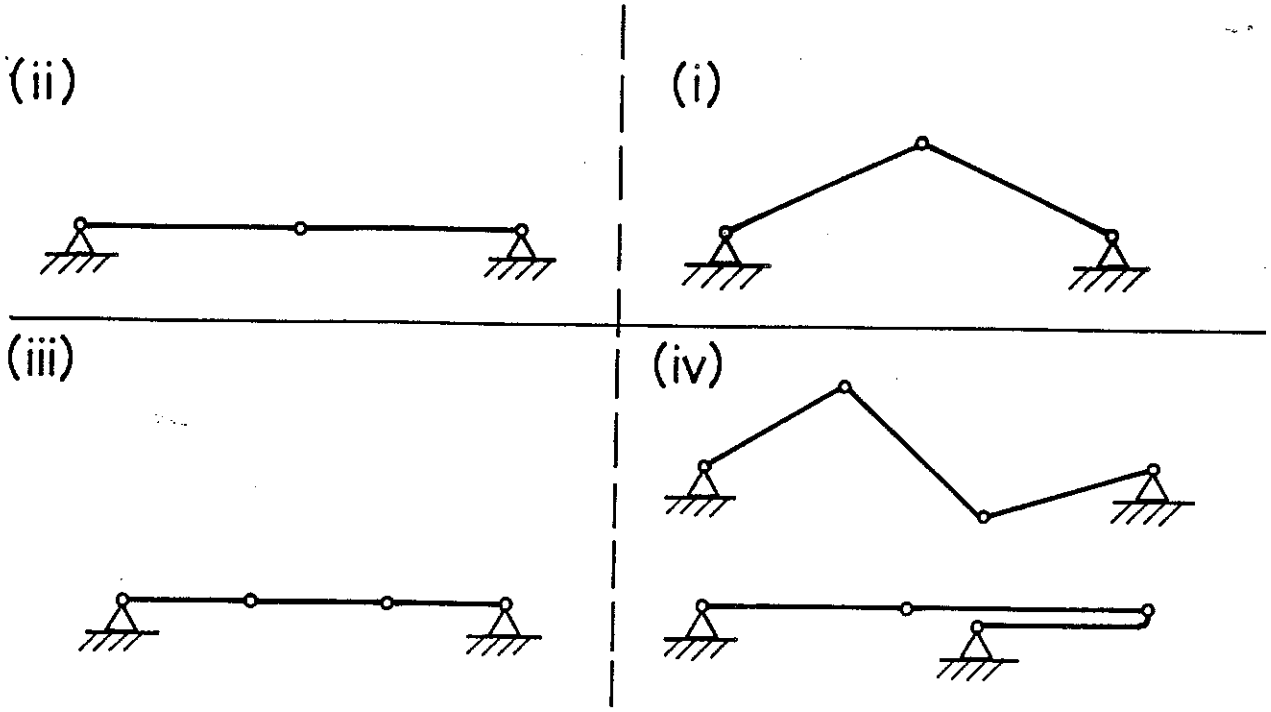

Fig. 2.13 Examples of the four classes of structures considered by Kuznetsov (1975, 1979). The broken line illustrates that -on distortion- (ii)->(i) and (iii)->(iv). From Kuznetsov (1979).

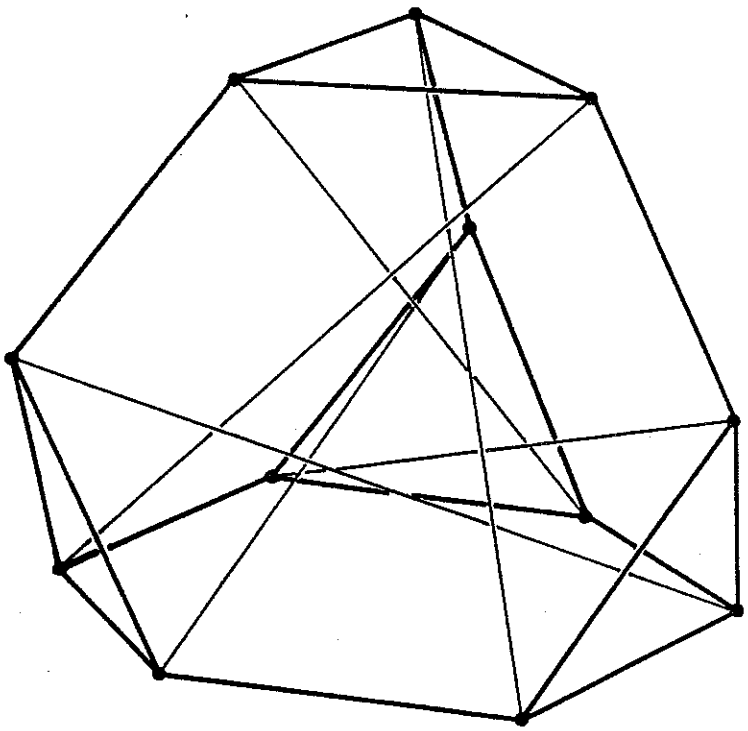

Fig. 2.14 "Tensegrity" structure investigated by Calladine (1978). The 18 external members have equal length, say =1, and the 6 inner diagonals have also equal length, =2.25. A photograph of a physical model of this structure is in Fig. k8 of Marks (1960).

made out of wires in Fuller's own model (Fuller, 1975, Marks, 1960). The structure was completed by adding six internal struts. The first point to be made, here, is that Fuller used to build all of his tensegrities with the outside segments made out of wire and therefore an initial state of pretension in all wires (and consequent precompression in the inner struts) was an essential ingredient of the physical structures: nevertheless all of this is a rather unimportant detail for the purpose of a theoretical investigation. In fact Calladine's paper refers to a physical model simply made out of plastic rods and rubber joints. The structure of Fig. 2.14 has n=12 and b=24; substitution of these quantities into (2.17) yields:

$$m-s=6 \qquad (2.18)$$

By inspection of this model, which had all the 'wire' lengths equal to 1 and all the 'strut' lengths equal to 2.25, only one state of selfstress was found. The assembly is therefore statically and kinematically indeterminate: s=1 => m=7, the implication being a consequence of (2.18). In fact Calladine verified that his model had seven independent mechanisms, but he also found that prestress had a stiffening effect on all of them; more generally, he concluded that prestress is necessary in order to build kinematically indeterminate frameworks with 'first order' stiffness in all modes.

The procedure described above constitutes a partial answer to the question posed at the beginning of Section 2.3; the same author pursued this approach even further in the study of the behaviour of saddle-shaped cable nets (Calladine, 1982).

Tarnai studied in detail various space trusses of the type shown in Figs 2.4 and 2.10. It was remarked in Section 2.2 that the ring-like assembly of Fig. 2.4a has been known to be statically and kinematically indeterminate since the times of Föppl; Tarnai (1980a) evaluated a closed form expression for the determinant of the equilibrium matrix of Föppl's ring, for a more general layout made out of a regular horizontal k-gon connected by 2k bars to a rigid foundation set out as the k vertices of an identical k-gon. The top k-gon was rotated through an angle θ relative to the bottom one, see Fig. 2.15. It turns out that, if one considers only $\theta \leq 2\pi$, the two configurations obtained for $\theta_1=\pi(k+2)/2k$ and $\theta_2=\pi(3k+2)/2k$ are statically and kinematically

indeterminate, with s=m=1; but they do not have any planes of mirror symmetry which, as will be demonstrated later on, is a crucial requirement if the mechanism is to be able to undergo 'large displacements'. If k is even, the determinant of the equilibrium matrix also vanishes in two other configurations: $\theta_3=\pi/k$ and $\theta_4=\pi(k+1)/k$. Tarnai pointed out that the special feature of these last configurations is that they do admit planes of mirror symmetry and therefore can undergo large inextensional displacements. It is easy to convince oneself that the joints of even numbers can move, say, towards the inside of the k-gon while the odd ones move outwards and that in so doing the nodes describe paths lying in the planes of mirror symmetry; hence the mechanism cannot tighten up. For k=4 the configurations θ_3 and θ_4 are shown in Fig. 2.16. In a more recent paper Tarnai (1984) has shown that, provided that there exists at least one plane of mirror symmetry which contains nodes i and i+k/2, even an irregular k-gon is a finite mechanism. This result is unexpectedly simple, if one compares it to Kötter's theorems in Section 2.2.

The structure shown in Fig. 2.16 and having the configuration θ_3 was also analysed and tested by Hoff & Fernandez-Sintes (1980).

Tarnai (1980a) also considered towers built from a number of rings having the configuration θ_3, see Fig. 2.10; the equilibrium matrix of this assembly has full rank if the number of sides of the constituent rings is odd, and in this case the resulting tower is statically and kinematically determinate. But an even number of sides leads to s=m=1: the statical indeterminacy is located in the bottom ring and the kinematical indeterminacy appears in the top one, while the remaining rings are statically determinate and rigid. This result is clearly independent of the number of constituent rings. Tarnai remarked that, unlike proper tensegrity structures, "it seems that prestress does not give stiffness" to the tower. This conclusion leads to some concern when one sees practical realizations of such towers in Figs 7 and 8 of Makowski (1966).

The work described above provided a firm foundation on which an analytical framework could be erected; C.R. Calladine and the present author presented communications along these lines at the XVI IUTAM Congress and the III International Conference on Space Structures. Chapters 4 and 6 will provide details of these communications.

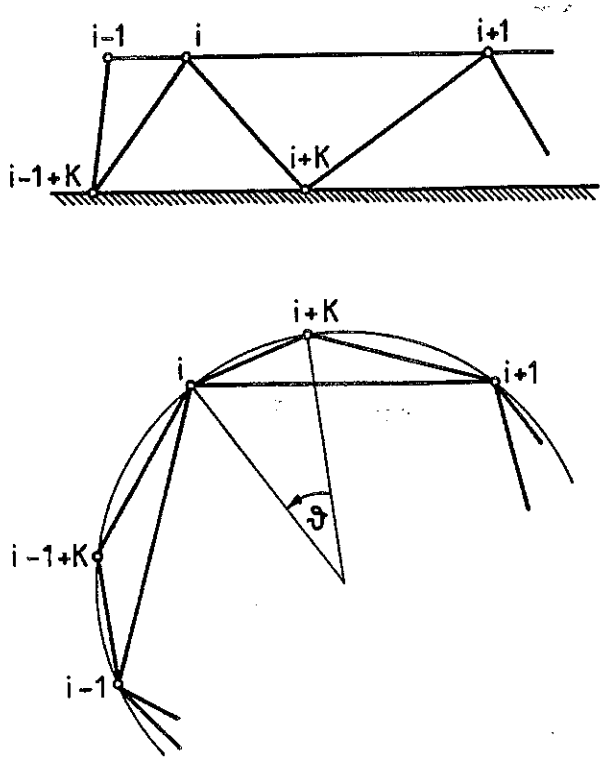

Fig. 2.15 Elevation and plan view of the bar forces acting on joint no. i of the 'ring' assembly studied by Tarnai (1980).

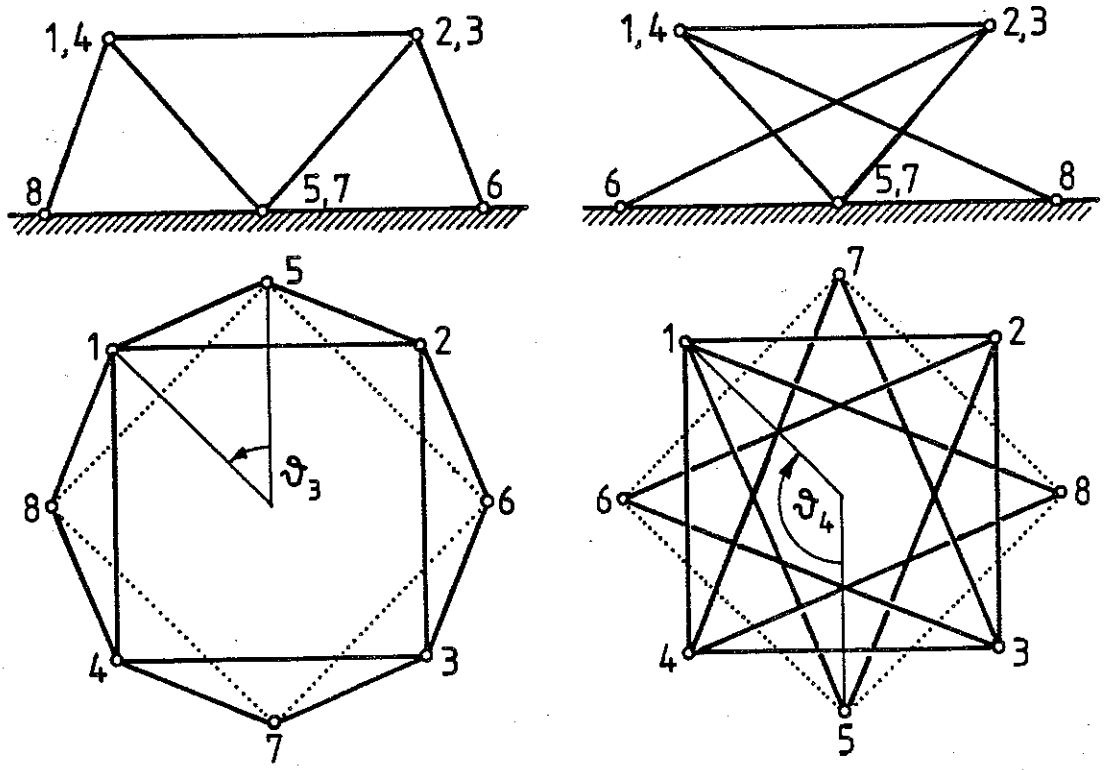

Fig. 2.16 Elevations and plan views of the only symmetrical configurations in which the 'ring' of Fig. 2.15 is both statically and kinematically indeterminate. From Tarnai (1980).

Research along similar lines has been made by Besseling. In an attempt to foster the use of the force method of structural analysis in some plastic analyses, Besseling (1978) first formulated the basic concepts of the analysis in terms of Linear Algebra and gave a description (but very compressed indeed) of the subspaces related to the equilibrium/compatibility matrices. The bases of the relevant subspaces appear to have been guessed rather than computed in a systematic fashion; the paper also discussed how to use the above subspaces to perform limit and elasto-plastic calculations. A deeper explanation of the Linear Algebra ideas was given subsequently by Besseling (1979, 1981), who also compared this approach to other numerical methods available. It is noteworthy that section 7 of Besseling (1979) has a formula for checking whether a framework with one or more mechanisms is 'stable', i.e. if a suitable state of prestress can be found to stiffen the mechanism; this formula coincides in essence with (2.15) obtained by Kötter in 1912 (see Section 2.2) and by Kuznetsov in 1975 (see Section 2.3). Chapter 4 of this dissertation will discuss the problem in more detail.

Motro (1983) followed a different approach in his doctoral thesis. In an initial qualitative study he used the theory of graphs to investigate the topological properties of tensegrities. A rather separate and more practically oriented study of a simple tensegrity followed: the "Simplex" is obtained by transforming an equilateral triangular prism, (see Fig. 2.17) the diagonals of which are simultaneously elongated until their length reaches a maximum value. This structure has n=6, b=12; it is therefore a statically and kinematically determinate truss in most configurations. From (2.17) m=s. Motro showed that a selfstressable configuration could be obtained by means of equilibrium considerations, i.e. he looked for values of θ in which a state of selfstress is admissible, which leads to $\theta=\pi/6$. And he obtained the same result by means of kinematical considerations, i.e. by maximizing the lengths of the diagonals. He compared this solution in closed form to the results given by Dynamic Relaxation, see Fig. 2.18: this numerical method has proved rather effective in solving a large class of problems concerned with finding an initial shape, according to Webster (1980). A coincise introduction to this method can be found in Day & Bunce (1969).

The performance of the "Simplex" under load was studied by Motro both experimentally, see Section 6.5, and numerically by means of a geometrically

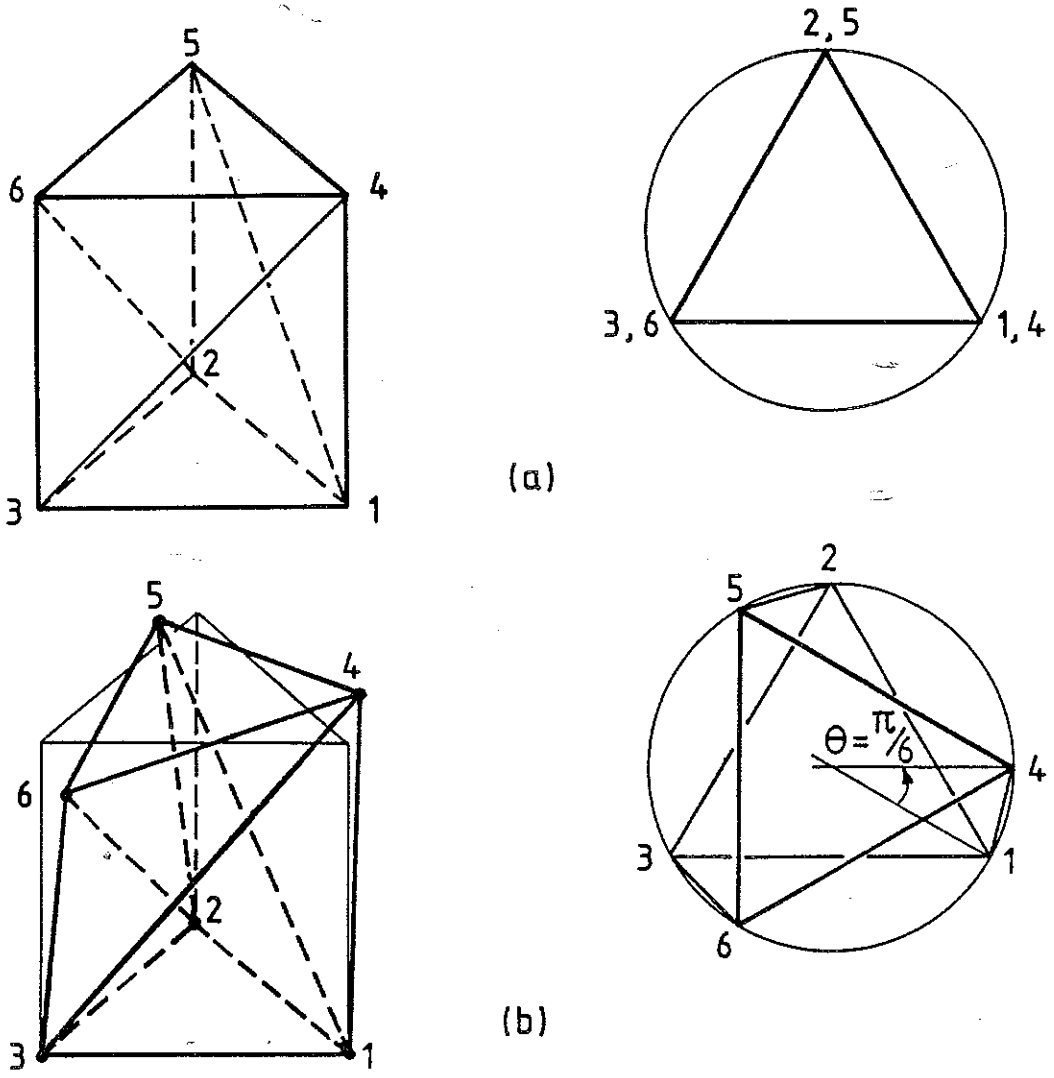

Fig. 2.17 Formfinding of "Simplex": a) initial configuration, $\theta=0$. b) selfstressable configuration, $\theta=\pi/6$.

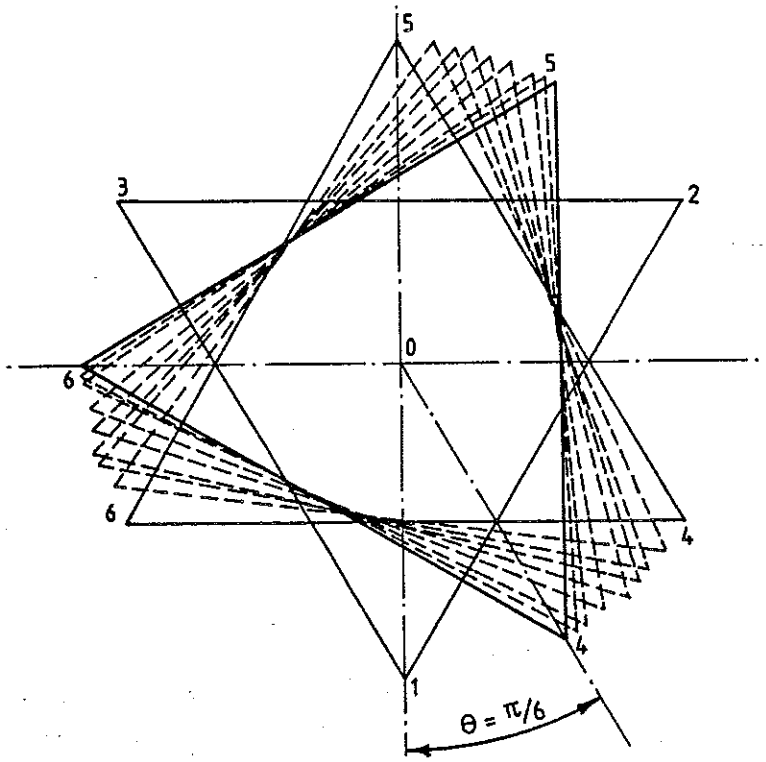

Fig. 2.18 Motro (1984) used the method of Dynamic Relaxation in order to obtain a prestressable configuration of the "Simplex". The figure shows a plot of the successive configurations of the top triangle.

non-linear computer program based on the displacement method of analysis. This work was presented in a condensed form by Motro (1984).

Vilnay also approached tensegrity structures using the same method; but his work (Vilnay, 1981, Vilnay & Soh, 1982) is full of misunderstandings as pointed out by Calladine (1983).

It should be clear from the above discussion that i) the geometrical problem of 'formfinding', i.e. the computation of the nodal coordinates of a configuration which is selfstressable and æsthetically pleasing, and ii) the structural behaviour of such a framework with its members made out of rods and wire, prestressed to improve its performance, are conceptually different operations even if some authors have applied the same numerical techniques to both i) and ii). The present work will take a very different line from such authors: its main thrust is the recognition, discussion and solution of various problems related to ii) with only Section 5.2 dedicated to i).

2.5 Recent contributions by geometers and mathematicians

It was noted in Section 2.2 that the interaction between engineers and geometers dealing with structural rigidity started to become more difficult towards the beginning of this century, mostly because the aims were different but also on account of the different terminologies used by each group. In recent years significant efforts to establish common ground have been made but the exchange of fruitful information is at present still rather slow.

The introductory section of a paper by Laman (1970) set out the main difficulties facing a mathematician who tried to investigate the rigidity of pin-jointed assemblies; in short, Laman had found a lot of "obscure and ambiguous notions" in the engineering literature, so that the first object of his paper was the definition of a new terminology and of precise concepts. Mathematical definitions of "skeletal structures", "length-preserving displacements", "infinitesimal and admissible infinitesimal displacements", "rigidity",... were given; and the meaning of these words in terms of structural mechanics should be easy to guess for all engineering readers. After this Laman started his own investigation. The main theorem proved in the paper is, for engineering purposes, just a little more powerful than Maxwell's rules on how to build stiff frameworks, and it will not be discussed here. An important effect of the paper by Laman was to provide an initial link

between engineering problems and mathematical techniques, because his definitions could be understood and therefore used and improved upon by other mathematicians. A number of related papers have been published from 1970 onwards, starting from a complete re-formulation of the problem of rigidity for pin-jointed assemblies in R^m by Asimow & Roth (1978, 1979) and the more practically oriented paper by Crapo (1979) which ascribes the lack of rigidity of a three-dimensional truss to either of the following reasons: i) a framework which fails to be rigid because it does not have enough bars fails for topological reasons; ii) a second type of failure is due to projective geometry reasons, if the nodes and bars happen to have special arrangements. Rigid, according to Crapo, means that an assembly cannot undergo even an infinitesimal displacement; and therefore the above description is correct. But his way of proceeding leads him into the misconception that all the structures that have been used in engineering practice must be rigid ones and therefore must have satisfied both the topological (i) and geometrical tests (ii). This is wrong: see e.g. tensegrities, cable nets,... It is curious to notice that, although Crapo (1979) introduced the four subspaces of the compatibility matrix (of which more details will be given in Chapter 4), he could not find any use for them, and in practice did not even compute them since his aim was to establish general theorems.

The definitions of rigidity and infinitesimal rigidity of various orders have received careful consideration by a number of authors, e.g. Connelly (1980) and Roth (1980). Having called "infinitesimally rigid" all of those frameworks which would be kinematically indeterminate, with infinitesimal mechanisms, according to the terminology introduced in Chapter 1, Connelly (1980) extended the notion to "infinitesimal rigidity of second order" by which he meant that no further deformation can be considered after an initial infinitesimal one, which is possible if the assembly is not first-order rigid. This class of definitions is almost equivalent to the 'engineering' definitions of higher-order mechanisms which will be given in Section 5.1. Connelly (1980) also demonstrated that second-order rigidity implies ordinary rigidity, but he was unable to extend his proof to the more general case in which nth-order rigidity implies ordinary rigidity as well. A list of various points in need of further investigation was given by Connelly (preprint), among which is the need for numerical algorithms. "Generically

rigid" frameworks were also defined in this paper to indicate assemblies that are rigid, so to speak, in most of their configurations. An engineer's answer to whether an assembly is generically rigid would just be through the combined use of 'common sense' and Maxwell's rule; but a different approach to this problem led to this matter being extensively investigated by Asimow & Roth (1978, 1979) and Roth (1980).

A clarifying point of Roth (1980) and Roth & Whiteley (1981) was the distinction between regular and singular configurations of a framework with a specified topology; it was clear to these authors that the general results mentioned above only refer to regular configurations and that ad hoc investigations are required in the singular ones. The study of singular configurations was inaugurated by Roth (1981), who noticed the link between infinitesimal rigidity and the possibility of equilibrating any applied load in the initial configuration by means of internal forces. He also referred to the rank of the equilibrium matrix as the "rigidity predictor" which one should look at in any circumstance. Most of this paper dealt with assemblies in m-dimensional space R^m but, with specific reference to R^3, Roth discussed the risks involved in using the formula $b=3n-6$ as a test for rigidity. He did not get as far as (2.17), which incidentally would have solved the problem entirely.

Connelly (1982) introduced "energy functions", obtained by adding up the product of the bar tension and the square of the length of some particular members, to demonstrate various theorems on the rigidity of frameworks. All these theorems are based on the idea that all assemblies made out of rods, struts and cables (the last two are members that can be subjected to compression or tension only, respectively) must be selfstressable in order to be rigid. Conditions relating the rigidity of assemblies consisting of cable segments and rods to that of ordinary frameworks are discussed by Roth & Whiteley (1981).

Infinitesimal mechanisms were referred to as "shaky structures" by Wunderlich (1982) and Wegner (1984). Consider a framework which satisfies the topological test described above but which is not rigid; Wunderlich showed that if the framework is an infinitesimal mechanism its deformability survives any linear transformation of the set of its nodal coordinates. "Shakyness is a projective property". But if the framework is a finite

mechanism a linear transformation will in general produce only an infinitesimal mechanism. The paper by Wunderlich is also a wealthy source of references on mechanisms. Wagner (1984) extended to assemblies in R^m the results obtained by Wunderlich in R^2.

Bolker & Roth (1980) and Whiteley (1979, 1982) investigated a class of structures commonly known as bipartite. The nodes of these belong to two disjoint sets and each node of one set is connected by bars to all the nodes of the other set. The first of these papers contains results on the rigidity in R^m of bipartite assemblies with a total number of i and j nodes in the two sets but when the authors built a model of the structure shown in Fig. 2.19 (i=j=4) they were unable to detect the expected number of mechanisms because the 'diagonal' bars touched each other. This led to rather disconcerting forecasts of how the assembly would behave if it was built out of cable segments and rods.

Wunderlich (1965) analysed rigid and deformable configurations of octahedral frameworks of the same type as Bricard's (1897). In a more recent investigation Wunderlich (1976) re-discovered the plane linkages shown in Fig. 2.20. Figure 2.20a shows a bipartite planar framework (i=j=3) with n=i+j=6, b=i×j=9 which satisfies Maxwell's rule but has m=s=1 and is a finite mechanism on account of its particular geometry. The mechanism of Fig. 2.20b is also a bipartite structure with i=j=3 which has the same statical and kinematical features although its outlook is quite different. Wunderlich indicated that these mechanisms certainly have spherical equivalents; it would be useful to know more about them. More examples of three-dimensional kinematically indeterminate frameworks have been presented by Goldberg (1978) and Crapo (1982): see Fig. 2.21.

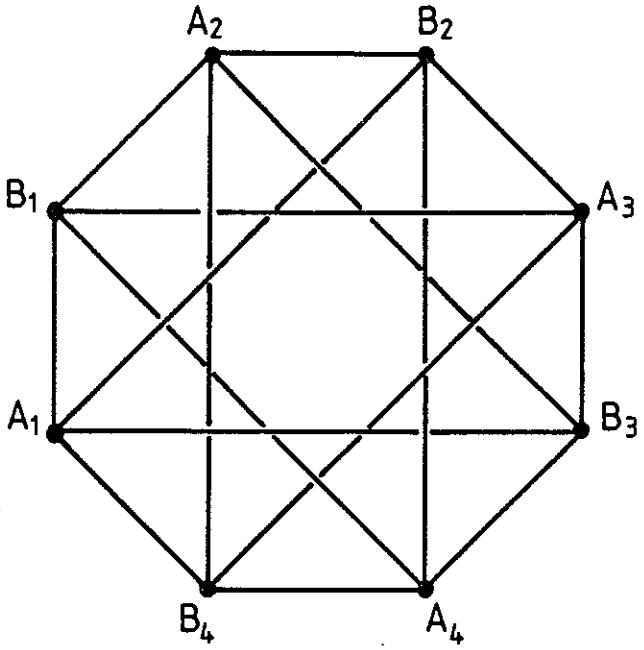

Fig. 2.19 One of the bipartite frameworks studied by Bolker & Roth (1980). All the vertices B_i are in the plane of the paper, vertices A_i lie in a parallel plane above it.

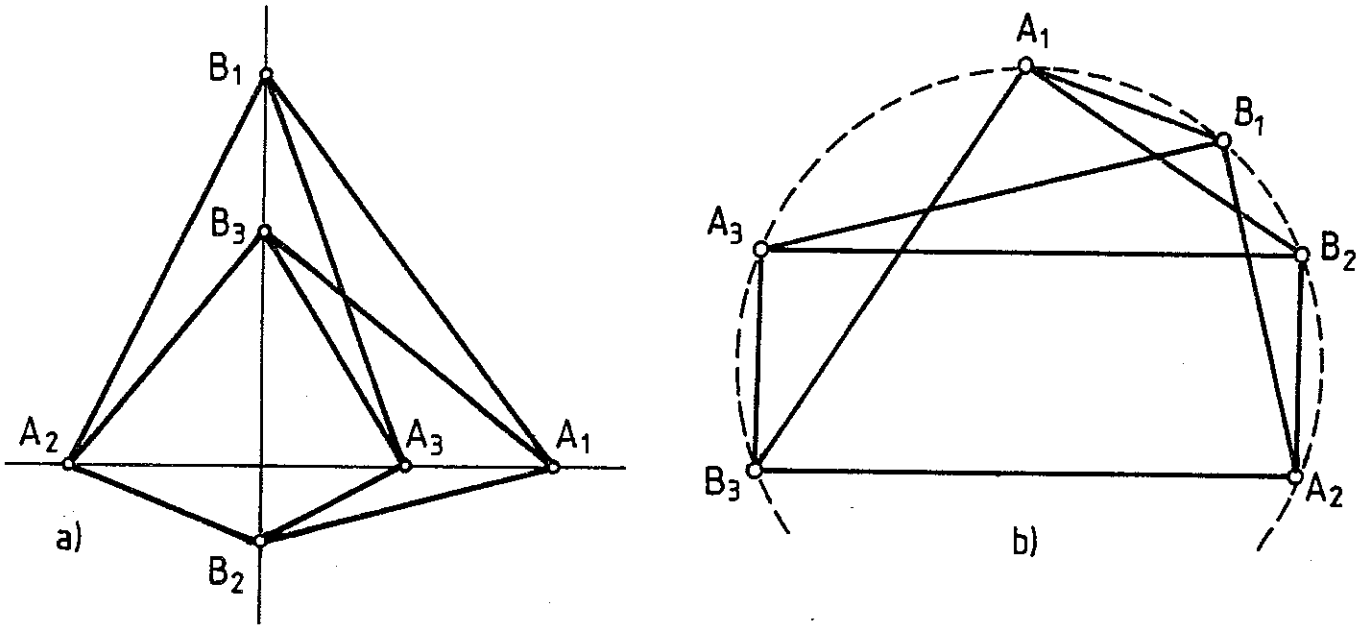

Fig. 2.20 Plane mechanisms first developed by Dixon (see Wunderlich (1976)).
a) Mechanism of the first kind. Points A_1,A_2,A_3 and B_1,B_2,B_3 lie on two orthogonal lines.
b) Mechanism of the second kind. $A_2B_2A_3B_3$ is a rectangle whose circumcircle passes through A_1 and B_1. $A_1B_1B_2A_2$ and $A_1B_1B_3A_3$ are isosceles trapezia.

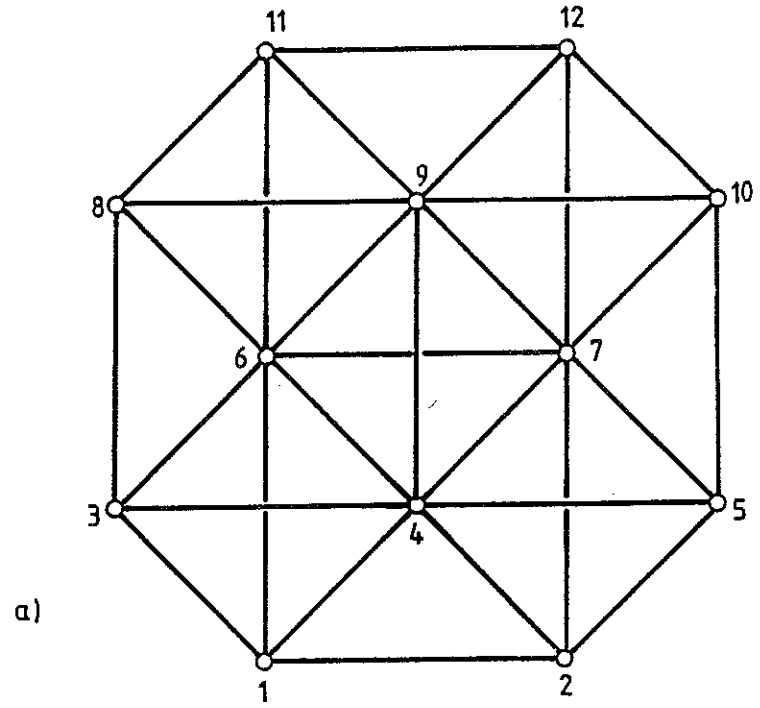

a)

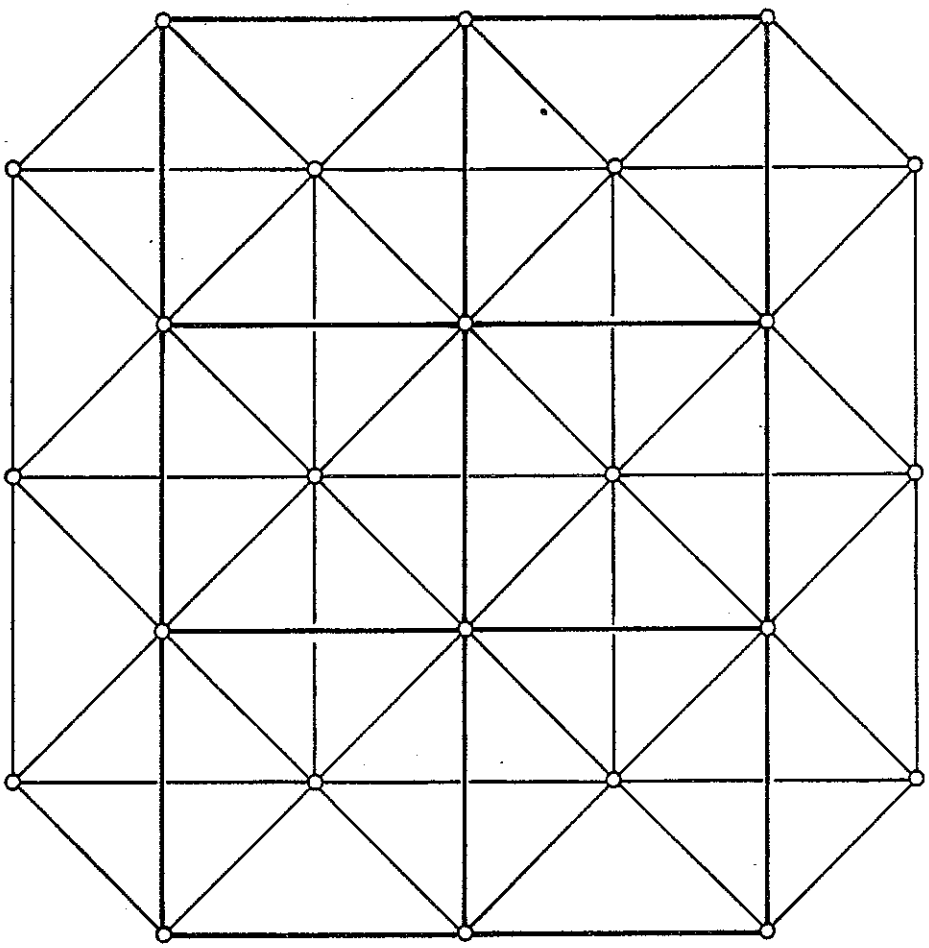

b)

Fig. 2.21 a) shows the simplest version of a category of frameworks called octahedral-tetrahedral trusses by Crapo (1982). They all consist of two square/rectangular grids lying in parallel planes, which are connected to one another by diagonal members. The framework in a) has s=m=1; the one in b) has s=5 and m=1.

3. Study of triangulated hyperbolic paraboloids

This chapter examines the rigidity of a particular class of triangulated hyperbolic paraboloids; and although the initial aim is merely to test some of the methods described in Chapter 2, a number of interesting results are obtained. The layout of the chapter is as follows: in Section 3.1 the geometry is described in detail and the basic relationship between the number of states of selfstress, s, and infinitesimal mechanisms, m, is introduced. The most intuitive method of classification, based on the direct evaluation of s by means of the zero-load test, is employed in Section 3.2. As the objective is to evaluate m and s for a structure with an arbitrary number of sides, two initial attempts which use the standard equilibrium matrices are made in Section 3.3 but without a complete solution emerging. The complete answer is obtained in Section 3.4 by means of a reformulation of the problem in terms of a stress function. Finally, some loose ends are tied up in Section 3.5 where the stiffening effects of pretension are examined; and concluding remarks follow in Section 3.6.

3.1 Geometrical description

The geometry of the triangulated hyperbolic paraboloid which is the subject of the present investigation, see Fig. 3.1, can be described in the following way: start from a twisted quadrangle which projects into a square, divide each of its sides into l parts of equal length and connect corresponding points lying on opposite sides with straight lines. Divide each one of the small quadrangles obtained in this way into two triangles by adding a diagonal (all the diagonals run in the same direction). Each of these 'lines' is a bar of the framework, each connection between different lines is a node; as elsewhere in this dissertation, all the nodes are ideal frictionless spherical hinges. Finally, connect all the nodes lying on the initial quadrangle to a rigid foundation by means of vertical pin-jointed bars, and add three horizontal bars connected to the foundation in order to suppress rigid-body displacements in which the initial quadrangle translates in the x or y directions, or rotates about a vertical axis. The perspective view of Fig. 3.1 shows the whole arrangement and the coordinate system for l=4. For the sake of simplicity it is assumed that the horizontal projection of each quadrangle is

a square with sides of unit length, see Fig. 3.2, and that the vertical projection of any one of the l parts in which the sides of the initial quadrangle has been divided is 1 (therefore in analytical terms: $Z_A=Z_C$, $Z_B=Z_D$, $Z_A-Z_B=1$); more general cases can be treated at the expense only of a more laborious computation of the numerical coefficients than in the present treatment.

This framework is not free in space, and therefore the six degrees of freedom corresponding to rigid-body motions have to be suppressed from the left-hand-side of (2.17). The complete Maxwell's rule for space frameworks constrained to a rigid foundation is:

$$3n-b=m-s \tag{3.1}$$

where all the symbols have their usual meanings. The hyperbolic paraboloid described above has:

$$\begin{aligned} &\text{No. of nodes:} \quad n=(l+1)^2 \\ &\text{No. of bars:} \quad b=2l(l+1)+l^2+(4l+3) \end{aligned} \tag{3.2}$$

The three elements of the lower sum refer to the number of sides of the quadrangles, their diagonals and connections to the foundation, respectively. Substitution of these quantities into (3.1) gives: $m-s=0$; therefore the frameworks of the type shown in Fig 3.1 are either statically and kinematically determinate or indeterminate, with s=m.

The set of nodal equilibrium equations yields a square equilibrium matrix of dimension 3n=b; details on it are given in Section 3.3. Other equilibrium matrices of smaller dimension are assembled in Sections 3.3 and 3.4; these are obtained by means of equivalent approaches in which about 1/3, in the first attempt, and then 2/3 of the global equilibrium requirements are satisfied automatically as a result of cunning formulations of the problem that take advantage of the lack of applied forces. Notice that in all formulations the equilibrium matrices assembled in this chapter are square in consequence of the algebraic relationship m=s.

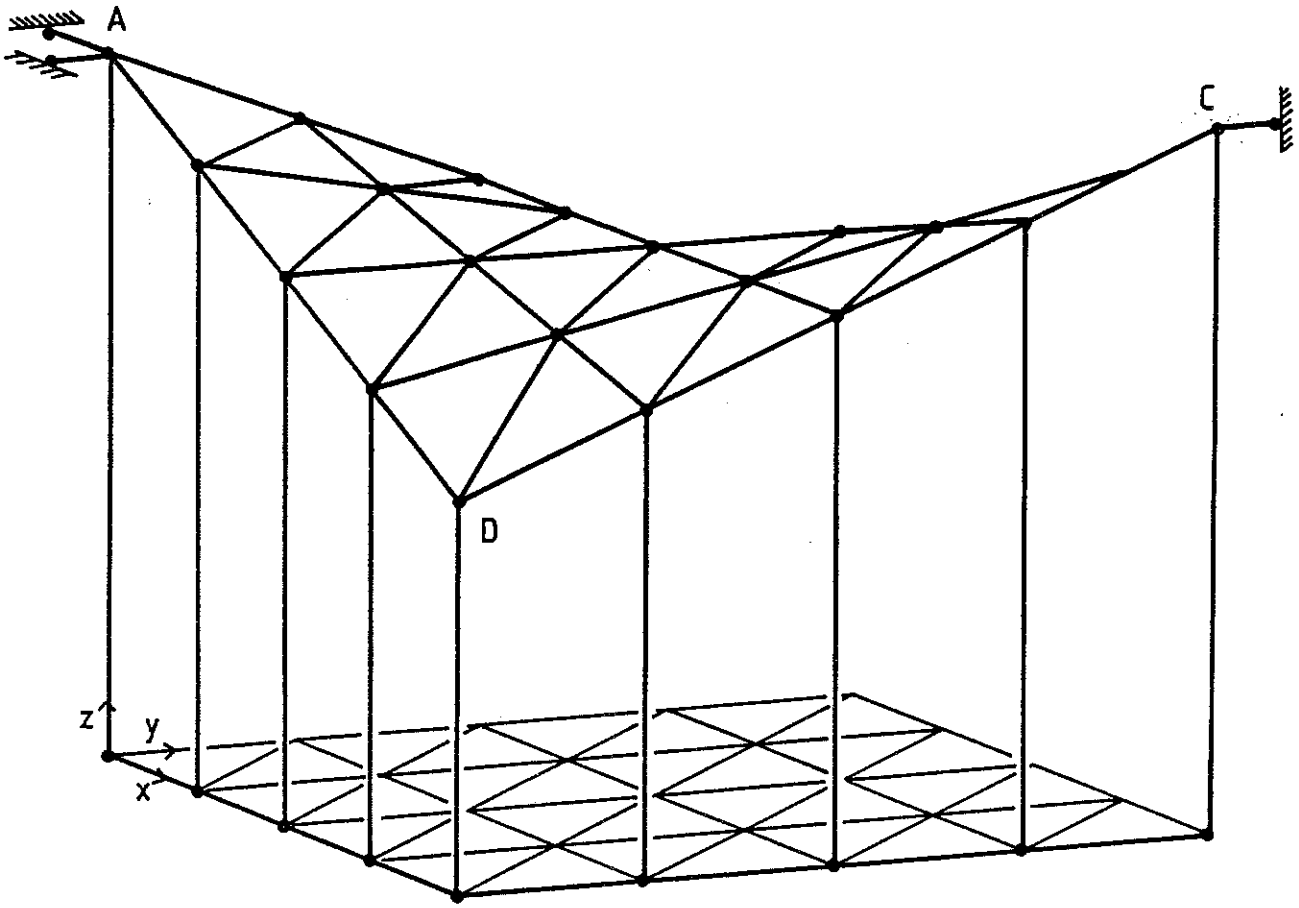

Fig. 3.1 Triangulated hyperbolic paraboloid studied in Chapter 3. For the sake of definiteness, the number of bays has been set equal to four (l=4). Some of the bars are not shown.

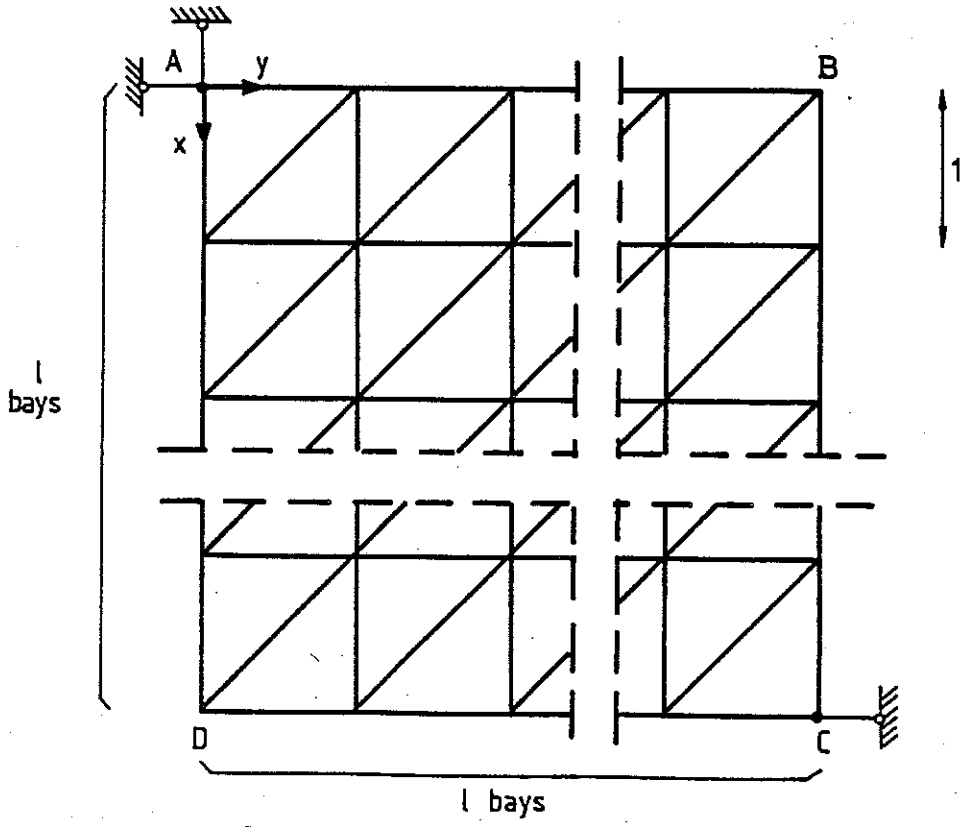

Fig. 3.2 General layout of the triangulated hyperbolic paraboloid. Plan view.

3.2 Direct evaluation of states of selfstress

In this section the number of states of selfstress (and hence mechanisms) and the bar tensions corresponding to each independent state are evaluated for hyperbolic paraboloids having l=1,...,7. This is done by use of the zero-load test briefly described in Section 2.1. The method consists of an exhaustive investigation of the admissible states of selfstress, one-at-a time; although this may seem to involve a fair amount of guesswork for an inexperienced user, it can be systematized in such a way as to produce reliable answers. The procedure is as follows: assign, say, a tension of one unit to one particular bar of the framework and evaluate the tensions in the other bars so that no external forces are required to satisfy the equilibrium equations of the nodes. This procedure may reach stages where the tensions in some bars are not uniquely determined, in which case the various alternatives have to be developed separately: choices that lead to the violation of one equilibrium equation can be ruled out, while the others produce independent states of selfstress. Eventually all the independent states of selfstress of the framework have been obtained; notice that the technique becomes impracticable in the case of large and complex frameworks because these may have several of the 'branching' points described above. It is obvious therefore that the evaluation of independent states of selfstress can be simplified by the introduction of some general 'rules'. For hyperbolic paraboloids of the type described in Section 3.1, these are the following:

(i) Equilibrium of the corners labelled A and C in Figs 3.1 and 3.2 can be only satisfied by having null tensions in the bars connected to them.

(ii) Any state of selfstress requires non-zero tension in at least one of the diagonal bars, otherwise all the remaining tensions would also vanish.

(iii) Equilibrium of any internal joint in the direction perpendicular to the plane containing the sides of the quadrangles requires that, if t_1 and t_2 are the tensions in the diagonal bars connected to that joint, $t_1=-t_2$. (This last observation enables one to carry out the entire study on an equivalent plane system).

Hyperbolic paraboloids with 1,2,...,7 sides were examined. No state of selfstress was found for l=1,2,3,5,7. Two were found in the case l=4 (see Fig. 3.3 for details; notice that both states of selfstress are symmetrical relative to the vertical plane passing through the corners B and D, and they

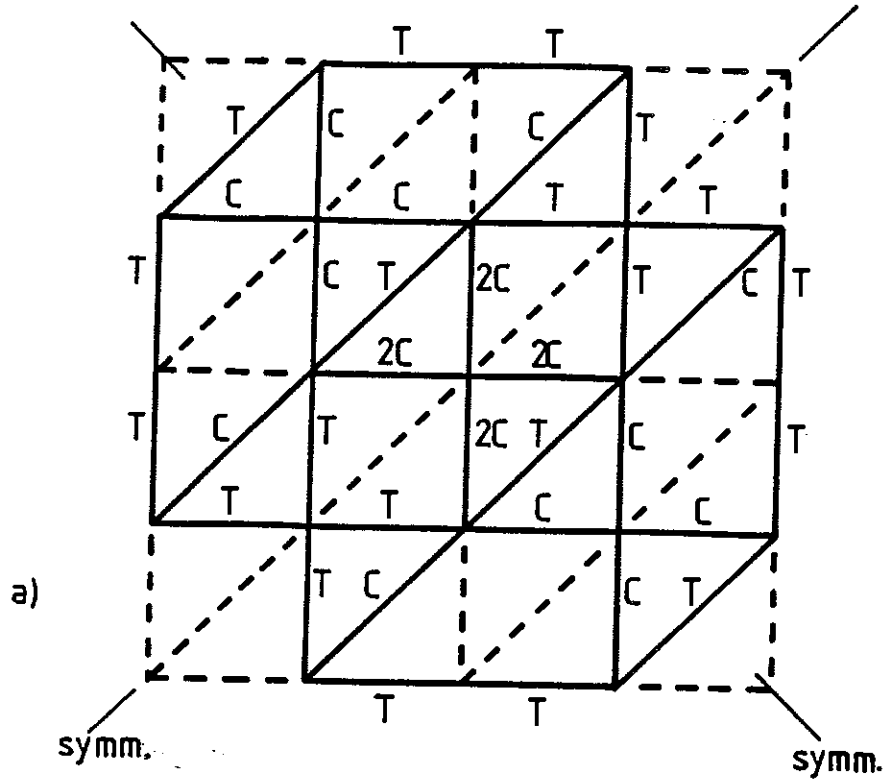

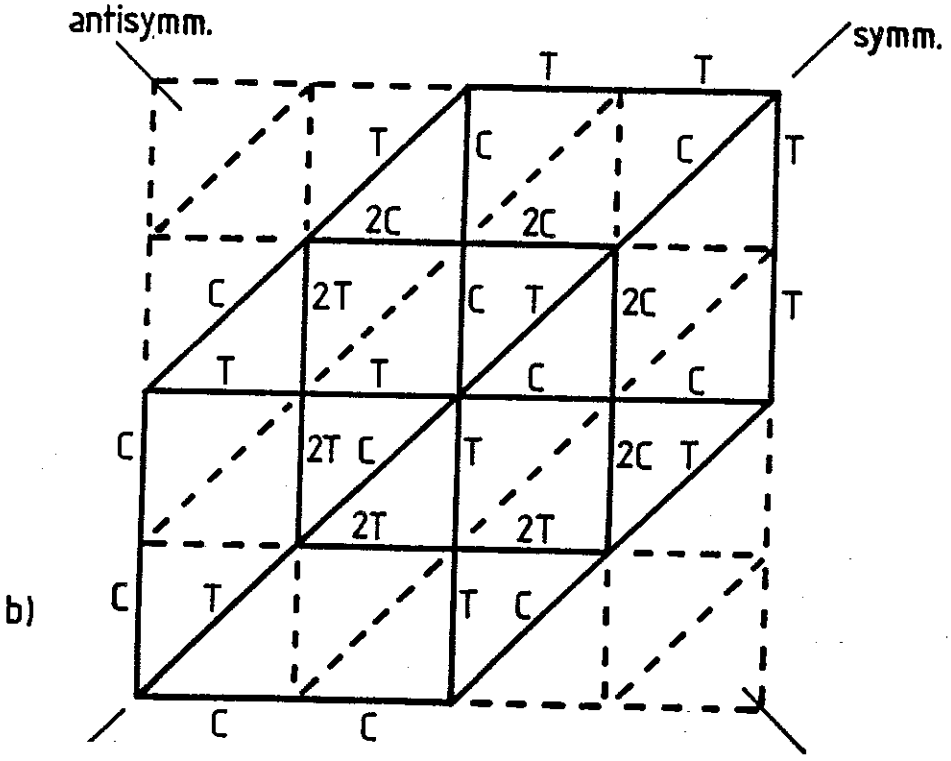

Fig. 3.3 States of selfstress of triangulated hyperbolic paraboloids with four sides (l=4). Solid lines represent bars carrying non-zero tension; T and C represent unit tensile and compressive tension coefficients, respectively. Each state of selfstress is associated to an infinitesimal mechanism; and the stress function Φ corresponding to a given state of selfstress gives the vertical components of nodal displacements.

are symmetrical and anti-symmetrical - respectively - relative to the plane through A and C) and four for l=6 (see Fig. 3.4; these states of selfstress also satisfy various properties of symmetry/anti-symmetry). It can be easily verified that all the states of selfstress satisfy the conditions (i), (ii) and (iii) above. Physical models were built from plastic rods and rubber joints for l=2 and l=4: the smaller one was rigid while the larger one displayed two mechanisms, with the same properties of symmetry and anti-symmetry of the states of selfstress shown in Fig. 3.3. The results obtained are summarized in Table 3.1.

Hyperboloids with a larger number of sides could not be examined because it was difficult to find several independent sets of tensions; this would be tricky even in frameworks not as complicated as the present ones. In general one of the disadvantages of the zero-load method is that, if s_1 independent states of selfstress have been determined, s_1 is a lower bound for s; on the other hand s_2=b is definitely an upper bound, but it is clearly a rather unsatisfactory one. In the present case the observations made earlier enable one to reduce s_2 to about 2b/3, but this is still high.

Another disadvantage of this method is that when s independent states of selfstress have been found the only information available on the inextensional (internal) mechanisms is their number, which leaves their details still to be determined.

l	1	2	3	4	5	6	7
s	0	0	0	2	0	4	0

Table 3.1 Dimensions of hyperbolic paraboloids, in terms of the number l of sides, against the number of states of selfstress s. These results have been obtained by use of the zero-load method.

3.3 Equilibrium matrices

Although in Section 3.1 the total number (=$3(l+1)^2$) of rows and columns of the complete equilibrium matrix was evaluated, here the (unknown) tensions in all the bars connecting the framework to the foundation will be dropped, together with the corresponding equations, in order to reduce the size of the equilibrium matrix with no loss of generality. The idea here is that the

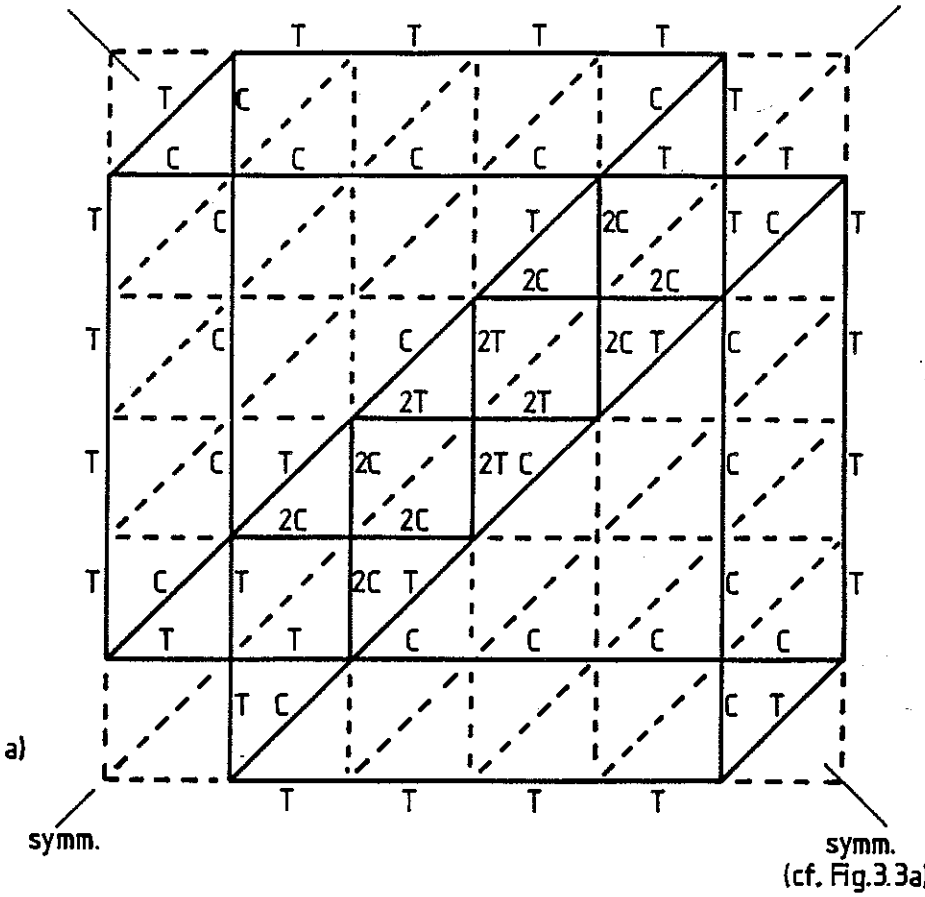

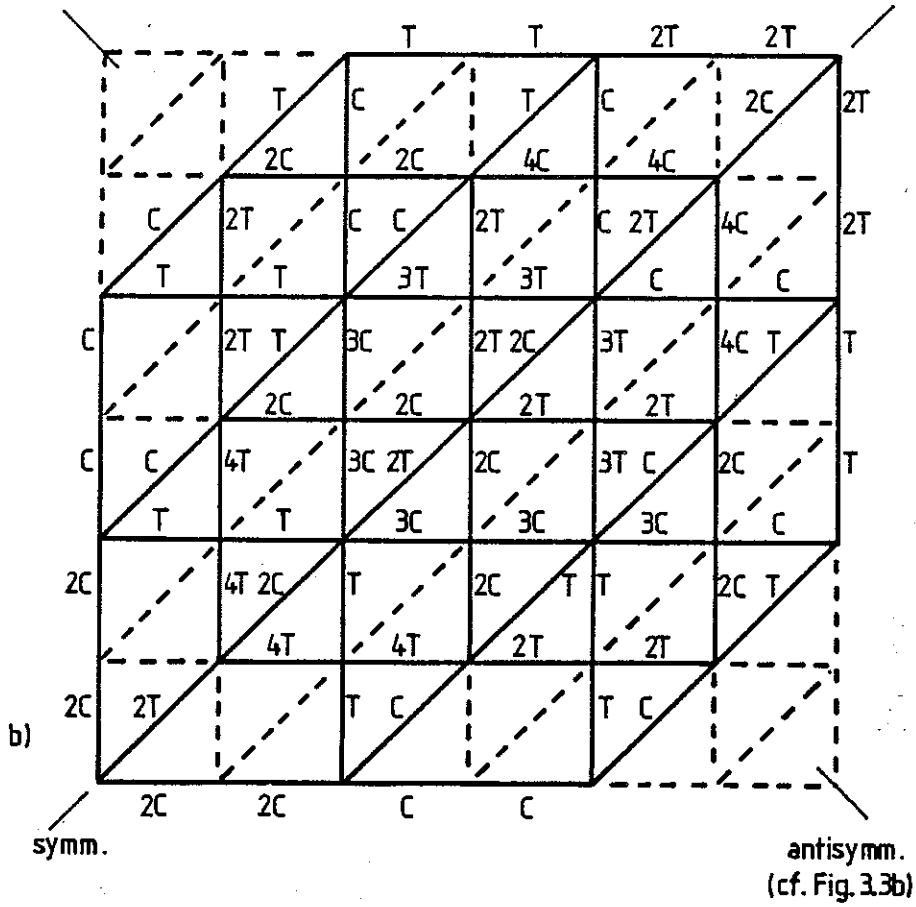

Figs 3.4a,b States of selfstress no. 1 and 2 of triangulated hyperbolic paraboloids with six sides (l=6). See caption of Fig. 3.3.

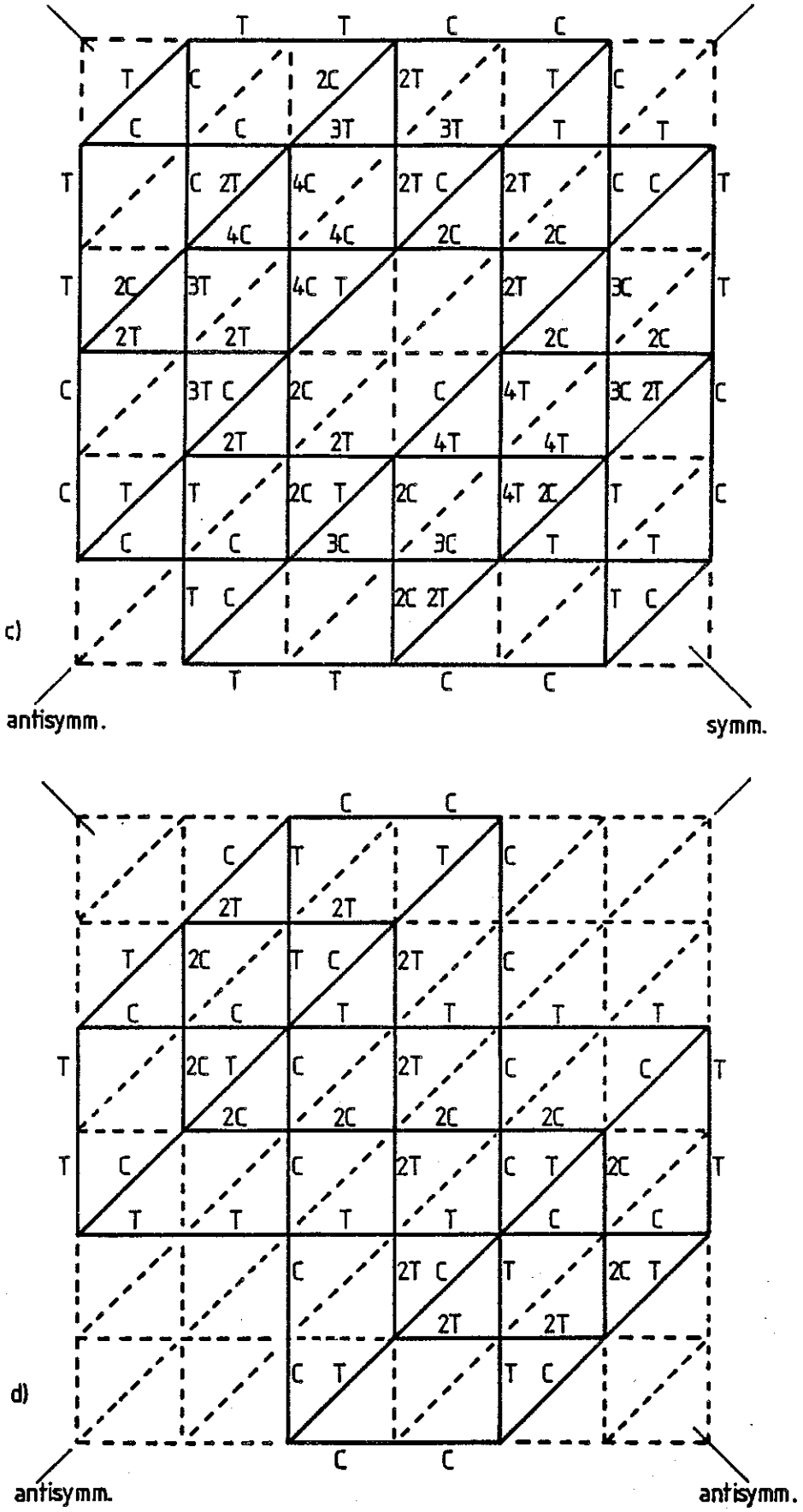

Figs 3.4c,d States of selfstress no. 3 and 4.

vertical equilibrium of the upper node of each vertical support determines its tension, once the tensions in the triangulated network have been decided; the tensions in the three horizontal supports of nodes A and C have to be zero, of course, for the overall equilibrium. In this way, the number of unknown bar tensions is reduced to only the first two terms of the sum for b in (3.2), and therefore $b=3l^2+2l$. The number of equilibrium equations to be considered is likewise reduced: equilibrium of the boundary nodes in the vertical direction can be satisfied at a later stage, and the equilibrium equation of node C in the y direction and both equations of node A in the horizontal plane are all automatically satisfied. Exactly $3l^2+2l$ equations are left to give a square equilibrium matrix.

The first step is now the choice of convenient numbering systems for the nodes and bars of the hyperbolic paraboloid; the most promising results have been obtained using the schemes illustrated in Fig. 3.5. In matrix form, and having denoted by $\{t/l\}$ the vector of dimension $3l^2+2l$ that contains the bar tension coefficients in the order specified in Fig. 3.5, the equilibrium equations are:

$$
\begin{array}{c}
\begin{array}{cc} & \begin{array}{cccccccc} 3l+1 & 3l+1 & & 3l+1 & 3l+1 & & 3l+1 & 3l+1 \quad 1 \end{array} \\
\begin{array}{c} 2l \\ 3l+1 \\ \\ 3l+1 \\ \\ 3l+1 \\ 2l+1 \end{array} & \left[\begin{array}{cccccccc}
L_1 & & & & & & & \\
N_2 & L_2 & & & & & & \\
 & \ddots & \ddots & & & & & \\
 & & & N_i & L_i & & & \\
 & & & & \ddots & \ddots & & \\
 & & & & & & N_1 & L_1 \\
 & & & & & & N_{l+1} & L_{l+1}
\end{array}\right]
\end{array}
\begin{array}{l} \{t/l\}=\{0\} \end{array}
\end{array}
\qquad (3.3)
$$

where all the entries of the submatrices L_l, N_{l+1}, L_{l+1} are either 0 or ± 1; but some of the entries of N_i, L_i $(i=2,\ldots,l)$ are not integer numbers as they depend on the relative inclination of the bars. The vector on the right-hand-side is zero as no external forces are considered. The system of equations (3.3) admits non-trivial solutions only if the equilibrium matrix does not have full rank; in particular the number of independent solutions, i.e. states of selfstress, is given by $s=3l^2+2l-\text{rank}$. This point will be discussed extensively in Chapter 4.

The structure of the matrix in (3.3) is such that the extended Laplace rule (Aitken, 1958) is the most promising procedure to obtain a closed-form expression of its determinant; indeed this technique has been successfully employed by Tarnai (1980a) in a case that has some similarities with the present one. But the expected answer, i.e. a formula giving the value of the determinant as a product of l+1 determinants which are simple to evaluate, could not be obtained in spite of several attempts to reorder rows and columns of the equilibrium matrix; the main difficulty is due to the non-squareness of submatrices L_1, N_{l+1} and L_{l+1}.

The third observation in Section 3.2 can be used to reduce further the number of unknown quantities and, at the same time, simplify the equilibrium matrix. Assume that the tensions in all of the diagonal bars can be obtained from the 2l-1 values indicated in Fig. 3.6 by using (iii): the total number of unknowns is in this way reduced to $2l^2+4l-1$ and each node is automatically in equilibrium in the direction of the local normal; in this way the non-integer entries disappear from (3.3). A general procedure for the transformation of the corresponding equilibrium matrix into a diagonal matrix has been devised; and the matrix rank is equal to the number of non-vanishing diagonal coefficients. Further details of this approach will not be given here because a different and more complete solution which leads to the evaluation of the states of selfstress and also of the infinitesimal mechanisms will be developed in the next section.

3.4 Stress function approach

A third formulation of the equilibrium approach which uses a stress function as the direct unknown of the problem (this function is entirely defined by the values it assumes at each joint) reduces the number of equations to be considered to the number of joints. It is well known (Den Hartog, 1952) that the use of a stress function can greatly simplify the analysis of a plane continuum by satisfying automatically the equations of equilibrium, and hence leaving only a (bi-harmonic) equation of compatibility to deal with.

In the context of a purely membranal formulation, a similar approach has been followed by Flugge (1973) to obtain solutions in closed form for shell structures of several shapes. This approach is based on the observation (Flugge, 1973) that the introduction of a stress function $\Phi=\Phi(x,y)$ such that:

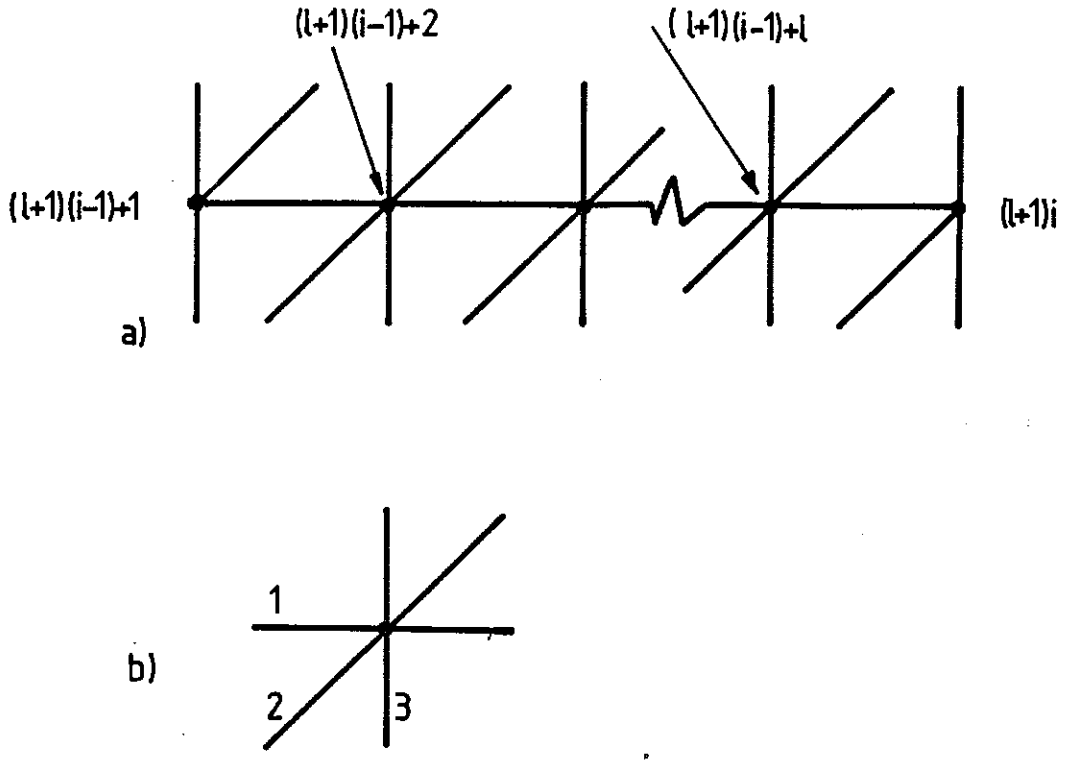

Fig. 3.5 a) View of 'row i' of Fig. 3.2, together with the node numbers. The numbering system of the bars follows from it: in each node the bars are taken in the order shown in b). These numbering systems lead to the equilibrium matrix in (3.3).

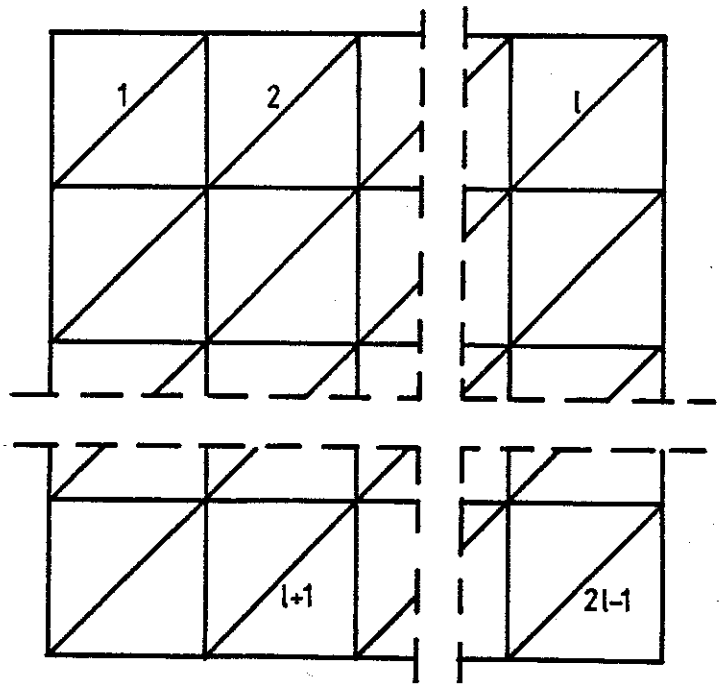

Fig. 3.6 Modified numbering system for the diagonal bars, which leads to the equilibrium matrix in 2D described in Section 3.3.

$$\bar{N}_x=\partial^2\Phi/\partial y^2 \qquad \bar{N}_y=\partial^2\Phi/\partial x^2 \qquad \bar{N}_{xy}=-\partial^2\Phi/\partial x\partial y \tag{3.4}$$

where $\bar{N}_x$, $\bar{N}_y$, $\bar{N}_{xy}$ are the components in the horizontal x-y plane of the stress resultants N_x, N_y, N_{xy}, automatically satisfies equilibrium in the x and y directions when no horizontal components of load are applied. Substitution of (3.4) into the system of three differential equations of equilibrium satisfies identically two of them; this leaves only one differential equation in Φ to be solved.

A second crucial point (Calladine, 1977) is the formal analogy between the equilibrium and compatibility equations of a thin, shallow shell; one of the interesting points of this analogy is that the stress function $\Phi(X,Y)$ and the vertical component of displacement $z(X,Y)$ satisfy formally identical differential equations: therefore one function can describe them both provided the boundary conditions are the same.[1]

Aiming at a reformulation of equations (3.4) suitable for a triangulated surface rather than a smooth shell structure, notice that an acceptable stress function must lead to stress resultants which are constant along any bar and equal to zero corresponding to empty spaces. The horizontal component of the tension in bar i is given by the change of the slope of $\Phi(X,Y)$ from one side to the other of the bar, in the direction normal to the bar. It is easy to verify that a stress function Φ made up of triangular patches, the horizontal projection of which coincides with the horizontal projection of the framework, satisfies the above requirements: this function defines for each bar a constant horizontal component of tension, equal to the change of slope across the crease. No tension components exist elsewhere because there are no other changes of slope. Φ is completely defined by the vertical coordinates of its vertices; its values at the boundary nodes must be such that there is zero stress in the 'empty space' around the assembly and in the three horizontal restraints of nodes A and C (see Fig. 3.2). This last condition follows from considerations of external equilibrium of the assembly. In conclusion, from the point of view of equilibrium, Φ can only vary linearly outside the assembly. But the analogy described above can be fully exploited only if Φ satisfies the boundary conditions on the vertical component of

[1] Notice that, as elsewhere in this dissertation, X, Y, Z denote the cartesian coordinates of a node; while x, y, z denote either its cartesian components of displacement or the coordinate axes.

displacement z. Therefore it is best to choose $\Phi(0,Y)=\Phi(X,0)=\Phi(l+1,Y)=\Phi(X,l+1)=0$, as in Fig. 3.7. The horizontal component of tension in each bar of a triangulated paraboloid of arbitrary l can be derived from Φ, and the coefficients that multiply the four values of Φ relevant to each bar are displayed in Fig. 3.8.

Does the relationship between stress function and bar tensions according to Fig. 3.8, lead to completely automatic satisfaction of the equilibrium of each node in the x and y directions? Using from now on the numbering system defined in Fig. 3.9, the equilibrium equation of an arbitrary (internal) node i, in the x direction, is:

$$-(t_1)_{xy}-(t_2)_{xy}/\sqrt{2}+(t_4)_{xy}+(t_5)_{xy}/\sqrt{2}=0 \qquad (3.5)$$

Substitute for the tensions their expressions in terms of Φ to obtain:

$$\begin{aligned}&-(-\Phi_{i-l-1}+\Phi_{i-l}-\Phi_{i}+\Phi_{i-1})-(\sqrt{2}\Phi_{i-l-1}-\sqrt{2}\Phi_{i-l}+\sqrt{2}\Phi_{i+1}-\sqrt{2}\Phi_{i})/\sqrt{2}+\\&+(-\Phi_{i}+\Phi_{i+1}-\Phi_{i+l+1}+\Phi_{i+l})+(\sqrt{2}\Phi_{i-1}-\sqrt{2}\Phi_{i}+\sqrt{2}\Phi_{i+l+1}-\sqrt{2}\Phi_{i+l})/\sqrt{2}=0\end{aligned} \qquad (3.6)$$

This equation is identically satisfied for any Φ; and the same is true in the y direction. This proves that the equilibrium in the horizontal plane is automatically satisfied when the bar tensions are derived from Φ in the way described. The second reference to shell theory, namely the analogy between Φ and z, will be proved in Section 3.5.

It now remains to determine what conditions on Φ are imposed by the conditions of equilibrium in the vertical direction. The equation of equilibrium of node i, see Fig. 3.9, is:

$$\sum_{j=1}^{6}(t_j)_z=p_i \qquad (3.7)$$

where the vertical external load p_i (=0) is positive if downwards. Multiplying the ratio between the vertical and horizontal projections of each bar by the coefficients of Fig. 3.8 one obtains the vertical components of tension in terms of Φ; and substitution into (3.7) gives:

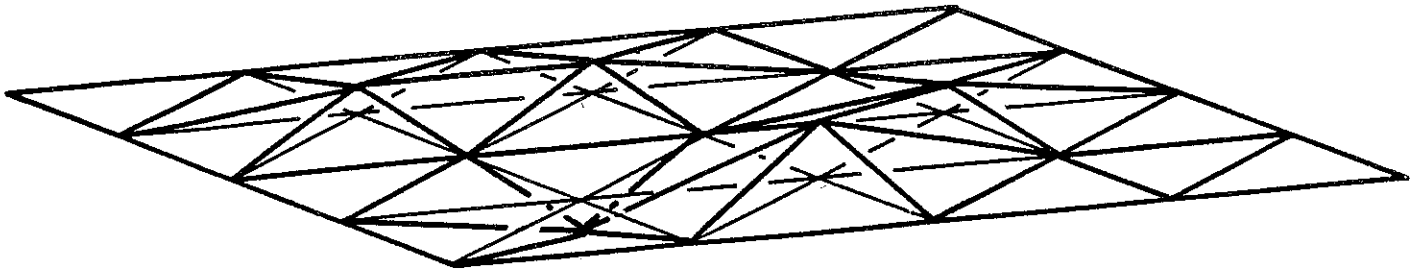

Fig. 3.7 Example of a stress function Φ of the type described in Section 3.4, for the hyperbolic paraboloid shown in Fig. 3.1. Only the nine values of Φ corresponding to the inner nodes are needed to define such a stress function. Starting from the back, and proceeding from left to right, the values of Φ are: $\Phi_1=\Phi_2=1$, $\Phi_3=\Phi_4=\Phi_5=0$, $\Phi_6=1$, $\Phi_7=-1$, $\Phi_8=2$ and $\Phi_9=0$.

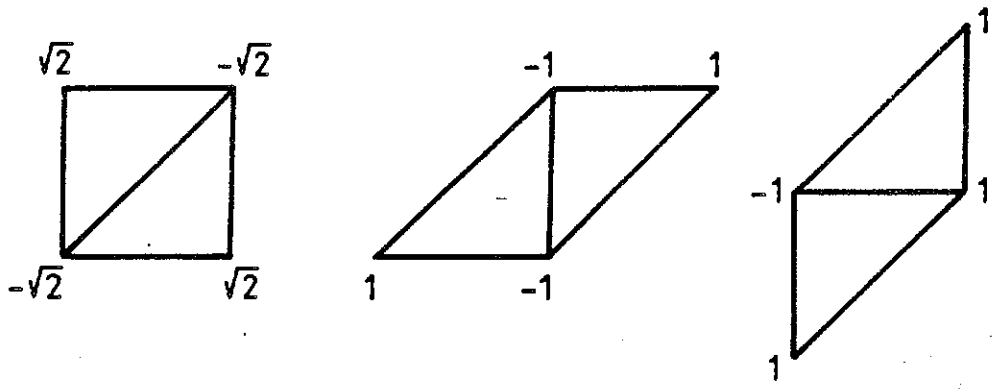

Fig. 3.8 Numerical coefficients that multiply the values of the stress function, in order to define the horizontal component of tension in a bar.

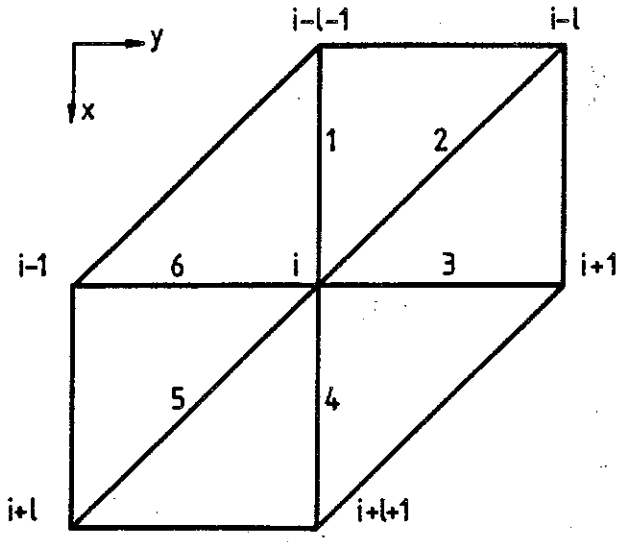

Fig. 3.9 Bar and node numbering systems used to set up the equations of equilibrium (3.5)-(3.8).

$$(2/l)(\Phi_{i-l-1}-\Phi_{i-l}+\Phi_{i-1}-2\Phi_{i}+\Phi_{i+1}-\Phi_{i+l}+\Phi_{i+l+1})=0 \qquad (3.8)$$

Only the internal nodes of the triangulated surface need to be considered, see Section 3.3; their total number is $(l-1)^2$, equal to the number of unknown parameters that define Φ. The system of equilibrium equations is in matrix form:

$$\underbrace{\begin{bmatrix} A & B & & & \\ B^TA & B & & & \\ & \ddots & \ddots & & \\ & & B^TA & B & \\ & & & B^TA & \end{bmatrix}}_{(l-1)^2} \cdot \{\Phi\}=\{0\} \qquad (3.9)$$

where:

$$A=\underbrace{\begin{bmatrix} -2 & 1 & & & \\ 1 & -2 & 1 & & \\ & \ddots & \ddots & \ddots & \\ & & 1 & -2 & 1 \\ & & & 1 & -2 \end{bmatrix}}_{l-1} \qquad B=\underbrace{\begin{bmatrix} 1 & & & \\ -1 & 1 & & \\ & \ddots & \ddots & \\ & & -1 & 1 \\ & & & -1 & 1 \end{bmatrix}}_{l-1} \Big\} l-1$$

and $\{\Phi\}$ is the vector containing the unknowns of this formulation: $\Phi_1,\Phi_2,\ldots,\Phi_{(l-1)^2}$. Notice that the equilibrium matrix is symmetrical, and therefore it is identical to its transpose, the compatibility matrix. This property is a condensed proof of the analogy between Φ and z.

3.4.1 Rank of equilibrium matrix

The rank of the equilibrium matrix (3.9) will indicate the number of non-trivial, independent solutions of the system of equations. Its computation is straightforward after performing a series of operations that, without altering the value of the rank, transform the matrix into the form:

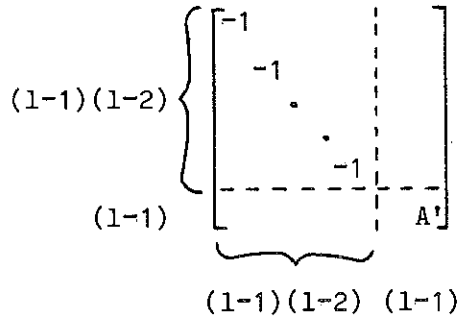

(3.10)

In fact,

$$\text{rank}=(l-1)(l-2)+\text{rank}(A') \tag{3.11}$$

The transformation of the matrix from the form (3.9) to (3.10) is done as follows. An important property of determinants (Aitken, 1958) allows linear transformation of rows: "The determinant of a matrix is unaltered when to any row is added a constant multiple of any other row". For the purposes of the following operations, each group of (l-1) rows, corresponding to one row of submatrices in (3.9), is referred to as a segment of the matrix; the whole matrix is therefore divided into (l-1) segments. Notice that the operation of addition of rows occupying corresponding positions in two segments will be referred to as addition of the two segments. Starting from (3.9) proceed as follows:

(0) Add to each segment all the following ones.

(1) Operations within segment 1: add row 1 to row 2, add the new row 2 to row 3,... Add segment 1 to segment 2. Transform segment 2 by subtracting rows 2,3,... (l-1) of segment 1 from rows 1,... (l-2) of segment 2.

(i) Operations within segment i: add row 1 to row 2, add the new row 2 to row 3,... Add segment i to segment (i+1). Transform segment (i+1) by subtracting rows 2,3,... (l-1) of segment i from rows 1,... (l-2) of segment (i+1).

(l-2) Follows from (i).

The equilibrium matrix is now in the form (3.10) but A' has different expressions in the two cases:

$$A' = \begin{bmatrix} -2 & 2 & -2 & 2 & . & . \\ 0 & -2 & 2 & -2 & . & . \\ 2 & 0 & -2 & 2 & . & . \\ -2 & 2 & 0 & -2 & . & . \\ . & . & . & . & . & . \\ . & . & . & . & . & . \end{bmatrix} \qquad \text{for } \underline{1 \text{ odd}}$$

$$A' = \begin{bmatrix} -2 & 2 & -2 & 2 & . & . \\ 2 & -2 & 2 & -2 & . & . \\ -2 & 2 & -2 & 2 & . & . \\ 2 & -2 & 2 & -2 & . & . \\ . & . & . & . & . & . \\ . & . & . & . & . & . \end{bmatrix} \qquad \text{for } \underline{1 \text{ even}}$$

The determinant of the upper matrix is not zero, hence the matrix has rank (l-1). The rank of the lower matrix is clearly 1, independently of l. The last step of the transformation that diagonalizes the equilibrium matrix is therefore:

(l-1) Operations within segment (l-1): add row 1 to rows 2,4,6,... and subtract row 1 from rows 3,5,... Substitute these results into (3.11) to obtain:

$$\text{rank} = \begin{cases} (l-1)^2 & \text{for } \underline{1 \text{ odd}} \\ (l-1)(l-2)+1 & \text{for } \underline{1 \text{ even}} \end{cases} \qquad (3.12)$$

This is the main result of the whole chapter, and it agrees with the special results presented in Table 3.1.

The hyperbolic paraboloid described in Section 3.1 is statically and kinematically determinate if the number of its sides is odd; but <u>it is indeterminate with s=m=l-2 for l even</u>.

3.4.2 States of selfstress

The remaining part of this section and the next complete the investigation of hyperbolic paraboloids with an <u>even</u> number of sides.

The first point is obviously the evaluation of l-2 vectors $\{\Phi\}$ which satisfy (3.9) and define the independent states of selfstress; although a more efficient way of solving the same problem will be described in Chapter 4, the following property of matrices (Aitken, 1958) can provide a solution in 'closed form': "Any permutation of the rows of a matrix can be done by premultiplying it by a matrix derived from the unit matrix by the same permutation of rows". And this can be generalized to include the addition or subtraction of rows. Let I_i, i=(0,1,...,l-1), be the matrix obtained by operating the transformation (i), defined in Section 3.4.1, on a unit matrix of dimension $(l-1)^2$. The original equilibrium matrix can be diagonalized by premultiplying it by $I_{l-1}I_{l-2}...I_1I_0$. In particular, the last l-2 rows of the equilibrium matrix are transformed into null rows and the entries of the last l-2 rows of the product $I_{l-1}...I_0$ define independent linear combinations of columns of (3.9) equal to {0}. Therefore they are the required states of selfstress expressed in terms of Φ. For l=4,6 this method re-obtains the states of selfstress which are shown in Figs 3.3 and 3.4.

3.5 Analogy between Φ and z. Computation of mechanisms

Simple considerations of geometrical compatibility can be employed to prove the analogy between the stress function Φ introduced in Section 3.4 and the vertical components of displacement z (as elsewhere in this dissertation, the nodal displacements will be assumed to be small). For the sake of simplicity the following proof only considers inextensional deformations of the framework.

Let z_i be the vertical component of displacement of node i, due to an inextensional distortion in which each triangle translates and rotates from its initial position. The obvious compatibility requirement is that the six triangles that meet in node i should fit together, therefore the following vector equation has to be satisfied:

$$\sum_{j=1}^{6} \{r_j\}=\{0\} \qquad (3.13)$$

where $\{r_j\}$ is the vector that represents the relative rotation of triangles j+1 and j. Equation (3.13) can be examined in scalar terms and one notices

that the horizontal components of the $\{r_j\}$'s automatically satisfy it. The only effective condition imposed on the deformation is therefore:

$$\sum_{j=1}^{6} (\{r_j\})_z = 0 \qquad (3.14)$$

The components of $\{r_j\}$ can be computed from z. The horizontal component of the relative rotation between two adjacent triangles, due to z, is essentially the same thing as the angle between two triangular patches defining Φ that was computed in Section 3.4 (see also Fig. 3.8). The horizontal components are easily transformed into the vertical ones, required for (3.14), by multiplying each horizontal component by the ratio of the vertical and horizontal components of length of the edge in common. The compatibility equation is therefore:

$$(2/l)(z_{i-l-1} - z_{i-l} + z_{i-1} - 2z_i + z_{i+1} - z_{i+l} + z_{i+l+1}) = 0 \qquad (3.15)$$

Equations (3.8) and (3.15) are formally equivalent; this proves the analogy. The system of equations (3.9) can be now regarded as a system of compatibility equations and the states of selfstress obtained in Section 3.4.2 are also vertical components of displacement of inextensional mechanisms.

It will be shown later on, see Chapter 4, that the scalar products of the vertical forces needed to equilibrate each joint of a statically and kinematically indeterminate framework, once a state of selfstress has been imposed and all the joints have been displaced by quantities proportional to a mechanism, and the various mechanisms are a meaningful way of classifying the mechanisms. Using the above results these scalar products have been computed for hyperbolic paraboloids with l=4,6. It turns out that the products never vanish and the 'sign' of the states of selfstress can be chosen in such a way that these products are positive; this means - as it will be shown - that these structures are only free to undergo rather small inextensional distortions. There is no reason why the same should not happen for larger number of sides.

3.6 Conclusions

The triangulated hyperbolic paraboloids of Fig. 3.1 are statically and kinematically determinate frameworks if their number of sides, l, is odd. But they are ill-conditioned frameworks with an equal number of infinitesimal mechanisms and statical redundancies, linearly growing with the number of sides, if l is even.

The states of selfstress/inextensional mechanisms found in two of the examples studied in this chapter satisfy simple properties of symmetry/anti-symmmetry relative to the vertical planes passing through the corners of the hyperboloids; yet no general rules which are valid for an arbitrary value of l have been found.

Structures consisting of a number of interconnected hyperbolic paraboloidal sheets may also show similar patterns of behaviour; this is a problem open for investigation. A large number of single layer triangulated hyperbolic paraboloids has been built in recent years (Makowski, 1981) some of which are very similar in layout to Fig. 3.1. The conclusions reached in this chapter may be relevant to their behaviour.

4. Structural mechanics of frameworks

This chapter deals with purely 'geometrical' analyses of pin-jointed assemblies. Section 4.1 introduces the four fundamental subspaces associated with the equilibrium matrix and relates them to the subspaces of the compatibility matrix. Sections 4.2 and 4.3 describe an efficient computational procedure for obtaining these subspaces, and demonstrate the calculations for a rather straightforward example. An essential refinement is introduced in Section 4.4 in order to separate 'rigid-body' from 'internal' mechanisms when dealing with frameworks which are either partly or entirely free in space. Leaving aside only assemblies with very special properties that will be the subject of a separate investigation in Chapter 5, Sections 4.5 and 4.6 conclude the study, enabling one to tackle any of the assemblies encountered in Chapters 2 and 3. The results obtained for some well-known and less well-known structures are given in Section 4.7. The chapter concludes with a discussion.

4.1 Equilibrium and compatibility of pin-jointed assemblies

The aim of this section is to set up a conceptual framework within which the behaviour of every pin-jointed assembly can be predicted and understood with absolute clarity; this requires the introduction of the equilibrium matrix, and its transpose the compatibility matrix, and the four vector subspaces associated with them.

Consider an assembly that consists of a total of n nodal points connected by b bars to each other and by a total of c kinematic constraints to a rigid foundation. Two sets of statical variables must be considered: the tensions in the bars and the external forces applied to the joints.

The tension in each bar is defined by a single number, and positive tensions will denote tensile axial forces; so there are altogether:

b tensions, assembled in the vector $\{t\}$.

Each unconstrained joint can be subjected to the action of a force with arbitrary components in the direction of the axes of the chosen cartesian system of reference (O,x,y,z). The three scalar components of the external force applied to each of the n joints would give a set of 3n force components

but there is in general no need to introduce into this set the three components of force acting upon a joint which is rigidly connected to the foundation by three kinematic constraints. Similarly, only one or two external components of force need to be considered for joints subjected to two or one constraints, respectively. The total number of force components is therefore:

3n-c loads, assembled in the vector {f}.

Notice that there has been no mention of the constraint reactions; their total number is c but, unless elastically or inelastically yielding constraints are present - in which case one can consider them as extra bars of the assembly - they play no part in the following analysis.

Similarly, two sets of variables are needed to perform the kinematical analysis: the elongations of the bars and the displacements of the joints. Each of these corresponds directly to one of the statical variables, and therefore the same 'positive sense' and order of numbering will be maintained. Thus the kinematical variables are:

b elongations, assembled in the vector {e};
3n-c displacements, assembled in the vector {d}.

4.1.1 Equilibrium approach

The three equilibrium equations for a general, unconstrained node i (see Fig. 4.1) which is connected by the bars p and q to the nodes j and k may be written as follows:

$$\begin{aligned}(X_i-X_j)t_p/l_p+(X_i-X_k)t_q/l_q&=f_{ix}\\(Y_i-Y_j)t_p/l_p+(Y_i-Y_k)t_q/l_q&=f_{iy}\\(Z_i-Z_j)t_p/l_p+(Z_i-Z_k)t_q/l_q&=f_{iz}\end{aligned} \qquad (4.1)$$

Here X_i, Y_i and Z_i are the cartesian coordinates of node i in the original configuration of the structure; f_{ix}, f_{iy} and f_{iz} are the components of the external force acting upon node i; l_p is the length of bar p and t_p is the tension in it. The equilibrium equations of kinematically constrained nodes are automatically satisfied, and therefore only 3n-c equations in b unknowns remain; these can be written in matrix form as:

$$
\begin{array}{c}
\qquad\quad p \qquad\qquad\quad q \\
3n\text{-}c \left\{ \underbrace{\begin{bmatrix}
 & \vdots & & \vdots & \\
\cdots & (X_i-X_j)/l_p & \cdots & (X_i-X_k)/l_q & \cdots \\
\cdots & (Y_i-Y_j)/l_p & \cdots & (Y_i-Y_k)/l_q & \cdots \\
\cdots & (Z_i-Z_j)/l_p & \cdots & (Z_i-Z_k)/l_q & \cdots \\
 & \vdots & & \vdots &
\end{bmatrix}}_{b} \right\}
\begin{Bmatrix} t_p \\ \\ t_q \end{Bmatrix}
=
\begin{Bmatrix} f_{ix} \\ f_{iy} \\ f_{iz} \end{Bmatrix}
\end{array}
\qquad (4.2)
$$

In short: $[A]\{t\}=\{f\}$ (4.3)

where [A] is the 3n-c by b equilibrium matrix. The matrix [A] provides a transformation of any b-dimensional vector {t} into a (3n-c)-dimensional vector {f} given by (4.3); it is therefore a linear operator between R^b, the space of tensions, and $R^{(3n-c)}$, the space of loads. Four subspaces are always associated with a matrix (for a detailed explanation of the standard terminology used in this section see any textbook on Linear Algebra, e.g. Strang (1980)). In the case of the equilibrium matrix [A] their names and dimensions are:

Space	Subspaces	Dimensions
bar space R^b	Row space of [A]	r_A
	Nullspace of [A]	s
joint space $R^{(3n-c)}$	Column space of [A]	r_A
	Left-nullspace of [A]	M

where r_A is the rank of the equilibrium matrix and

$$s=b-r_A$$
$$M=3n-c-r_A \qquad (4.4)$$

A vector subspace can be defined either in terms of the properties that characterize its vectors or by providing one of its bases, i.e. a set of independent vectors that span the given subspace. Each of these two kinds of description is useful for different purposes. For the sake of clarity only algebraic 'definitions' and their interpretations in terms of structural

mechanics will be given at this initial stage; the convenient terms of row and column vectors will be used to denote the entries in a row or column of [A], respectively.

The row space of [A] is the subspace of the bar space R^b spanned by the row vectors of [A]; its dimension is r_A because the rank of [A] is equal to the number of independent row (or column) vectors. It is easy to convince oneself that any tension vector whose components are equal to a row of the equilibrium matrix cannot be in equilibrium without external forces, unless all its components vanished. Therefore the row space of [A] consists of the tension vectors {t} that require external loads to be in equilibrium.

The nullspace of [A], also called the kernel of [A], is the subspace of R^b consisting of the solutions of the system of equations

$$[A]\{t\}=\{0\} \tag{4.5}$$

The solutions of (4.5) are all the states of selfstress of the assembly, therefore the dimension of the nullspace of [A], equal to the number of independent states of selfstress, is $s=b-r_A$.

The column space or range of [A] is the subspace of R^{3n-c} spanned by the columns of [A]; its dimension is r_A. Column number i of the equilibrium matrix contains the nodal loads that are required to equilibrate the assembly if the tension in bar number i is set equal to one, and the remaining tensions are zero. Only a total of r_A columns of [A] are independent, which means that there are r_A independent systems of load that the assembly can sustain and r_A bars corresponding to them. Following Vilnay (private communication) these load systems will be called the "fitted loads" of the assembly. The remaining bars are redundant and one can obtain a statically determinate assembly by removing them.

The left-nullspace of [A] is the subspace of R^{3n-c} consisting of the solutions of the system of equations

$$[A]^T\{f\}=\{0\} \tag{4.6}$$

By similarity to the nullspace, the dimension of the left-nullspace is

$M=3n-c-r_A$. Transpose (4.6) to obtain $\{f\}^T[A]=\{0\}^T$. This is a relationship that can provide some insight: the dot product of a vector $\{f\}$ that satisfies (4.6) and any column of [A] vanishes. Since any column of [A] represents a load system in equilibrium with a tension of 1 in one particular bar of the assembly (see above), the solutions of (4.6) are orthogonal to all such load systems. Therefore the left-nullspace of [A] contains all the force systems that cannot be equilibrated whatever value the bar tensions take: they cannot be carried by the assembly in its original configuration. In conclusion, column space and left-nullspace are orthogonal i.e. any vector from the first space is orthogonal to all the vectors of the second one. The row space and nullspace are also orthogonal: this is easily demonstrated by evaluating the dot product of two vectors $\{t_1\}$ and $\{t_2\}$ belonging to the rowspace and nullspace, respectively. By definition there exists at least one vector $\{f_1\}$ of the column space such that $\{t_1\}=[A]^T\{f_1\}$; substitute this expression into $\{t_1\}^T\{t_2\}$ to obtain $\{f_1\}^T[A]\{t_2\}$, which vanishes as $[A]\{t_2\}=\{0\}$ because $\{t_2\}$ is a state of selfstress. In fact these subspaces are not merely orthogonal, since one of them contains all the vectors orthogonal to the other: the two subspaces are thus orthogonal complements of each other.

In conclusion, any set of bar tensions $\{t\}$ can be uniquely decomposed into two orthogonal sets of tensions: its projection onto the row space of the equilibrium matrix, which equilibrates any applied permissibile loads, and its projection onto the nullspace which is self-equilibrated but, of course, influences the geometrical compatibility of an elastic structure. Similarly, an arbitrary load condition $\{f\}$ can be uniquely decomposed into two orthogonal load systems: its projection onto the column space of [A], which can be sustained by the assembly in its initial shape, and its projection onto the left-nullspace that may be carried only if the assembly adopts a deformed configuration. See Fig 4.2. More details on these last remarks will be given in Section 4.5 and Chapter 6.

4.1.2 Compatibility approach

The elongation of bar p of the framework, which connects two unconstrained nodes j and k, caused by an assigned nodal displacement (see Fig 4.3) is:

$$e_p=\sqrt{(X_i+x_i-X_j-x_j)^2+(Y_i+y_i-Y_j-y_j)^2+(Z_i+z_i-Z_j-z_j)^2}-l_p \qquad (4.7)$$

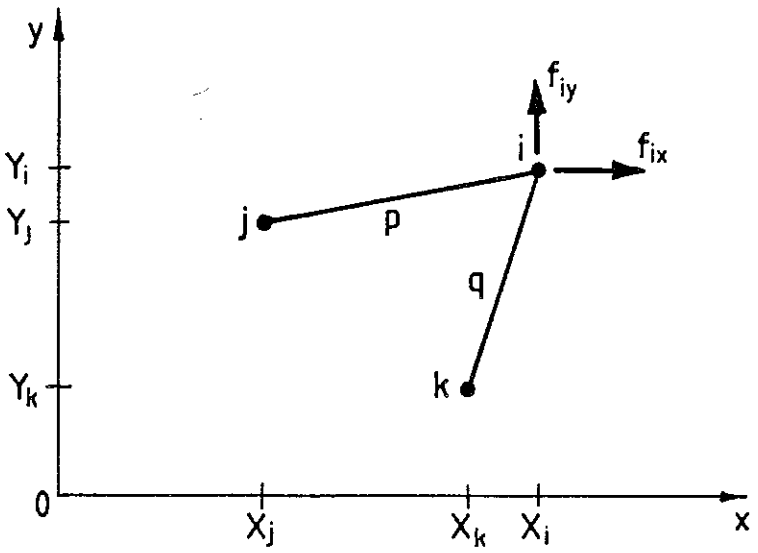

Fig. 4.1 View along the axis Oz of a joint i which carries external forces, and which is connected by bars p, q to joints j, k.

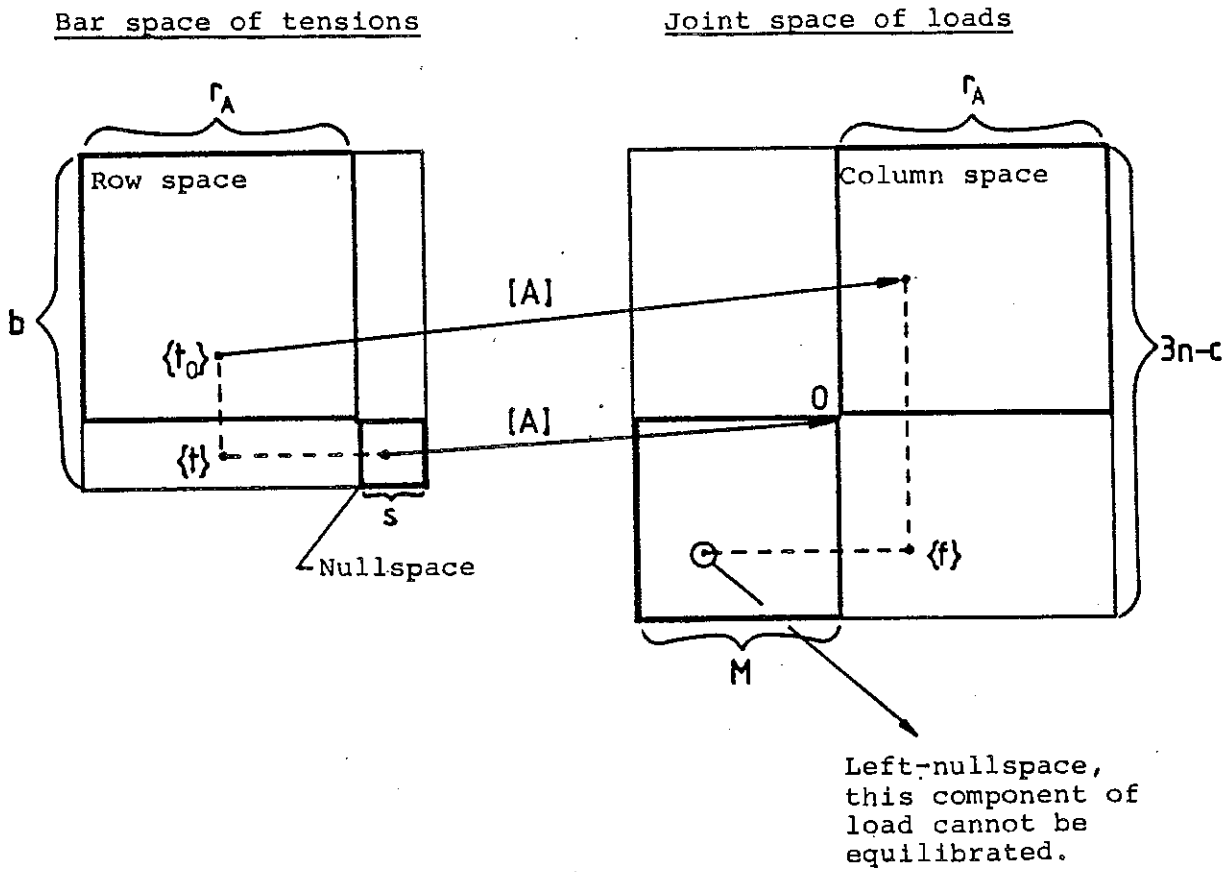

Fig. 4.2 The equilibrium matrix [A] is a linear operator between the vector spaces R^b and R^{3n-c}; it associates nodal loads with bar tensions. The above picture refers to an assembly which is statically indeterminate (s>0) and kinematically indeterminate (M>0).
{t} and {f} are arbitrary points of the bar and joint spaces, respectively. See Section 4.1.1.

where x_i, y_i, z_i are the cartesian components of displacement of node i; l_p is the length of bar b measured in the original configuration of the assembly, and e_p is its elongation. On the hypothesis of small displacements, all the terms of order higher than one can be neglected and the following linear expression is obtained:

$$(X_i-X_j)(x_i-x_j)/l_p+(Y_i-Y_j)(y_i-y_j)/l_p+(Z_i-Z_j)(z_i-z_j)/l_p=e_p \quad (4.8)$$

A similar equation of geometrical compatibility relates displacements and elongations of any bar of the assembly; in matrix form the whole system of compatibility equations is:

$$b\left\{\begin{array}{c}\\\\\\\\\end{array}\right.\underbrace{\left[\begin{array}{cccccccccc} \cdot & \cdot & \frac{X_i-X_j}{l_p} & \frac{Y_i-Y_j}{l_p} & \frac{Z_i-Z_j}{l_p} & \cdot & \cdot & \frac{X_j-X_i}{l_p} & \frac{Y_j-Y_i}{l_p} & \frac{Z_j-Z_i}{l_p} \end{array}\right.}_{3n-c}\left.\begin{array}{c}\\\\\\\\\end{array}\right]\left\{\begin{array}{c} x_i \\ y_i \\ z_i \\ \\ x_j \\ y_j \\ z_j \end{array}\right\}=\left\{\begin{array}{c}\\\\\\\\\end{array}\right.e_p\left.\begin{array}{c}\\\\\\\\\end{array}\right\} \quad (4.9)$$

in short: $[B]\{d\}=\{e\}$. Here [B] is the b by 3n-c <u>compatibility matrix</u>. Everything said about the equilibrium matrix [A] in Section 4.1.1 is also valid for [B], bearing in mind that the compatibility matrix operates from the (3n-c)-dimensional space of nodal displacements R^{3n-c} to the b-dimensional space of bar elongations R^b. In particular, the four fundamental subspaces of the compatibility matrix are:

The <u>row space</u>, a subspace of the joint space R^{3n-c}, spanned by the row vectors of [B]: its dimension is r_B. Row p of the compatibility matrix [B] defines a displacement {d} in which each end of bar i moves by 1 in the same direction as the bar; the corresponding elongation e_p is therefore +2; the other bars of the assembly deform accordingly. This shows that the row space of the compatibility matrix contains all the displacements which require the

elongation of one or more bars, i.e. all modes of deformation which are not inextensional mechanisms.

The nullspace, is the subspace of the joint space formed by the solutions of $[B]\{d\}=\{0\}$; it is therefore the space of all inextensional motions (mechanisms), including rigid-body and internal ones, of the assembly. Its dimension is

$$M'=3n-c-r_B \tag{4.10}$$

The range, the subspace of the bar space R^b spanned by the columns of [B]: its dimension is r_B. Any particular column of the compatibility matrix defined in (4.9) contains the bar elongations due to a displacement {d} which has +1 as its entry corresponding to the chosen column and zero elsewhere. This demonstrates that the bar elongations in the range of [B] are all geometrically compatible.

The left-nullspace consists of the solutions of $[B]^T\{d\}=\{0\}$, its dimension is

$$s'=b-r_B \tag{4.11}$$

Following the discussion of the left-nullspace of [A] as a guideline it should be plain that this subspace contains all combinations of bar elongations which are forbidden by the conditions of geometrical compatibility of the assembly.

The conclusions of Section 4.1.1 on the orthogonality of the four subspaces also apply. Some noteworthy kinematical conclusions can be drawn: any nodal displacement {d} can be uniquely decomposed into two orthogonal vectors, its extensional and inextensional components; these are the projections of {d} onto the row space and nullspace of [B], respectively. Similarly, any set of bar elongations {e} can be uniquely decomposed into its compatible and incompatible components, these are its projections onto the column space and left-nullspace. See Fig. 4.4.

The similarity between the equilibrium and compatibility approaches cannot have passed unnoticed. In fact the link between corresponding results

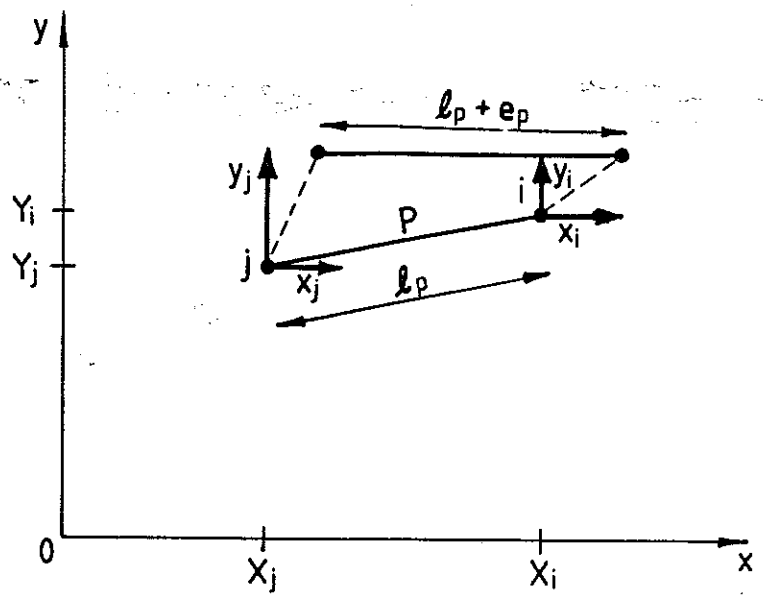

Fig. 4.3 View along the axis Oz of a bar p the end nodes of which move from the initial configuration (X,Y) to the final one (X+x,Y+y).

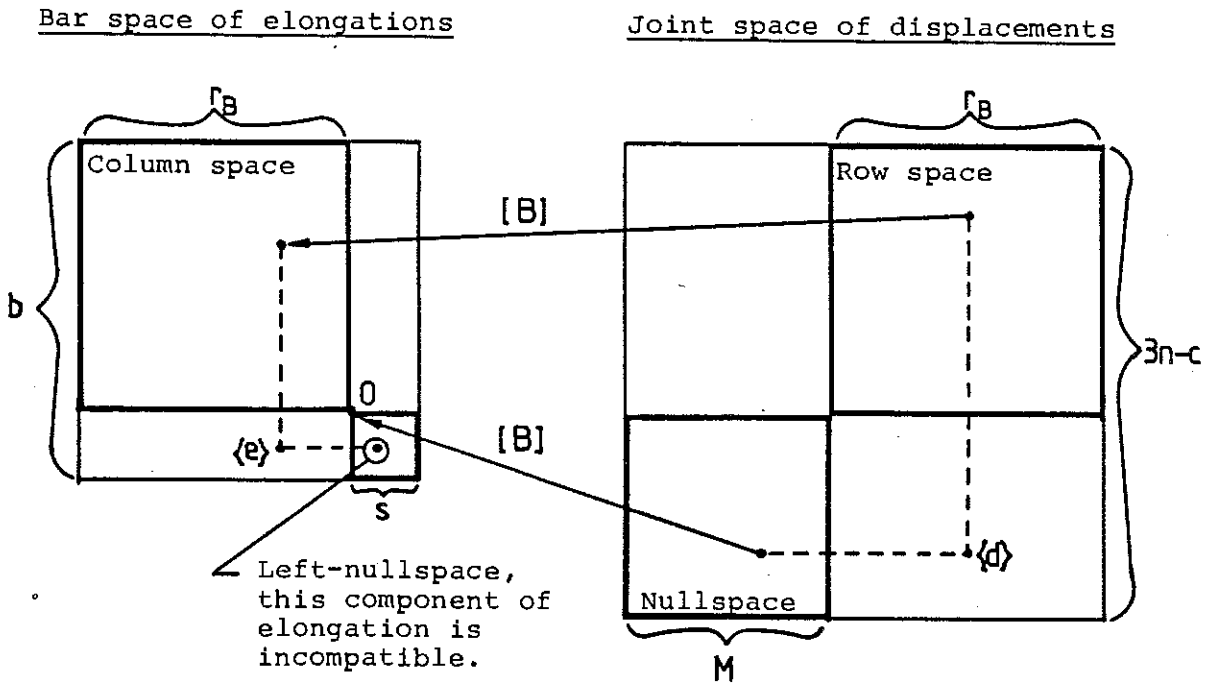

Fig. 4.4 The compatibility matrix [B] is a linear operator between the vector spaces R^{3n-c} and R^b; it associates nodal displacements with bar elongations. See Section 4.1.2.

is much stronger. Thus compare row number p of the compatibility matrix shown in (4.9) with column p of the equilibrium matrix in (4.2); although the former shows a complete version while the latter does not, all their entries will be equal in the end. This demonstrates by induction that the compatibility matrix is the transpose of the equilibrium matrix, and that the two sets of subspaces introduced above are the same thing, see Table 4.1. Their dimensions

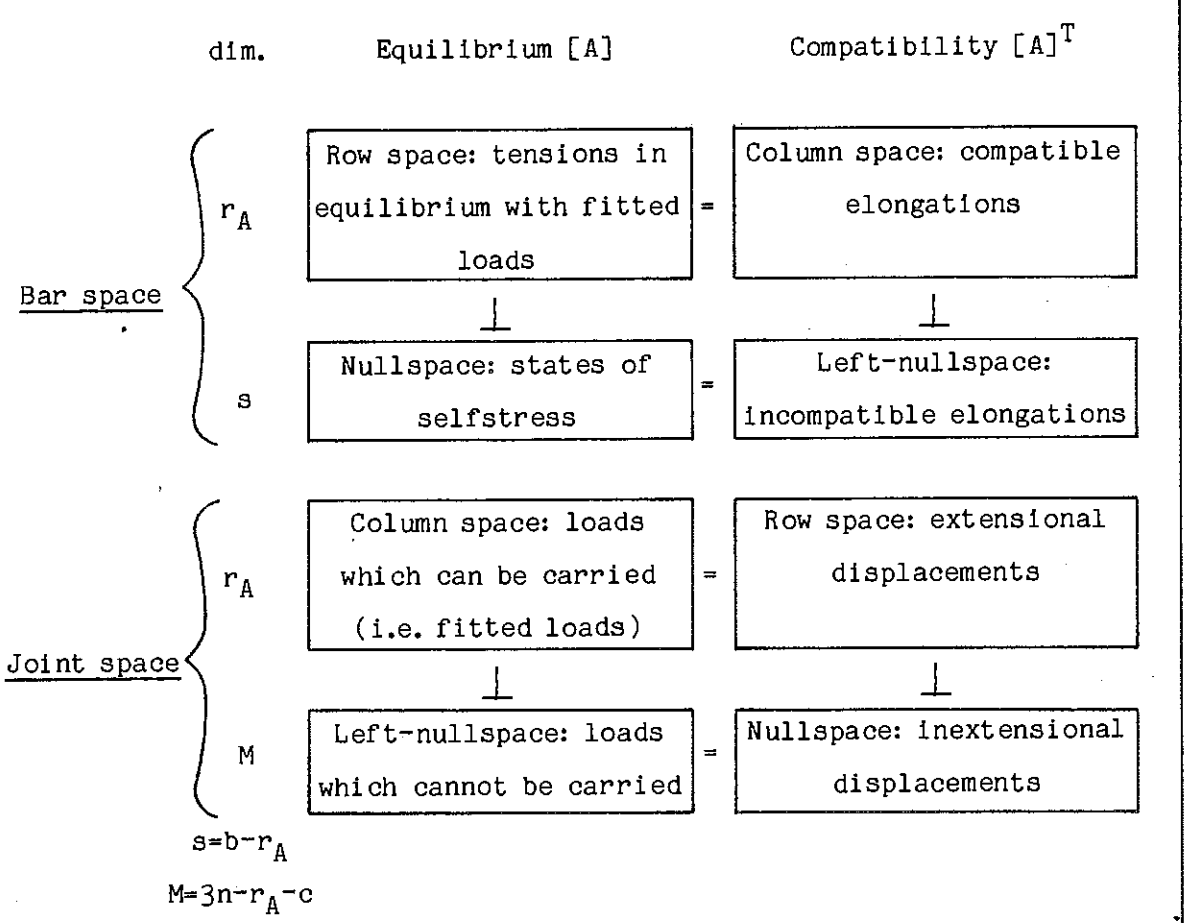

Table 4.1 The relationship between the fundamental subspaces of the equilibrium and compatibility matrices. b, n and c are the number of bars, nodes and kinematical constraints, respectively; r_A is the rank of the equilibrium matrix [A]. s is the number of states of selfstress, and M is the total number of inextensional mechanisms (including 'internal' and 'rigid-body' motions).

also coincide, hence: $r_A=r_B$, $s=s'$, $M=M'$ and subtraction of the first of the relationships (4.4) from the second one yields $M-s=3n-c-b$ for an assembly free in space $M=m+6$ and $c=0$, and so this formula agrees with (2.17).

The last result obtained in this section, i.e. $[B]=[A]^T$, is well known in Structural Analysis, see Livesley (1975) or Calladine (1978), but the usual way of demonstrating it relies on virtual work, which is a less direct way of making the statements about equilibrium and compatibility: these are exactly equivalent to those made here.

4.2 A scheme of computation

The four subspaces defined in Section 4.1 will be an essential element in the exposition, but little progress can be made until a more operational approach is taken. As already noticed, this can be only achieved by computing a basis for each subspace, i.e. a set of independent vectors that span the space. This is the objective of the present section, which describes an algorithm for the automatic computation of the rank of the equilibrium matrix (and hence, by (4.4), the number of independent mechanisms M and states of selfstress s) and of bases for the four fundamental subspaces.

Start by writing out the matrix [A] with an adjoining identity matrix [I] of dimension 3n-c, as shown in Fig. 4.5a, and then proceed to operate on the rows of the extended matrix [A|I] with the aim of transforming [A] into a 'staircase pattern' with 0's in the lower-left of the 'triangle' schematically shown in Fig. 4.5b: this is called echelon form of the matrix (Strang, 1980). The transformation is performed by a modified Gaussian elimination. The matrix [I] associated with [A] is sometimes known as the 'record matrix', since it records precisely the row operations performed during the elimination sequence. In the first stage of the transformation the aim is to have a non-zero entry in position (1,1), with 0's in the remainder of the column. In the operations leading to this, exchange row 1 of [A|I] with the row that contains the largest entry in column 1 and use this as the pivotal row to transform the rows below it. Next perform similar operations on the matrix obtained by disregarding the first row and first column, with the aim of securing a non-zero entry at (2,2) and 0's in the lower part of the second column. Now while these operations are being carried out it sometimes happen that no pivot can be found in the column under investigation; in which case attention is transferred successively one column to the right until a pivot is eventually found or the last column of [A] has been processed. When the transformation has been completed the bottom $M=3n-c-r_A$ rows of [A] are filled

by 0's; the rank of the matrix is equal to the total number of pivots found. Thus in the transformed matrix $[\tilde{A}|\tilde{I}]$ shown schematically in Fig. 4.5b, pivots were found in columns 1, 2 and 5 but not in columns 3, 4, 6 and 7; hence $r_A=3$. The columns with pivots are marked * in Fig. 4.5b; these denote in fact r_A linearly independent columns of the original matrix, which are also marked * after the transformation is complete. The bars of the framework wich correspond to columns not marked * are 'redundant' bars. Notice that the choice of which bars are considered redundant here depends on the numbering systems of bars and joints, and on the numerical strategy adopted; Livesley (1967) has argued that procedures like the one described above aim at 'the best' set of redundancies. For a comparison of different procedures see Domaszewski & Borkowski (1979). Since all non-trivial applications of the method described above require the use of a digital computer to assemble $[A|I]$ and transform it into $[\tilde{A}|\tilde{I}]$, the entries of these matrices will be expressed as floating-point numbers. How many digits are stored at any time depends on the particular computer which is used: in any case small errors creep in at each step of the calculation and add to the initial error made when defining the geometry of the assembly. Modern numerical analysis (Morris, 1983) makes available a variety of techniques to prevent the build-up of unacceptable errors and improve therefore the numerical stability of a large-scale computation. See Fig. 4.6 for a schematic flow chart of the elimination subroutine that has been used in all tests described in this dissertation; the smallest acceptable number has been 10^{-4}.

Only a little more effort is now required in order to obtain bases for the four subspaces of the equilibrium/compatibility matrix.

Column space of [A]. The r_A columns of [A] that provide a pivot (marked * in Fig. 4.5a) form a basis for this subspace.

Left-nullspace of [A]. The bottom $M=3n-c-r_A$ rows of $[\tilde{I}]$ form a basis for this subspace. This follows from the fact that the equations $[\tilde{A}]\{t\}=[\tilde{I}]\{f\}$ are precisely equivalent to the original equilibrium equations (4.3), and the bottom M equations then state that each of the bottom M rows of $[\tilde{I}]$ is orthogonal to $\{f\}$. See also Livesley (1973).

Row space of [A]. The upper r_A rows of $[\tilde{A}]$ form a basis for this space.

Nullspace of [A]. A basis for this subspace is found in the following way. Consider $[\tilde{A}]\{t\}=\{0\}$. Set t=1 for the first redundant bar and t=0 for the

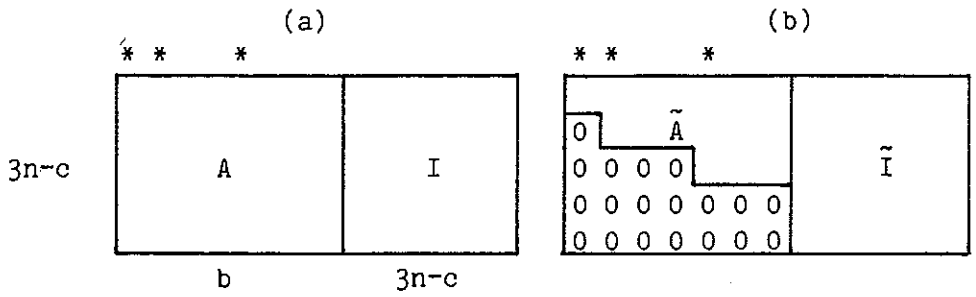

Fig. 4.5 Diagram to show the way that the equilibrium matrix [A] together with the identity matrix [I] is transformed by row-operations into the 'echelon' form $[\tilde{A}|\tilde{I}]$. Pivots are found in columns 1, 2 and 5.

Choice of pivotal row:	For rows i, i+1,...3n-c, if the entry in column j - a, say - is greater than the smallest acceptable number, choose the largest entry of the row not in column j - b, say - and evaluate a/b. Otherwise skip the row. If the previous check was never satisfied the column is dependent and the computation moves to column j+1. Otherwise the pivotal row corresponds to the greatest computed ratio. (This technique is called scaled pivoting). Pivotal row and row i are exchanged.
Transformation of pivotal row:	All entries of the pivotal row are divided by the pivot. The entry of position (i,j) is now 1.
Transformation of entries below pivot:	For rows i+1,...3n-c, if the entry below the pivot is smaller than the smallest acceptable number, skip the row. If the row can be considered proportional to the pivotal row, set all its entries equal to zero. Otherwise subtract the entry below the pivot multiplied by the pivotal row.

Fig. 4.6 Transformation of column j of [A]. In the above description i-1 pivots have been found in the first j-1 columns, in previous stages of the elimination; therefore the first i-1 rows and j-1 columns of [A] have to be disregarded.

remaining s-1; and solve (uniquely) for the tensions in the non-redundant bars. This is easily done because $[\tilde{A}]$ is an upper triangular matrix. The vector {t} so obtained is a base vector of the nullspace. The other s-1 base vectors are obtained similarly by having t=1 for each of the redundant bars in turn. Since the equations $[A]\{t\}=\{f\}$, $[\tilde{A}]\{t\}=[\tilde{I}]\{f\}$ are equivalent, the solutions of $[\tilde{A}]\{t\}=\{0\}$ are the states of selfstress of the assembly.

Each of the four bases decribed above is just <u>one</u> possible choice; according to the type of analysis that one is going to perform the most convenient starting basis may be different, see Section 6.1. For instance, the set of M inextensional mechanisms that form a basis for the left-nullspace might not show any properties of symmetry, which would be revealed by a different treatment or by the choice of a different coordinate system.

4.3 An example

Figure 4.7 shows an assembly of three collinear bars of equal length, connected to a rigid foundation at nodes 1 and 4. The assembly is regarded as lying in a plane; consequently the dimension of the joint space will be $2n-c=2\times4-4=4$ (c=4 since joints 1 and 4 are fully constrained in the plane) and b=3. The statical and kinematical variables introduced in Section 4.1 are now:

$$\{t\}=\begin{Bmatrix} t_a \\ t_b \\ t_c \end{Bmatrix},\quad \{f\}=\begin{Bmatrix} f_{2x} \\ f_{2y} \\ f_{3x} \\ f_{3y} \end{Bmatrix},\quad \{e\}=\begin{Bmatrix} e_a \\ e_b \\ e_c \end{Bmatrix} \text{ and } \{d\}=\begin{Bmatrix} x_2 \\ y_2 \\ x_3 \\ y_3 \end{Bmatrix}$$

By inspection, the equilibrium matrix of (4.2) is given by:

$$[A]=\begin{bmatrix} 1 & -1 & 0 \\ 0 & 0 & 0 \\ 0 & 1 & -1 \\ 0 & 0 & 0 \end{bmatrix} \quad \text{thus} \quad [A|I]=\left[\begin{array}{ccc|cccc} 1 & -1 & 0 & 1 & 0 & 0 & 0 \\ 0 & 0 & 0 & 0 & 1 & 0 & 0 \\ 0 & 1 & -1 & 0 & 0 & 1 & 0 \\ 0 & 0 & 0 & 0 & 0 & 0 & 1 \end{array}\right]$$

(* *)

and by following the procedure described above, which here involves merely the replacement of row 2 by 1×(row 3)-0×(row 2) and of row 3 by

1×(row 2)-0×(row 3) one obtains

$$[\tilde{A}|\tilde{I}]=\left[\begin{array}{ccc|cccc} 1 & -1 & 0 & 1 & 0 & 0 & 0 \\ 0 & 1 & -1 & 0 & 0 & 1 & 0 \\ 0 & 0 & 0 & 0 & 1 & 0 & 0 \\ 0 & 0 & 0 & 0 & 0 & 0 & 1 \end{array}\right]$$

clearly $r_A=2$ and so, by (4.4), s=1 and M=2. Thus the plane assembly of Fig. 4.7 is statically and kinematically indeterminate with one state of selfstress; bar c is redundant; and there are two mechanisms.

The nullspace of [A], i.e. the one state of selfstress, is obtained by back-substitution from

$$\left[\begin{array}{ccc} 1 & -1 & 0 \\ 0 & 1 & -1 \\ 0 & 0 & 0 \\ 0 & 0 & 0 \end{array}\right]\left\{\begin{array}{c} t_a \\ t_b \\ 1 \end{array}\right\}=\left\{\begin{array}{c} 0 \\ 0 \\ 0 \\ 0 \end{array}\right\} \qquad \text{so: } \{t\}=\{1\ 1\ 1\}^T$$

The other three subspaces are found exactly as described above, and are displayed in Fig. 4.8. The various features pointed out in Table 4.1 may be verified by inspection, and the orthogonality of the subspaces may be checked directly.

4.4 Rigid-body and internal mechanisms

The scheme described in Section 4.2 gives, in particular, M independent inextensional mechanisms of the assembly which span the left-nullspace of the equilibrium matrix [A]. In the case where the assembly is unattached to a rigid foundation, these will obviously include six independent inextensional motions of the assembly as a rigid-body in space, in addition to any 'internal' inextensional mechanisms which the assembly may possess. It is clear that the procedure described above does not make this distinction, and that a new algorithm is needed to segregate the rigid-body mechanisms from the others. The following scheme does this by treating any framework as a rigid body, and it can cope with assemblies having any number between zero and

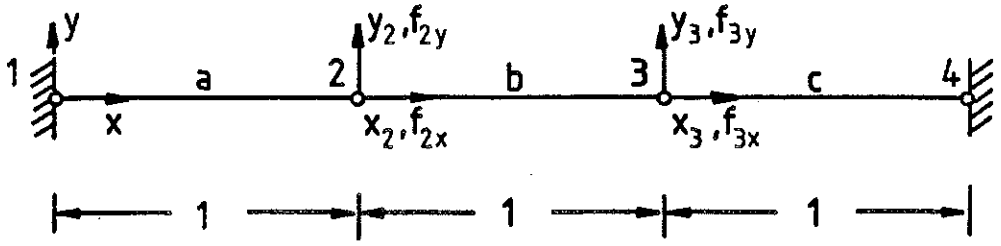

Fig. 4.7 Plane assembly analysed in Section 4.3.

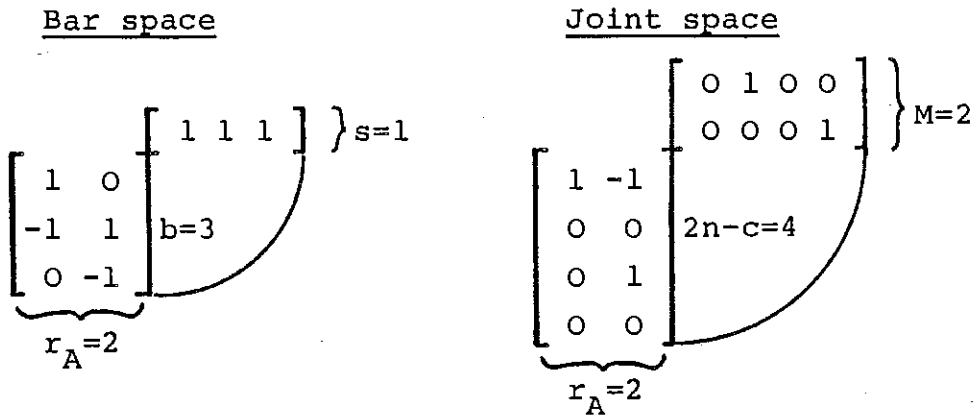

Fig. 4.8 Bases of the four subspaces of the assembly shown in Fig. 4.7. In this schematic representation orthogonal subspaces are denoted by row and column vectors.

six of rigid-body motions.

Consider the previous general pin-jointed assembly, having a total of c kinematic constraints to a rigid foundation, and let the locations of the joints in the original configuration be described, as before, with respect to a fixed system of cartesian coordinates (O,x,y,z). Any rigid-body displacements of the assembly may be described by one translation and one rotation vector $\{n_0\}=\{n_{0x}\ n_{0y}\ n_{0z}\}^T$ and $\{r\}=\{r_x\ r_y\ r_z\}^T$ respectively. Here $\{n_0\}$ represents the displacement of that point of the assembly which lies at the origin of the coordinates in the original configuration; $\{r\}$ is the rotation about this point. In such a rigid-body motion the displacement of a point i having position vector $\{q\}=\{X_i\ Y_i\ Z_i\}^T$ is given by

$$\{x_i\ y_i\ z_i\}^T=\{n_0\}+\{r\}\times\{q\} \qquad (4.12)$$

Now if i is a joint of the assembly which is fully restrained to the foundation, the three kinematic conditions $x_i=y_i=z_i=0$ are imposed on any rigid-body motion; they give three simultaneous equations:

$$\begin{cases} n_{0x} & & & +Z_i r_y & -Y_i r_z & =0 \\ & n_{0y} & -Z_i r_x & & +X_i r_z & =0 \\ & & n_{0z} & +Y_i r_x & -X_i r_y & =0 \end{cases} \qquad (4.13)$$

If this joint had only two or one degrees of kinematic constraint, then only two or one of the above three equations would apply. In this way, each of the external constraints imposes one condition on $\{n_0\}$ and $\{r\}$, and hence the c external constraints together give a system of c equations in six unknowns:

$$[C]\left\{\begin{matrix} n \\ r \end{matrix}\right\}=\{0\} \qquad (4.14)$$

Here [C] is a c×6 kinematic matrix. The rank r_C of this matrix indicates how many of the external constraints effectively suppress rigid-body degrees of freedom of the assembly; this rank can be determined by the procedure described earlier in relation to the equilibrium matrix [A]. Thus the number rb of rigid-body motions is:

$$rb=6-r_c \tag{4.15}$$

The independent solutions of the system of equations (4.14), which span the nullspace of [C], provide a basis for the subspace of these rigid-body motions in terms of the six scalar components of $\{n_0\}$ and $\{r\}$. These may be used in (4.12) to obtain, for each of these motions, the components of displacement of each joint of the assembly.

The next step is to find a basis for the m-dimensional space of internal mechanisms, where

$$m=M-rb \tag{4.16}$$

Since by definition the internal mechanisms are orthogonal to the subspace of rigid-body mechanisms, the M mechanisms $\{d_1\},\ldots,\{d_M\}$ computed in Section 4.2 have to be separated from their components in that subspace. Assemble the nodal displacements corresponding to each rigid-body mechanism in the $(3n-c)\times rb$ matrix [RB]. Any rigid-body motion can be expressed as a linear combination of the columns of [RB], and in particular the 'rigid-body' component of mechanism $\{d_i\}$ will be $[RB]\{x_i\}$. And

$$\{d_i\}-[RB]\{x_i\} \tag{4.17}$$

is orthogonal to any rigid-body motion; hence $[RB]^T(\{d_i\}-[RB]\{x_i\})=0$. Solve this system of rb equations for $\{x_i\}$ and substitute into (4.17) to obtain the component of $\{d_i\}$ orthogonal to the subspace of rigid-body mechanisms:

$$\{d_i\}-[RB]([RB]^T[RB])^{-1}[RB]^T\{d_i\} \tag{4.18}$$

This formula gives an answer in closed form to the problem. But the same result can be achieved by orthogonalizing the rigid-body mechanisms to each other, i.e. transforming the initial basis into an orthogonal one $\{a_1\},\ldots,\{a_{rb}\}$, and subtracting from each mechanism its components onto the subspace of rigid-body motions:

$$\{d_i\}=\{d_i\}-\sum_{j=1}^{rb}(\{a_j\}\{d_i\}/|a_j|^2)\{a_j\}$$

This operation transforms the initial mechanisms into a set of M internal mechanisms. But only m of these are linearly independent; and the modified Gaussian elimination described in Section 4.2 can be used to detect which columns of the $(3n-c)\times M$ matrix $[\{d_1\},\ldots\ \{d_M\}]$ are dependent on the others. These are then suppressed and the remainder form the required basis for the space of internal inextensional mechanisms of the assembly.

4.5 Stiffening effects of selfstress

The preceding description of the four fundamental vector subspaces of the equilibrium matrix of a pin-jointed framework and the computational scheme for their evaluation in any given case are an essential preliminary to a complete understanding of the mechanics of such assemblies. Most usual engineering frameworks will prove to be kinematically determinate when subjected to the analysis described and they can be treated without difficulty following the standard methods of Structural Analysis: see e.g. Parkes (1974) or Timoshenko & Young (1965). The reader will have noticed that the approach described in Sections 4.1 and 4.2 is strongly biased towards the force method of analysis. If the scheme described above is used to establish that a given assembly is kinematically determinate, it would be wasteful to dispose of all the results of those computations, states of selfstress in particular, and to start again by assembling a conventional stiffness matrix, see Section 6.1.1.

Some other assemblies will turn out to be kinematically indeterminate. The study of how they respond to an applied loading is the main objective of Chapter 6. But it is convenient here to take a necessary preliminary step in the analysis by computing the total number of independent loads that a prestressed assembly can carry.

In order to investigate further an assembly with $s>0$ and $m>0$ (for reasons that will become clear later the rb rigid-body mechanisms will not be considered) first give the assembly a state of selfstress, and then impart a small amplitude to one or more of the internal inextensional mechanisms. In its original configuration, of course, the assembly would be in equilibrium

under zero external load. But when the geometry is altered slightly this will no longer be true, in general, since the coefficients of (4.3) will have changed. Indeed it has already been shown (Calladine, 1978, 1982) that in some relatively simple examples a state of selfstress can 'stiffen' one or more inextensional mechanisms. The key to the situation is the so-called product-force vector (Pellegrino & Calladine, 1984) associated with any given mechanism of a structure which sustains a given state of selfstress. For this purpose, suppose that the state of selfstress does not change when the mode of inextensional displacement is excited: certainly it need not change in an assembly of elastic bars since, at least to the first order, the lengths of the bars do not alter.

Rewrite the equilibrium equations (4.1) for an infinitesimally displaced configuration to obtain:

$$\begin{aligned}
&[(X_i+x_i)-(X_j+x_j)]t_p/l_p+[(X_i+x_i)-(X_k+x_k)]t_q/l_q=f_{ix}\\
&[(Y_i+y_i)-(Y_j+y_j)]t_p/l_p+[(Y_i+y_i)-(Y_k+y_k)]t_q/l_q=f_{iy}\\
&[(Z_i+z_i)-(Z_j+z_j)]t_p/l_p+[(Z_i+z_i)-(Z_k+z_k)]t_q/l_q=f_{iz}
\end{aligned} \qquad (4.19)$$

where x_i, y_i, z_i,... are the components of displacement of joint i,... according to the inextensional mechanism considered, and t_p,... are now understood to denote a state of selfstress. The external forces in (4.19) define the product-forces associated with the state of selfstress and the inextensional displacement imposed. Subtraction of (4.1), written in the original configuration, from (4.19) gives:

$$\begin{aligned}
p_{ix}&=(x_i-x_j)t_p/l_p+(x_i-x_k)t_q/l_q\\
p_{iy}&=(y_i-y_j)t_p/l_p+(y_i-y_k)t_q/l_q\\
p_{iz}&=(z_i-z_j)t_p/l_p+(z_i-z_k)t_q/l_q
\end{aligned} \qquad (4.20)$$

Equations of this type can be used, for each unconstrained component of joint displacement and for each internal mechanism, to assemble a set of m product-force vectors of dimension 3n-c:

$$\{p_1\},\ldots,\{p_m\} \qquad (4.21)$$

For example, in the assembly of Fig. 4.7 the state of selfstress consists of a uniform tension t. Let the product-forces be evaluated separately for each of the two mechanisms already determined: by inspection they are proportional to

$$\{p_1\}=\{0 \quad 2 \quad 0 \quad -1\}^T$$
$$\{p_2\}=\{0 \quad -1 \quad 0 \quad 2\}^T$$

When each column is multiplied by the product of t and the (small) amplitude of joint displacement, it gives the product-force vector.

The earlier analysis completed the classification summarized in Table 4.1, and revealed a vector subspace of the load space, the column space of [A] of dimension equal to r_A, of "fitted loads" which could be carried by the assembly in its original configuration. This subspace can be supplemented by the m-dimensional subspace of product-forces. The question is now: does the sum of the two subspaces span the entire load space? One way of answering this is to compare the dimension of this new subspace to 3n-c. A set of column vectors that span it is certainly given by the $(3n-c)\times(r_A+m)$ matrix [A'] shown in Fig. 4.9.

Notice that the subspace of product-forces is quite different in principle from the subspace of 'forbidden' loads, equal to the subspace of inextensional mechanisms, revealed by the initial analysis. That space consists of those loads which <u>cannot</u> be carried in the original configuration; but the product-forces are those loads which <u>can</u> be carried on account of selfstress when the inextensional modes are given small displacements.

It is obvious without any manipulation that the rigid-body motions develop <u>zero</u> product-forces: the product-force at any joint is a consequence of relative rotations of the bars meeting at the joint, which are obviously zero in any rigid-body motion. This is the reason why only product-forces corresponding to internal mechanisms need to be assembled in [A']. When rb=0 [A'] is square; and it follows immediately that there is a possibility that, when the assembly is allowed to distort in its inextensional modes it will be able, after all, to support a <u>completely arbitrary</u> set of loads, although the amplitude of the resulting inextensional modes may not be acceptable in some applications, of course. This will be the case if the matrix [A'] is of full

rank; the same ideas can be applied to non-square matrices [A'], but one needs to exclude rb rigid-body motions and the corresponding loads.

For example, the assembly of Fig. 4.7 has

$$[A'] = \left[\begin{array}{cc|cc} 1 & -1 & 0 & 0 \\ 0 & 0 & 2 & -1 \\ 0 & 1 & 0 & 0 \\ 0 & 0 & -1 & 2 \end{array}\right]$$

and it is easy to see that $r_{A'}=4$: hence this particular arrangement of bars is capable of withstanding arbitrary vertical and horizontal loading at the joints. The example of Fig 4.7 is, in fact, a primitive sort of cable net and it has been shown already, see Calladine (1982) and Pellegrino & Calladine (1984), that certain simple types of cable net can sustain a completely arbitrary pattern of loads although they have a substantial number of mechanisms.

The computation of $r_{A'}$ is not the only way to evaluate the number of extra load conditions that an assembly is enabled to carry in consequence of prestress. In a different approach one can aim at the dimension of the subspace intersection of the left-nullspace of [A] and the subspace of product-forces, which contains the loads that - although not "fitted"- can be equilibrated through inextensional deformation. Some projection work along the same lines as in Section 4.4 would lead to a solution in closed form. However, for assemblies with a very small number of mechanisms one need only prove that there exists one product-force $\{p_i\}$ such that

$$\{d_j\}\{p_i\}>0 \qquad (4.22)$$

to demonstrate that the product-force associated with mechanism number i can stiffen mechanism j.

Checking the sign of (4.22) is always a useful addition to the computation of the rank of [A']. If the chosen state of selfstress is changed to one of opposite sign the signs of all product-forces also change and the dot product in (4.22) then becomes <0, which denotes negative stiffness and therefore an unstable case. Although the envisaged unstable case has been

obtained here simply by changing the sign of a state of selfstress, which would not be possible in a tensegrity structure (because, if one tries to shorten - rather than lengthen - a bar the length of which is maximum, the structure becomes 'floppy' and no prestressing is achieved), more elaborate cases can be found.

A paper by Kuznetsov (1979) has an example, shown in Fig. 4.10, which is a variant of Fig 4.7 and also has s=1, m=2 but in which the dot products (4.22) for the two mechanisms have opposite signs. This implies that one of the two mechanisms is unstable whatever the sign of the selfstress; and in fact the assembly is free to distort as a four-bar-chain with s=0, m=1. Compare this with Fig. 2.12.

All of this leads to the conclusion that an assembly with m>0 is not stiffened by a state of selfstress if it can be recognized that changing sign to the selfstress makes 'no difference'.

4.6 Infinitesimal mechanisms of first order

This section will give a first estimate of the amplitude of 'inextensional' displacements which can take place in a structure for which the matrix methods described above indicate kinematical indeterminacy. Specific reference will be made to statically and kinematically indeterminate frameworks, mostly of the type envisaged by Maxwell (1864) and discussed in Section 2.1; this is because assemblies with m>0 but s=0 can usually undergo displacements of finite amplitude, although the possibility of the "dead points" of Figs 2.12 and 4.10 has to be borne in mind.

Tarnai (1980b) conjectured that it is only the infinitesimal inextensional mechanisms that can be stiffened by states of selfstress. The assembly of Fig. 4.7 which is stiffened by prestress, as well as the examples in Section 4.7, illustrate this conjecture: a state of selfstress imparts first-order stiffness to some mechanisms, but does not impart any stiffness to others which are already known to be finite mechanisms.

How can one explain the mechanics behind this conjecture, and thereby demonstrate that the conjecture is true?

Consider the assembly of Fig. 4.7, prestressed and subjected to a load in the vertical direction. The assembly provides some stiffness against this loading, because the change in geometry according to the inextensional

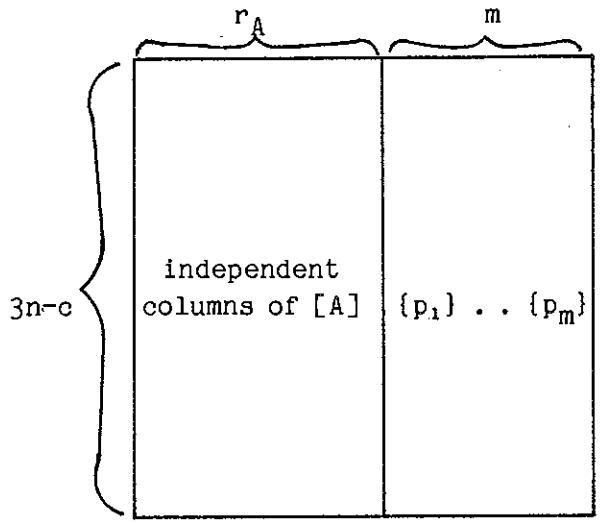

Fig. 4.9 The general form of [A']. The left-hand r_A columns represent the column space of [A] (Sections 4.1.1 and 4.2), and the right-hand m columns are the product-force vectors (Section 4.5) corresponding to the internal inextensional mechanisms. [A'] is square in the case (rb=0) of assemblies properly constrained to a rigid foundation.

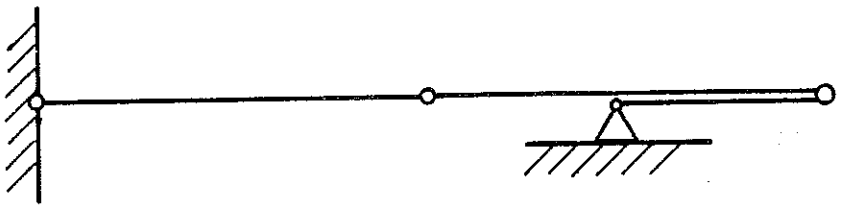

Fig. 4.10 A pin-jointed framework which is a finite mechanism, not an infinitesimal one, although [A'] has full rank. See Section 4.5. From Kuznetsov (1979).

mechanisms enables the prestressed bars to balance any vertical loads. The assembly thus has some first-order stiffness. Therefore it absorbs some energy as the load increases; and this energy is stored in the assembly in the only possible way, as strain energy associated with a second-order elongation of the bars. In this example it is clear from Pythagoras' theorem that second-order changes of length are needed for the distortion of this mechanism. It is also clear that this type of second-order stretching will in general tend to increase the level of prestress in the assembly, so that the relationship between transverse load and transverse deflection will in general be non-linear: it is only linear for sufficiently small deflections (see Chapter 6). When the assembly is prestressed, the transverse displacement which gives, geometrically, second-order changes in the length of the bars also gives a change in the strain energy of the same order, and thus imparts the first-order stiffness which is detected by the matrix method of Section 4.5.

The conclusion is that any first-order stiffness which a state of selfstress imparts to an inextensional mechanism may be taken as evidence that the geometry of distortion in fact requires second-order changes of length in the bars. If no first-order stiffness is detected by this method, then the inextensional mechanism is either a second- or higher-order infinitesimal mechanism or a finite mechanism, see Section 5.1. Tarnai's conjecture is thus confirmed.

4.7 Applications

This section looks at some applications of the methods described earlier in this chapter. All of the computations have been performed by means of a digital computer and the two Fortran programs GEAN1 and GEAN2 described in Fig. 4.11. Most of the figures have also been drawn by the computer. In order to highlight some common features, the examples are divided into four groups.

Plane trusses. Two types of Dixon linkages have already been encountered in Section 2.5, see Fig. 2.20. Starting from the simpler case of Fig. 2.20a it can be seen that it satisfies Maxwell's rule: n=6, b=9, therefore 2n-3=b; but a more complete analysis of it was done using GEAN2. The layout shown in Fig. 4.12 was tested, with the rigid-body motions suppressed by fully constraining node 1 and only allowing motions in the x direction for node 2;

GEAN1: Geometric analysis of 3D trusses

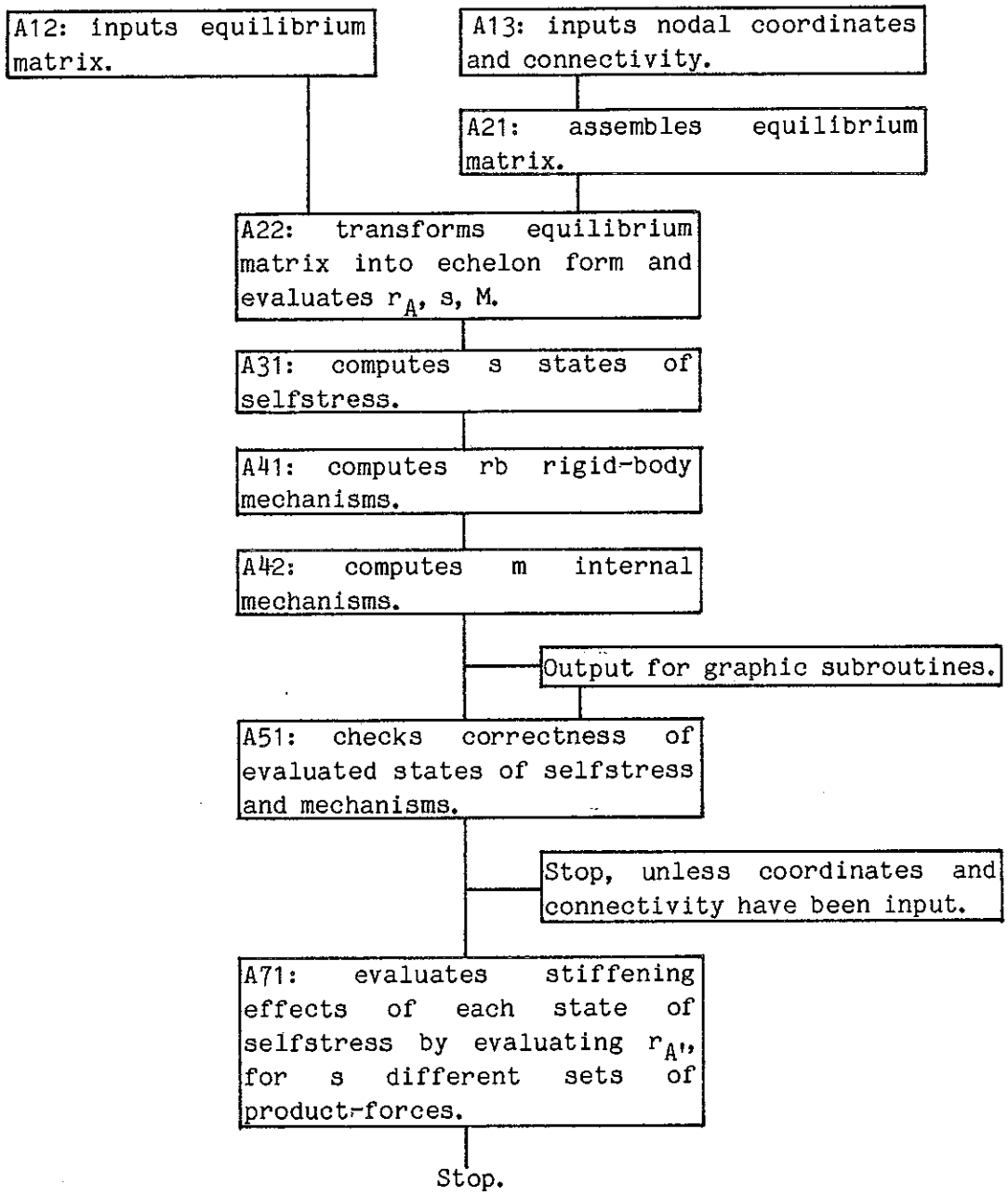

Fig. 4.11a Schematic flow chart of the program GEAN1 showing only essential subroutines. Note that the analysis can be started from a given equilibrium matrix by calling the subroutine A12.

GEAN2: Geometric analysis of 3D trusses
without rigid-body mechanisms.

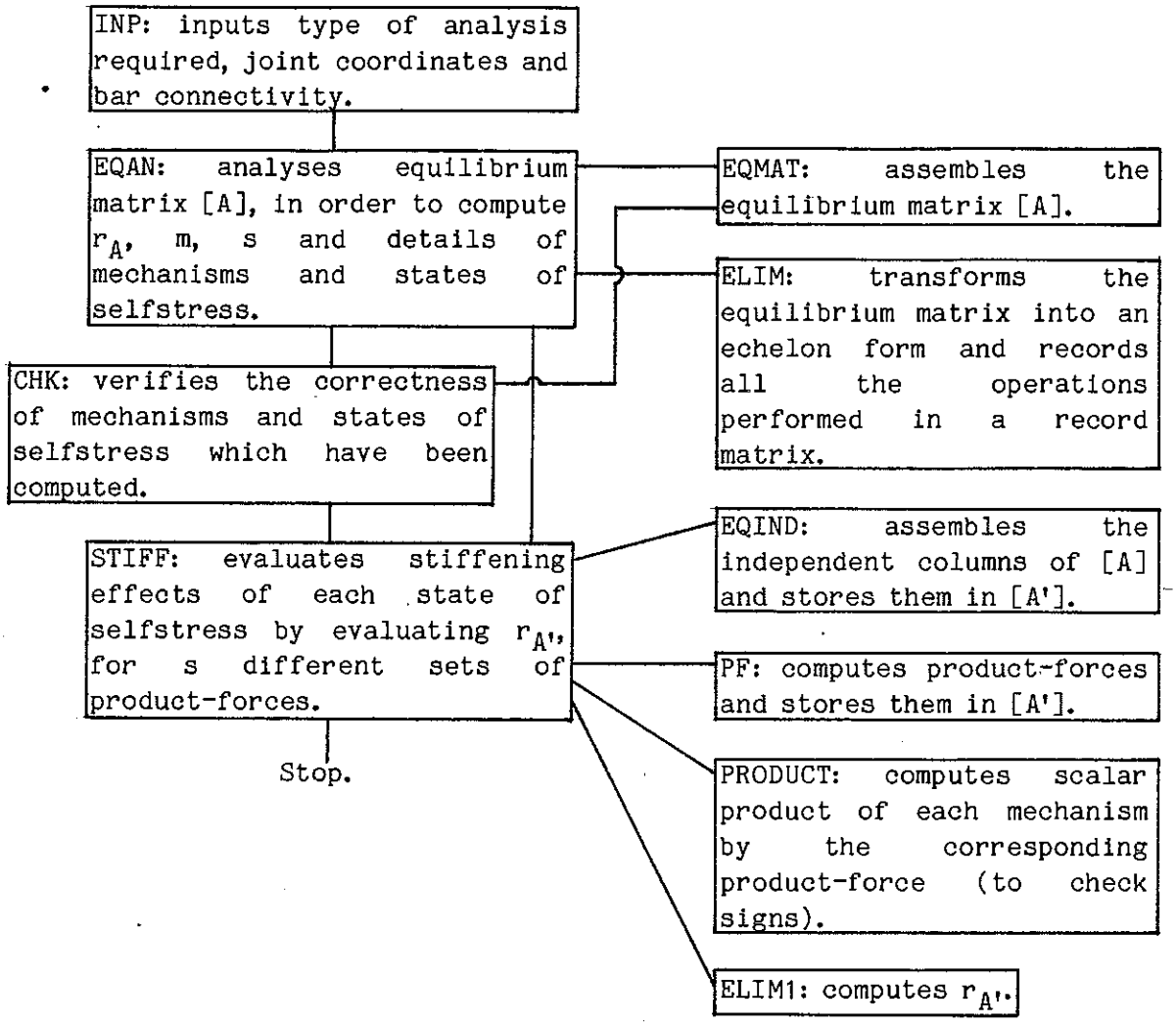

Fig. 4.11b Flow chart of the program GEAN2.

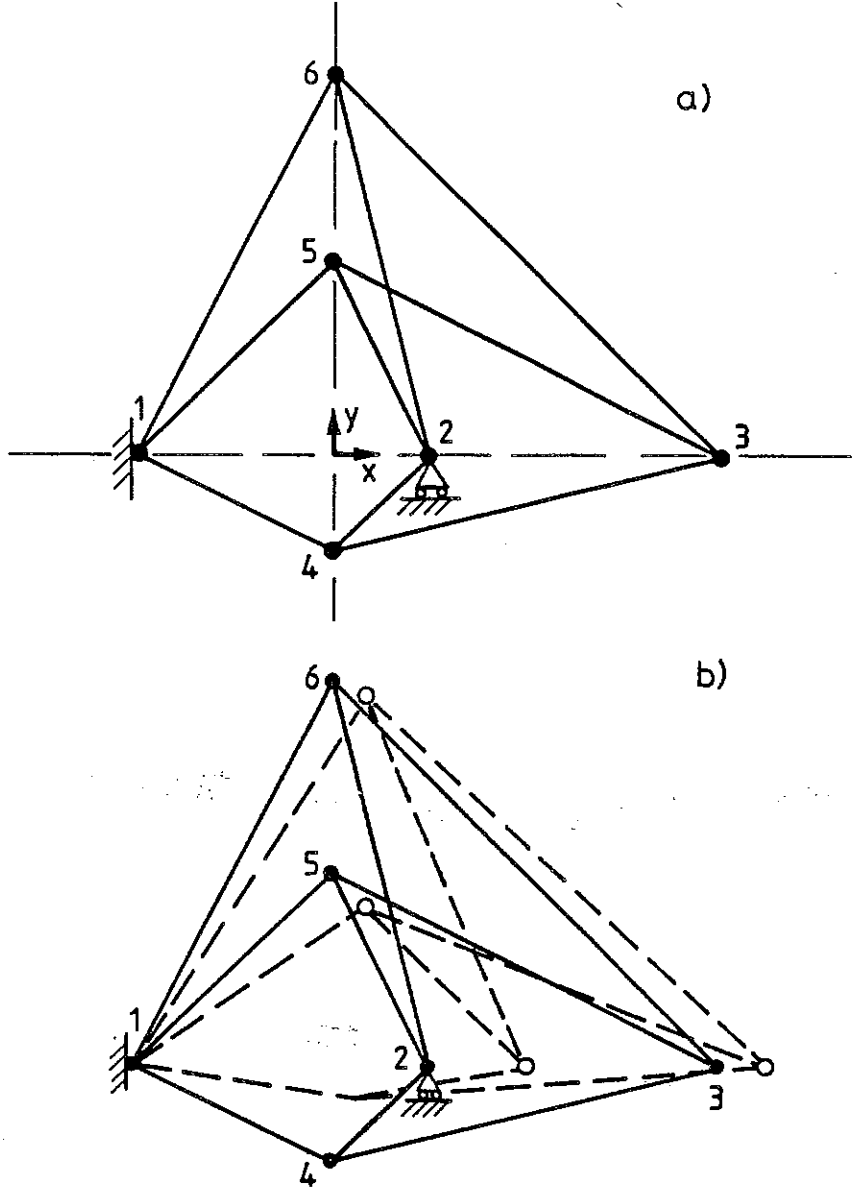

c)

Node no.	X	Y	Z	xc	yc	zc
1	-1.	0	0	1	1	1
2	.5	0	0	0	1	1
3	2.	0	0	0	0	1
4	0	-.5	0	0	0	1
5	0	1.	0	0	0	1
6	0	2.	0	0	0	1

Bar no.	Node no.	Node no.
1	1	4
2	1	5
3	1	6
4	2	4
5	2	5
6	2	6
7	3	4
8	3	5
9	3	6

Fig. 4.12 Dixon's linkage of the first kind (see also Fig. 2.20a) shown in its original position a). The linkage has been redrawn in b), with the infinitesimal mechanism shown in broken lines. The geometrical data for GEAN2 are shown in c): the last three columns of the array on the left define the nodal constraints (free=0, constrained=1).

obviously all nodes are 'constrained' to lie in the x-y plane. The geometrical data for the program are shown in Fig. 4.12c. The 9×9 equilibrium matrix has r_A=8; and so m=s=1. The components of the infinitesimal mechanism are displayed in Fig. 4.12b. The state of selfstress involves tensile forces in all the bars on the external contour, and in bar 5. There is only one product-force and its dot product with the mechanism is zero: prestress does not provide first-order stiffness, hence no second-order elongations are associated with the mechanism. This result is confirmed by the analysis of the matrix [A'] of Fig. 4.9: $r_{A'}$=8 so the product-force lies in the column space of [A].

One Dixon linkage of the second type (Fig. 2.20b) was also tested; it is easy to verify that the assembly in Fig. 4.13 satisfies all the geometrical conditions listed in the caption to Fig. 2.20b. All nodes were constrained to the x-y plane, 6 being fully constrained and 1 only allowed to move in the x direction. The results of the analysis were essentially the same as above. All of this agrees with Section 2.5: in fact both linkages are finite mechanisms.

'Ring' trusses. Figure 4.14 shows an assembly like the one already examined in Sections 2.1 and 2.4 (see Fig. 2.4a): a regular four-sided 'ring' on a level rigid base. The 12×12 matrix [A] is found to have r_A=11, and so m=s=1. The simple inextensional mechanism involves the upper square distorting into an out-of-plane diamond shape, as shown in Fig. 4.14b. There is one 'forbidden' load system (=mechanism), consisting of equal horizontal forces acting inwards along one of the diagonals of the top square and outwards along the other. The product-force consists of horizontal forces acting in the direction of the tangent to the square circumcircle, and following a common direction; it is therefore orthogonal to the 'forbidden' load condition. Hence $r_{A'}$=11, and this ring behaves like the plane mechanisms examined above. In fact, this assembly can undergo finite inextensional distortions, as one can verify with a cardboard model or by elementary trigonometry.

The assembly in Fig. 4.15 (cf. Fig. 2.10) consists of three rings like that of Fig. 4.14 on top of each other. It has been pointed out already that this assembly satisfies Maxwell's rule but is statically and kinematically indeterminate; the computer analysis shows that r_A=35 and s=m=1. It also shows that the bar tensions due to the state of selfstress vanish in all rings except the bottom one; while the inextensional mechanism only involves

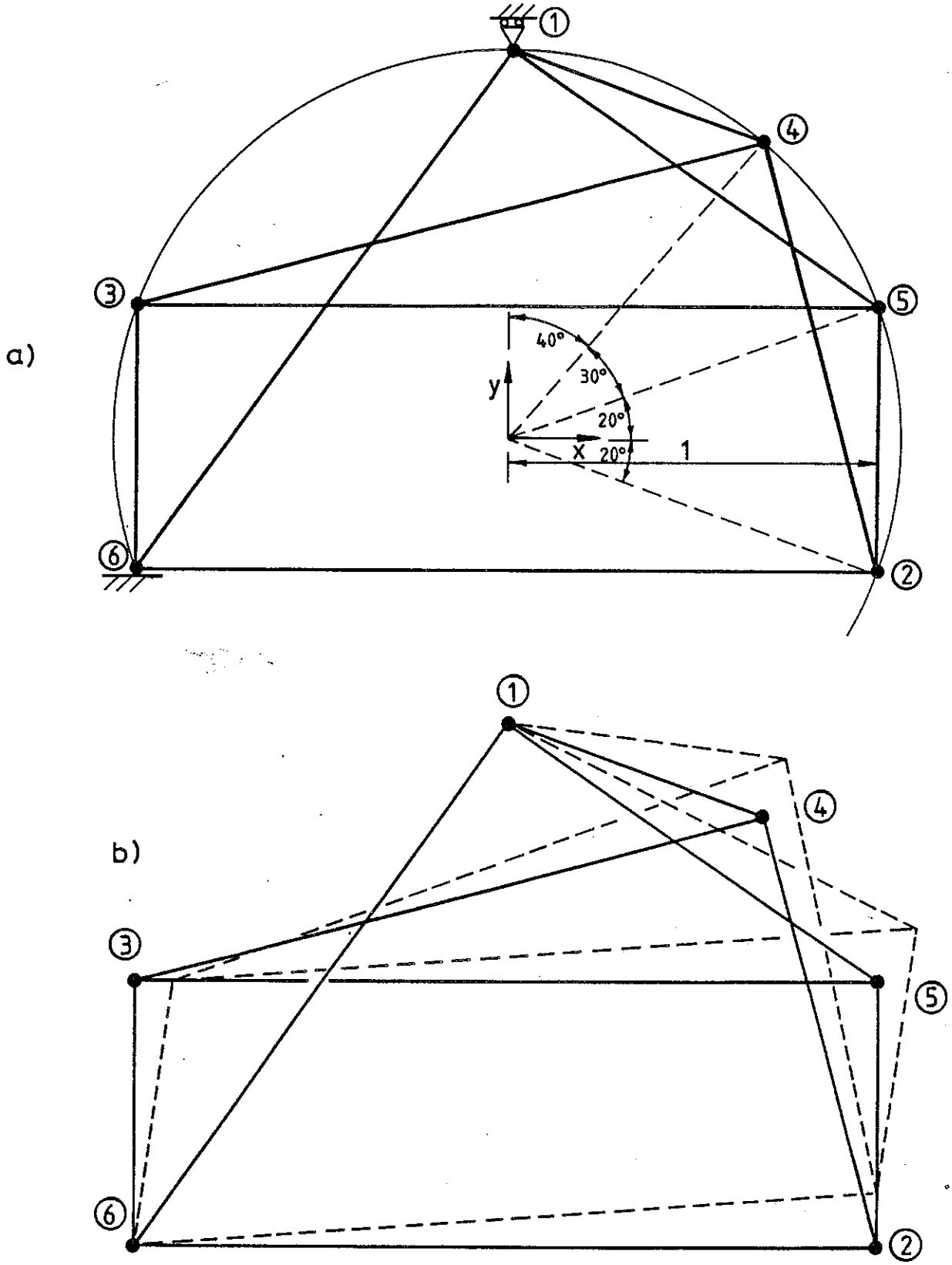

Fig. 4.13 Dixon's linkage of the second kind (see also Fig. 2.20b). b) shows the inextensional mechanism in broken lines.

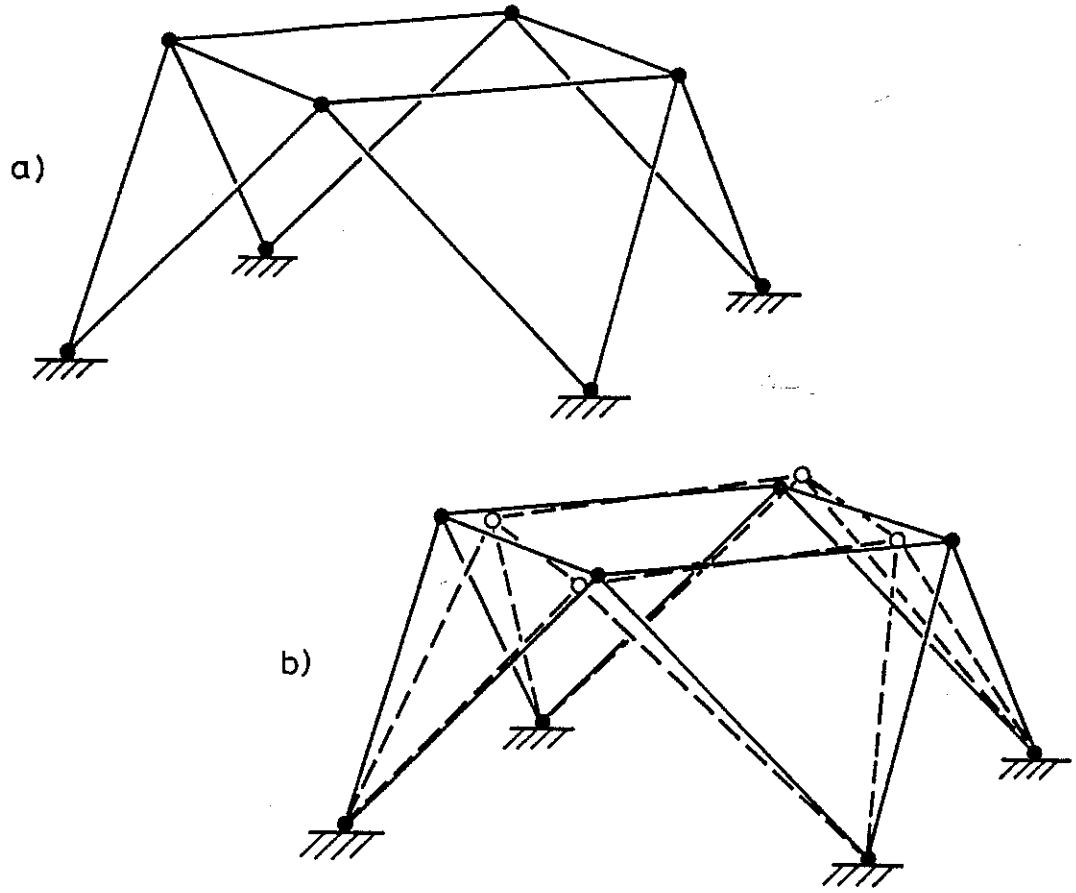

Fig. 4.14 'Ring' assembly consisting of a top square, with each corner connected by two bars to a level foundation. b) shows its free mechanism of inextensional displacement.

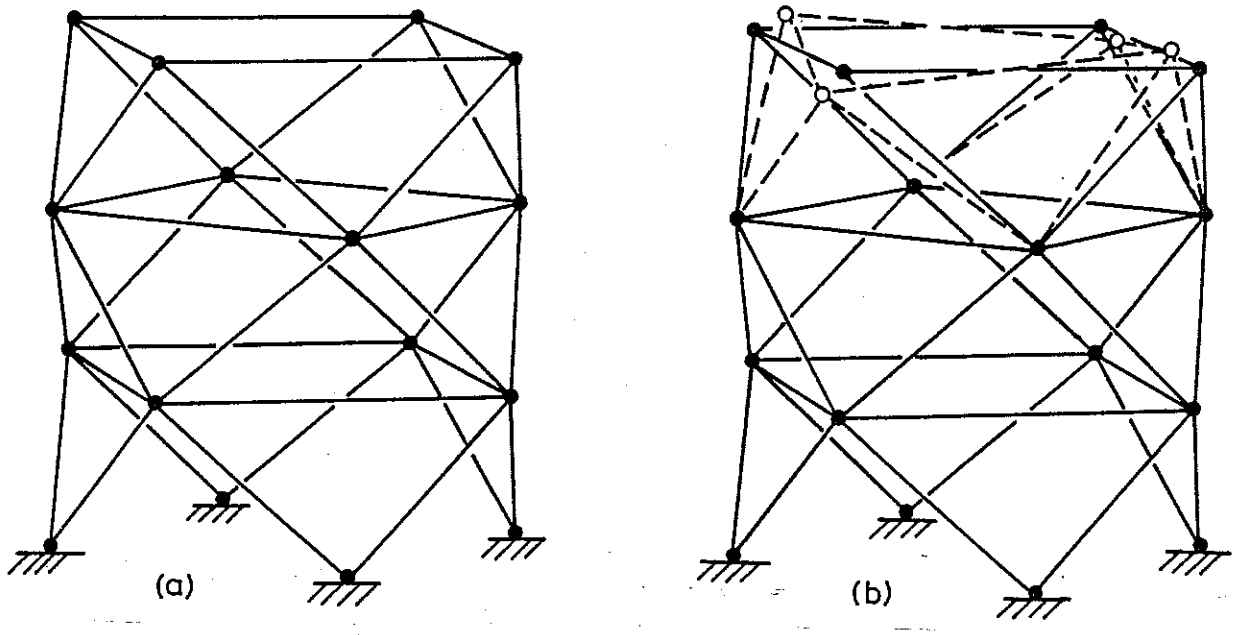

Fig. 4.15 Cylindrical tower consisting of three rings similar to Fig. 4.14. The computer analysis shows that the bottom ring is statically indeterminate, with one redundancy, while the top ring is kinematically indeterminate.

displacements of the top ring. Clearly the product-force is zero and $r_{A'}=35$.

The ring assembly shown in Fig. 4.16 has most of the features of the one shown in Fig. 4.14: in fact it satisfies Maxwell's rule with $3n-c=b=12$ and its equilibrium matrix has $r_A=11$, too. The mechanism is shown in Fig. 4.16b; the state of selfstress is also easy to visualize: two parallel four-hinge-arches carry compressive forces while the other two are in tension. Again the product-force has only horizontal components and $r_{A'}=11$; in fact this structure is a finite mechanism too.

Two variants of Fig. 4.16 are shown in Figs 4.17 and 4.18. Both of these trusses share the same horizontal projection but, while the foundation joints lie on one horizontal plane in Fig. 4.16, in Fig. 4.17 the 'legs' are shorter in one direction than in the other; and in Fig. 4.18 the square lies half-way between the horizontal planes containing the foundation joints. Both variants have $r_A=11$, and $m=s=1$ as in the ring considered first, but their mechanism is infinitesimal of first order as $r_{A'}=12$.

Some more trusses that satisfy Maxwell's rule. The truss in Fig. 4.19, a plan view of which is shown in Fig. 2.21a, consists of two pairs of adjacent quadrangles, lying in different horizontal planes and interconnected by diagonal members. In fact the truss is made out of five tetrahedra and four half-octahedra with various faces in common; the description of the structural geometry in these terms can be useful in understanding some of its kinematical properties. The tetrahedron in the middle of the framework - with vertices in nodes 4,6,7,9 of Fig. 2.21a - is a rigid structure and therefore all rigid-body motions can be suppressed by properly connecting it to the foundation. Six external constraints have been introduced in the analysis for this reason, but the pictures do not show them. The assembly has $n=12$, $b=30$ and $c=6$, hence $3n-c=b=30$; the 30×30 equilibrium matrix has $r_A=29$, thus $m=s=1$. The mechanism deforms the quadrangles in a twisting mode, as shown in Fig. 4.19b. Look at the plan view of Fig. 2.21a: the state of selfstress has equal compressive forces of two units in the bars joining nodes (6,7) and (4,9), which are the edges common to adjacent quadrangles; tensile and compressive unit axial forces alternate in the internal diagonals. For instance (1,4) and (2,4) are in compression while (4,7) is in tension; the eight bars on the outside of the figure (1,2),(2,5),... (3,1) are in tension; the remaining bars carry zero tension. The dot product between the product-force due to the

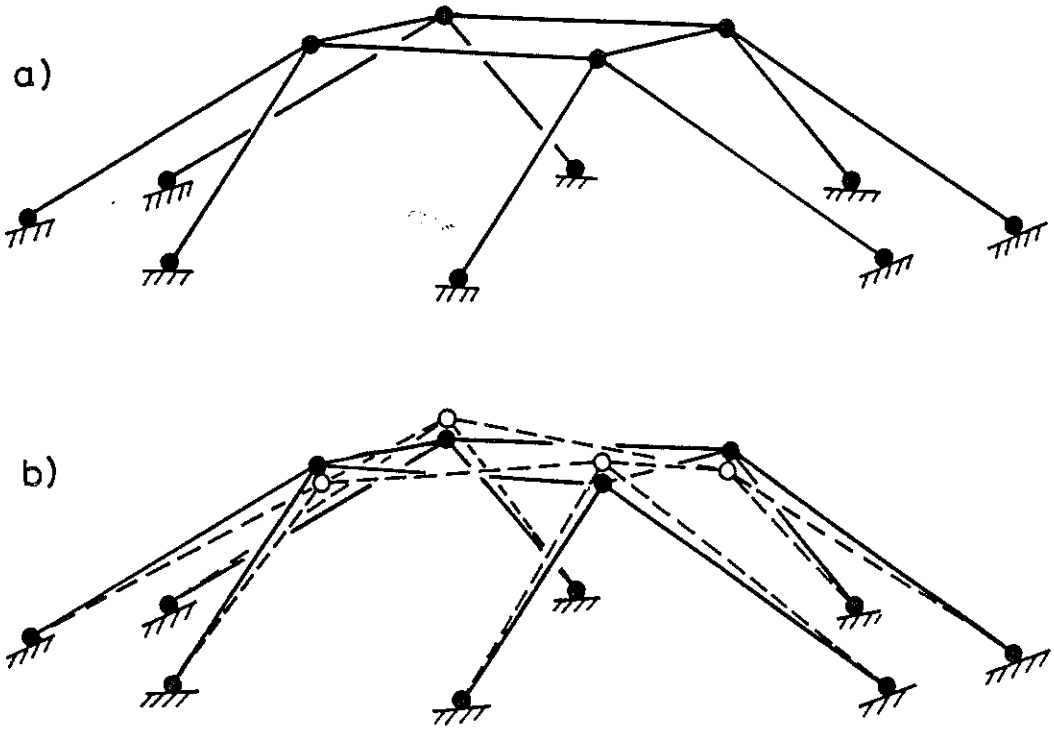

Fig. 4.16 Modified version of Fig. 4.14. Here there are eight foundation joints, all of which lie in a plane. b) shows the 'free' inextensional mechanism.

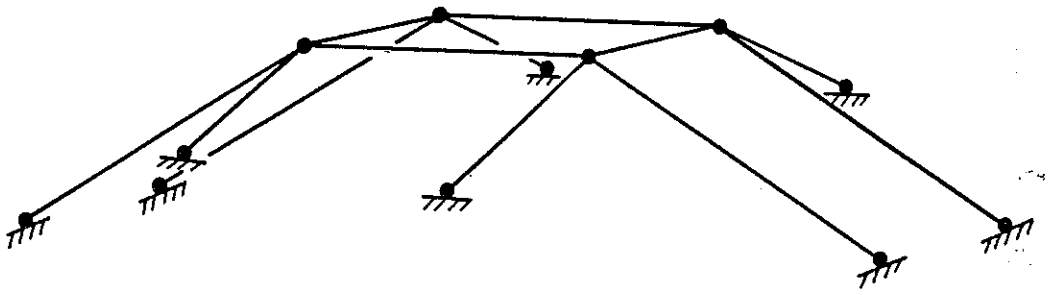

Fig. 4.17 Variant of Fig. 4.16. Four of the foundation joints lie on a higher horizontal plane than the remainder. Unlike the assemblies in Figs 4.14 and 4.16, this assembly is an infinitesimal mechanism, of first order.

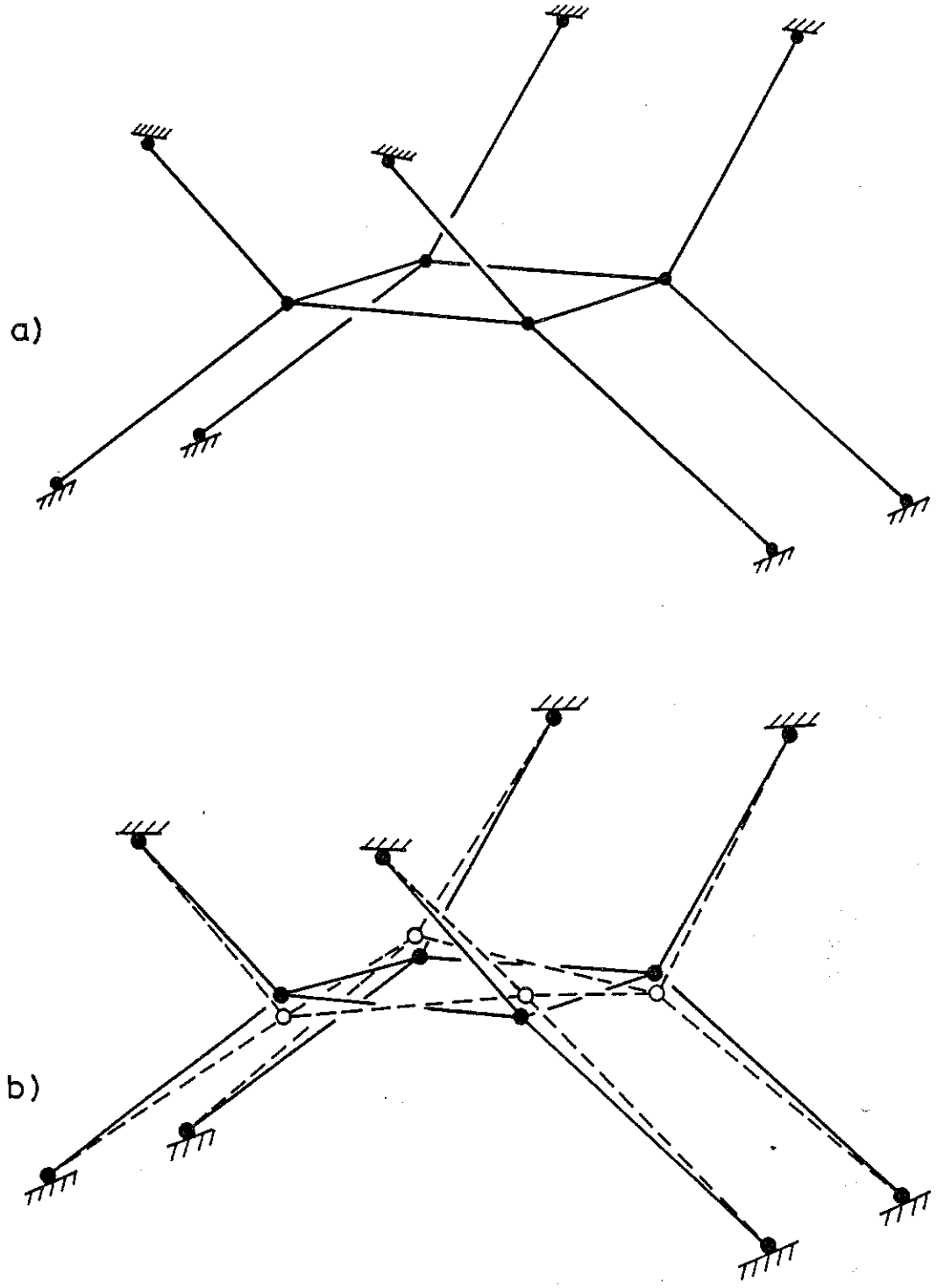

Fig. 4.18 Variant of Fig. 4.16. The foundation joints are now at equal distance above and below the horizontal plane containing the square. This assembly is an infinitesimal mechanism, of first order.

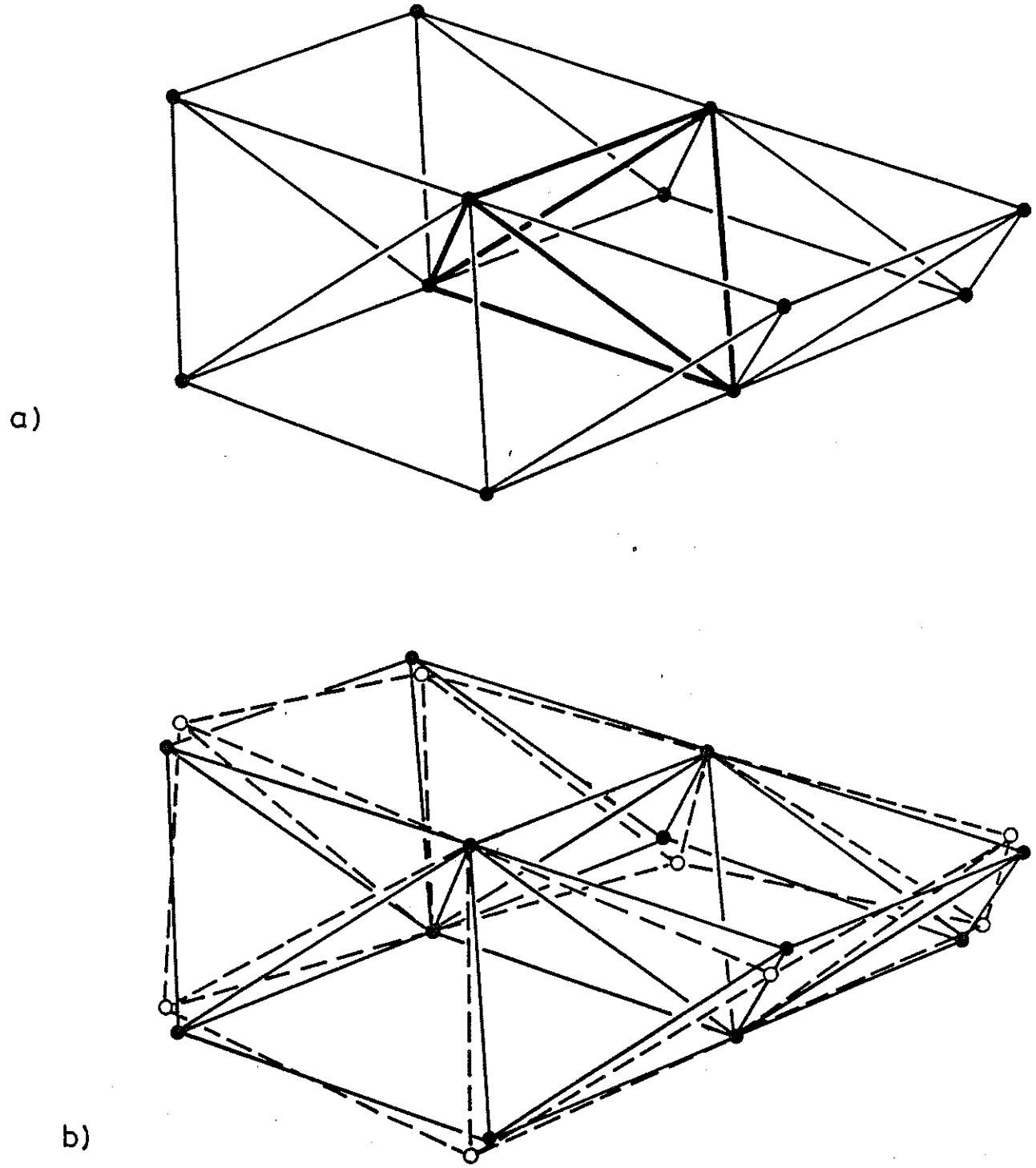

Fig. 4.19 "Tetrahedral-octahedral" truss. For the sake of simplicity, the internal tetrahedron - drawn with thicker lines - has not been allowed to move. See Fig. 2.21a.

above tensions and the mechanism is positive, therefore the mechanism is infinitesimal of first order. This conclusion can be verified by means of a physical model of this structure.

The triangulated hyperbolic paraboloids of Figs 4.20, 4.21 and 4.22 have been discussed already in Chapter 3; in fact their geometry fits with the geometrical description of Section 3.1. Each of these assemblies satisfies Maxwell's rule but the computer analysis shows that, although assemblies with two and three sides (shown in Figs 4.20 and 4.21) are statically and kinematically determinate, the hyperboloid with four sides (Fig. 4.22) has s=m=2. This result is in agreement with the formula s=m=(l-2) for l even found in Section 3.4.1. The two mechanisms produced by the computer analysis in this case are shown in Figs 4.22b and 4.22c. Of the two states of selfstress produced, the first one coincides with Fig. 3.3b while the second one can be obtained by adding up the two sets of tensions in Fig 3.3. The analysis of the matrices [A'], containing in their last two columns the product-forces due to either of the above independent states of selfstress, produces an interesting result. Only the second of the states of selfstress provides (equal) first-order stiffnesses to both mechanisms, which are therefore infinitesimal; but, in contrast, the first state of selfstress can only cause an increase by one of the rank of [A'].

Tensegrities. Only the first of the frameworks to be presented in this group satisfies Maxwell's rule, as all the others have fewer bars than would be required. Yet all of them have one state of selfstress, which involves tensile forces on the 'outside' of the framework and compressive 'inside', as in proper tensegrity systems. (The 'sign' of the selfstressing forces cannot be reversed, as noted at the end of Section 4.5). After the initial considerations on the formfinding of the "Simplex" made in Chapter 2 (see Fig 2.17), here it will be assumed that only one specific configuration is of interest, which is the one shown in Fig. 2.17b. A further examination of the ways in which this configuration can be determined will be deferred until the next chapter. All rigid-body motions of this assembly can be suppressed by imposing six kinematic constraints on the motion of the bottom triangle so that n=6, b=12 and c=6. The equilibrium matrix [A] is 12×12 with r_A=11; hence m=s=1. In the inextensional motion shown in Fig. 4.23b the top triangle rotates about a vertical axis while translating vertically; the

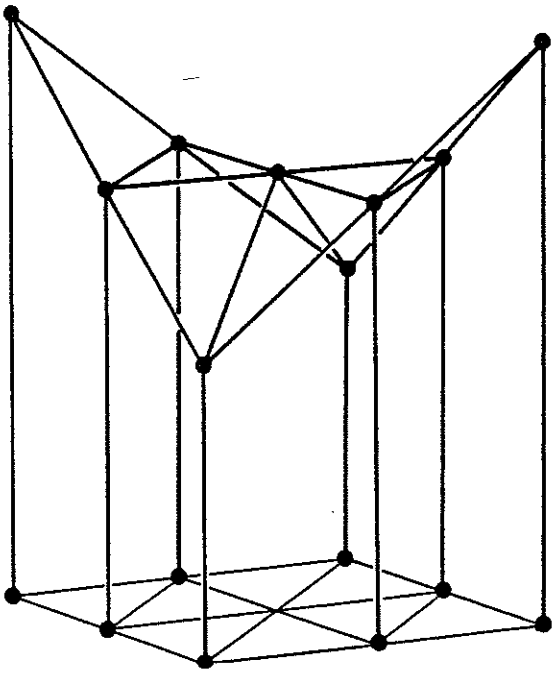

Fig. 4.20 Triangulated hyperbolic paraboloid, with l=2. The analysis described in Section 4.6 shows that s=m=0.

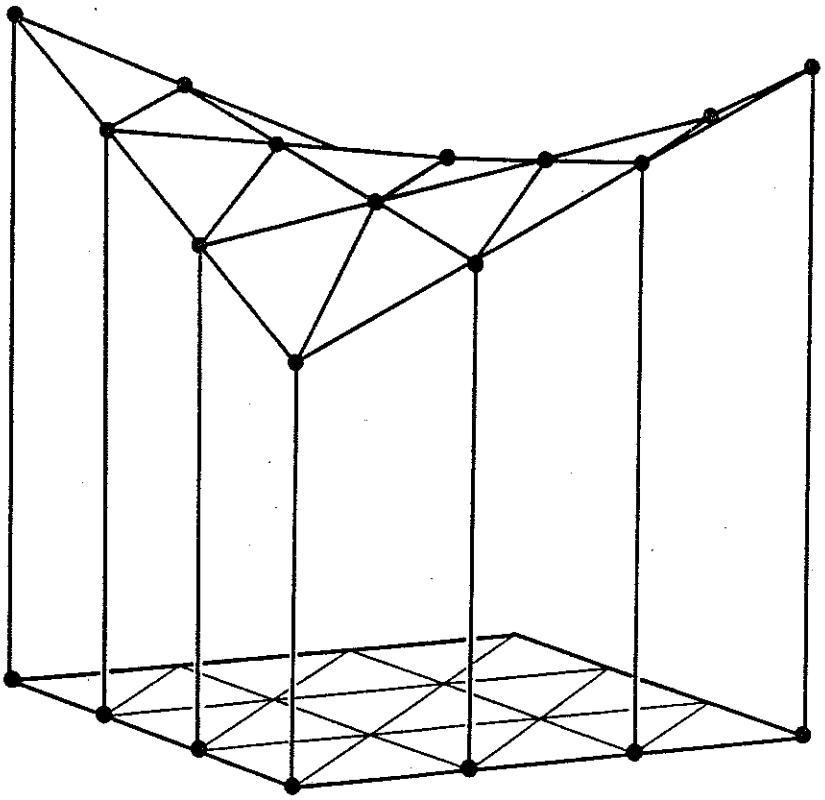

Fig. 4.21 Triangulated hyperbolic paraboloid, with l=3. Some of the bars are not shown. The analysis described in Section 4.6 shows that s=m=0.

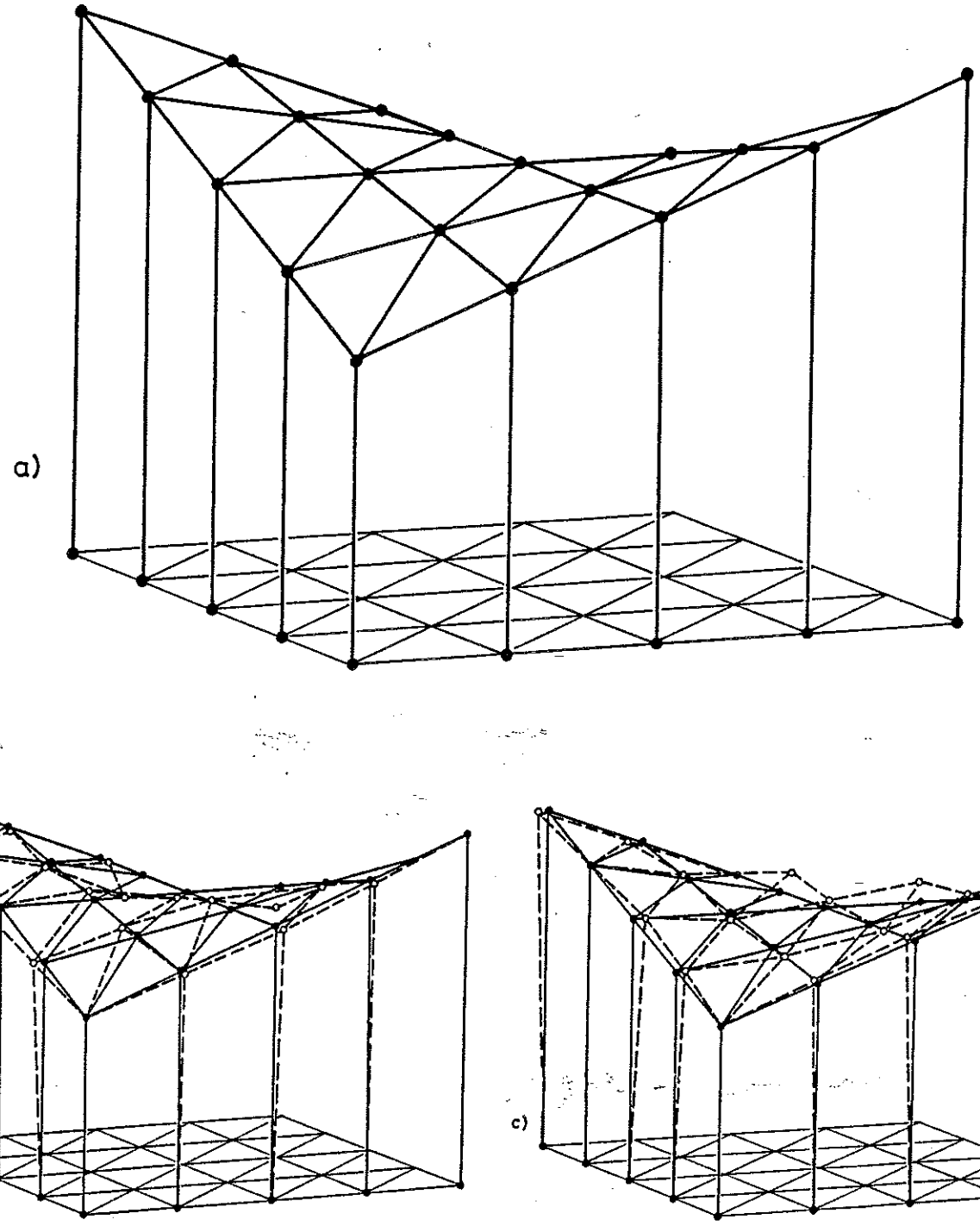

Fig. 4.22 Triangulated hyperbolic paraboloid, with l=4. Some of the bars are not shown. This assembly satisfies Maxwell's rule but s=m=2. b) and c) show the two infinitesimal mechanisms.

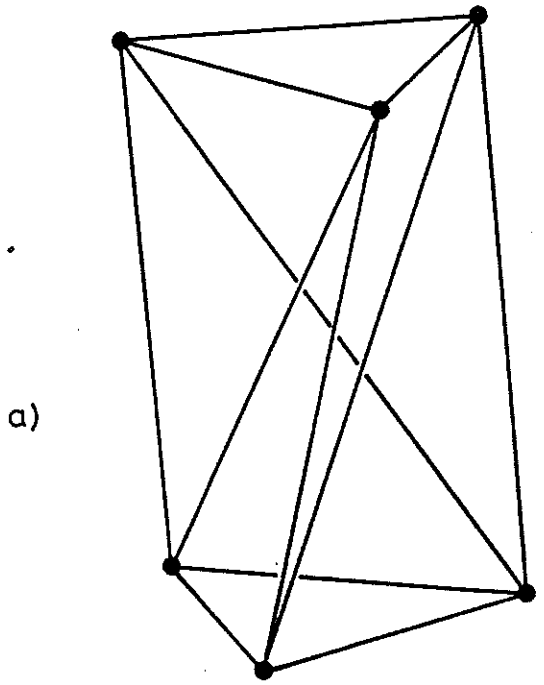

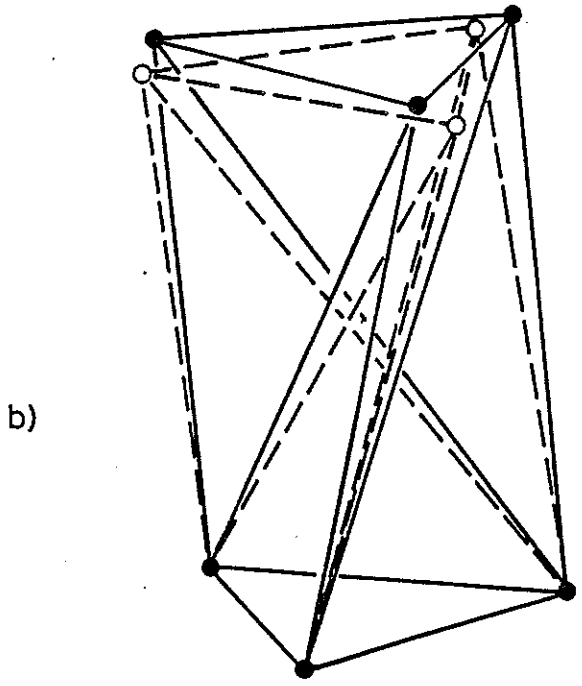

Fig. 4.23 "Simplex", cf. Fig. 2.17. b) shows the infinitesimal mechanism.

self-equilibrated tensions consist of tensile forces in all bars on the outside of the "Simplex", and compression in the three diagonals. [A'] has full rank and therefore the mechanism is infinitesimal of first order. This result, that is a common feature of tensegrities (Calladine, 1978), is no surprise after the experimental studies conducted by Motro (1983, 1984).

The next structure, Fig. 4.24a, has nodes which coincide with the vertices of a cube, and the outside bars also coincide with its edges; four inner diagonals complete the structure. This assembly has been studied 'free' in space, with n=8, b=16 and c=0. The equilibrium matrix has dimensions 24×16; its analysis shows that r_A=15, s=1, M=9. Clearly six of the mechanisms are rigid-body motions and only the three internal ones (m=M-6=3) are of interest. The internal mechanisms, computed along the lines of Section 4.4, are also shown in Fig. 4.24. In the first mode (Fig. 4.24b) top and bottom squares rotate through equal angles about a vertical axis anticlockwise and clockwise, respectively. In the second mode (Fig. 4.24c) top and bottom squares deform into two plane rhombi. Only in the third mode (Fig. 4.24d) these squares undergo an out-of-plane deformation: two opposite vertical edges go up, while the other two go down. The state of selfstress prescribes tensile forces in all the bars on the outside, and compression in the diagonals. When the product-forces are computed and assembled in [A'], it is found that $r_{A'}$=12; and thus the (prestressed) assembly has first-order stiffness against any load condition which is externally equilibrated. Therefore all three mechanisms are infinitesimal of first order. Calladine (1978) built and inspected a physical model of this truss and reached the same conclusions although the mechanisms he considered were all of the type shown in Fig. 4.24d; these are obviously a linear combination of the ones obtained in the present analysis and define an equivalent basis of the left-nullspace of [A].

The last example of this section is the truncated tetrahedral assembly of Fig. 4.25 (see also Fig. 2.14) first developed in 1952 by Della Sala. An investigation of this structure by Calladine (1978) has been summarized in Section 2.4; this study can be possibly regarded as a final test for the analytical approach developed here. The starting problem is obviously the evaluation of the initial geometry of the assembly: this will be assumed to be known a priori at present (Section 5.2 will give details on the simple

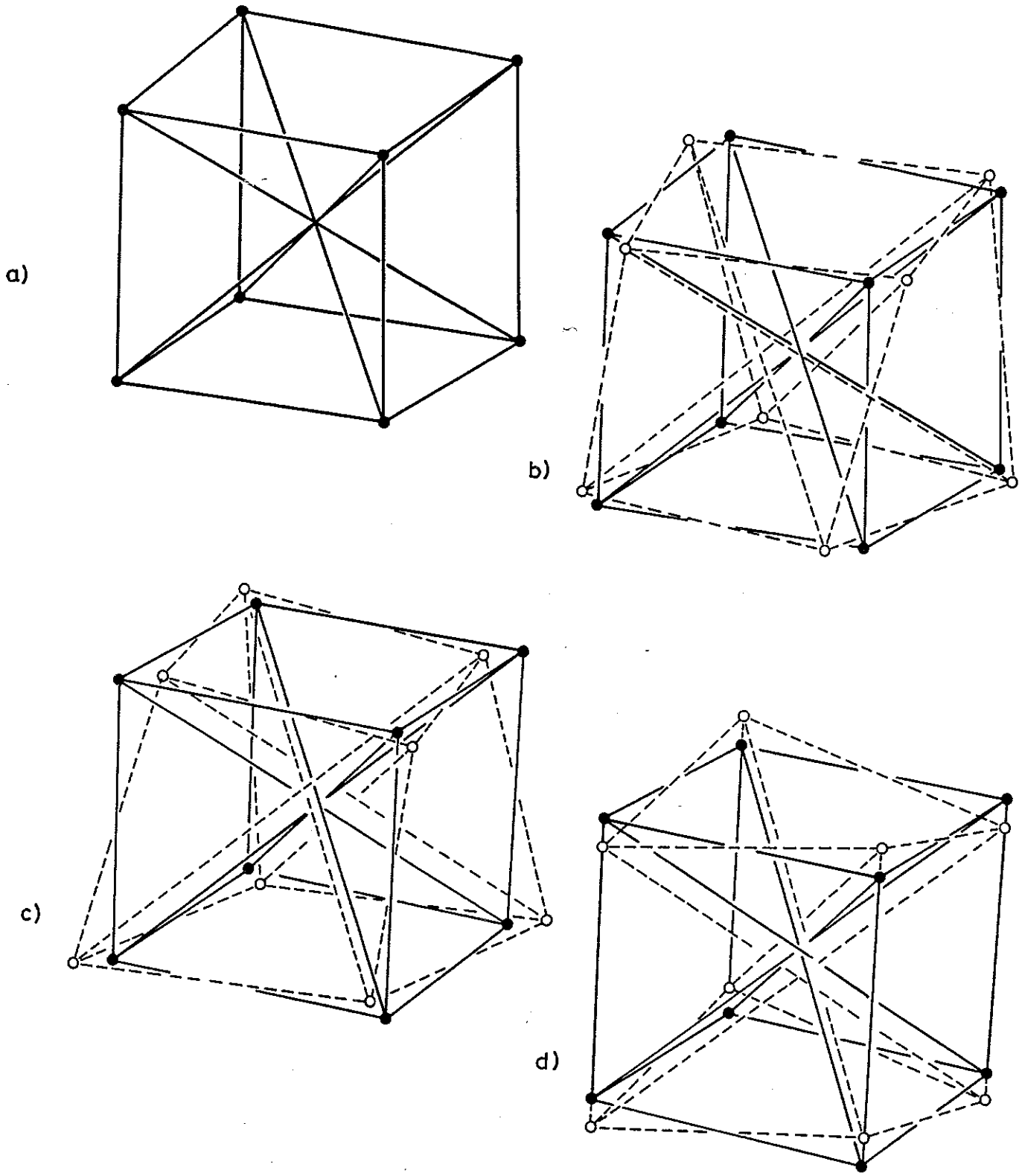

Fig. 4.24 Tensegrity cube. This is one of the assemblies that were examined by Calladine (1978). An alternative, equivalent, set of mechanisms can be obtained by displacing only parallel edges, as in d).

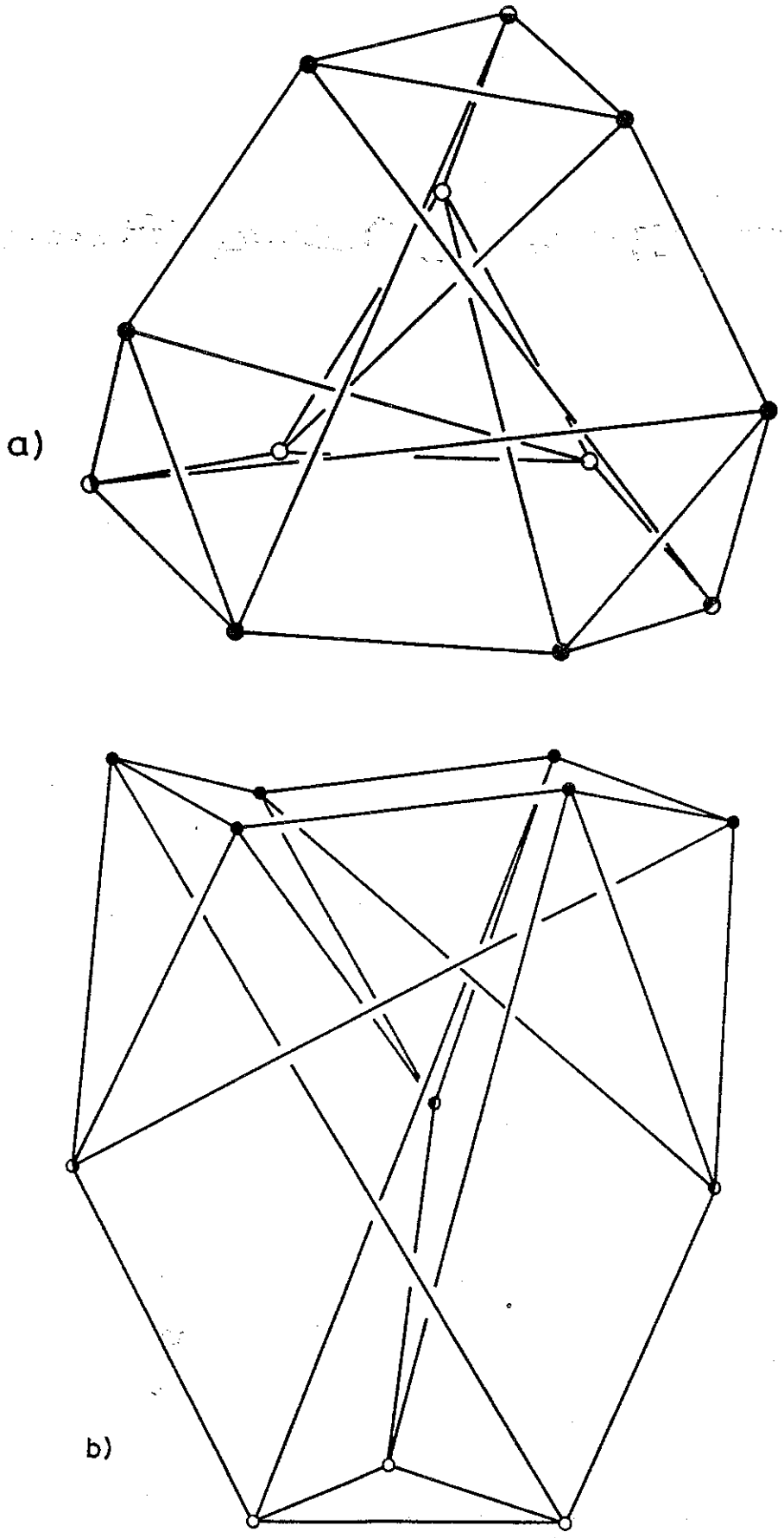

Fig. 4.25 Plan view and elevation of truncated tetrahedron studied in Section 4.7. In a), note the top hexagon and the three triangles connected to it; the bottom triangle lies in the middle of the plan view.

techniques that one may use to generate the nodal coordinates in this and similar cases). The bottom triangle has been connected to a rigid foundation by six constraints. By inspection, n=12, b=24 and c=6; the 30×24 matrix [A] has r_A=23; hence m=7 and s=1. All seven internal mechanisms have been computed in the usual manner, but only two representative ones are shown in Figs 4.26 and 4.27. The mechanism in Fig. 4.26 is actually the same as one described in the paper by Calladine, with one triangle rotating about an axis of three-fold symmetry of the initial geometry while the rest of the assembly does not move. The second mechanism reproduced here is a rather intricate combination of simple motions of the type described above. The state of selfstress has tensions of 1.5 units in the sides of the triangles (twelve bars in all), 2.066 in the remaining six bars on the outside of the framework, and compressive forces of 2.25 units in the six diagonals. The seven product-forces are independent of the 23 loads in the column space of [A], hence $r_{A'}$=30. All of this is in complete agreement with Calladine (1978).

4.8 Discussion

The theory developed in this chapter provides a comprehensive conceptual framework for the work started by Möbius (1837) and developed intermittently since then, as described in Chapter 2. It also clarifies and develops recent studies by Kuznetsov (1975, 1979), Calladine (1978) and Besseling (1978, 1979, 1981); a recent paper by Pellegrino & Calladine (1986) was the first attempt to divulge it.

It is noteworthy that Section 4.1 starts off from the definition of two 'geometrical' matrices and then pursues a line which would appear to be rather unorthodox to most structural analysts of the present day, since the displacement method of analysis appears to be used almost universally. Using the terminology and symbols of Section 4.1, the stiffness matrix - which is crucial for this conventional type of approach - of a framework with n nodes, b bars and c constraints is a square matrix [K] of dimension 3n-c such that

$$[K]\{d\}=\{f\} \qquad (4.23)$$

see ,e.g., Livesley (1975) or McGuire & Gallagher (1979). This matrix can be

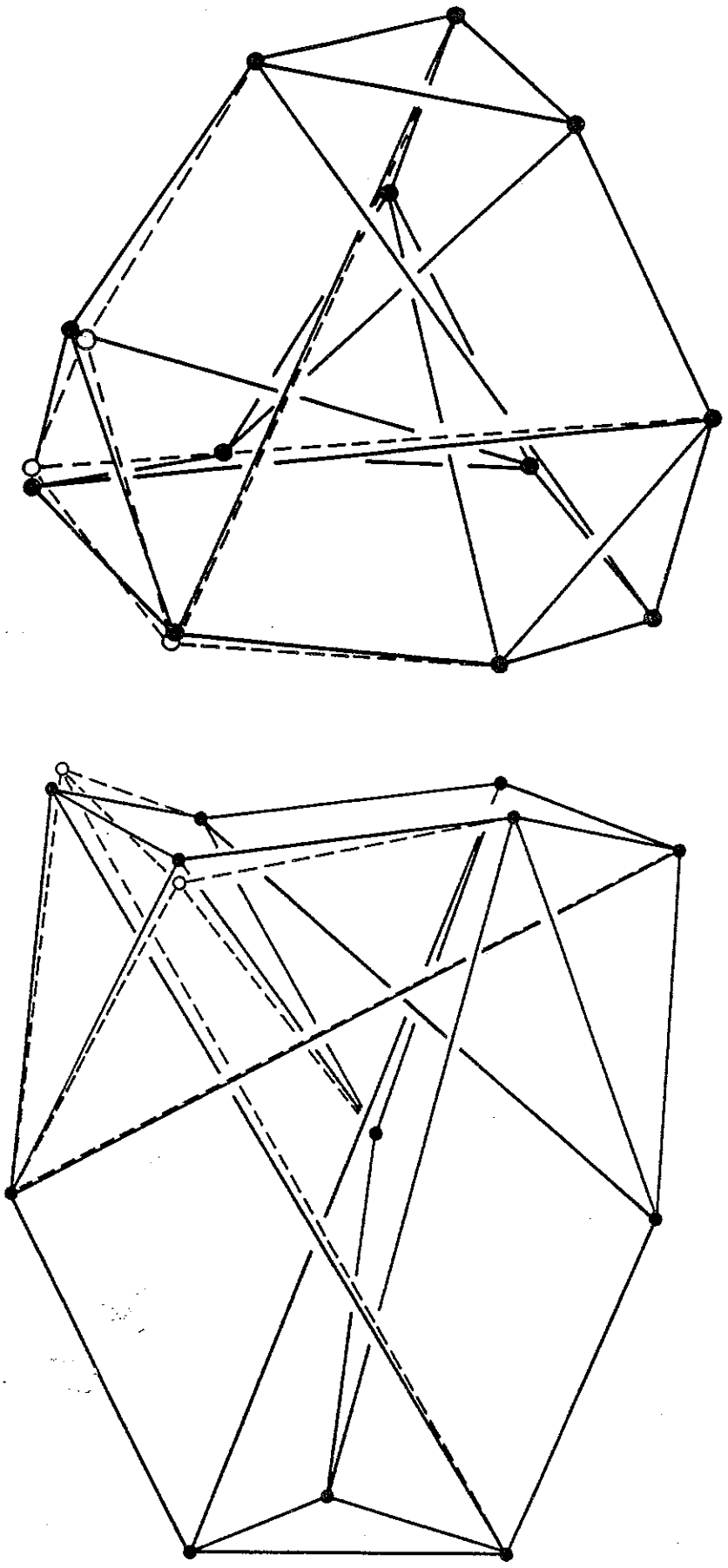

Fig. 4.26 Plan view and elevation of one of the seven infinitesimal mechanisms of the truncated tetrahedron shown in Fig. 4.25. In this particular mechanism, one of the triangles rotates about an inclined axis of three-fold symmetry.

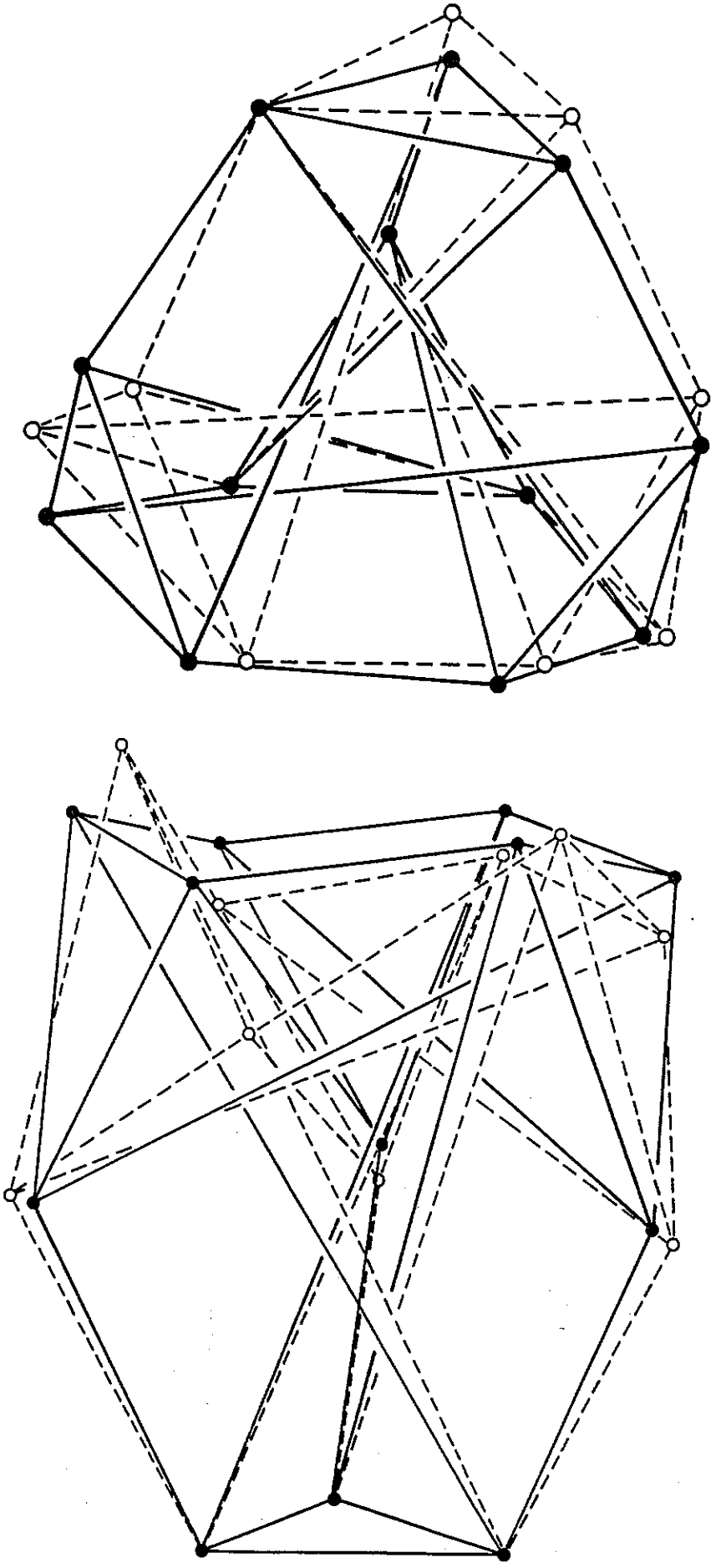

Fig. 4.27 Plan view and elevation of one of the seven infinitesimal mechanisms of the truncated tetrahedron shown in Fig. 4.25.

constructed by performing various operations on the equilibrium and compatibility matrices; and it is a linear operator that transforms any (3n-c)-dimensional vector {d} into a vector {f} of the same dimension. Further examination of this transformation in terms of the present ideas would be a topic worth investigating in some detail. Here it will be noted only that the solutions of the system of equations

$$[K]\{d\}=\{0\} \qquad (4.24)$$

are all sets of compatible nodal displacements in equilibrium without loads, and hence are the inextensional mechanisms of the assembly (also equal to the 'forbidden' load conditions in the left-nullspace of [A], see Table 4.1). The formulation (4.24) may lead numerically to a rather unstable method, yet it provides a way of obtaining some of the present results from a formulation which is widely used. Once m (or M) is known, s can be computed from (2.17) but this is all that can be obtained from [K].

An essential feature of the present work is that <u>all</u> the vital information about the behaviour of a structure can be obtained from an analysis of the equilibrium matrix. It seems unlikely that the same information can be abstracted from the conventional 'stiffness' formulation without considerable effort.

5. Further analysis. Formfinding

Although essentially self-contained, this chapter answers two questions left over from Chapter 4. Its first section deals with statically and kinematically indeterminate frameworks in which the activation of one of the mechanisms involves bar elongations which are of third- or higher-order in the magnitude of the given displacement, and also provides some examples of them. The present approach follows an entirely different route from that of Chapter 4, and leads eventually to a technique of analysis that - unlike the one based on Linear Algebra - can be refined according to the needs of the problem in hand. The second section tackles the formfinding of some of the tensegrity systems encountered in Section 4.7, i.e. it determines the shape in which an assembly of assigned 'connectivity' is able to sustain self-equilibrated states of tension.

5.1 Infinitesimal mechanisms of higher order

The linkage of Fig. 5.1a is a statically and kinematically determinate two-dimensional assembly in which the (rigid) triangle 1 2 3 is connected to a rigid foundation by three members which do not meet in one point. If A and B coincide, see Fig. 5.1b, 1 2 3 can rotate about A: the assembly has now one mechanism and one state of selfstress, as demonstrated by the analysis of Chapter 4. This analysis also provides the vectors indicated in the caption of Fig. 5.1. It is intuitive that such a linkage cannot undergo very large displacements if the member lengths are to be preserved; this is confirmed by the computation of the rank of [A'], equal to 6, and is most easily checked by evaluation of the dot product: $\{\text{product-force}\}^T\{\text{mechanism}\}=1.875$ (>0; of course, reversing the signs of the selfstressing tensions would give negative stiffness). The state of selfstress can therefore impart first-order stiffness to the linkage; this means - as noted elsewhere - that the 'small' displacement indicated in Fig. 5.1 is associated with second-order bar elongations.

Now consider the linkage of Fig. 5.2a, which is obtained by moving point 5 of Fig. 5.1b to a different position, still collinear with A3; and also the one in Fig. 5.2b where both 3 and 5 are in different positions. These two assemblies are also statically and kinematically indeterminate, because all

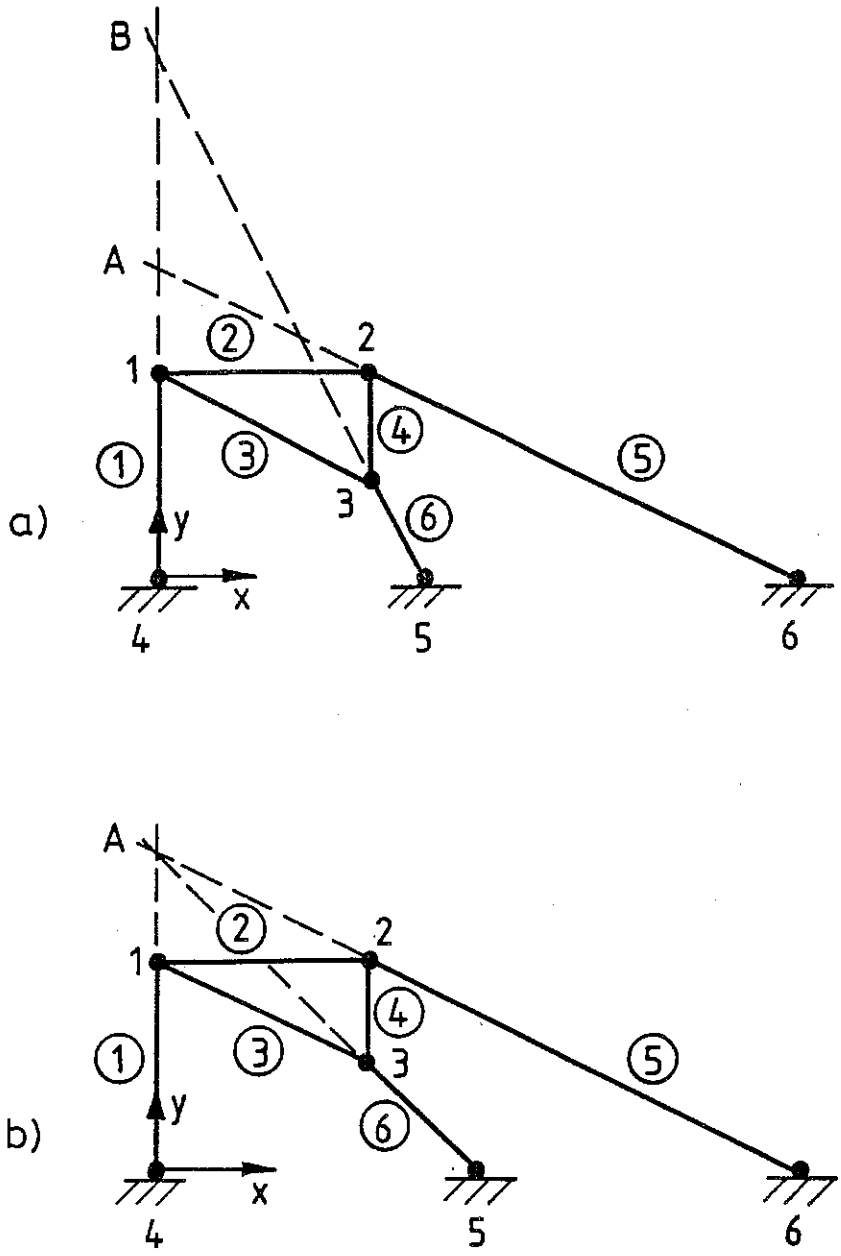

Node no.	x	y
1	0.	2.
2	2.	2.
3	2.	1.
4	0.	0.
5a	2.5	0.
5b	3.	0.
6	6.	0.

Fig. 5.1 Plane linkages examined in Section 5.1; their nodal coordinates are indicated above.
a) has $2n=b=r_A=6$, and hence it is statically and kinematically determinate.
b) has $2n=b>r_A=5$, hence it is statically and kinematically indeterminate, with $m=s=1$. The components of its mechanism are

$$\{0.5 \;\; 0 \;\; 0.5 \;\; 1 \;\; 1 \;\; 1\}^T$$

and the state of selfstress (tension coefficients) is

$$\{-.25 \;\; -.50 \;\; +.50 \;\; +.50 \;\; -.25 \;\; +1.00\}^T$$

The corresponding product force is:

$$\{-.375 \;\; 0 \;\; -.375 \;\; -.750 \;\; +1.500 \;\; +1.500\}^T$$

It is shown in the text that b) is an infinitesimal mechanism, of first order.

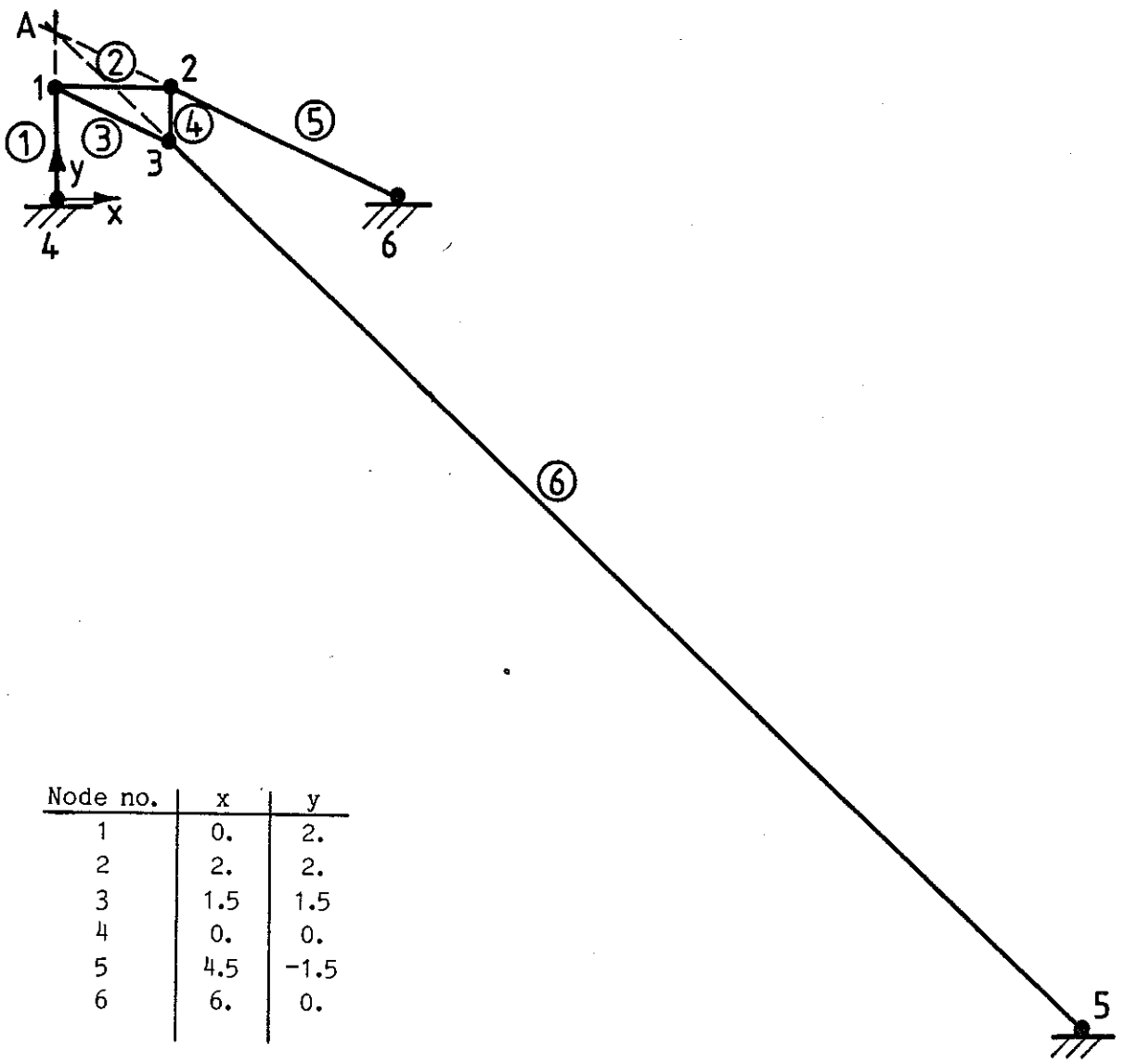

Node no.	x	y
1	0.	2.
2	2.	2.
3	1.5	1.5
4	0.	0.
5	4.5	-1.5
6	6.	0.

Fig. 5.2a Plane linkage examined in Section 5.1. It has $2n=b=6>r_A=5$, hence it is statically and kinematically indeterminate, with $m=s=1$. The components of its mechanism are

$$\{0.5 \quad 0 \quad 0.5 \quad 1 \quad 1 \quad 1\}^T$$

and the state of selfstress (tension coefficients) is

$$\{-4 \quad -8 \quad 8 \quad 8 \quad -4 \quad 1\}^T$$

The corresponding product-force is

$$\{-6 \quad 0 \quad -6 \quad -12 \quad 9 \quad 9\}^T$$

It is shown in Section 5.1.2 that this linkage is an infinitesimal mechanism, of order two.

the members connecting the triangle to the foundation meet in one point; this is confirmed by the the results of the analyses of the respective equilibrium matrices. An unexpected result of these calculations is that $r_{A'}=r_A=5$ in both cases, which can be verified as the product of product-force by mechanism gives zero. Does this contradict the 'intuitive' statement above and imply that the two linkages are finite mechanisms? The answer is no.

These assemblies have been provided by J.M. Prentis for their special characteristics. In the first assembly (Fig. 5.2a) node 5 coincides with the centre of curvature of the path described by node 3 so that no second-order elongation of bar 6 is required; the second assembly (Fig. 5.2b) also satisfies the above condition but 3 is now also a point for which the rate of change of path curvature vanishes, hence no third-order elongation of bar 6 takes place. These are therefore examples of structures in which an infinitesimal distortion provokes only third-order and fourth-order elongations of bar 6, respectively. All of this assumes that no change of length occurs in the remaining members of the linkage.

Although kinematically indeterminate layouts that one encounters in practice may well prove to have the properties detected above, these properties seem to have received very little attention in the past, apart from the rather theoretical studies described in Section 2.5. A suitable starting point for the present study is the following classification proposed by Koiter (1984) and Tarnai (1984a).

Consider a structure which is kinematically indeterminate, with m=1; its mechanism can be either <u>finite</u>, in which case "there exists a finite motion such that the elongation of every bar is zero" (Tarnai, 1984a), or <u>infinitesimal</u> if the activation of the mechanism provokes some bar elongations. Infinitesimal mechanisms can be classified by considering the McLaurin expansion of the elongation of one of the bars in the assembly - on the assumption that the remaining bars are of infinite axial stiffness - in terms of a displacement parameter δ:

$$e(\delta)=a_1\delta+a_2\delta^2+a_3\delta^3+... \qquad (5.1)$$

where the coefficient $a_1=0$ if δ activates an infinitesimal mechanism. "An infinitesimal mechanism of order n has $a_1=a_2=...=a_n=0$ but $a_{n+1}\neq 0$" (Tarnai,

1984a). This definition is in agreement with Connelly (1980). Tarnai (1984b) has constructed the structure of Fig. 5.3 as an example that can turn itself into a mechanism belonging to any of the defined categories. Tarnai (1984a) has also pointed out that, although a finite mechanism is also an infinitesimal mechanism of infinite order, for which all the terms of (5.1) vanish, the McLaurin expansion (5.1) is unsuitable to distinguish between finite and infinitesimal mechanisms of infinite order.

According to the classification proposed, the assemblies of Figs 5.1b, 5.2a and 5.2b are of first, second and third order, respectively.

To classify a kinematically indeterminate framework one can use the matrix method of Chapter 4, or just compute the dot product indicated above, to decide if the mechanism is of first order. If $r_A=r_{A'}$, the mechanism is either infinitesimal of order ≥ 2 or finite; and this may already be an answer good enough for practical purposes. If more precise information is needed one may think of computing the coefficients of (5.1) by expanding in a power series the elongation of one particular bar of the given framework, while the lengths of the remaining members are kept fixed. This requires an ad hoc formulation for each different configuration and it may well prove to be unfeasible in case of large three-dimensional structures.

An approach which is sufficiently general, and which might be proved to be equivalent to the one described above, is based upon the analysis of the stability of the assembly in its initial configuration - an idea first appeared in Kuznetsov (1975). The following description uses the terminology which is standard in investigations of elastic stability: see, e.g., Thompson & Hunt (1973, 1984). It is intuitive that any kinematically indeterminate framework - now regarded as an assembly of linear-elastic bars - which has a position of stable equilibrium, under no loads, in its original configuration is an infinitesimal mechanism. The order of the mechanism is related in a simple way to the order of the analysis required to ascertain that the given configuration is stable. The mechanism is finite if the initial configuration is of neutral equilibrium.

Consider a space framework which has m=1. The analysis of the stability of this assembly can be done, in general terms, by looking at its Total Potential Energy (Thompson & Hunt, 1973): therefore the initial step must be the introduction of this function.

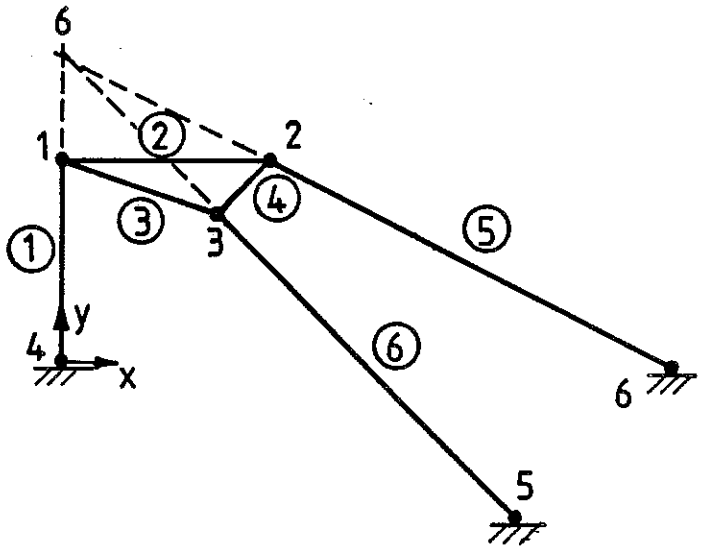

Node no.	x	y
1	0.	2.
2	2.	2.
3	2.	1.0
4	0.	0.
5	18.	-15.
6	6.	0.

Fig. 5.2b Infinitesimal mechanism of third order examined in Section 5.1. This plane linkage has m=s=1, the mechanism components are

$$\{0.50 \quad 0 \quad 0.50 \quad 1 \quad 0.75 \quad 0.75\}^T$$

and the state of selfstress (tension coefficients) is

$$\{-.750 \quad -2.25 \quad 3 \quad 3 \quad -.750 \quad .750\}^T$$

The corresponding product-force is

$$\{-1.125 \quad 0 \quad -1.125 \quad -2.25 \quad 2.25 \quad 2.25\}^T$$

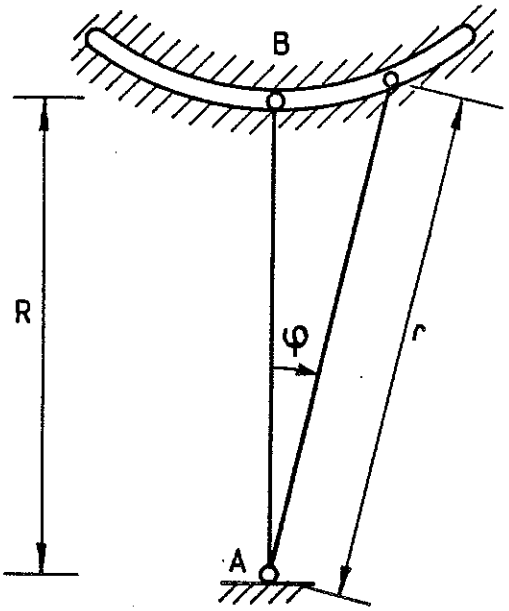

Fig. 5.3 Example proposed by Tarnai (1984b): bar AB can rotate about A while B slides in the rigid slot of equation $r(\phi)=R+C_1\phi^{n+1}+C_2e^{-1/\phi^2}$.
The following cases can be obtained:

$C_1 \neq 0$, $n=0$ -> the structure is not a mechanism
$C_1 \neq 0$, $n \geq 1$ -> mechanism of order n
$C_1 = 0$, $C_2 \neq 0$ -> mechanism of ∞ order
$C_1 = C_2 = 0$ -> finite mechanism.

In the initial stress-free configuration let node i have coordinates X_i, Y_i, Z_i; consider a small distortion of the assembly which brings node i to (X_i+x_i), (Y_i+y_i), (Z_i+z_i). Geometrical compatibility obviously requires that the lengths of the connecting bars also change by corresponding amounts, and the elongation of bar p (see Fig. 4.3) linking nodes i and j is $e_p=(l_p)_{new}-l_p$,

where: $l_p=\sqrt{(X_i-X_j)^2+....}$

$$(l_p)_{new}=\sqrt{(X_i+x_i-X_j-x_j)^2+....}=$$
$$=\sqrt{l_p^2+2[(X_i-X_j)(x_i-x_j)+...]+(x_i-x_j)^2+...}$$

and the work absorbed by this (linear-elastic) bar during the deformation is:

$$(AE/2l)_p\{\sqrt{l_p^2+2[(X_i-X_j)(x_i-x_j)+...]+(x_i-x_j)^2+...}-l_p\}^2$$

The strain energy in the whole assembly is obtained by adding up the contributions from all members. As there are neither applied forces - hence the change of potential energy of the external loads is zero - nor any initial prestress - hence the strain energy associated with the initial configuration is zero - the strain energy/elastic work absorbed described above coincides with the Total Potential Energy (TPE):

$$TPE=\frac{1}{2}\sum_{p=1}^{b}(AE/l)_p\{\sqrt{l_p^2+2[(X_i-X_j)(x_i-x_j)+...]+(x_i-x_j)^2+...}-l_p\}^2 \quad (5.2)$$

The initial configuration of the framework is of stable equilibrium if it corresponds to a local minimum of TPE; it is of neutral equilibrium if there exists one path starting from it along which TPE vanishes identically. This allows a classification of mechanisms in terms of an analytical condition on a function of 3n-c variables. However, one last problem has to be dealt with before any calculation can be started: the initial problem looks 'purely geometrical' but the function in (5.2) depends upon the elastic constants of the bars. This contradiction has its roots in the very definition of structural mechanisms. Strictly speaking a <u>purely geometrical</u> analysis of the rigidity of an ideal assembly whose rods are inextensible would only segregate <u>finite mechanisms</u> from <u>rigid structures</u>. For present purposes the bars of the assembly must not be absolutely inextensible although the actual

value of their elastic constants is of no consequence because TPE is the sum of b non-negative definite functions and the whole point of the analysis is the identification of paths on which TPE, and hence all b terms of the summation (5.2), vanish within a chosen degree of accuracy. In conclusion it can be assumed that $(AE)_p=1$ in (5.2).

The next subsection attempts the standard textbook analysis associated with the computation of an analytical minimum; this will clarify the points described above but will also show that realistic situations cannot be tackled in this way. A more cunning technique will therefore be developed and tested on the linkages of Figs 5.1b and 5.2a. In case of kinematically indeterminate frameworks with m>1 everything said above is still valid for each of the mechanisms, separately; but further work is required to assess the validity of the computational procedure in Section 5.1.2.

5.1.1 Analysis of TPE using total differentials

The analysis broadly indicated in the previous secion is now developed and applied to the two-bar plane linkage of Fig. 5.4. The Total Potential Energy can be obtained by substituting the nodal coordinates of 1,2,3 into (5.2); or alternatively by considering the bar elongations due to an arbitrary change of configuration:

$$e_1=\sqrt{(1+x)^2+y^2}-1,\quad e_2=\sqrt{(1-x)^2+y^2}-1$$

$$\begin{aligned} e_1^2/l_1&=2+2x+x^2+y^2-2\sqrt{1+2x+x^2+y^2}\\ e_2^2/l_2&=2-2x+x^2+y^2-2\sqrt{1-2x+x^2+y^2}\end{aligned} \qquad (5.3)$$

from which, assuming AE=1, $TPE=(e_1^2/l_1+e_2^2/l_2)/2$. The results of the rather laborious computation of all the derivatives of TPE with respect to the variables x,y, in the initial configuration x=y=0, are displayed in Table 5.1. This is the raw material for the analysis.

The linkage of Fig. 5.4 is certainly an infinitesimal mechanism, therefore its TPE should be minimum for x=y=0. The McLaurin expansion of TPE can be written (Fiorenza & Greco, 1978) in the form:

$$TPE(x,y)=dTPE+d^2TPE/2!+d^3TPE/3!+... \qquad (5.4)$$

1st order	$\partial TPE/\partial x=0$	3rd order	$\partial^3 TPE/\partial x^3=0$
	$\partial TPE/\partial y=0$		$\partial^3 TPE/\partial x^2\partial y=0$
2nd order	$\partial^2 TPE/\partial x^2=2$		$\partial^3 TPE/\partial x\partial y^2=0$
	$\partial^2 TPE/\partial x\partial y=0$		$\partial^3 TPE/\partial y^3=0$
	$\partial^2 TPE/\partial y^2=0$	4th order	$\partial^4 TPE/\partial x^4=0$
			$\partial^4 TPE/\partial x^3\partial y=0$
			$\partial^4 TPE/\partial x^2\partial y^2=-4$
			$\partial^4 TPE/\partial x\partial y^3=0$
Table 5.1			$\partial^4 TPE/\partial y^4=6$

where:

$$dTPE=[(\partial TPE/\partial x)dx+(\partial TPE/\partial y)dy]_{x=y=0}=0$$

$$d^2TPE=[\partial^2 TPE/\partial x^2)dx^2+2(\partial^2 TPE/\partial x\partial y)dxdy+(\partial^2 TPE/\partial y^2)dy^2]_{x=y=0}=2dx^2$$

$$d^3TPE=[(\partial^3 TPE/\partial x^3)dx^3+3(\partial^3 TPE/\partial x^2\partial y)dx^2dy+ \quad (5.5)$$
$$+3(\partial^3 TPE/\partial x\partial y^2)dxdy^2+(\partial^3 TPE/\partial y^3)dy^3]_{x=y=0}=0$$

$$d^4TPE=[(\partial^4 TPE/\partial x^4)dx^4+4(\partial^4 TPE/\partial x^3\partial y)dx^3dy+6(\partial^4 TPE/\partial x^2\partial y^2)dx^2dy^2+$$
$$+4(\partial^4 TPE/\partial x\partial y^3)dxdy^3+(\partial^4 TPE/\partial y^4)dy^4]_{x=y=0}=-4dx^2dy^2+6dy^4$$

a general expression - which resembles Leibniz' formula for the nth power of a sum - can provide d^nTPE but only the four terms given above are needed at present.

(i) $dTPE=0$, therefore the Total Potential Energy is stationary in the original configuration and may be minimum in it.

(ii) There would definitely be a minimum if $d^2TPE>0$ for any choice of dx,dy but it is clear from (5.5) that $d^2TPE=0$ for any change of configuration with $dx=0$; subject to the above condition the analysis has to continue. Incidentally, notice that the displacements $\{0\ dy\}^T$ - that must be considered from now on - are the same as those that would be provided by the matrix method of Chapter 4; in fact the two calculations are equivalent. Also notice that a kinematically indeterminate assembly with m mechanisms is bound to have $d^2TPE=0$ along m paths starting from its original configuration.

(iii) The third and fourth order differentials have to be examined: the necessary condition for a minimum is that $d^3TPE=0$; which is satisfied.

(iv) As in (ii) the condition $d^4TPE>0$ is sufficient for a minimum. Is $6dy^4-4dx^2dy^2>0$? Certainly yes, since $dx^2=0$.

The linkage of Fig. 5.4 is therefore an infinitesimal mechanism, of order one because the above analysis only went up to second-order elongations.

The first comment on the calculation just performed is that, of course, the product-force calculation of Chapter 4 would have been perfectly adequate for the structure in hand; but any more interesting mechanism of order, say, two would also require the examination of d^5TPE and d^6TPE. This could be rather an achievement if the framework has more than one node and two members! This leads to a second remark which will appear trivial to the reader expert in differential calculus but is stated here as a warning against possible misunderstandings: the condition $dx^2=0$ obtained in (ii) does not have any implications on the higher-order increments of x. This will be emphasized in the next section; here it suffices to say that the method described above requires the computation of a very large number of derivatives of TPE, because only few of them can be recognized a priori as giving no contribution to the differential of a particular order.

5.1.2 Analysis of TPE along suitable paths

The impracticality of considering total differentials, which derives from the rapidly increasing number of derivatives one has to compute to perform higher-order analyses, is resolved by the present simplified method of attack in which variations of TPE will now be considered only along one direction. The crucial point to grasp is that the initial analysis of dTPE and d^2TPE does provide some information on the equation of the path along which the nodes of the framework move during an inextensional displacement, although it may not coincide with the straight 'line' which has direction cosines proportional to the first-order components of the infinitesimal mechanism. Thus the third- and fourth-order differentials required for the classification of Fig. 5.4 cannot be limited to the y direction. More precisely, one has to consider all the paths which are tangent to the computed mechanism, or indeed to the path computed in a lower-order analysis, if the same idea is to be employed for differentials of arbitrary order. Among all of these paths, one has to consider the one for which the change of TPE is minimum. See Fig. 5.5.

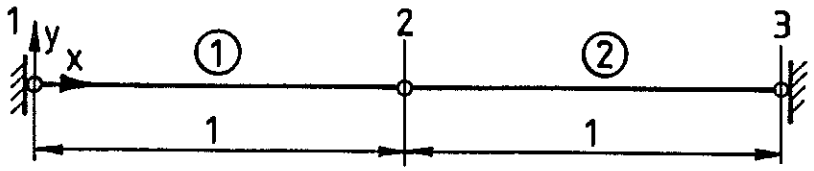

Fig. 5.4 Plane linkage with $2n=b=2>r_A=1$ studied in Sections 5.1.1 and 5.1.2.

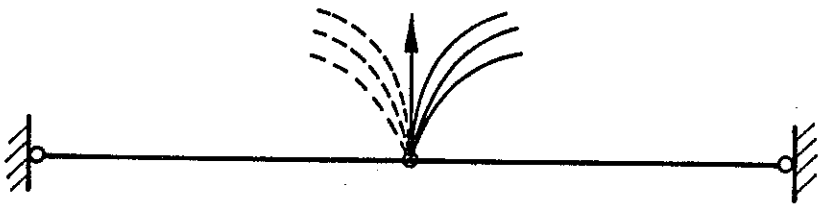

Fig. 5.5 Various node paths tangent to the infinitesimal mechanism -indicated by a solid arrow- of the assembly shown in Fig. 5.4.

The mechanics of the procedure will be explained by repeating the analysis for the linkage of Fig. 5.4. An independent parameter λ can be taken to denote the nodal component of displacement in the y direction; on the assumption that only paths with a polynomial expression need to be considered here, the most general equation for a path is:

$$x=\sum_{i=1}^{n} a_i\lambda^i,\quad y=\lambda$$

where the n constants a_i are all unspecified at the beginning. Only the first term of the summation is required for d^3TPE and d^4TPE, giving a quadratic path:

$$x=a_2\lambda^2,\quad y=\lambda \qquad (5.6)$$

Substitute (5.6) into (5.3) to obtain:

$$e_1^2/l_1=2+(1+2a_2)\lambda^2+a_2^2\lambda^4-2\sqrt{1+(1+2a_2)\lambda^2+a_2^2\lambda^4}$$
$$e_2^2/l_2=2+(1-2a_2)\lambda^2+a_2^2\lambda^4-2\sqrt{1+(1-2a_2)\lambda^2+a_2^2\lambda^4}$$

which define $TPE(\lambda)=(e_1^2/l_1+e_2^2/l_2)/2$. The list of derivatives provided in Table 5.2 enables one to obtain the following:

$$(TPE)_{\lambda=0}=(2-2+2-2)/2=0$$
$$(dTPE/d\lambda)_{\lambda=0}=0$$
$$(d^2TPE/d\lambda^2)_{\lambda=0}=[2(1+2a_2)-2(1+2a_2)+2(1-2a_2)-2(1-2a_2)]/2=0$$
$$(d^3TPE/d\lambda^3)_{\lambda=0}=0$$
$$(d^4TPE/d\lambda^4)_{\lambda=0}=\{24a_2^2-[24a_2^2-1.5(2+4a_2)^2]+24a_2^2-[24a_2^2-1.5(2-4a_2)^2]\}/2=$$
$$=6+24a_2^2$$

therefore $dTPE=d^2TPE=d^3TPE=0$ and everything said in Section 5.1.1 is still valid. This leads to the analysis of $d^4TPE=(6+24a_2^2)d\lambda^4$, the minimum value of which is 6; hence TPE is minimum in the initial configuration and the assembly is confirmed to be a mechanism of first order.

1	$(f'/\sqrt{f})_{\lambda=0}=0$
2	$(f''/\sqrt{f})_{\lambda=0}$
3	$(f'''/\sqrt{f})_{\lambda=0}$
4	$(f^{iv}/\sqrt{f}-1.5(f'')^2/f^{3/2}))_{\lambda=0}$
5	$(f^{v}/\sqrt{f}-5f''f'''/f^{3/2})_{\lambda=0}$
6	$(f^{vi}/\sqrt{f}-5[1.5f''f^{iv}-(f''')^2]/f^{3/2}+11.25(f'')^3/f^{5/2})_{\lambda=0}$

Table 5.2 The derivatives of $2\sqrt{f(\lambda)}$, with f differentiable six times and $f'(0)=0$.

The above technique, which was first introduced by Thompson & Hunt (1973), displays its full potential when applied to the study of the linkages of Figs 5.1b and 5.2a. Starting from the framework of Fig. 5.1b, the elongations in (5.3) are replaced by:

$$
\begin{aligned}
e_1^2/l_1&=[x_1^2+(y_1+2)^2+4]/2-2\sqrt{x_1^2+(y_1+2)^2}\\
e_2^2/l_2&=[(-x_1+x_2+2)^2+(y_1-y_2)^2+4]/2-2\sqrt{(-x_1+x_2+2)^2+(y_1-y_2)^2}\\
e_3^2/l_3&=[(-x_1+x_3+2)^2+(y_1-y_3+1)^2+5]/\sqrt{5}-2\sqrt{(-x_1+x_3+2)^2+(y_1-y_3+1)^2}\\
e_4^2/l_4&=(x_2-x_3)^2+(y_2-y_3+1)^2+1-2\sqrt{(x_2-x_3)^2+(y_2-y_3+1)^2}\\
e_5^2/l_5&=[(x_2-4)^2+(y_2+2)^2+20]/\sqrt{20}-2\sqrt{(x_2-4)^2+(y_2+2)^2}\\
e_6^2/l_6&=[(x_3-1)^2+(y_3+1)^2+2]/\sqrt{2}-2\sqrt{(x_3-1)^2+(y_3+1)^2}
\end{aligned}
\qquad (5.7)
$$

For the linkage of Fig. 5.2a the only change is that the bottom line of (5.7) is replaced by:

$$e_6^2/l_6=[(x_3-16)^2+(y_3+16)^2+512]/16\sqrt{2}-2\sqrt{(x_3-16)^2+(y_3+16)^2}$$

The 'first-order' analysis could be now repeated by solving the system of equations $d^2TPE=0$ but for the sake of brevity the infinitesimal mechanism will not be recomputed here. Denote, as above, by an independent parameter λ the vertical component of displacement of node 3; a 'straight' displacement tangent to the infinitesimal mechanism has $x_1=x_2=.5\lambda$, $y_1=0$, $y_2=x_3=y_3=\lambda$. And the path equation of the lowest order that one must consider is now:

$$
\begin{aligned}
x_1 &= .5\lambda + a_1\lambda^2 \qquad & y_1 &= \quad a_2\lambda^2 \\
x_2 &= .5\lambda + a_3\lambda^2 \qquad & y_2 &= \lambda + a_4\lambda^2 \\
x_3 &= \lambda + a_5\lambda^2 \qquad & y_3 &= \lambda
\end{aligned}
\tag{5.8}
$$

Substitution of (5.8) into (5.7) provides the expressions for e_i^2/l_i in the six bars of the framework, from which TPE(λ) is obtained. The values of TPE and of its differentials up to the fourth order, obtained by using the derivatives in Table 5.2, are

$$TPE)_{\lambda=0} = dTPE)_{\lambda=0} = d^2TPE)_{\lambda=0} = d^3TPE)_{\lambda=0} = 0$$

$$
\begin{aligned}
d^4TPE)_{\lambda=0} = k[&13.7243a_1^2 + 9.4311a_2^2 + 10.8622a_3^2 + 16.7155a_4^2 + 11.3812(6.0779)a_5^2 \\
&-5.7243a_1a_2 - 16a_1a_3 - 11.4487a_1a_5 + 5.7243a_2a_5 - 2.8622a_3a_4 + \\
&-7.5777a_1 + 2.7889a_2 + 3.1056a_3 + 4.4472a_4 - 7.7360(+3.5335)a_5 + \\
&+7.0670(1.4115)]
\end{aligned}
$$

where the coefficients in brackets refer to the structure of Fig. 5.2a and k denotes a positive constant. Of all the displacement paths (5.8), the one which minimizes d^4TPE has to be chosen; this is done by differentiating it with respect to $a_1, a_2, \ldots, a_5$, equating each derivative to zero and solving a linear system of five equations. At this stage it is also necessary to verify that the determinant of the system and its top-left entry are >0 (Fiorenza & Greco, 1978). These minimizations have been performed in both cases, and the results are shown in Table 5.3. It can be seen that the linkage of Fig. 5.1b has $d^4TPE>0$ and is therefore a mechanism of order one. All that can be said about the linkage of Fig. 5.2a is that it is a mechanism of order two, at least. A higher-order analysis of the second linkage requires a more complete path equation than just (5.8), subject to the conditions listed in Table 5.3:

$$
\begin{aligned}
x_1 &= .5\lambda + .3438\lambda^2 + b_1\lambda^3 \\
y_1 &= \quad -.0625\lambda^2 + b_2\lambda^3 \\
x_2 &= .5\lambda + .0938\lambda^2 + b_3\lambda^3 \\
y_2 &= \lambda - .1250\lambda^2 + b_4\lambda^3 \\
x_3 &= \lambda + .0625\lambda^2 + b_5\lambda^3 \\
y_3 &= \lambda
\end{aligned}
\tag{5.9}
$$

Linkage of Fig. 5.1b	$a_1 = .3109$ $a_2 = -.0583$ $a_3 = .0692$ $a_4 = -.1271$ $a_5 = .0158$	$d^4TPE = 5.4822k > 0$
Linkage of Fig. 5.2a	$a_1 = .3438$ $a_2 = -.0625$ $a_3 = .0938$ $a_4 = -.1250$ $a_5 = .0625$	$d^4TPE = 0$

Table 5.3 Path constants that minimize d^4TPE.

The path equation is substituted once more into (5.7) and the derivatives of TPE up to the sixth order are computed to obtain:

$$TPE)_{\lambda=0} = dTPE)_{\lambda=0} = \ldots = d^5TPE)_{\lambda=0} = 0$$

$$\begin{aligned} d^6TPE)_{\lambda=0} = k[&306.88b_1^2 + 210.88b_2^2 + 242.88b_3^2 + 373.77b_4^2 + 135.9057b_5^2 \\ &- 128.b_1b_2 - 357.77b_1b_3 - 256b_1b_5 + 128b_2b_5 - 64b_3b_4 + \\ &+ 21.18b_1 - 9.25b_2 - 8.68b_3 - 12.43b_4 - 10.0618b_5 + 1.8038] \end{aligned}$$

This is always positive, as shown by the results of the minimization of d^6TPE shown in Table 5.4. In conclusion the linkage is indeed a mechanism of order two as anticipated at the beginning of the section. A similar analysis would confirm that the linkage shown in Fig. 5.2b is an infinitesimal mechanism, of order three.

More generally, it would be straightforward to implement the above procedure in a computer program, one application of which would be in the field of infinitesismal mechanisms of infinite order/finite mechanisms - several examples of which have been given in Section 4.7.

$b_1 = -.0411$
$b_2 = .0116$
$b_3 = -.0103$ } $d^6TPE = 1.3k > 0$
$b_4 = .0157$
$b_5 = -.0071$

Table 5.4 Path constants which minimize d^6TPE for the linkage of Fig 5.2a.

5.2 Formfinding of tensegrity systems

Various tensegrities have been encountered so far but, apart from some remarks on the geometry of the "Simplex" in Section 2.4, the computation of their nodal coordinates has not yet been discussed in any depth.

Start from an assembly of pin-jointed bars, of which the nodal coordinates and bar connectivity are assumed to be known. The present aim is not to use the assembly in the given configuration, but rather to elongate one of its bars (or more than one bar, maintaining prescribed length ratios) until a configuration is reached in which a state of selfstress can be sustained. At this stage any further elongation would induce, in principle at least, the computed state of selfstress. (In practice the geometry-change effects due to the finite rigidity of the members have also to be considered). Most tensegrity systems are physically built in this way: turnbuckles are inserted into the bars to be lengthened (or in the wires to be shortened) and a prescribed number of turns in each of them produces the required shape and level of pretension.

How does one evaluate the 'exact' geometry of a tensegrity, at the point where prestress becomes possible?

Various relationships and numerical tables are provided by Kenner (1976), who uses only simple mathematics and ingenious arguments of symmetry to compute the nodal coordinates of some tensegrity systems. Several numerical methods have been put forward in the context of cable-net formfinding, one of which has met with particular success in recent years. This is the Dynamic Relaxation method already referred to in Section 2.4. This is a 'vector' method in which the process of converging towards a particular configuration, in equilibrium with or without external loads, is transformed into a

fictitious dynamical problem and integrated by means of a finite-difference procedure. Some artificial damping is introduced in order to obtain convergence. Motro (1983, 1984) has made use of this technique to obtain the prestressable configuration of the "Simplex".

Here a purely 'geometrical' formulation is proposed which reduces the formfinding of any tensegrity to the solution of a standard problem of Non-Linear Programming, for which library subroutines are available.

The "Simplex" is obtained by starting from a triangular prism all the edges of which have unit length, replacing the edges by pin-jointed bars and adding three diagonals, as in Fig. 2.17a, to brace the square faces of the prism. Such a truss has n=6, b=12 and therefore it satisfies Maxwell's rule; it has m=s=0 as do all closed triangulated surfaces which are convex (Cauchy, 1813). Clearly, after Section 2.1, an ill-conditioned configuration with s=m=1 can be obtained by elongating simultaneously the three diagonals until they reach a maximum length; and this is the configuration of interest. Figure 5.6 shows a plan view of the top and bottom bases of the prism: it is assumed that the bottom triangle does not move when the diagonals elongate. See Fig. 2.17. The simultaneous elongation of the diagonals causes the top triangle to rotate about the z-axis and translate in the vertical direction; therefore the axis through the centres of area of the two triangles is an axis of three-fold symmetry for all successive configurations. The translation associated with a rotation through an angle α of the top triangle can be evaluated by imposing that the distance between two corresponding vertices of the triangles has to remain equal to one:

$$\overline{14}^2=\overline{25}^2=\overline{36}^2=(\sin\alpha/2\sin60^\circ)^2+[(1-\cos\alpha)/2\sin60^\circ]^2+z^2=1$$

this gives the third coordinate of nodes 4,5,6, for arbitrary α:

$$z=\sqrt{1-(1-\cos\alpha)/2\sin^2 60^\circ} \qquad (5.10)$$

The corresponding length of a diagonal is

$$\overline{15}^2=\sqrt{(.5+\sin\alpha/2\sin60^\circ)^2+(\cos\alpha/2\sin60^\circ+.5\tan30^\circ)^2-(1-\cos\alpha)/2\sin^2 60^\circ+1} \qquad (5.11)$$

a)

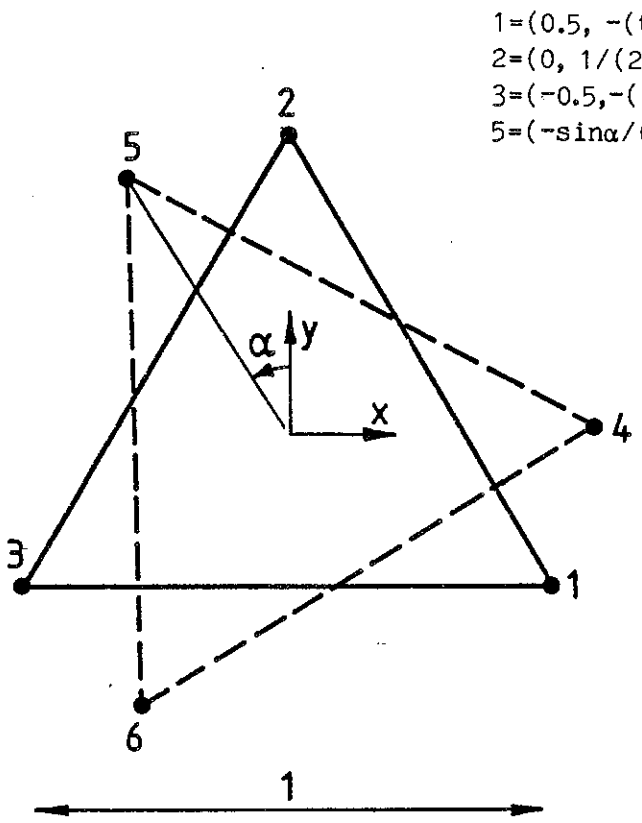

b)

bar no.	node no.	node no.	
1	1	4	
2	2	5	upright members
3	3	6	
4	4	5	
5	5	6	top triangle
6	6	4	
7	1	5	
8	2	6	diagonal members
9	3	4	

Fig. 5.6 a) Plan view of top and bottom triangles of the "Simplex", along the z-axis. The top triangle has been rotated through an arbitrary angle α. b) Bar numbering system. (Not all the bars are shown in the figure). Note that the sides of the bottom triangle need not be part of the structure.

and the value of α for which the diagonal length is maximum corresponds to a stationary value of the expression under the root of (5.11). This value is given by the solution of the equation $\tan\alpha=1/\sqrt{3}$ which has only one solution in $[0°,180°]$, given by $\alpha=30°$. The corresponding nodal coordinates of the "Simplex" are shown in Table 5.5; and the length of the diagonals is 1.4679.

		x	y	z
i)	1	.5000	-.2887	.0000
	2	.0000	.5774	.0000
	3	-.5000	-.2887	.0000
	4	.5774	.0000	.9543
	5	-.2887	.5000	.9543
	6	-.2887	-.5000	.9543
ii)	4	.5773	.0000	.9543
	5	-.2887	.5000	.9543
	6	-.2887	-.5000	.9543
iii)	4	.5770	.0240	.9471
	5	-.3093	.4877	.9471
	6	-.2673	.5117	.9471

Table 5.5 Nodal coordinates of "Simplex", in the cartesian system of axes shown in Fig. 5.6: i) solution in closed form, ii) numerical solution using a NAG subroutine, iii) results from Motro (1983).

The above calculation has taken full advantage of the three-fold symmetry of the problem being tackled, which enables one to obtain the configurations of the prism, for any chosen length of the diagonal members, as function of the one parameter α. In this example the length of the diagonal bars could be maximized by means of direct differentiation. A similar approach would be clearly desirable in all circumstances, but it is not practical in most 'realistic' cases. If no symmetries can be spotted at the onset, the above formulation becomes practically impossible: the main difficulty lies in the large number of variables.

The following reformulation of the "Simplex" formfinding will introduce an equivalent but more general way of proceeding, which may be extended to more complicated assemblies.

Following the connectivity scheme displayed in Fig. 5.6, the relationships

$$l_1=l_2=\ldots=l_6=1; \quad l_7=l_8=l_9=\text{Max} \tag{5.12}$$

entirely define the problem. Here the positions of nodes 1,2,3 are being considered fixed in space, therefore only the nodal coordinates of 4,5,6 have to be determined. It takes little effort to transform the first set of equations (5.12) into six quadratic equations:

$$l_1^2=l_2^2=\ldots=l_6^2=1 \tag{5.13}$$

Once the function $F=-(l_7)^2$ has been defined, the remaining conditions can be written in the form:

$$\begin{aligned} &F=\text{Minimum} \\ &l_7^2-l_8^2=0 \\ &l_7^2-l_9^2=0 \end{aligned} \tag{5.14}$$

The relationships (5.13) and (5.14) define the following problem of Non-Linear Programming, see Luenberger (1984):

$$\begin{aligned} &\text{"Minimize } F(x)=-[(x_5+.5)^2+(y_5+.2887)^2+z_5^2] \\ &\text{subject to: } (x_4+.5)^2+(y_4+.2887)^2+z_4^2=1 \\ &x_5^2+(y_5-.5774)^2+z_5^2=1 \\ &(x_6+.5)^2+(y_6+.2887)^2+z_6^2=1 \\ &(x_5-x_4)^2+(y_5-y_4)^2+(z_5-z_4)^2=1 \\ &(x_6-x_5)^2+(y_6-y_5)^2+(z_6-z_5)^2=1 \\ &(x_4-x_6)^2+(y_4-y_6)^2+(z_4-z_6)^2=1 \\ &x_5^2+y_5^2+z_5^2-x_6^2-y_6^2-z_6^2-x_5+.5774y_5+1.1548y_6=0 \\ &-x_4^2-y_4^2-z_4+x_5^2+y_5^2+z_5^2-x_4-x_5-.5774(y_4-y_5)=0 \text{ "} \end{aligned} \tag{5.15}$$

This can be solved by means of the NAG (1984) subroutine E04VDF; the results obtained are shown in Table 5.5. The corresponding length of the diagonal members is 1.468. For the sake of comparison, the table also shows the results of the formfinding performed by Motro.

This approach has also been successful in generating the nodal coordinates of the tensegrity truncated tetrahedron analysed in Section 4.7, see Fig. 4.25 and Table 5.6. In this case the objective function to be minimized, equal to the negative of the length of bar no. 24, has to satisfy 23 constraint equations. In this application a Fortran subroutine which prepared the data input required by the minimization routine replaced the explicit formulation in (5.15); the triangle with vertices in 10, 11 and 12 was prevented from moving by defining equal top and bottom bounds of the interval in which they vary. The final length of bar no. 24 is 2.2507, very close to 2.25 which is the value quoted by Calladine (1978).

In conclusion, a novel and reliable way of obtaining the prestressable configuration of any tensegrity structure has been presented. An advantage of the present system is that it is entirely general, as it does not rely on the choice of a particular system of coordinates.

Joint no.	x	y	z
1	.95602	-.08948	1.67408
2	.59356	.83643	1.56771
3	-.40013	.87334	1.67359
4	-1.02083	.09648	1.56773
5	-.55609	-.78256	1.67411
6	.42706	-.93418	1.56807
7	1.07667	.39845	.80957
8	-.88340	.73362	.80934
9	-.19355	-1.13120	.80981
10	.50000	.28868	.00000
11	-.50000	.28868	.00000
12	.00000	-.57735	.00000

bar no.	joint no.	joint no.
1	1	2
2	2	3
3	3	4
4	4	5
5	5	6
6	6	1
7	1	7
8	2	7
9	3	8
10	4	8
11	5	9
12	6	9
13	7	10
14	8	11
15	9	12
16	10	11
17	11	12
18	12	10
19	1	11
20	2	9
21	3	12
22	4	7
23	5	10
24	6	8

Table 5.6 Joint coordinates and connectivity of tensegrity truncated tetrahedron of Fig. 4.25.

6. Response to loads

Cable structures tend to exhibit a non-linear response to most 'normal' load conditions. This is visually confirmed by the plots of load vs. displacement and tension from any of the tests to be described in Chapter 7. In the past this has led to their being analysed by means of numerical methods in which all configuration changes are accounted for within an iterative procedure. Yet the key to the understanding of the behaviour of this structural type is in the analysis of its linear response to a set of rather special load conditions, which were introduced in a different context in Chapter 4. Consequently the main objective of this chapter is the development of a novel technique for the 'linear' analysis of cables and cable nets; and the limitations of the technique are then examined and removed. In fact the results of this chapter are not restricted to cable systems, and they will be described in relation to arbitrary kinematically indeterminate assemblies.

The layout of the chapter is as follows: Section 6.1 describes how to use the four fundamental subspaces of the equilibrium matrix, introduced in Chapter 4, in order to perform linear-elastic or plastic computations for 'ordinary' rigid assemblies under arbitrary load conditions. Building on these results, Section 6.2 tackles the analysis of an arbitrary pin-jointed assembly; in the case of kinematically determinate assemblies the procedure described coincides with the well-known force method. This analysis is completed in Section 6.3; Section 6.4 investigates the possible sources of non-linear effects and introduces the required corrections. Finally, the validity of the method is tested and verified, mostly in Section 6.5, by comparing its results with data from experiments and calculations available in the literature.

6.1 Linear-elastic and plastic analyses of rigid assemblies

The study of the general assembly introduced in Section 4.1, consisting of n nodal points connected by b bars to each other and by c constraints to a rigid foundation, will be continued in this section. It is assumed that the geometrical analysis leading to the four subspaces related to the equilibrium matrix, summarized in Table 4.1, has been performed already; so that their dimensions r_A, s and m are known, and a basis for each subspace is also

available. This section shows what to do with them, in order to solve 'straightforward' structural problems. Therefore only rigid assemblies with M=m=0 will be analysed, and so each result has a well known counterpart in the textbook descriptions; these analogies will be pointed out as the analysis develops.

6.1.1 Linear-elastic analyses

Assume that a linear-elastic relationship exists between the elongation e_i of bar i of the framework and the axial tension t_i:

$$e_i=(lt/AE)_i \qquad (6.1)$$

where l_i, A_i, E_i are the length, cross-sectional area and Young's modulus, respectively, of bar i. The ratio $(l/AE)_i$, which is the axial flexibility of bar i, will be denoted by the symbol f_i. Thus the b-dimensional diagonal matrix [F], with f_i as its entry of position (i,i), relates the vectors {e} and {t} introduced in Section 4.1:

$$\{e\}=[F]\{t\} \qquad (6.2)$$

Obviously, the inverse relationship is $\{t\}=[F]^{-1}\{e\}$ where $[F]^{-1}$ is the diagonal matrix of entries $1/f_i$.

Statically determinate assemblies ($b=3n-c=r_A$, M=0, s=0) have both bar and joint spaces entirely filled by the row space and column space of the equilibrium matrix, respectively; hence all load conditions can be equilibrated and there is a one-to-one correspondence between sets of bar tensions {t} and applied loads {f}. Furthermore, any prescribed nodal displacement requires certain bar elongations to occur, in other words it is 'extensional', and there is only one vector {e} corresponding to it. All sets of bar elongations are compatible. As all the columns of [A] are independent, they will obviously provide a basis for the column space (see Section 4.2) while the rows of an r_A-dimensional identity matrix furnish a basis for the row space. The correspondence between vectors of the row space and column space is illustrated in Fig. 6.1. The complete structural analysis of a

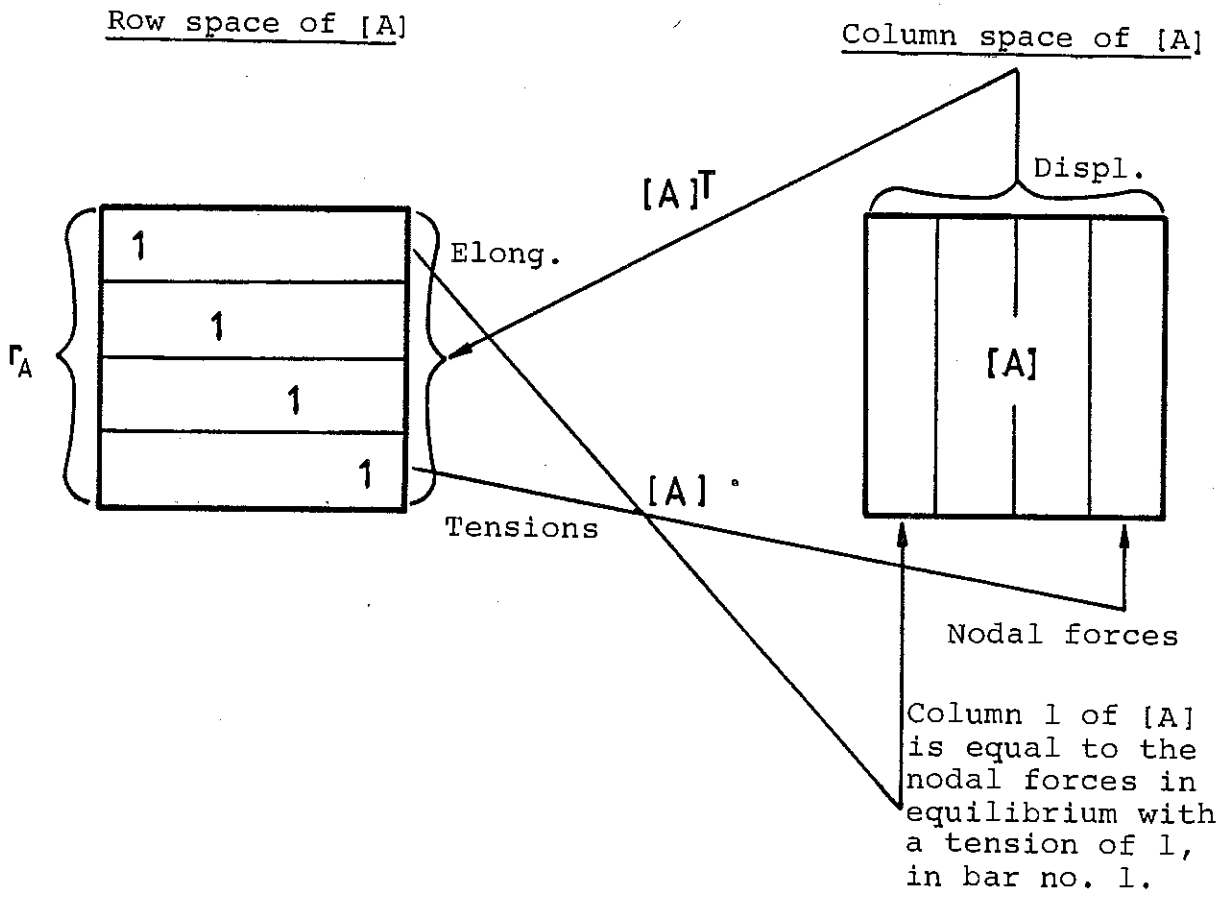

Fig. 6.1 The correspondence between vectors of the row and column spaces of the equilibrium matrix [A], for a statically and kinematically determinate framework. [A] transforms each row vector of the row space into a column vector of the column space; but the compatibility matrix $[A]^T$ achieves a one-to-one correspondence between displacement and elongation vectors only if the columns of [A] are replaced by $([A]^{-1})^T$, in the column space.

statically and kinematically determinate framework is now easily done by use of the two subspaces of Fig. 6.1: any assigned load {f} has to be decomposed into r_A components, each of which corresponds to a change of tension in only one of the bars. This operation requires the computation of the coefficients $\alpha_1, \alpha_2, \ldots \alpha_{r_A}$ from:

$$[A]\{\alpha\}=\{f\} \tag{6.3}$$

which has a unique solution. Obviously $\{\alpha\}=\{t\}$, and solving (6.3) is precisely the same as computing the bar tensions by means of the equilibrium equations of the assembly, see McGuire & Gallagher (1979). Once the tensions are known, the bar elongations are obtained from (6.2). As noted in the caption to Fig. 6.1, the nodal displacement due to a unit elongation of bar i is row number i of $[A]^{-1}$; the nodal displacement {d} due to the elongation $\{e\}=[F]\{t\}$ will be:

$$\{d\}=([A]^{-1})^T[F]\{t\} \tag{6.4}$$

Similarly, the displacements produced by a given set of elongations (due to thermal distortions, lack of fit,..) $\{e_o\}$ are just given by $\{d\}^T=([A]^{-1})^T\{e_o\}$. These results are not unexpected if one recalls that $[A]^T$ is the compatibility matrix of the assembly.

Redundant assemblies ($b>3n-c=r_A$, $M=0$, $s=b-r_A$) The left-nullspace is empty as in the statically determinate case, and therefore any load condition {f} can be equilibrated in the initial configuration; but the row space does not fill the bar space and - although it is of course possible to define a one-to-one correspondence between the vectors {t'} in the row space of [A] and any applied load - the elongations corresponding to {t'} will not, in general, satisfy the conditions of geometrical compatibility. This is because {t'} is orthogonal to the nullspace but the elongations due to it, possibly added to a set of initial elongations $\{e_o\}$, may not be. As shown in Section 4.1.2, the nullspace of the equilibrium matrix contains all the possible incompatible elongations; therefore the elongations due to {t'} in general have an incompatible component. This point will be clarified later on,

and the orthogonality condition mentioned above will be used to obtain the set of compatibility equations; but some essential details regarding the three non-empty subspaces of the equilibrium matrix need to be discussed first.

A basis for the column space of [A] is formed by the r_A independent columns of the equilibrium matrix; for the sake of convenience the (3n-c) by r_A matrix containing these columns will be indicated as $[A_o]$. s independent states of selfstress, assembled in the b by s matrix [SS], are a basis for the nullspace. A simple way to obtain a basis of the row space can be derived from the statically determinate case (Fig. 6.1), with the difference that now the rows of the r_A-dimensional identity matrix have to be augmented by $b-r_A$ extra columns which make the resulting row vectors orthogonal to the nullspace (this is an application of Section 4.2).

Although the bases provided above are all correct, in the sense that they do span the three subspaces, their vectors have not been chosen with enough care that [A], say, associates each base vector of the row space with a corresponding base vector of the column space.

The following two alternative bases of the column space, though, satisfy this need in different ways. First consider the column vectors the entries of which are the nodal forces in equilibrium with the systems of bar tensions considered for the row space and assemble them in the matrix $[A_1]$; the equilibrium matrix [A] now transforms one basis into the other in a way similar to that shown in Fig. 6.1. But the compatibility matrix does not operate the inverse transformation. See Fig. 6.2a.

Now consider the r_A-dimensional matrix $[\tilde{I}]^T$ of Section 4.2 as an alternative basis for the column space: the compatibility matrix $[A]^T$ transforms the columns of $[\tilde{I}]^T$ into the rows of the row space of [A]. Obviously there is no such correspondence in terms of equilibrium. See Figs 6.2b and 6.3.

As noted before, any load can be equilibrated by the assembly; the first stage in the determination of the bar tensions due to the load {f} is to evaluate a vector {t'} which belongs to the row space of [A] and is in equilibrium with {f}. This problem has been already encountered when dealing with statically determinate assemblies: one needs to solve the system of r_A equations

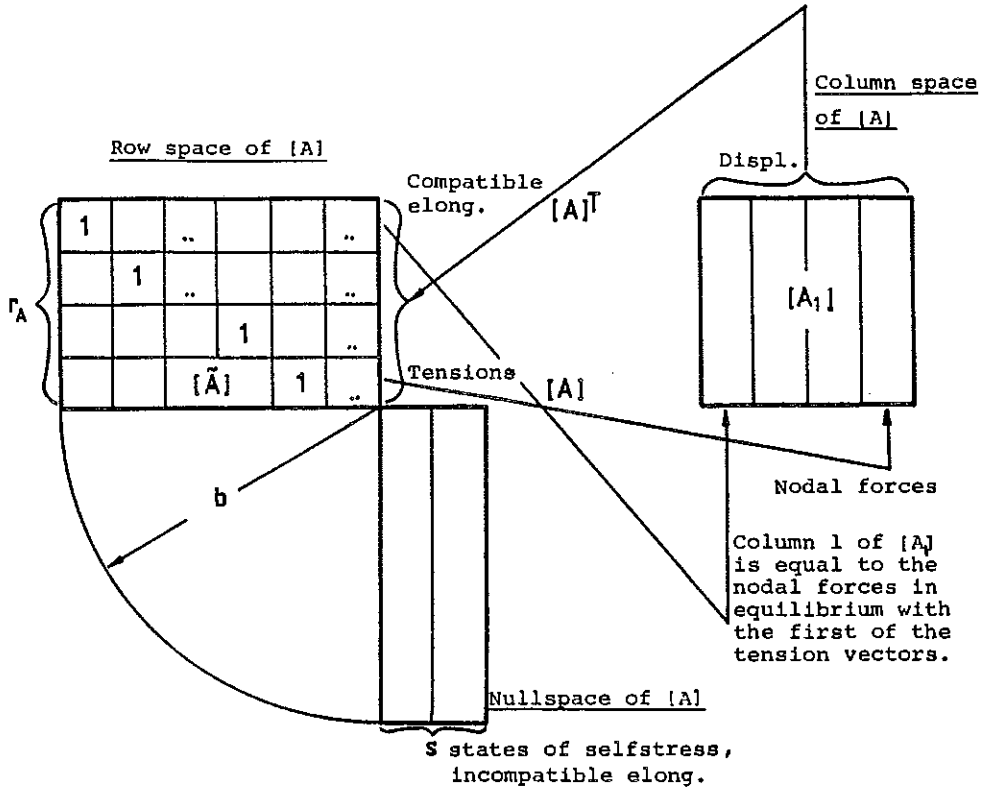

Fig. 6.2a The correspondence between vectors of the row and column spaces of the equilibrium matrix [A], for a statically indeterminate but kinematically determinate assembly.
The basis of the column space chosen here is such that [A] transforms each row of the row space into a column vector of the column space; and all of the vectors of the nullspace into the origin, of course. But $[A]^T$ does not achieve the same one-to-one correspondence.

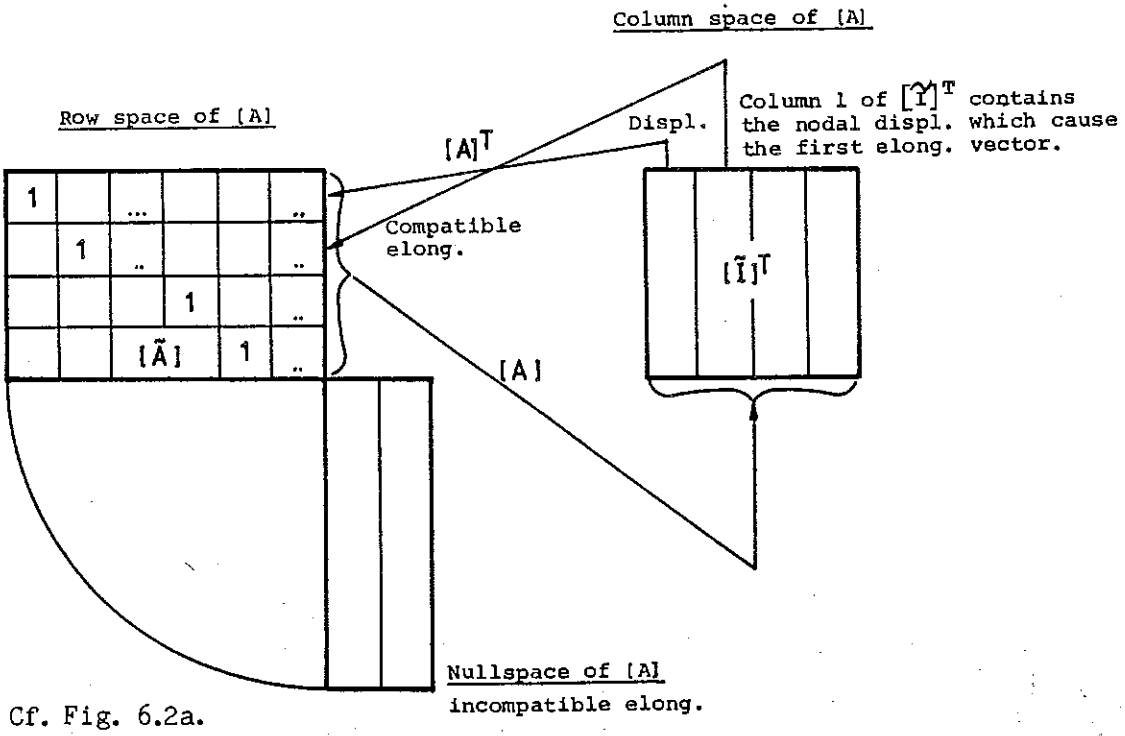

Fig. 6.2b Cf. Fig. 6.2a.

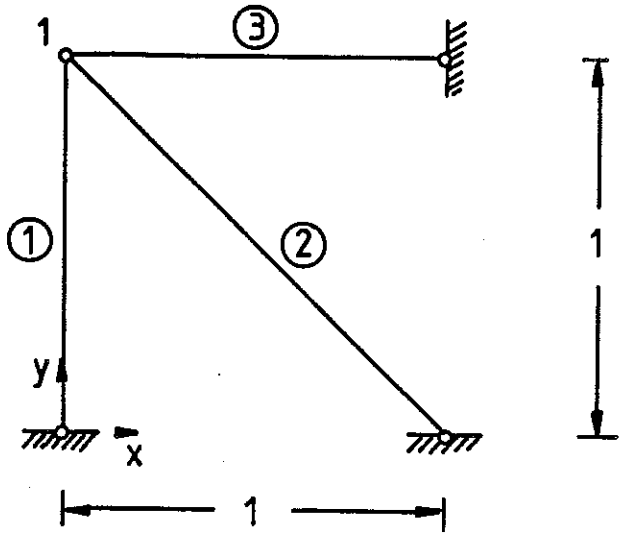

$$[A] = \begin{bmatrix} 0 & -1/\sqrt{2} & -1 \\ 1 & 1/\sqrt{2} & 0 \end{bmatrix}$$

The transformation described in Section 4.2 yields:

$$[\tilde{A}|\tilde{I}] = \left[\begin{array}{ccc|cc} 1 & 0 & -1 & 1 & 1 \\ 0 & 1 & \sqrt{2} & -\sqrt{2} & 0 \end{array}\right]$$

Hence $r_A=2$, $m=2-2=0$ and $s=3-2=1$. Substituting numerical values into the scheme shown in Fig. 6.2a one obtains:

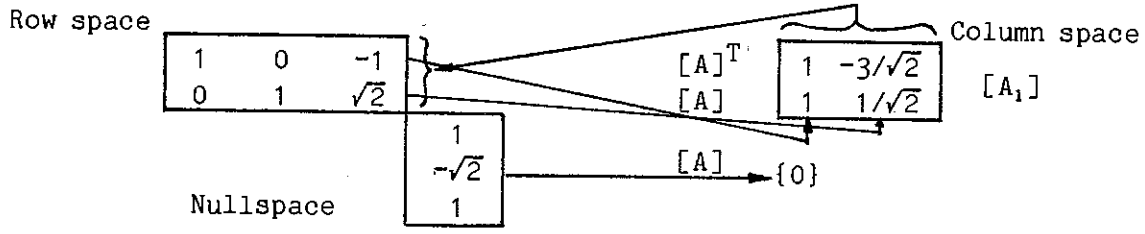

Substitute into Fig. 6.2b to obtain:

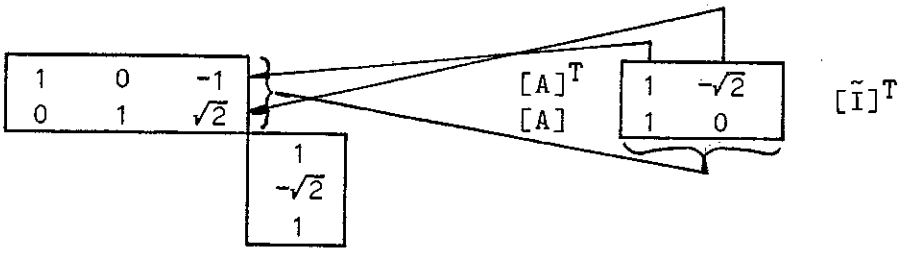

Fig. 6.3 Example of statically indeterminate assembly. All the points discussed in Section 6.1.1 can be verified by inspection.

$$[A_1]\{\alpha\}=\{f\} \tag{6.5}$$

And then the desired tension vector is

$$\{t'\}=[\tilde{A}]^T\{\alpha\} \tag{6.6}$$

in other words the ith vector of the standard basis of the row space, which coincides with row i of $[\tilde{A}]$, has to be multiplied by the corresponding coefficient α_i and the contributions from all the vectors of the basis have to be added up. To use a term well known in the theory of framed structures (Heyman, 1974), the computation of $\{t'\}$ is equivalent to sketching a 'free' bending moment diagram in the analysis of a continuous beam. The vector $\{t'\}$ obtained from (6.6) is orthogonal to the nullspace; the bar elongations are now $[F]\{t'\}+\{e_o\}$, with $\{e_o\}$ denoting a set of initially imposed elongations. These elongations are compatible only if they too are orthogonal to the nullspace; otherwise a set of self-equilibrated tensions has to be superimposed to the initial solution. The most general state of self-equilibrated tensions is given by $[SS]\{x\}$, in which x_i is the coefficient that multiplies the state of selfstress number i. All x_i's would vanish if $\{t'\}$ happened to satisfy the compatibility of deformation.

The bar tensions are in total:

$$\{t\}=\{t'\}+[SS]\{x\} \tag{6.7}$$

and the total elongations are:

$$\{e\}=\{e_o\}+[F](\{t'\}+[SS]\{x\}) \tag{6.8}$$

The s-dimensional vector $\{x\}$ is unknown, therefore one needs to write down s independent equations of compatibility; precisely s equations of this type are obtained by imposing the condition that $\{e\}$, as expressed in (6.8), is orthogonal to the nullspace, i.e. that the dot product of $\{e\}$ by each column vector of $[SS]$ vanishes. In matrix form the compatibility equations are therefore:

$$[SS]^T\{e\}=\{0\} \qquad (6.9)$$

Substitute (6.8) into (6.9), expand and take all known quantities to the right-hand-side to obtain:

$$[SS]^T[F][SS]\{x\}=-[SS]^T\{e_0\}-[SS]^T[F]\{t'\} \qquad (6.10)$$

This is a system of s linear equations in s unknowns; the matrix $[SS]^T[F][SS]$ is not singular because the s rows of [SS] are independent and [F] is a diagonal matrix (Strang, 1980). The interpretation of this result is trivial; indeed it is well known in the analysis of a redundant structure by the force method that one has to solve a system of linear equations the dimension of which is equal to the number of redundancies. This system of equations is precisely (6.10).

A more usual way of obtaining (6.10) is by means of virtual work: see Pestel & Leckie (1963). In this case the proof considers s independent systems of 'forces' in equilibrium, each of which is merely a state of selfstress; and only one system of 'displacements', the real one. The orthogonality argument described above and the more traditional approach based on virtual work are entirely equivalent; this becomes apparent if one compares the statements of equilibrium and compatibility made in Chapter 4, and embodied in the four fundamental subspaces of [A], to the proof of the virtual work equation in the explicit case of trusses (Neal, 1964). Equivalent equations that minimize the total energy in the assembly were used by Robinson (1966) in the development of the rank force method, which has many points in common with the above derivation, and by Przemieniecki (1968).

Once {x} has been determined from (6.10), (6.7) and (6.8) provide the bar tensions and elongations due to {f} (+$\{e_0\}$). The final step is the evaluation of the nodal displacement vector {d}. For this purpose the elongation vector {e} has to be decomposed into r_A components, each of which is proportional to a vector in the basis of the row space, by solving:

$$[\tilde{A}]^T\{\alpha\}=\{e\} \qquad (6.11)$$

Thus the nodal displacement vector is $\{d\}=[\tilde{I}]^T\{\alpha\}$. In fact the elongations of the bars of the framework that correspond to linearly independent columns of [A], denoted by * in Fig. 4.5a, correspond to rows of $[\tilde{A}]^T$ which only contain one non-vanishing entry (=1). Therefore there is no need to solve (6.11): $\{\alpha\}$ has to contain the elongations of the independent bars, which one can extract from $\{e\}$. In conclusion

$$\{d\}=[\tilde{I}]^T\{e^*\} \tag{6.12}$$

where $\{e^*\}$ contains the elongations of the independent bars. This completes the analysis.

In practice some inconsequential simplifications can be introduced: $[A_1]$ can be replaced by $[A_0]$ in (6.5), and $[\tilde{A}]^T$ by [I] in (6.6). Then $\{t_0\}$ is directly computed from

$$[A_0]\{t'\}=\{f\} \tag{6.13}$$

and is no longer orthogonal to the nullspace of [A], but this does not matter too much.

In conclusion, the structural analysis of a statically indeterminate truss requires the solution of (6.13) and (6.10), and the evaluation of (6.7), (6.8) and (6.12). These results will be useful for the analysis of kinematically indeterminate assemblies, in the next section.

6.1.2 Plastic analyses

The fundamental subspaces of the equilibrium matrix [A] can be utilized in order to compute the multiplier λ_c, of all applied loads (proportional loading), under which collapse of a redundant structure occurs according to simple plastic theory (Baker & Heyman, 1969). Therefore the load vector $\{f\}$ in this section will merely denote the 'shape' of the applied loading, $\lambda\{f\}$ being its actual value. Strictly speaking, all conclusions will be only valid for pin-jointed assemblies but it would be straightforward to extend the present treatment to framed structures and continua.

For the purposes of this section, it is assumed that every bar of the assembly is made of rigid-perfectly plastic material, see Fig. 6.4; this is equivalent, see Baldacci, Ceradini & Giangreco (1974), to considering a slightly more realistic elastic-perfectly-plastic constitutive relationship and also postulating that the elastic displacements are small enough not to influence the bar tensions. Furthermore each bar is assumed to have equal strength in tension or compression, and the possibility that any bar in compression may buckle is excluded.

The upper- and lower-bound theorems are well known in the theory of plastic design of structures (Neal, 1964, Baker & Heyman, 1969): according to the lower-bound theorem any multiplier λ' such that the applied load $\lambda'\{f\}$ can be in equilibrium with a set of tensions which do not violate the yield condition is always less than, or at most equal to, the true load factor λ_c. Also, according to the upper-bound theorem, for any hypothetical mechanism of collapse, the multiplier λ'' - obtained by equating the work done by the load $\lambda''\{f\}$ during collapse, to the plastic energy dissipated - is always greater than, or at most equal to, λ_c.

For an assembly having s=0 the evaluation of λ_c is trivial.

To produce lower bound estimates of λ_c in the more general case s>0, one has to satisfy equilibrium and yield conditions at the same time: Equilibrium provides, for any assigned load (shape) $\{f\}$, a set of tensions $\{t_o\}$, solution of (6.13), in equilibrium with it; the bar tensions $\lambda\{t_o\}$ are in equilibrium with $\lambda\{f\}$. An arbitrary set of self-equilibrated tensions $[SS]\{x\}$ can be added to $\{t_o\}$ without altering the equilibrium requirements, as in (6.7). In order to introduce the Yield condition in the calculation, define two b-dimensional vectors $\{t_{min}\}=-\{t_y\}$ and $\{t_{max}\}=\{t_y\}$, where $\{t_y\}$ is the vector which contains the yield tensions for all bars of the assembly. Clearly

$$\{t_{min}\}\leq\{t\}\leq\{t_{max}\} \qquad (6.14)$$

The inequalities (6.14) determine an admissible set within the space of bar tensions, and any multiplier λ is a lower bound for λ_c if a linear combination $[SS]\{x\}$ can be found such that the vector $\lambda\{t_o\}+[SS]\{x\}$ lies in the 'admissible' region of the bar space. See Fig. 6.5.

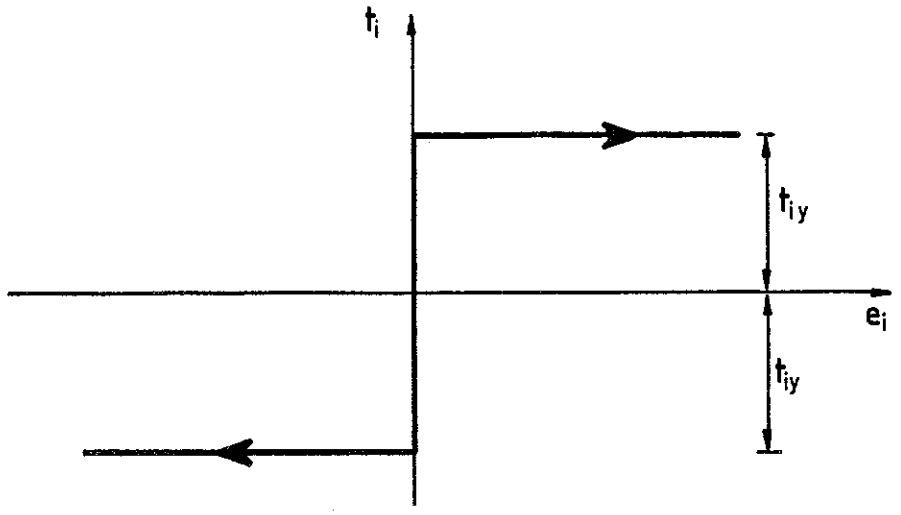

Fig. 6.4 Constitutive relationship assumed in Section 6.1.2 for bar i of the assembly.

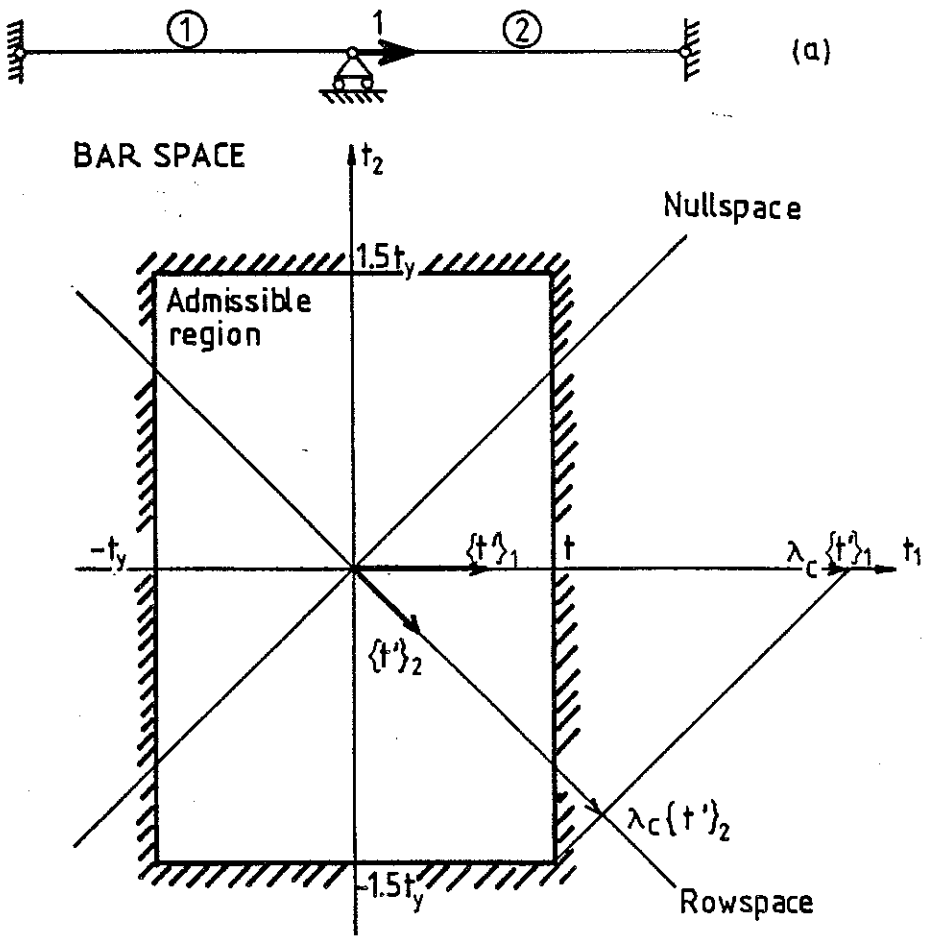

Fig. 6.5 Two-dimensional bar space of the plane assembly shown in (a). Bars 1 and 2 have different yield tensions: $t_{1y}=t_y$ and $t_{2y}=1.5t_y$. Plainly there is one state of selfstress, in which the bars carry equal tensions. The row space is perpendicular to the nullspace. Two different systems of tensions in equilibrium with the unit load applied are $\{t'\}_1$, obtained from (6.13), and $\{t'\}_2$, obtained from (6.5). The maximum value of λ ($=\lambda_c$) has been found graphically. Obviously both initial solutions yield the same λ_c.

The maximum lower bound can be found by solving the following problem of Linear Programming: "Maximize λ subject to the condition

$$\{t_{min}\} \leq [t' | SS] \begin{Bmatrix} \lambda \\ x \end{Bmatrix} \leq \{t_{max}\} \text{ "} \qquad (6.15)$$

The adjoint matrix in (6.15) has b rows and s+1 columns. It is easy to solve the problem defined above by using a library routine, see Luenberger (1984). It is important to notice that this approach decouples the equilibrium problem from the yield condition. Thus (6.15) only deals with the yield condition, which reduces substantially one of the dimensions of the matrix: the number of columns is reduced from b, as in (Livesley, 1973), to s+1. An equivalent formulation has been described concisely by Besseling (1978).

Upper bound calculations can be also made by use of the fundamental subspaces, and for this purpose one of the formulations of Section 6.1.1 will be particularly useful: this is the one in which a one-to-one correspondence was established between the basis of the row space and the columns of $[\tilde{I}]^T$, which contain the nodal displacements due to the elongations in the row space. Each of these displacement vectors defines an independent mechanism of collapse for the rigid-plastic assembly being investigated; thus a total of $r_A=3n-c$ independent mechanisms is obtained. All the mechanisms of collapse, among which is the true one, can be expressed as a linear combination of the above mechanisms, and hence any mechanism has the form $[\tilde{I}]^T\{y\}$; here the r_A dimensional vector $\{y\}$ allows one to choose any particular mechanism of collapse by a suitable choice of its components. The corresponding plastic bar elongations will be $[\tilde{A}]^T\{y\}$. In order to compute the load factor associated with a chosen mechanism of collapse, the external work done by the applied load $\{y\}^T[\tilde{I}]\lambda\{f\}$ has to be equated to the plastic energy dissipated $ABS(\{y\}^T[\tilde{A}])\{t_y\}$ (the notation ABS( ) here denotes the vector with entries equal to the the absolute value of the entries of the vector inside the brackets). If the external work associated with a particular mechanism does not vanish, the corresponding load factor is provided by the ratio:

$$\lambda=(ABS(\{y\}^T[\tilde{A}])\{t_y\})/(\{y\}^T[\tilde{I}]\{f\}) \qquad (6.16)$$

Formula (6.16) defines a scalar function of the vector {y}. The collapse multiplier of the load {f} is the minimum of the function $\lambda=\lambda(y_1,y_2,\ldots,y_{r_A})$ defined in (6.16).

The above approach is suitable for both statically determinate and indeterminate assemblies, and promises to be a substantial improvement of the more usual upper bound formulations suggested in, e.g., Besseling (1978) which lead to a problem of Linear Programming which is the dual to (6.15). Therefore it may contribute to the development of more efficient algorithms for the limit analysis of structures; it is somewhat surprising to read in Livesley (1975) that "the calculation of the collapse load factor ... takes about five times as long as an elastic analysis of the same structure". It may also be possible to explain some unexpected difficulties found by Heyman (1975) in the evaluation of the collapse load of simple space frames. Another area for further investigation is how to utilize best the fundamental subspaces of [A] for elasto-plastic calculations; a recent paper by Domaszewski & Borkowski (1984) may be of some guidance in this task.

6.2 Linear response of kinematically indeterminate frameworks

A calculation of the product-forces of a pin-jointed assembly with s>0, m>0 was first performed in Section 4.5. The consequent assemblage and analysis of [A'] led to the distinction between infinitesimal mechanisms of first order and mechanisms of higher order. An equivalent approach can also be introduced for assemblies with s=0, m>0: formulae like (4.20) can define the product-forces due to an initially applied set of loads and an identical matrix [A'] can be assembled. In this section the linear behaviour of an assembly with arbitrary s and m will be analysed in general terms; this is possible because the most significant differences of behaviour between a kinematically indeterminate assembly which is statically determinate and a 'similar' assembly which is statically and kinematically indeterminate are in the non-linear range, leaving aside of course the need for extra equations of compatibility in the latter case. In particular, it will turn out that the linear-elastic analyses of Section 6.1.1 can be derived as special cases from it.

In the present section it will be assumed that the displacements due to the applied loads are rather 'small', in a sense that will be more clearly

defined in Section 6.4. The initial computation of the linear response of an assembly to any load condition, though, is the first and essential component of the present method; its validity will be tested and extended when necessary in Section 6.4. For the sake of clarity, it will be assumed that dimensions and bases of the four fundamental subspaces related to the equilibrium matrix [A] are known a priori, although in practice several of the calculations described here find their most natural location within the elimination procedure of Section 4.2.

Consider a three-dimensional assembly of n spherical, frictionless hinges connected to each other by b bars, and to an external foundation by c constraints. The vectors {t}, {e}, {f}, {d} have already been introduced in Section 4.1 to denote the b-dimensional vectors of bar tensions and elongations, and the (3n-c)-dimensional vectors of nodal components of force and displacement, respectively. In this context these vectors will be used to denote global quantities; therefore if an initial set of - say - tensions is present in a particular analysis, these will be denoted by $\{t_0\}$ and the subsequent increment that brings their values up to {t} will be denoted by $\{\delta t\}$.

For this assembly, the geometrical analysis described in Chapter 4 reveals that the rank of the equilibrium matrix is r_A: therefore the assembly is $s=b-r_A$ times redundant and has $M=m=3n-c-r_A$ internal mechanisms (the introduction of rb rigid-body mechanisms into the present formulation would be possible at the only expense of more complicated symbols).

Which load systems can the assembly equilibrate in the context of a linear analysis? All the "fitted loads", of course, can be carried by the assembly in its initial configuration, hence all the load conditions that belong to the column space of [A]: of a total of 3n-c independent load vectors one can think that their 'components' along the r_A-dimensional column space do not excite any of the inextensional modes. Therefore these can be dealt with, in principle, in exactly the same way as they would be in a kinematically determinate framework (see Section 6.1.1). The components of that load onto the m-dimensional left-nullspace are still left. A state of selfstress may provide, as noted in Section 4.5, first-order stiffness against some or all of the m inextensional modes which were the forbidden load conditions above. This is not an unusual situation: it is common practice to prestress

statically and kinematically indeterminate engineering structures by imposing an initial set of distortions which generates a state of self-equilibrated tensions $\{t_o\}$, e.g. cable nets. It is also standard practice to rely on the effect of any existing tension when dealing with statically determinate but kinematically indeterminate assemblies, e.g. cables hanging under their own weight and loaded by live loads. This is just a variant of the above situation, with $\{t_o\}$ now being the consequence of an initial loading $\{f_o\}$ which is itself a "fitted load" for the assembly, and hence can be in equilibrium with $\{t_o\}$. As $\{t_o\}$ and $\{f_o\}$ are in equilibrium

$$[A]\{t_o\}=\{f_o\} \tag{6.17}$$

Here [A] has 3n-c rows and b columns and 3n-c>b, but there exists <u>one</u> (and only one because s=0) solution to (6.17) as $\{f_o\}$ is "fitted". Now rewrite the equilibrium equations of node i of the framework, see Fig. 4.1, for an infinitesimally displaced configuration assuming that the values of the bar tensions are unchanged -as for (4.19)-:

$$\begin{aligned}
&[(X_i+x_i)-(X_j+x_j)]t_{op}/l_p+[(X_i+x_i)-(X_k+x_k)]t_{oq}/l_q=f_{oix}+p_{ix}\\
&[(Y_i+y_i)-(Y_j+y_j)]t_{op}/l_p+[(Y_i+y_i)-(Y_k+y_k)]t_{oq}/l_q=f_{oiy}+p_{iy}\\
&[(Z_i+z_i)-(Z_j+z_j)]t_{op}/l_p+[(Z_i+z_i)-(Z_k+z_k)]t_{oq}/l_q=f_{oiz}+p_{iz}
\end{aligned} \tag{6.18}$$

here x_i, y_i, z_i,... are the components of displacement of joints i,... according to the inextensional mechanism considered. Subtract from (6.18) the corresponding equations of (6.17) and exchange right- and left-hand-side to obtain:

$$\begin{aligned}
p_{ix}&=(x_i-x_j)t_{op}/l_p+(x_i-x_k)t_{oq}/l_q\\
p_{iy}&=(y_i-y_j)t_{op}/l_p+(y_i-y_k)t_{oq}/l_q\\
p_{iz}&=(z_i-z_j)t_{op}/l_p+(z_i-z_k)t_{oq}/l_q
\end{aligned} \tag{6.19}$$

These formulae define a set of product-forces for any preloaded assembly, in the same way as (4.20) did for prestressed assemblies only. So far as the linear analysis goes the vector of initial tensions $\{t_o\}$, whatever its origin,

is the only datum required. The product-forces define a new subspace of loads that 'can be carried', and they may have beneficial effects on the structural performance of the assembly. It was noted that there is usually no close resemblance between a mechanism and the product-force vector due to it and to the initial tensions $\{t_o\}$; an important implication of this is that "fitted loads" and product-forces have to interact when a load is applied. That is, if one particular applied load needs to activate an inextensional mode to benefit from the product-forces consequent to it, these product-forces usually have a non-vanishing component in the subspace of "fitted loads"; this component has to be included in all computations. See Fig. 6.6. Also, as the effect of any "fitted load" component is to alter the bar tensions and hence the product-forces, [A'] will need to be updated and the calculation repeated.

In conclusion any prestressed assembly has m product-force vectors which may or may not carry the m forbidden loads through the geometry-changes associated with the inextensional modes, without any change of tension in the bars. The distinction between stiff (extensional) and soft (inextensional) modes of a prestressed mechanism, a cable net in the specific case, was first pointed out by Calladine (1982). Pellegrino & Calladine (1984) utilized a minor modification of [A'], see Fig. 4.9, to analyse the linear response of a saddle-shaped cable net. In a more general form the same approach will be followed here.

The matrix [A'] introduced in Chapter 4 has the r_A independent columns of the equilibrium matrix [A], i.e. all the "fitted loads" of the assembly, as columns 1,... r_A; plainly all the columns of [A] are independent if s=0. The remaining m columns are the product-force vectors which can be now computed for each one of the m mechanisms from (6.19). The resulting matrix is square because rb=0. The rank of [A'] will indicate how many independent load conditions can be considered in the context of the present linear analysis, as in Section 4.5.

The main use of [A'] here is as a replacement of the standard equilibrium matrix; while [A] is only valid in the initial configuration of the assembly, [A'] also incorporates equilibrium conditions in all the configurations obtainable through small, inextensional distortions from the initial configuration. In this new function obviously only the first r_A columns of

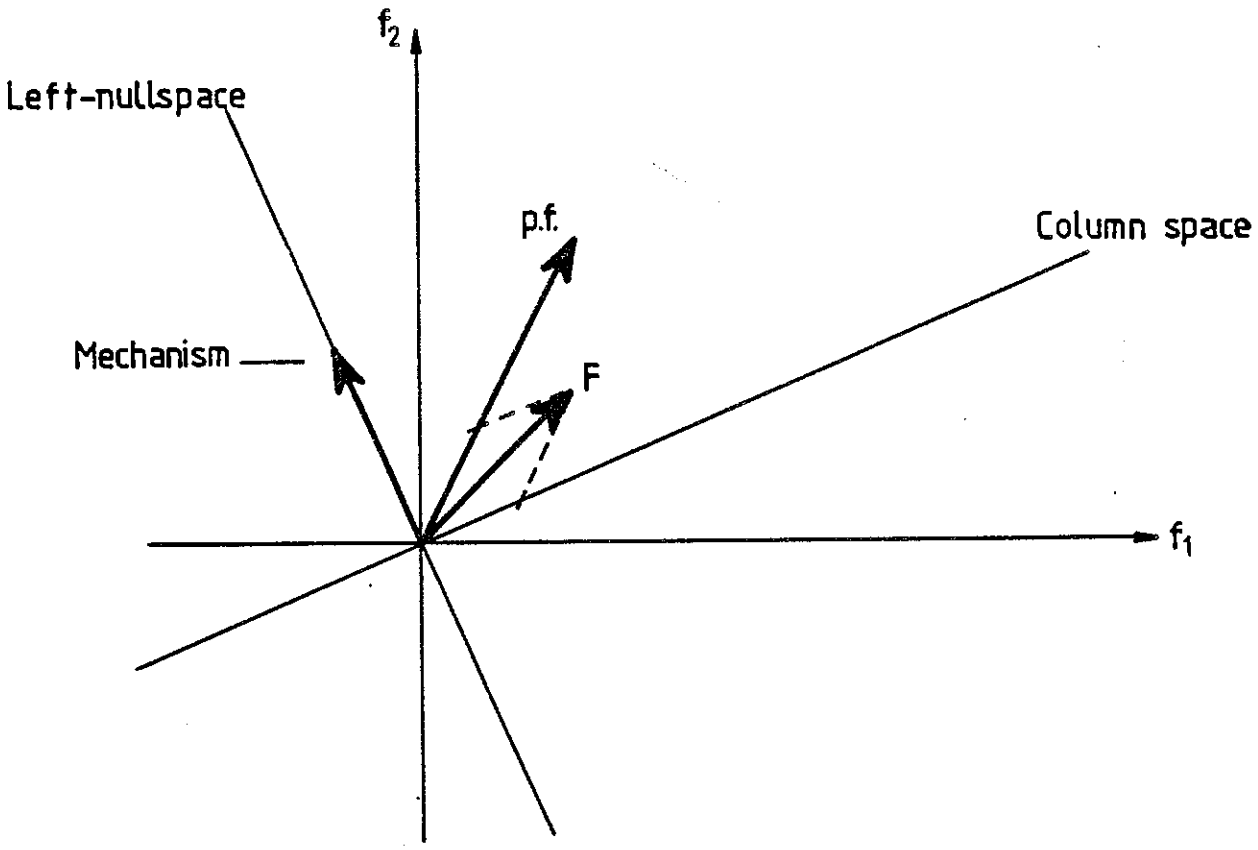

Fig. 6.6 Two-dimensional joint space of an hypothetical assembly which has $r_A=1$, $m=1$. Obviously there is only one fitted load; the only product-force has been computed according to an hypothetical set of existing pretensions, and its components are $\{1\ 2\}^T$. The applied load $F=\{1\ 1\}^T$ has been decomposed into its 'fitted' and 'product-force' components.
Notice that loads proportional to the product-force, not to the mechanism, would be carried purely inextensionally, and hence would not alter the bar tensions.

[A'] have to be multiplied by the tension in the corresponding bars, which are statically determinate and were indicated by * in Fig. 4.5a. The remaining columns are multiplied by the magnitudes of the (small) inextensional displacements. In short:

$$[A']\{\frac{\delta t}{\alpha}\}=\{\delta f\} \qquad (6.20)$$

where the first r_A components of the vector $\{\frac{\delta t}{\alpha}\}$ represent changes of tension in the statically determinate bars which were picked out by the elimination procedure. The same numbers, interspersed by 0's corresponding to the redundant bars, constitute $\{\delta t\}$. The remaining m components of $\{\frac{\delta t}{\alpha}\}$, α_1, ..,α_m are the quantities by which each inextensional mechanism has to intervene. $\{\delta f\}$ is the 'live' load vector.

The solution of (6.20) can be pursued using Gaussian elimination, or any algorithm which is able to detect load conditions which cannot be carried if [A'] does not have full rank.

The calculation just described has been made for the plane assembly of Fig. 6.7: it is easy to verify that, although the structure has one mechanism, $\{f_o\}$ is certainly a "fitted load" because it is equal to the linear combination of the columns of [A] with coefficients $2\sqrt{1.25}$, 2, $2\sqrt{1.25}$. The initial tensions are therefore $\{t_o\}=\{2\sqrt{1.25}\ 2\ 2\sqrt{1.25}\}^T=\{2.2361\ 2\ 2.2361\}^T$. It is also easy to verify that the components of the inextensional mechanism are $\{-.5\ 1.\ -.5\ -1.\}^T$. The columns of the equilibrium matrix being independent, [A'] is obtained by adjoining the product-force to it; hence (6.20) becomes:

$$\begin{bmatrix} 1/\sqrt{1.25} & -1 & 0 & -1 \\ 1/2\sqrt{1.25} & 0 & 0 & 6 \\ 0 & 1 & -1/\sqrt{1.25} & -1 \\ 0 & 0 & 1/2\sqrt{1.25} & -6 \end{bmatrix} \begin{Bmatrix} \delta t_1 \\ \delta t_2 \\ \delta t_3 \\ \alpha_1 \end{Bmatrix} = \begin{Bmatrix} 0 \\ 0 \\ 0 \\ 1 \end{Bmatrix} \qquad (6.21)$$

the solution vector is $\{\frac{\delta t}{\alpha}\}=\{1.0320\ \ 1.\ \ 1.2040\ \ -.0769\}^T$, from which $\{t\}=\{3.2681\ \ 3.\ \ 3.4401\}^T$.

A straightened out version of this assembly, see Fig. 6.8, was first examined in Section 4.3. Only two columns of [A] are independent (the Gaussian elimination picked out columns 1 and 2) and they are the first two columns of

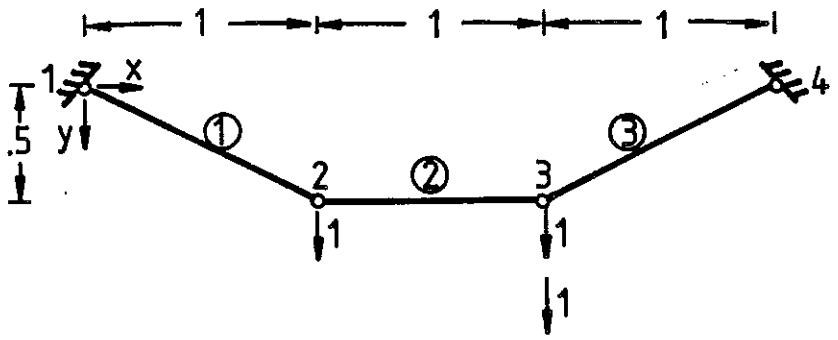

$$[A] = \begin{bmatrix} 1/\sqrt{1.25} & -1 & 0 \\ 1/2\sqrt{1.25} & 0 & 0 \\ 0 & 1 & -1/\sqrt{1.25} \\ 0 & 0 & 1/2\sqrt{1.25} \end{bmatrix} \qquad \{f_o\} = \begin{Bmatrix} 0 \\ 1 \\ 0 \\ 1 \end{Bmatrix}$$

$r_A = 3 \rightarrow$ $m = 4-3 = 1$, $s = 3-3 = 0$

$$[A'] = \begin{bmatrix} 1/\sqrt{1.25} & -1 & 0 & -1 \\ 1/2\sqrt{1.25} & 0 & 0 & 6 \\ 0 & 1 & -1/\sqrt{1.25} & -1 \\ 0 & 0 & 1/2\sqrt{1.25} & -6 \end{bmatrix}$$

Fig. 6.7 Example discussed in Section 6.2.

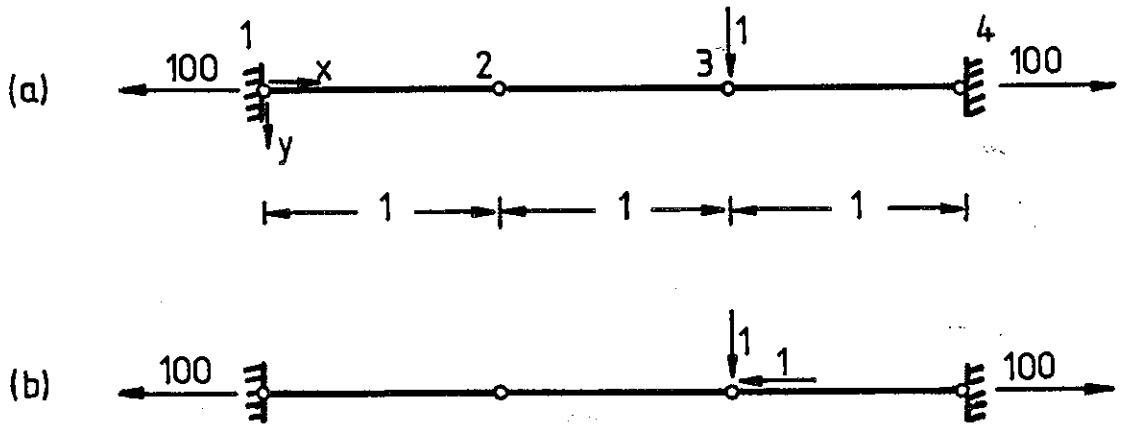

Fig. 6.8 (a) is an example of a load condition which causes no change of bar tension, and hence there is no need for the extra computations that restore the geometrical compatibility. These calculations have been done for (b) in Section 6.2.

[A']; hence the first two entries of $\{\frac{\delta t}{\alpha}\}$ are the tensions of bars 1, 2. The remaining two columns of [A'] are the product-forces, which were first computed in Section 4.5; the level of prestress has been set at 100 (force units) in the present example. For the load condition shown in Fig. 6.8a (6.20) can be written as:

$$\begin{bmatrix} 1 & -1 & 0 & 0 \\ 0 & 0 & 200 & -100 \\ 0 & 1 & 0 & 0 \\ 0 & 0 & -100 & 200 \end{bmatrix} \begin{Bmatrix} \delta t_1 \\ \delta t_2 \\ \alpha_1 \\ \alpha_2 \end{Bmatrix} = \begin{Bmatrix} 0 \\ 0 \\ 0 \\ 1 \end{Bmatrix} \qquad (6.22)$$

The solution of this system of equations confirms that the assigned load is only carried through geometry-change effects, hence the final tensions are $\{t\}=\{t_0\}=\{100\ 100\ 100\}^T$.

Formula (6.20) relies, as noted already, on the knowledge of the 'exact' product-forces although these cannot be computed until the final tensions $\{t_0\}+\{\delta t\}$, as opposed to $\{t_0\}$, are known. There is clearly no difficulty if the applied load $\{\delta f\}$ involves no change of bar tensions, but in most cases (6.20) has to be incorporated in an iterative procedure in which the product-forces are updated at the beginning of each step. The number of iterations required depends on various factors. For instance, if the subspace of the product-forces is orthogonal to the column space only two iterations will be needed; in more general circumstances it depends on the ratio between the norms of the tension vectors before and after application of the loads.

This calculation has been done for the first of the above examples: a new product-force has been computed and adjoined to [A] to obtain an updated version of (6.21)

$$\begin{bmatrix} 1/\sqrt{1.25} & -1 & 0 & -1.4615 \\ 1/2\sqrt{1.25} & 0 & 0 & 8.9231 \\ 0 & 1 & -1/\sqrt{1.25} & -1.5385 \\ 0 & 0 & 1/2\sqrt{1.25} & -9.0769 \end{bmatrix} \begin{Bmatrix} \delta t_1 \\ \delta t_2 \\ \delta t_3 \\ \alpha_1 \end{Bmatrix} = \begin{Bmatrix} 0 \\ 0 \\ 0 \\ 1 \end{Bmatrix}$$

Its solution is $\{\frac{\delta t}{\alpha}\}=\{1.0232\ .9901\ 1.1952\ -.0513\}^T$, from which $\{t\}=\{3.2593\ 2.9901\ 3.4313\}^T$. The norm of this tension vector is 5.5980, very close to 5.6138

of the previous step.

The above treatment is all that is required in the case of statically determinate assemblies; but redundant assemblies need an extra computation: every time a new set of bar tensions in equilibrium with the "fitted loads" is available, a self-equilibrated system of tensions has to be added to restore compatibility by means of (6.7) and (6.10). No correction has to be made to the above examples, because the first one (Fig. 6.7) is statically determinate while the other (Fig. 6.8a), although redundant, is loaded in a way which gives purely inextensional displacements.

As an example consider the load condition shown in Fig. 6.8b; for this new $\{\delta f\}$, (6.22) yields $\{\delta t\}=\{-1\ -1\ 0\}^T$. If the three bars have equal axial stiffness (6.10) gives $x=2/3$; and the updated tension vector is therefore

$$\{t\}=\{t_0\}+\begin{Bmatrix}-1\\-1\\0\end{Bmatrix}+2/3\begin{Bmatrix}1\\1\\1\end{Bmatrix}=\begin{Bmatrix}100-1/3\\100-1/3\\100+2/3\end{Bmatrix}$$

At this stage one can go back to (6.22) with updated product-forces and start the same procedure again.

The above calculation generates, together with the changes of bar tensions, the inextensional displacements $\{di\}$ of the nodes:

$$\{di\}=[\{d_1\},\ldots,\{d_m\}]\{\alpha\} \qquad (6.23)$$

here the column vectors $\{d_1\},\ldots,\{d_m\}$ are the m inextensional mechanisms, and the m-dimensional vector $\{\alpha\}$ contains the last m entries of $\{\frac{\delta t}{\alpha}\}$. The final inextensional displacements $\{di\}$ are $\{0.0256\ -0.0513\ 0.0256\ 0.0513\}^T$ and $\{0.\ 0.0333\ 0.\ 0.0667\}^T$ for the assemblies of Figs 6.7 and 6.8a, respectively. To obtain the total nodal displacements one still has to compute the extensional displacements $\{de\}$ due to the "fitted loads", which will be discussed in the next section. One last remark on the displacements $\{di\}$ is that they are not rigorously inextensional, yet the source of the appreciable error connected with this can be removed at no expense by subtracting these unwanted elongations from $\{e\}$ before entering the procedure described in Section 6.3.

The approach presented in this section is substantially different from all the iterative techniques based on tangent/secant stiffness matrices often used to analyse cable structures (see, e.g., Argyris & Scharpf, 1972, Møllmann, 1974 and Baron & Venkatesan, 1971). The work of Szabo' (1973) has some points in common with the present one in that equilibrium and compatibility statements are kept separate throughout; in fact although his equilibrium, compatibility and flexibility matrices are submatrices of one hypermatrix, in most parts of the analysis they are used independently. He also attaches some importance to the rank of the equilibrium matrix. The paper by Szabo' also deals with the response of kinematically indeterminate structures to applied loads but he proposes to use the same approach as for stiff structures within an iterative procedure. This technique has been expanded and applied to the analysis of cable nets by Szabo' & Kollar (1984).

J. Argyris is frequently acknowledged as one of the great contributors to the advancement of the displacement method of analysis and its application to non-linear problems, documented in, e.g., Argyris (1964) and Argyris & Scharpf (1972). Here it is interesting to note that a whole chapter of Argyris (1964) is dedicated to the use of the force method in non-linear problems; an iterative procedure allows for the (elastic) distortion of the structure when the equilibrium equations are written, by means of "imaginary loads" which have some resemblance to the product-forces in [A'] although they are introduced for modes of deformation which are extensional, see Section 6.4.2.

Kuznetsov (1973) wrote a theoretical contribution on the mechanics of assemblies with s=0, m>0: he proposed to divide any applied load into "equilibrium" and "supplementary" components, and he derived a formula equivalent to (6.19) by differentiating the equation of the constraint imposed by a bar on the displacements of its end nodes. Kuznetsov's approach, though, differs in a number of details from the present method and its validity is limited to small inextensional displacements.

6.3 Computation of extensional displacements

The nodal displacements of a rigid structure due to a compatible set of bar elongations {e} are easy to compute: it was shown in Section 6.1.1 that it is a matter of 'compacting' the elongation vector by discarding the elongations of the statically indeterminate bars and then computing {d} from (6.12).

Structural mechanisms cannot be treated in the same way because there is not a unique solution when only geometrical conditions are invoked. In fact the compatibility matrix $[A]^T$ enforces all such conditions, plainly in the hypothesis of small extensional displacements; but the number of independent equations (r_A) is smaller than the number of unknown components of displacement (3n-c). Therefore the system of equations

$$[A]^T\{de\}=\{e\} \tag{6.24}$$

cannot be solved uniquely; here {de} is the vector of extensional displacements. Some more equations are needed. It might be argued that, all the inextensional displacements {di} having been computed already, the extensional displacement vector has to be orthogonal to the left-nullspace of [A] and hence to the m inextensional mechanisms computed earlier. A total number of m independent conditions of orthogonality of the form $\{d_i\}^T\{de\}=0$, which are precisely the number of extra equations that are needed to solve (6.24), would be obtained in this way. But no sound structural principle guarantees the validity of such conditions, and in fact they are wrong. A correct set of equations is obtained by substitution of the m product-forces for the inextensional mechanisms; and the correctness of this can be demonstrated by writing m equilibrium equations in inextensionally deformed configurations. The following proof relies on the existence of m product-forces, and hence of a set of initial tensions $\{t_o\}$ in equilibrium with initial loads $\{f_o\}$, before any displacement takes place. If there is no prestress, no further conditions can be imposed and {de} is not uniquely determined.

For the purpose of this demonstration, start by considering a set of entirely general bar elongations $\{e_o\}$. First this is to be transformed into a compatible set of elongations {e}; if s=0 $\{e\}=\{e_o\}$, otherwise (6.8) gives, for {t}={0},

$$\{e\}=\{e_o\}+[F][SS]\{x\} \tag{6.25}$$

where the unknown {x} is obtained from (6.10).

The initial forces $\{f_o\}$ are in equilibrium with the bar tensions $\{t_o\}$ when the assembly is in its initial configuration; and the displacements $\{de\}$ are compatible with the assigned elongations $\{e\}$. Virtual work relates the external and internal work done by the systems defined above (Neal, 1964):

$$\{f_o\}^T\{de\}=\{t_o\}^T\{e\} \tag{6.26}$$

Now consider the the new configuration of the assembly obtained by imposing the (small) inextensional distortion due to mechanism $\{d_i\}$. Because of the way in which the product-forces were defined in Section 4.5, the forces $\{f_o\}+\{p_i\}$ are in equilibrium with the bar tensions $\{t_o\}$ ($\{p_i\}$ is the vector of product-forces due to the mechanism $\{d_i\}$). Starting from the distorted configuration, the displacements $\{de\}$ are still compatible with the elongations $\{e\}$ since the change of configuration considered was small. Virtual work can be used again, this time to obtain:

$$(\{f_o\}+\{p_i\})^T\{de\}=\{t_o\}^T\{e\} \tag{6.27}$$

Subtract (6.26) from (6.27) to obtain:

$$\{p_i\}^T\{de\}=0 \tag{6.28}$$

which is precisely the anticipated relationship. Formula (6.28) provides m equations in the unknown components of displacement, one for each product-force. They supplement the r_A independent equations in (6.24) and can be written in matrix form as:

$$[A']^T\{de\}=\{\frac{e}{0}\} \tag{6.29}$$

where $[A']^T$ is the transpose of the matrix defined in Fig. 4.9. The $(3n-c)$-dimensional vector $\{\frac{e}{0}\}$ contains the elongations of the statically determinate bars as its first r_A components; the remaining m entries are 0 in order to impose the orthogonality of the last m rows of $[A']^T$ (=product-forces) to $\{de\}$.

Formula (6.29) completes the analogy between the standard equilibrium matrix [A], whose transpose is the compatibility matrix of (4.9), with [A'] which performs similar functions in the more general class of problems treated here.

The linear analysis of any kinematically indeterminate assembly is now complete: inextensional and extensional displacement vectors can be added up to obtain the total displacements, as shown in the following examples. Notice that the procedures described for updating the product-forces while computing $\{\frac{\delta t}{\alpha}\}$ and for eliminating undesired bar elongations due to the mechanisms, result in a (small) non-linearity in the overall behaviour of the assembly. The method can cope, in its present form, with a large range of statically determinate structures, but the computation may need to be expanded when dealing with redundant assemblies; these further developments will be investigated in the Section 6.4.

6.3.1 Examples and experiments

The extensional displacements of the plane frameworks in Figs 6.7 and 6.8 can be computed by use of (6.29). For the sake of simplicity the axial stiffness $(AE)_i$ of bar i of either framework is taken as 100 (expressed in the appropriate units). Starting from the assembly in Fig. 6.7 the elastic bar elongations are given by (6.2):

$$\{e\}=[F]\{\delta t\}=\begin{bmatrix}\sqrt{1.25}/100 & & \\ & 1/100 & \\ & & \sqrt{1.25}/100\end{bmatrix}\begin{Bmatrix}1.0232\\0.9901\\1.1952\end{Bmatrix}=\begin{Bmatrix}.0114\\.0099\\.0134\end{Bmatrix}$$

The inelastic elongation of each bar, in consequence of the inextensional displacements computed in Section 6.2, is equal to the difference between the exact length in the 'inextensionally' distorted configuration (computed by Pythagoras' theorem) and the original one. The vector of inelastic elongations turns out to be

$$\{e_0\}=\{.0014\ \ .0052\ \ .0015\}^T$$

All the bars of this truss are statically determinate, hence all the above

elongations are certainly compatible. The first three entries of $\{\frac{e}{0}\}$ in (6.29) are given by

$$\{e\}-\{e_0\}=\{.0100\ \ .0047\ \ .0119\}^T$$

Using the final expression of [A'], (6.29) becomes:

$$\begin{bmatrix} 1/\sqrt{1.25} & 1/2\sqrt{1.25} & 0 & 0 \\ -1 & 0 & 1 & 0 \\ 0 & 0 & -1/\sqrt{1.25} & 1/2\sqrt{1.25} \\ -1.4615 & 8.9231 & -1.5385 & -9.0769 \end{bmatrix} \{de\}=\begin{Bmatrix} .0100 \\ .0047 \\ .0119 \\ \underline{0} \end{Bmatrix}$$

The solution of this is $\{de\}=\{-.0035\ \ .0293\ \ .0012\ \ .0291\}^T$. The total nodal displacements of the assembly of Fig. 6.7 are therefore

$$\{d\}=\{di\}+\{de\}=\begin{Bmatrix} .0256 \\ -.0513 \\ .0256 \\ .0513 \end{Bmatrix}+\begin{Bmatrix} -.0035 \\ .0293 \\ .0012 \\ .0291 \end{Bmatrix}=\begin{Bmatrix} .0221 \\ -.0220 \\ .0268 \\ .0804 \end{Bmatrix}$$

The assembly of three collinear bars in Fig. 6.8a has no extensional displacement, but the largest bar elongation due to {di} is in this case .0022. So long as this error is negligible, the results of the linear analysis are acceptable and {d}={di}.

Now consider the second load condition, displayed in Fig. 6.8b. The main difference from the computation shown above is that no improvement in the accuracy of the solution is usually achieved by subtracting the inelastic elongations $\{e_0\}$ from the elastic ones. This result is not unexpected since, in assemblies with s>0 and m>0, $\{e_0\}$ is not merely a side-effect of an essentially correct computation but it may be an important factor (see Section 6.4) which leads to an increase in the level of selfstress. Therefore this effect will be neglected altogether in this example. Taking all axial stiffnesses to be 100 the compatible elongations of bars 1 and 2, which are statically determinate, are

$$\{e\}=[F]\{d\}=\begin{bmatrix}1/100 & \\ & 1/100\end{bmatrix}\begin{Bmatrix}-1/3\\-1/3\end{Bmatrix}=\begin{Bmatrix}-1/300\\-1/300\end{Bmatrix}$$

And (6.29) becomes, with [A'] from (6.22),

$$\begin{bmatrix}1 & 0 & 0 & 0\\ -1 & 0 & 1 & 0\\ 0 & 200 & 0 & -100\\ 0 & -100 & 0 & 200\end{bmatrix}\{de\}=\begin{Bmatrix}-1/300\\-1/300\\ \hline 0\\ 0\end{Bmatrix}$$

The extensional and total displacements are therefore:

$$\{de\}=\{-.0033\ 0\ -.0067\ 0\}^T$$
$$\{d\}\ =\{-.0033\ .0033\ -.0067\ .0667\}^T.$$

The theoretical foundations of the method described in this section are clearly sound and one would expect its results to be correct, within the limits of validity already discussed. For the sake of completeness the theoretical argument presented above has been supplemented by several experimental and numerical tests.

For instance, two very simple experiments were conducted to test the accuracy of (6.29) with reference to statically determinate assemblies; in the first one, see Fig. 6.9, two equal weights were hung from a thin copper wire whose ends were fixed to a vertical board by means of drawing pins at the same level. The assembly consisted therefore of two inclined cable segments on either side of a horizontal one, as in Fig. 6.7. Incidentally, notice that the product-forces of the assemblies in Figs 6.7 and 6.9 are proportional and can be assumed for present purposes to be equal, so that [A'] is known already. The test consisted in measuring the displacements caused by a shortening of 10mm of one of the side members, which was obtained by letting 10mm of wire slide through the left-hand pin. No extra loads were added and the measured displacements were indeed small compared to the overall dimensions: the elastic elongations of the segments are negligible compared to the imposed one. A sheet of graph paper stuck on the board holding the pins was used for

all the measurements; no magnifying instruments were used to take readings. Two independent estimates of the nodal displacements were obtained from (6.29) and from the non-linear finite element program described in the Appendix; the results are presented in Fig. 6.9 and they demonstrate the accuracy of the present method.

A similar experiment was done on the layout of Fig. 6.10. Again the first segment was shortened by 10mm and the nodal displacements were measured and compared to theoretical estimates.

Other equally successful but purely numerical tests were conducted on redundant assemblies: these employed the f.e. program described in the Appendix and will not be described here.

6.4 Corrections to the linear theory

Limitations of the linear theory developed in Sections 6.2 and 3 have been pointed out already; in essence that theory is valid if the nodal displacements are sufficiently small. In order to extend the validity of the linear computations to a wider range of nodal displacements two entirely independent corrections will be introduced here, the first of which applies only to redundant assemblies. An elementary example will introduce the problem.

Figure 6.11 shows an assembly of two collinear bars; plainly m=s=1 and the inextensional motion consists of a vertical displacement of the node. The state of selfstress consists of equal bar tensions, which have been set to t_o. The load shown in Fig. 6.11b excites the inextensional mode and, within a small range of vertical displacements, the linear analysis applies. The layout is very simple and therefore its response can be obtained in closed form: the only component of displacement is y_2 and the bar tensions have to be equal for any value of W because the load condition is symmetrical. The above remarks apply to displacements of any magnitude, of course. It can be initially assumed that the tensions in the bars stay constant although y_2 might impose considerable elongations. On this hypothesis the force W_p ('p' stands for prestress) which equilibrates the assembly in the distorted configuration defined by y_2 can be obtained from an equation of equilibrium in the vertical direction:

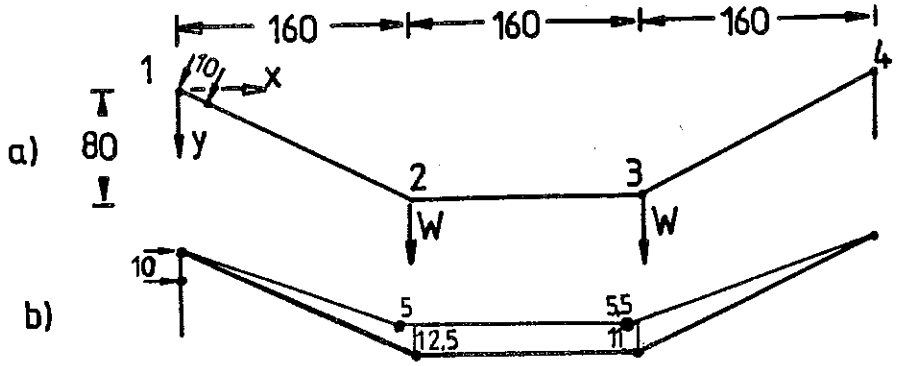

Displ.	Experimental	from (6.29)	from f.e.
x_2	-5.	-5.2	-5.0
y_2	-12.5	-12.1	-12.7
x_3	-5.5	-5.2	-5.1
y_3	-11.	-10.4	-11.1

Fig. 6.9 Schematic description of an experiment to test the validity of (6.29). a) shows the initial configuration. Both configurations are shown in b), where the final configuration has been drawn with a thinner line. The table compares measured and estimated nodal displacements. All dimensions are in [mm].

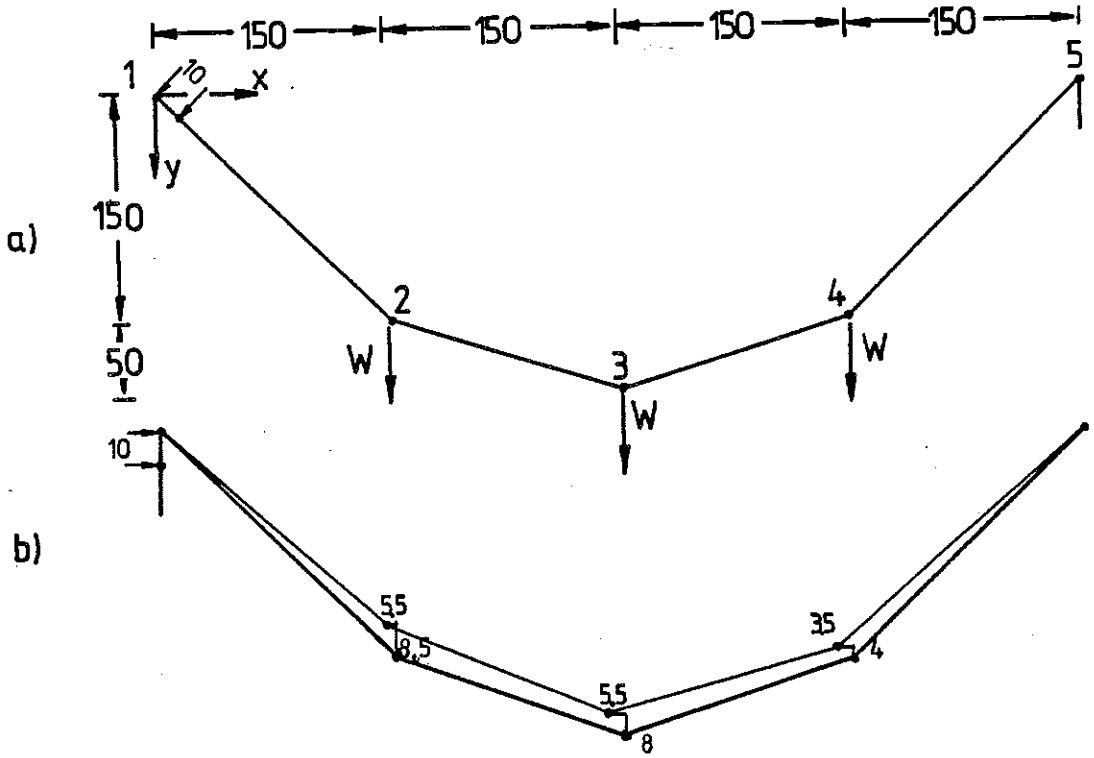

Displ.	Experimental	from (6.29)	from f.e.
x_2	-5.5	-5.4	-5.4
y_2	-8.5	-8.7	-8.8
x_3	-5.5	-5.5	-5.5
y_3	-8.	-8.2	-8.4
x_4	-3.5	-4.2	-4.2
y_4	-4.	-4.2	-4.3

Fig. 6.10 Cf. Fig. 6.9.

$$W_p = 2t_0 \sin \arctan \frac{y_2}{l} \qquad (6.30)$$

This expression resembles (6.19), which defined the product-forces, and in fact the two coincide if $\frac{y_2}{l}$ is small. The elastic bar elongations due to y_2 are equal to $(1/\cos \arctan \frac{y_2}{l})-1$ and the consequent change of bar tensions is $\delta t = AE[(1/\cos \arctan \frac{y_2}{l})-1]$. The vertical force W_e ('e' for elastic) in equilibrium with δt is obtained by replacing t_0 in (6.30) by δt:

$$W_e = 2AE[(1/\cos \arctan \frac{y_2}{l})-1] \sin \arctan \frac{y_2}{l} \qquad (6.31)$$

In conclusion:

$$W = W_p + W_e = 2\{t_0 + AE[(1/\cos \arctan \frac{y_2}{l})-1]\} \sin \arctan \frac{y_2}{l} \qquad (6.32)$$

The load/deflection curve according to this expression has been plotted in Fig. 6.12. For small values of $\frac{y_2}{l}$, $\sin \arctan \frac{y_2}{l} \approx \arctan \frac{y_2}{l} \approx \frac{y_2}{l}$ and $\cos \frac{y_2}{l} \approx 1-(\frac{y_2}{l})^2/2$. Neglecting terms of higher order (6.32) becomes:

$$W = AE(\frac{y_2}{l})^3 + 2t_0 \frac{y_2}{l} \qquad (6.33)$$

This is plotted in Fig. 6.12. In most structural applications the strain in the material is not too large and it can be assumed that (6.33) gives an accurate description of the behaviour of the structure in Fig. 6.11. The right-hand-side of (6.33) consists of a linear term, which accounts for the 'geometrical' stiffness of the assembly due to prestress, and of a cubic term due to the increase in the level of bar tension. Results from the linear theory are acceptable so long as $AE(\frac{y_2}{l})^3$ is small compared to $t_0 \frac{y_2}{l}$: the linear theory does not 'know' that part of the applied load will be equilibrated by the 'elastic' component W_e and therefore it overestimates the nodal displacement y_2 but underestimates the bar tensions.

This can be corrected by the introduction of a reducing factor γ ($0<\gamma<1$) that multiplies the initial estimate, $\bar{y}_2$, obtained from the linear computation; an equation of equilibrium in the unknown γ is then obtained by substituting $\gamma\bar{y}_2$ to y_2 in (6.33):

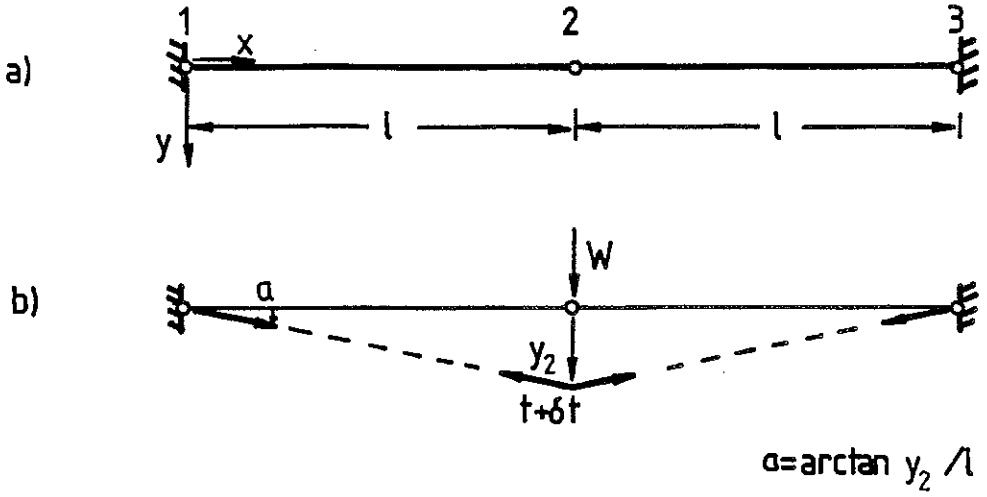

Fig. 6.11 a) Initial configuration. The axial stiffnesses of the bars are equal. The prestressing tensions are $\{t_0\}=t_0\{1\ 1\}^T$.
b) Distortion due to W.

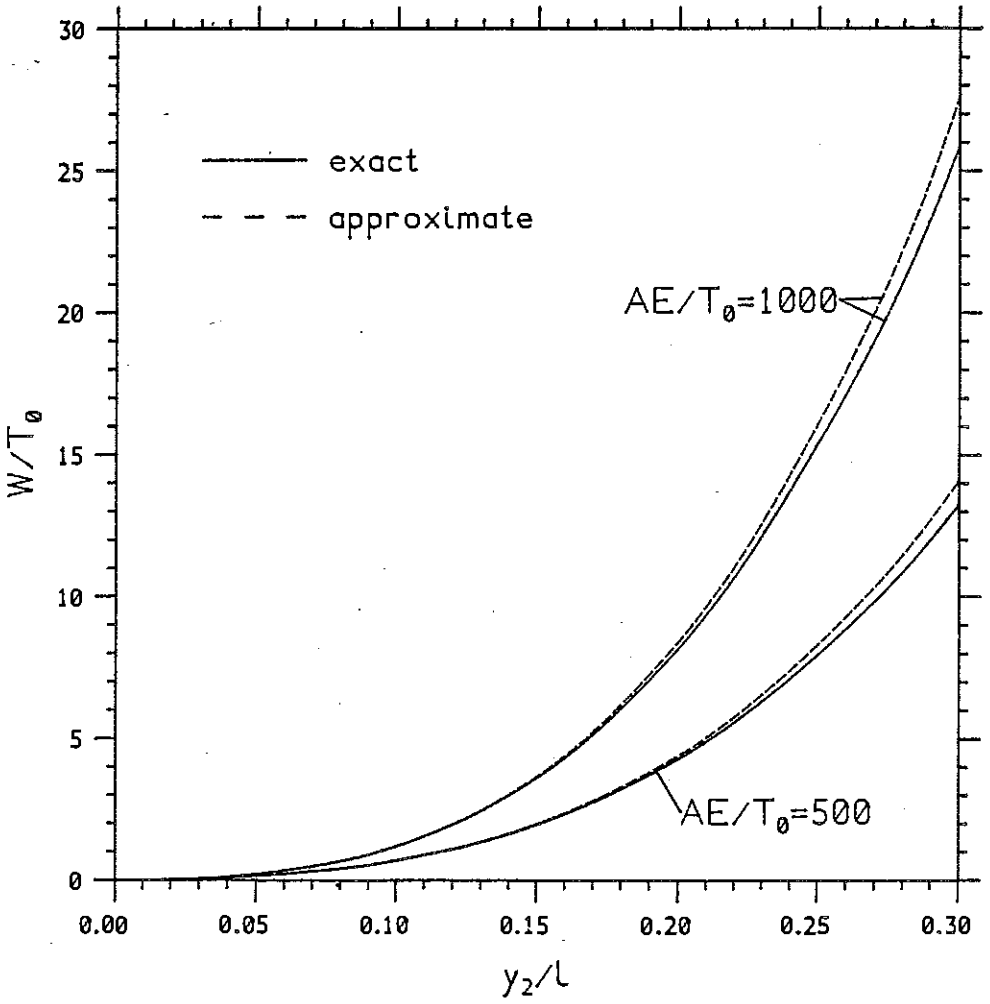

Fig. 6.12 Comparison between (6.32) and (6.33). The lower value of AE/t_0 corresponds to a rather low value of the initial prestress, if the assembly of Fig. 6.11 is made of steel.

$$W=AE(\bar{y}_2/l)^3\gamma^3+2t_0(\bar{y}_2/l)\gamma \qquad (6.34)$$

Apart from the initial displacement $\bar{y}_2=Wl/2t_0$, computed according to Section 6.2, the numerical coefficients of (6.34) depend on the elastic axial stiffness of the bars and on the level of prestress. This approach was first proposed by Pellegrino & Calladine (1984). It should be added that the level of selfstress does not change appreciably in statically determinate assemblies.

Do these conclusions apply to more general situations?

The answer is yes, and this can be demonstrated by analysing the response of the saddle-shaped cable net shown in Fig. 6.13, a more complicated redundant assembly, to a system of product-forces. The components of load are

$$\{\ 3.23\ \ -3.23\ \ -9.68\ \ 0\ \ -.62\ \ 0\ \ -3.23\ \ -3.23\ \ 9.68$$
$$\ \ .62\ \ \ 0\ \ \ 0\ \ \ 0\ \ \ 0\ \ \ 0\ \ -.62\ \ \ 0\ \ \ 0$$
$$\ \ 3.23\ \ 3.23\ \ 9.68\ \ 0\ \ .62\ \ 0\ \ -3.23\ \ 3.23\ \ -9.68\ \}^T$$

equal to the product-forces corresponding to the inextensional mechanism

$$\{\ \ 1.\ \ \ -1.\ \ \ -2.5\ \ 0\ \ -.6887\ \ 0\ \ \ -1.\ \ \ -1.\ \ \ 2.5$$
$$\ .6887\ \ \ 0\ \ \ \ 0\ \ \ 0\ \ \ \ 0\ \ \ 0\ \ -.6887\ \ \ 0\ \ \ \ 0$$
$$\ \ \ 1.\ \ \ \ 1.\ \ \ \ 2.5\ \ 0\ \ .6887\ \ 0\ \ \ -1.\ \ \ \ 1.\ \ \ -2.5\ \}^T$$

The finite element program has been used to predict the behaviour of this cable net for different values of the load factor. This assembly has also been tested experimentally, and in fact the level of prestress in this numerical test has been set the same as in one of the experiments, which will be described in Chapter 7. Figure 6.14 shows a plot of the load factor against the components of displacement of node 5, chosen arbitrarily; although each graph is non-linear the ratio between these components of displacements remains approximately constant at 1/-1/-2.5, as in the infinitesimal mechanism. The figure also shows a plot of equation $-1.1479.10^5z^3-.0408z$, the coefficients of which were chosen to obtain a good fit with the 'exact' curve.

As a further test the same cable net was loaded by the vector of product-forces corresponding to the mechanism

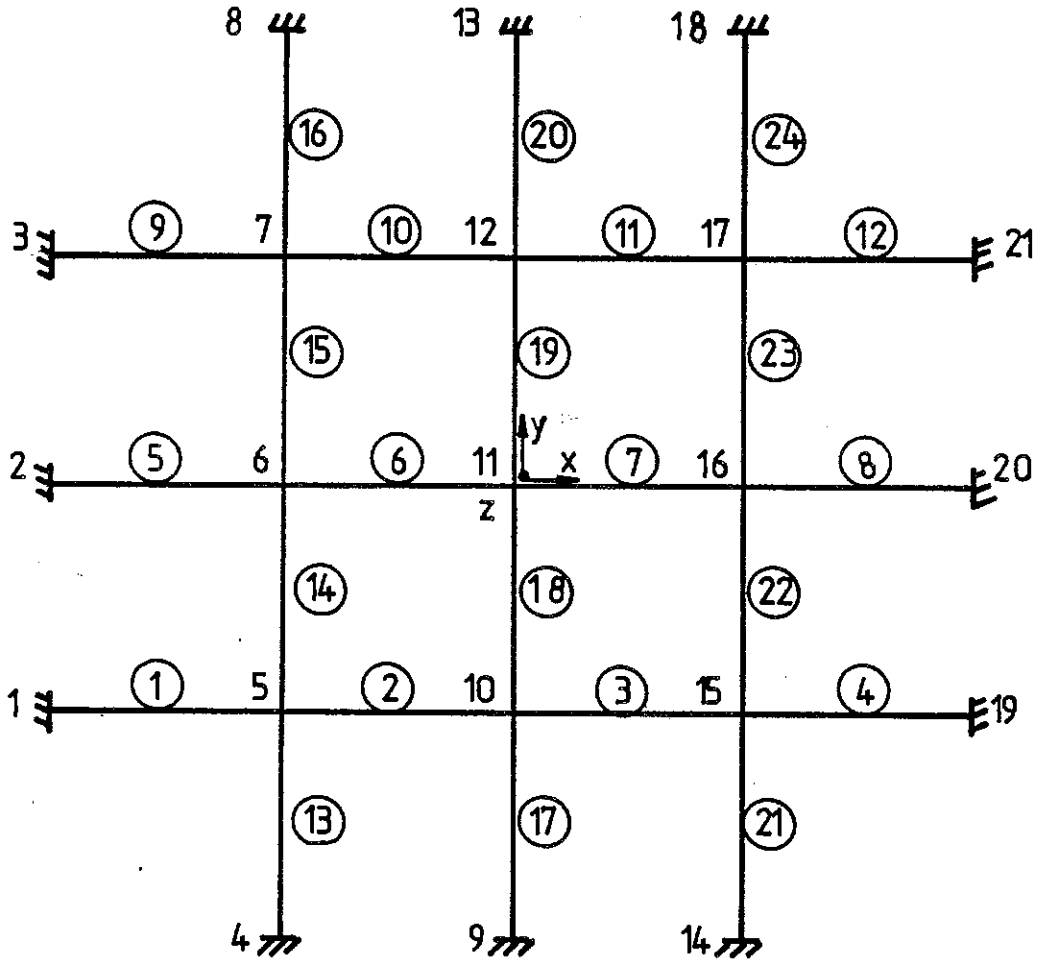

Fig. 6.13 Plan view of the saddle-shaped cable net first examined in Section 6.4. All the boundary nodes are fully constrained; more details of the geometry, material properties and prestress are given in Chapter 7.
By inspection, this structure has n=21, b=24, c=36 and hence 3n-b-c=3. the analysis described in Chapter 4 shows that r_A=59, s=1 and m=4.
The z-axis is directed upwards. The 3 cables parallel to the x,z plane are hogging (i.e. have negative curvature), the others are sagging.

$$\{\ .9042\ \ -.9042\ \ -2.2605\ \ -1.\ \ -.3113\ \ 2.5\ \ 0\ \ 0\ \ 0$$
$$0\ \ 0\ \ 0\ \ .3113\ \ 1.\ \ 2.5\ \ -.3443\ \ .3443\ \ -2.7648$$
$$0\ \ 0\ \ 0\ \ 0\ \ 0\ \ 0\ \ 0\ \ 0\ \ 0\ \}^T$$

This mechanism clearly does not enjoy the same properties of symmetry as the one considered above, but Fig. 6.15 shows that all the properties noted in Fig. 6.14 still hold.

All of these remarks demonstrate that, provided the numerical coefficients of the third-order equation that replaces (6.34) in more general cases are estimated correctly, the non-linear response of a cable net to any of its product-forces is comparatively easy to predict.

6.4.1 Non-linear corrections for redundant assemblies

The need to compute a factor Υ that reduces the 'inextensional' displacements $\{d_i\}$ obtained from (6.20) and (6.23), and proportionally increases the level of prestress of a redundant framework which is loaded by 'large' forces, has been stressed already. In this section virtual work will be used to demonstrate the validity of a generalized form of equation (6.34); this new equation will allow the computation of Υ. Notice that, although all the results obtained here are qualitatively the same for all statically indeterminate assemblies, the treatment will be confined to the case s=1 which is of interest at present.

A side-effect of the linear theory is that a set of elongations $\{e_o\}$ - first introduced in Section 6.3 for statically determinate assemblies - is associated with an 'inextensional' distortion. In the case of redundant assemblies this effect becomes a little more complicated, because any 'inextensional' distortion is also accompanied by an increase of the level of pretension, and will be introduced here by means of an example.

The assembly shown in Fig. 6.16 is similar to Fig. 6.11, and in particular its bars still have equal AE, but the line of action of W - which still coincides with the direction of the mechanism - is no longer an axis of symmetry of the assembly; hence the substantial change in the prestress level which accompanies any large 'inextensional' distortion due to W leads to bar elongations which are not equal to those associated with the mechanism. See Fig. 6.16b. Therefore loading this assembly by force components which are

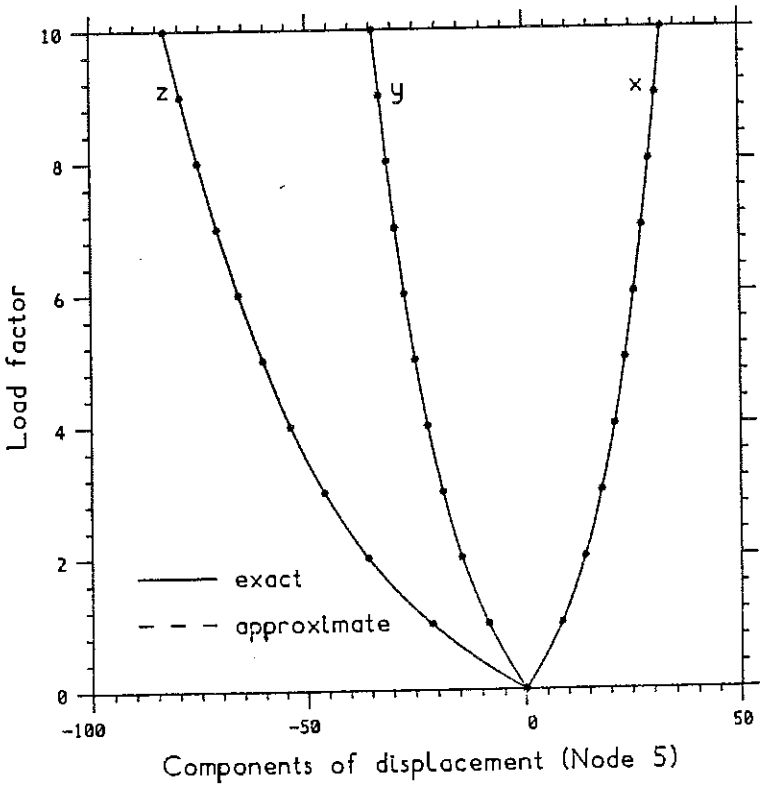

Fig. 6.14 Load/displacement graphs for the cable net of Fig. 6.13, under the first load system described in Section 6.4. Starred points correspond to results from a finite element computation; an 'approximate' dotted line of equation $-1.1479.10^{-5}z^3-0.0408z$ has been fitted.

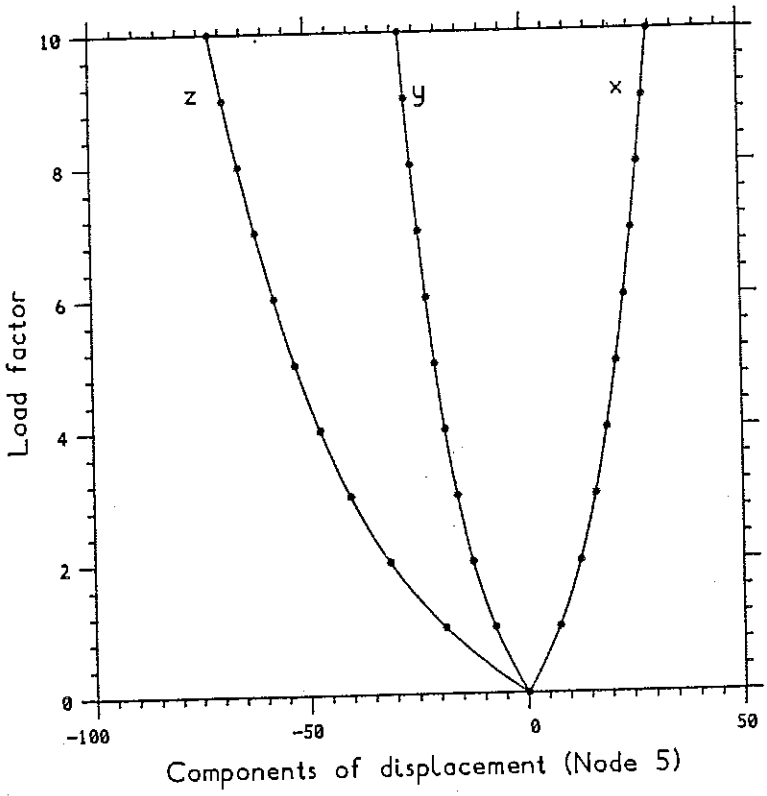

Fig. 6.15 Load/displacement graphs for the cable net of Fig. 6.13, under the second loading system described in Section 6.4.

proportional to the vector of product-forces causes its only node to move along a path tangent to the vector representing its inextensional and infinitesimal motion. In the case of Fig. 6.16b such a path has been obtained graphically, but the knowledge of the entire paths described by all nodes of a complicated framework is not needed in practice.

Thus, the first requirement at the end of the linear analysis is to restore the violated 'geometrical compatibility' by letting each node return to its path (equilibrium considerations are left aside at this stage): the undesired elongation of each bar associated with the inextensional displacement, computed from (6.23), is calculated as the difference between final and initial lengths (both computed by Pythagoras' theorem). In the case of statically determinate assemblies these elongations $\{e_0\}$, changed in sign, could be used in (6.29) to compute the related extensional displacements. In the present case $-\{e_0\}$ may not be compatible and therefore, after (6.8) and (6.10), the elongations to be used in the computation are:

$$\{e\}=-\{e_0\}+[F][SS]x \qquad (6.35)$$

where $x=[SS]^T\{e_0\}/[SS]^T[F][SS]$.

Here [SS] is just a column vector, as s=1.

Obviously the elongations of 'dependent' bars have to be dropped when one solves:

$$[A']^T\{dc\}=\{\frac{e}{0}\} \qquad (6.36)$$

Here {dc} denotes the vector of correcting nodal displacements such that the configuration defined by {di}+{dc} is geometrically compatible.

But equilibrium will not be satisfied in this configuration because the level of selfstress has in the meantime increased to $\{t_0\}+[SS]x$. A parameter γ is therefore introduced in the analysis ($0<\gamma<1$) to reduce the inextensional displacements by γ and increase accordingly the initial selfstress by $1/\gamma$. The correcting displacements will be reduced to $\gamma^2\{dc\}$; the reason for the power two appearing at this stage is that the bar elongations - and hence the correcting displacements - associated with an infinitesimal

mechanism of order one are of second order. Note that this is, visually, in agreement with Fig. 6.16.

Now the assembly will be allowed to move with its nodes resting firmly on rigid rails of 'parabolic shape', in search of an equilibrated configuration. The equation that determines Υ will be obtained from virtual work, and the configuration in equilibrium under the applied loads will be:

$$\Upsilon\{di\}+\Upsilon^2\{dc\} \qquad (6.37)$$

In this configuration the total load $\{f\}$ is in equilibrium with the bar tensions given by the sum $\{t_0\}+\{\delta t\}+[SS] \times \Upsilon^2$, the individual terms of which are the initial prestress, the bar tensions due to the "fitted" component of $\{f\}$ and the increase in selfstress level computed above, respectively. The last term of the sum contains Υ^2 because, being a consequence of the non-inextensionality of the mechanism, it varies with the same law as $\{dc\}$.

An infinitesimal displacement from the configuration defined in (6.37) is obtained by differentiating it with respect to its only variable, Υ; this gives

$$(\{di\}+2\{dc\}\Upsilon)d\Upsilon$$

The elongations compatible with this displacement are $2[F][SS] \times \Upsilon d\Upsilon$. This is because the correcting elongations that correspond to the configuration (6.37) are $\Upsilon^2\{e_0\}$ from the argument used above. Differentiation yields $2\{e_0\}\Upsilon d\Upsilon$ but only the component of $\{e_0\}$ which gives rise to selfstress needs to be considered, hence the expression given above.

	Forces	Displacements
External	$\{f\}$	$(\{di\}+2\{dc\}\Upsilon)d\Upsilon$
Internal	$\{t_0\}+\{\delta t\}+[SS] \times \Upsilon^2$	$2[F][SS] \times \Upsilon d\Upsilon$

Table 6.1 Terms of the equation of virtual work in Section 6.4.1. All symbols have their usual meaning; x is from (6.35).

All the terms needed in the equation of virtual work have been summarized in Table 6.1; equate external to internal work and divide by dY to obtain:

$$\{f\}^T\{di\}+2\{f\}^T\{dc\}Y=$$
$$2(\{t_0\}+\{\delta t\})^T[F][SS]xY+2[SS]^T[F][SS]x^2Y^3$$

This equation can be written in the form:

$$2[SS]^T[F][SS]x^2Y^3+2[(\{t_0\}+\{\delta t\})^T[F][SS]x-\{f\}^T\{dc\}]Y+$$
$$-\{f\}^T\{di\}=0 \qquad (6.38)$$

This is a third-order equation of the type $a_3Y^3+a_1Y-a_0=0$, the solution of which completes this non-linear correction. This equation has been successfully used in several hand and automatic calculations. The coefficients a_1 and a_0 have always turned out to be about equal and, taking advantage of this, one can divide both sides of (6.38) by a_0 and use the simplified form:

$$\frac{2[SS]^T[F][SS]x^2}{\{f\}^T\{di\}}\,Y^3+Y-1=0 \qquad (6.39)$$

The equality of a_1 to a_0 is a direct consequence of the linear theory. In fact, on the assumption that the level of prestress does not increase, the loading procedure consists of a gradual increase of load from $\{0\}$ to $\{f\}$ while only the inextensional displacement $\{di\}$ develops. Finally, the correcting displacement $\{dc\}$ takes place. The work done by the applied load in this process is $\frac{1}{2}\{f\}^T\{di\}+\{f\}^T\{dc\}$.

The bar tensions have in the meantime increased from $\{t_0\}$ to $\{t_0\}+\{\delta t\}$, hence their work is $(\{t_0\}+\{\delta t\})^T[F][SS]x$. Equating external and internal work one obtains

$$\frac{1}{2}\{f\}^T\{di\}+\{f\}^T\{dc\}=(\{t_0\}+\{\delta t\})^T[F][SS]x$$

from which the equality of a_1 to a_0 is plain.

Does (6.39) agree with, say, (6.34)? The results of the linear analysis for the framework of Fig. 6.11 are $\{\delta t\}=\{0\}$, $\{di\}=\{0\ Wl/2t_0\}^T$, $\{de\}=\{0\}$. The vector of undesired bar elongations is $\{e_0\}=e_0\{1\ 1\}^T$ with $e_0=\sqrt{l^2+\bar{y}_2^2}-l\approx W^2l/8t_0^2$. The equation $[SS]^T[F][SS]\{x\}=[SS]^T\{e_0\}$ now becomes:

$$\{1\ 1\}\begin{bmatrix}1/AE & \\ & 1/AE\end{bmatrix}\begin{Bmatrix}1\\1\end{Bmatrix}x=\{1\ 1\}\begin{Bmatrix}1\\1\end{Bmatrix}\frac{W^2l}{8t_0^2}$$

from which $x=AEW^2/8t_0^2$. Substitution of all these quantities into (6.39) yields:

$$(AEW^2/8t_0^3)\gamma^3+\gamma-1=0$$

and (6.34) can be easily put in the same form.

6.4.2 Product-forces corresponding to extensional modes

The stiffening effects of prestress, in the form of the so-called product-forces corresponding to each of the m inextensional mechanisms, have been extensively discussed. Indeed the modified equilibrium matrix [A'] has been used throughout this chapter for the linear analysis of arbitrary kinematically indeterminate frameworks.

Prestress has a similar linear effect on the extensional modes of the assembly and these can be also included in (the first r_A columns of) [A'].

Consider again the assembly of Fig. 6.7, the linear analysis of which was done in Section 6.2. In order to focus on this effect a load condition which is purely "fitted" will be considered, consisting of equal downward loads of magnitude W applied at nodes 2, 3. The live load vector is therefore $\{\delta f\}=\{0\ W\ 0\ W\}^T$. Equation (6.21) gives the tension changes due to this load: $\delta t_1=\delta t_3=2\sqrt{1.25}W$, $\delta t_2=2W$. Of course, this result ignores any stiffening effects of $\{t_0\}$. The elastic bar elongations and the consequent nodal displacements due to these changes of tension will upset (6.21), resulting in unbalanced forces whose direction is shown in Fig. 6.17. These forces are 'linear' functions of the nodal displacements as well as of the initial tensions $\{t_0\}$; they also depend on $\{\delta t\}$ but this can be neglected if $\{\delta t\}$ is small compared

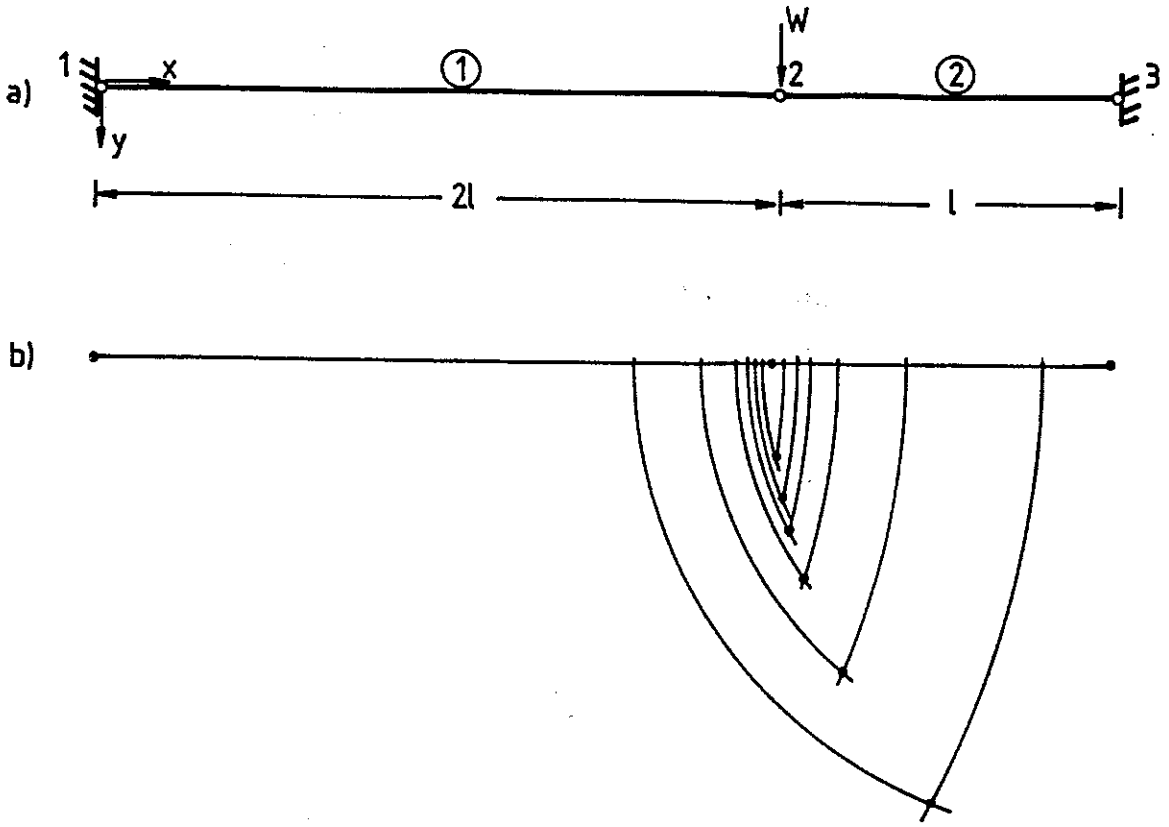

Fig. 6.16 a) A modified version of the assembly in Fig. 6.11. The state of prestress is unchanged. Small loads W are equilibrated through geometry-change effects; but larger loads cause an increase in the level of bar tensions. This increase is about equal to a change in selfstress level, if the deflections are not too large. Any increase of prestress involves bar elongations e_1 and e_2 in the ratio $e_1/e_2=0.5$. The path of node 2 is shown in (b).

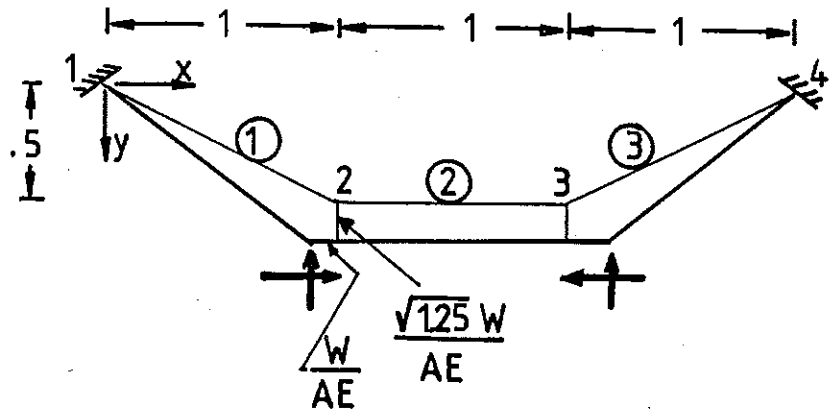

Fig. 6.17 Extensional distortion and consequent 'unbalanced' forces in the assembly of Fig. 6.7, under the fitted load $\{0\ W\ 0\ W\}^T$. AE is constant for all bars.

to $\{t_o\}$.

Let bar h of the framework be one of the r_A independent ones. A unit change of tension in this bar produces an elongation vector $\{e_o\}$ in which the component of position h is $(1/AE)_h$ and the others are zero. If $s\neq 0$, $\{e_o\}$ may not be compatible, in which case compatible elongations $\{e\}$ have to be derived from (6.35); otherwise $\{e\}=\{e_o\}$. The (extensional) nodal displacements $\{d^h\}$ due to $\{e\}$ are then computed from

$$[A']^T\{d^h\}=\{\frac{e}{0}\}$$

Now, as in Section 4.5, one can define the product-forces at node i, corresponding to the extensional mode $\{d^h\}$:

$$\begin{aligned}
&[(X_i+x_i)-(X_j+x_j)]t_{op}/(l_p+e_p)+[(X_i+x_i)-(X_k+x_k)]t_{oq}/(l_q+e_q)=f_{oix}+p_{ix}\\
&[(Y_i+y_i)-(Y_j+y_j)]t_{op}/(l_p+e_p)+[(Y_i+y_i)-(Y_k+y_k)]t_{oq}/(l_q+e_q)=f_{oiy}+p_{iy}\\
&[(Z_i+z_i)-(Z_j+z_j)]t_{op}/(l_p+e_p)+[(Z_i+z_i)-(Z_k+z_k)]t_{oq}/(l_q+e_q)=f_{oiz}+p_{iz}
\end{aligned} \qquad (6.40)$$

Here all the symbols have their usual meanings. Note that the only difference between (6.40) and (6.18) is that the bar lengths have now been 'updated'. Neglecting terms of higher order, the product-forces are:

$$\begin{aligned}
p_{ix}&=\left[\frac{x_i-x_j}{l_p}\frac{-e_p}{l_p}\frac{X_i-X_j}{l_p}\right]t_{op}+\left[\frac{x_i-x_k}{l_q}\frac{-e_q}{l_q}\frac{X_i-X_k}{l_q}\right]t_{oq}\\
p_{iy}&=\left[\frac{y_i-y_j}{l_p}\frac{-e_p}{l_p}\frac{Y_i-Y_j}{l_p}\right]t_{op}+\left[\frac{y_i-y_k}{l_q}\frac{-e_q}{l_q}\frac{Y_i-Y_k}{l_q}\right]t_{oq}\\
p_{iz}&=\left[\frac{z_i-z_j}{l_p}\frac{-e_p}{l_p}\frac{Z_i-Z_j}{l_p}\right]t_{op}+\left[\frac{z_i-z_k}{l_q}\frac{-e_q}{l_q}\frac{Z_i-Z_k}{l_q}\right]t_{oq}
\end{aligned} \qquad (6.41)$$

These approximate expressions are certainly acceptable for $\|\delta t\|K<<\|t_o\|$. The above formulae define, for the extensional mode corresponding to a unit change of tension in bar h, a vector of product-forces to be added to the corresponding column of [A']. This takes into account the stiffening effects of $\{t_o\}$ but, unlike the product-forces associated with the inextensional

mechanisms which must always be considered, the present ones merely refine the calculation and are not needed in all circumstances.

Despite the complicated symbolism used by Argyris (1964), the "imaginary" loads that he introduced are equivalent to (6.41). If one is using the displacement method, the addition of the matrix of geometrical stiffness to the elastic one corresponds to the suggested modification of [A'].

6.5 Comparisons with theoretical and experimental results

Three structures will be considered in this section: the first one is a plane assembly (Fig. 6.7) already encountered in Sections 6.2 and 6.3; the second is the "Simplex", a three-dimensional tensegrity first introduced in Section 2.4 (Fig. 2.17), and the third is the saddle-shaped cable net of Fig. 6.13.

The 'hanging cable' of Fig. 6.7 was the object of an extensive numerical investigation by Baron & Venkatesan (1971). These authors developed a computer program for the analysis of geometrically non-linear structures in which, for any given configuration of a cable structure, the stiffness matrix is assembled by adding up elastic and geometrical contributions in a way similar to that described in the Appendix to this chapter. They used their program to analyse the response of the assembly of Fig. 6.7 to different live loads.

The geometry of the cable, see Fig. 6.18, is defined under an initial load which consists of equal vertical loads of magnitude 17.792kN applied at joints no. 2 and 3. The additional load systems for which Baron and Venkatesan published results are also shown in the figure. Tables 6.2 and 6.3 show the results of their analysis. The load condition no. 3 had been previously examined by Michalos & Birnstiel (1960), who devised an iterative procedure in which one guesses a value for the horizontal component H of the bar tensions (this has the same value in all bars because no horizontal forces are applied to the joints) and then computes the nodal displacements required to equilibrate the nodes. Having moved from one end of the cable to the other, one finds that the end node has moved, although in fact it is constrained in both the x and y directions. A new value of H is then assumed and the entire procedure is repeated; a plot of end displacements versus trial values of H provides its correct value.

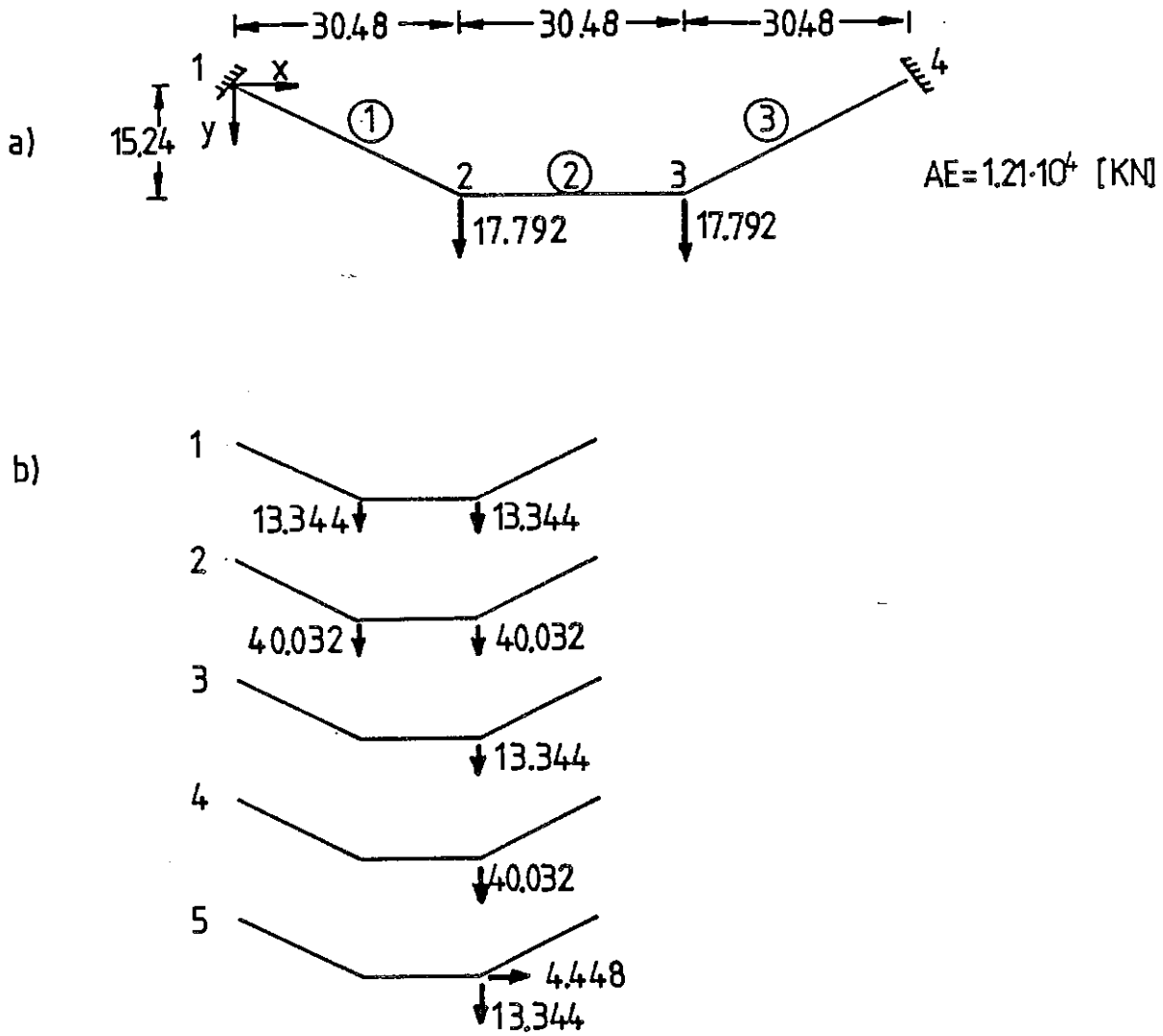

Fig. 6.18 Cable structure analysed by Michalos & Birnstiel (1960), Baron & Venkatesan (1971), J.W. Leonard (Personal communication) and by the present author. (a) Shows the initial geometry, which is defined with an initial symmetrical loading. (b) Shows the load cases examined in Section 6.5. Length and force units are [m,kN].

J.W. Leonard (personal communication) also examined the response to load condition no. 3 by means of a non-linear finite element program. Another full set of estimates was obtained by the present author using the f.e. program described in the Appendix. All of these results are given in Tables 6.2 and 6.3: the reader can verify that all the answers more or less coincide. A common aspect of the finite element computations is the comparatively large number of increments in which the load has to be divided (or the number of iterations needed to reach convergence), always >10.

Finally, this cable structure was analysed in the way described in Sections 6.2 and 6.3 with the computer program SINCA, also described in the Appendix. The analysis is in this case essentially linear; some iterations are performed only at the beginning in order to allow for the change $\{\delta t\}$ of the initial bar tensions $\{t_o\}$ due to the "fitted" component of the load. The total number of iterations was two for loading cases 1, 2, 3, 5; and it was three for loading case 4. In all cases the total load was applied in one step. The results of this computation are also given in Tables 6.2 and 6.3. It has been noted already in Section 6.2 that load conditions such as 1 and 2 are "fitted"; now compare the bar tensions estimated by SINCA, for these load conditions, with all the other methods: it is plain that they are over-estimated and, in particular, that the error associated with load condition 2 is significantly larger. This is a consequence of having neglected the product-forces corresponding to the extensional modes, introduced in Section 6.4.2. The elastic bar elongations and (extensional) displacements computed by SINCA are consequently overestimated, see Table 6.2.

The remaining load cases involve significant inextensional components of displacement; note that all estimates almost coincide in the case of loading case 3. In terms of displacements, the largest error made by SINCA is in loading case 5, in the x-component of node 2, with an overshoot of 13mm that corresponds to an error of 8.5% (compared to the largest displacement). Tensionwise the largest error is of 2.8kN in loading case 4: the corresponding error is 3.3%.

Motro (1983) tested a physical realization of the "Simplex", see Figs 6.19, 2.17 and 4.23a, made out of three steel tubes and nine high-tensile steel cables. Steel plates, welded at the tube ends and stiffened by gusset

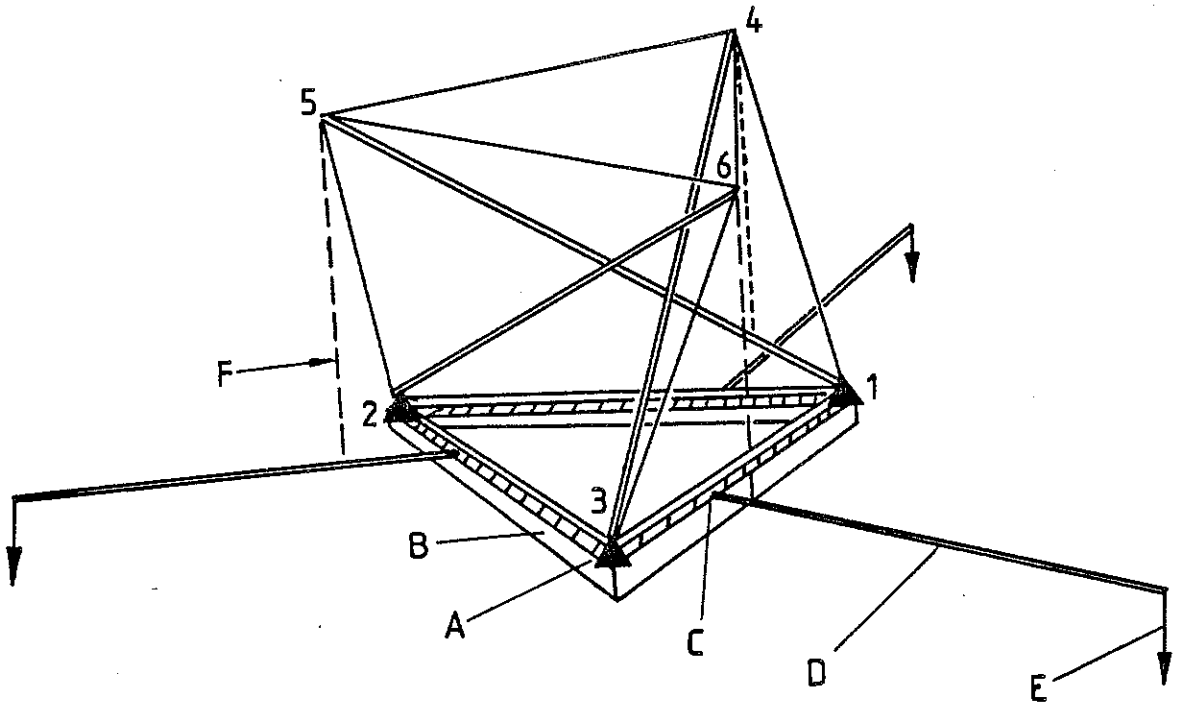

A Constraint
B Rigid base
C Hinge connecting lever to rigid base
D Lever
E Applied load
F Cable transferring load to upper node

Axial stiffnesses: cables $(AE)_{equivalent}$=1.60MN

tubes AE=65.0MN

Fig. 6.19 Loading scheme adopted by Motro (1983) for his investigation into the behaviour of the "Simplex". See Section 6.5.
Equal vertical forces are applied to nodes 4, 5 and 6. Notice that only node 2 is fully fixed: nodes 1 and 3 are free to move in the x-direction and 3 can also move in the y-direction (the system of axes is shown in Fig. 5.6). The total number of constraints is therefore six.
The figure is based on Fig. 114.1 of Motro (1983).

	Component of displ.	Loading case 1	2	3	4	5
	x_2			.668		
Michalos &	y_2			-1.32		
Birnstiel	x_3			.596		
(1960)	y_3			1.23		
	x_2	$-3.23.10^{-3}$	$-9.36.10^{-2}$	.667	1.33	.765
Baron &	y_2	.244	.704	-1.32	-2.69	-1.52
Venkatesan	x_3	$3.23.10^{-3}$	$9.36.10^{-2}$	.594	1.04	.671
(1971)	y_3	.244	.704	1.23	2.20	1.35
	x_2			.660		
J.W.Leonard	y_2			1.33		
(private comm.)	x_3			.604		
	y_3			1.25		
	x_2	$-3.23.10^{-3}$	$-9.40.10^{-2}$	.668	1.33	.765
f.e. program	y_2	.244	.706	-1.32	-2.69	-1.52
see Appendix	x_3	$3.23.10^{-3}$	$9.40.10^{-2}$	.595	1.04	.668
	y_3	.244	.706	1.23	2.20	1.35
	x_2	$-3.36.10^{-3}$	-.101	.673	1.32	.778
SINCA	y_2	.255	.764	-1.33	-2.79	-1.54
see Appendix	x_3	$3.36.10^{-3}$	-.101	.599	1.09	.679
	y_3	.255	.764	1.23	2.22	1.36

Table 6.2 Components of displacement [m] of the cable structure shown in Fig. 6.18.

plates, were the points of anchorage of the cables. In Motro's model the length of all cables was 1420mm and the tubes were of length 2085mm. Hence the nodal coordinates of the selfstressable configuration can be obtained by multiplying the values in Table 5.5 by 1420mm. Figure 6.19 shows the loading device used to apply three equal vertical loads at the top nodes; and it is possible that the applied load did not remain purely vertical during the test. The nodal components of displacement were measured by using theodolites, and most member tensions were derived from the measured displacements of their ends. (A more complete description of the model,

	Member number	Loading case 1	2	3	4	5
Michalos &	1			53.7		
Birnstiel	2			49.2		
(1960)	3			56.0		
Baron &	1	68.5	125.	53.8	82.3	56.5
Venkatesan	2	61.4	110.	49.4	77.8	52.0
(1971)	3	68.5	125.	56.0	89.0	53.8
	1			53.5		
J.W.Leonard	2			49.0		
(private comm.)	3			55.7		
	1	68.7	124.	53.7	82.4	56.4
f.e. program	2	61.2	110.	49.2	77.6	51.9
see Appendix	3	68.7	124.	56.0	89.0	54.0
	1	69.6	129.	53.5	80.5	56.0
SINCA	2	62.3	116.	48.8	75.0	51.3
see Appendix	3	69.6	129.	55.7	87.4	53.6

Table 6.3 Bar tensions in the cable structure shown in Fig. 6.18 [kN].

details of measurement techniques and treatment of data are available in Motro's thesis).

In one of Motro's experiments the (adjustable) cable lengths were given precisely the value required to obtain a prestressable structure and, without prestress, the vertical loads were increased from 0 to 5kN in four equal increments. Figures 6.20 and 6.21 show the experimental results, as presented in Fig. 135 of (Motro, 1983), together with numerical predictions based on the program MULCA, described in the Appendix. This computer program was primarily intended for prestressed cable systems but it can be used equally for structures the members of which are either in tension or compression; it can be also applied to assemblies in which the level of initial prestress is zero, by assigning a fictitious prestress and treating all the results accordingly.

The measured member tensions compare satisfactorily with the results from the present method, see Fig. 6.21. The corresponding nodal displacements

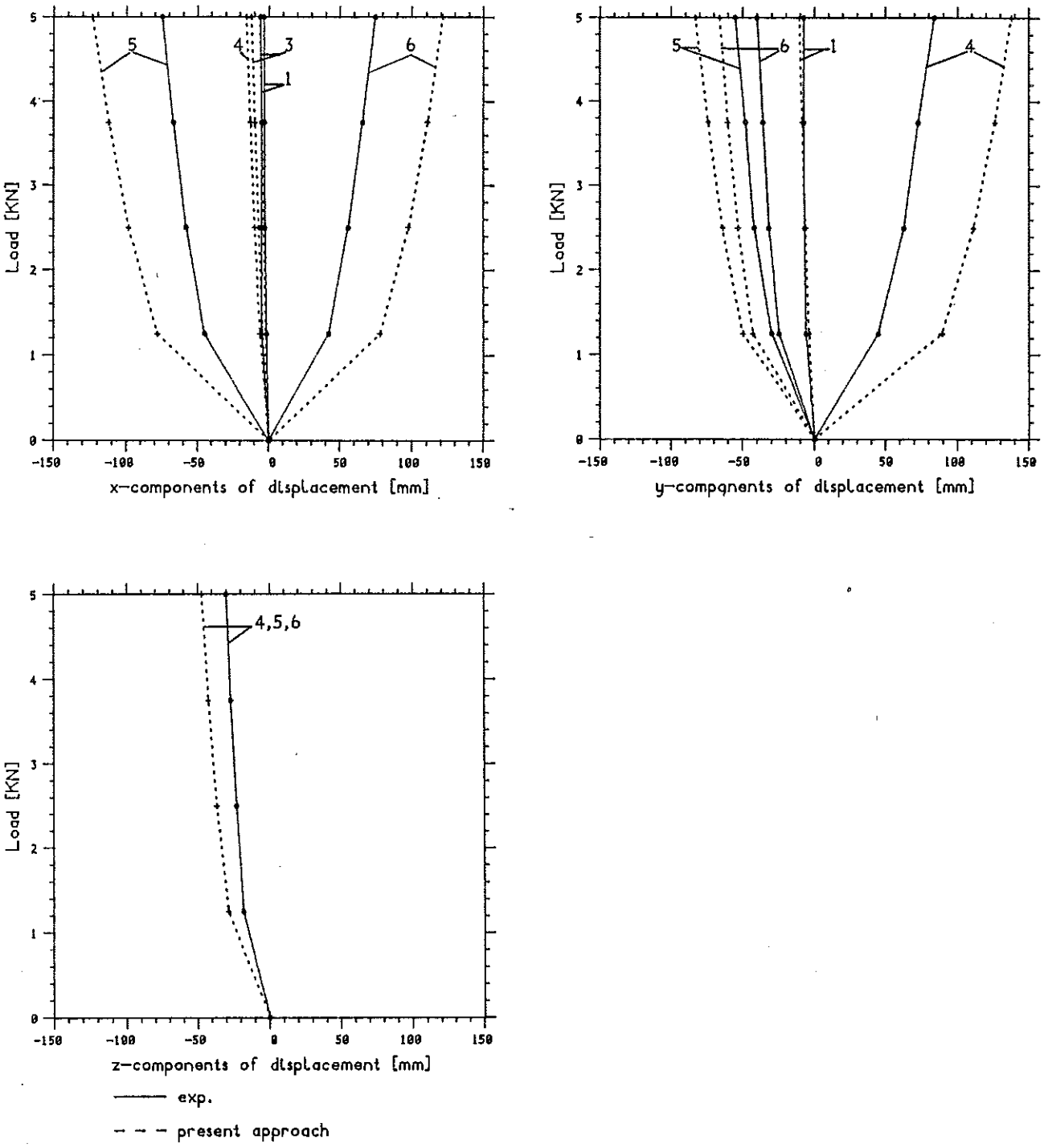

Fig. 6.20 Comparison of experimental and theoretical nodal displacements of the "Simplex". The experiments were performed by Motro (1983). The horizontal components of displacement are much larger than the vertical components, as in the inextensional mechanism shown in Fig. 4.23b. The discrepancy between experiment and theory is discussed in the Section 6.5.

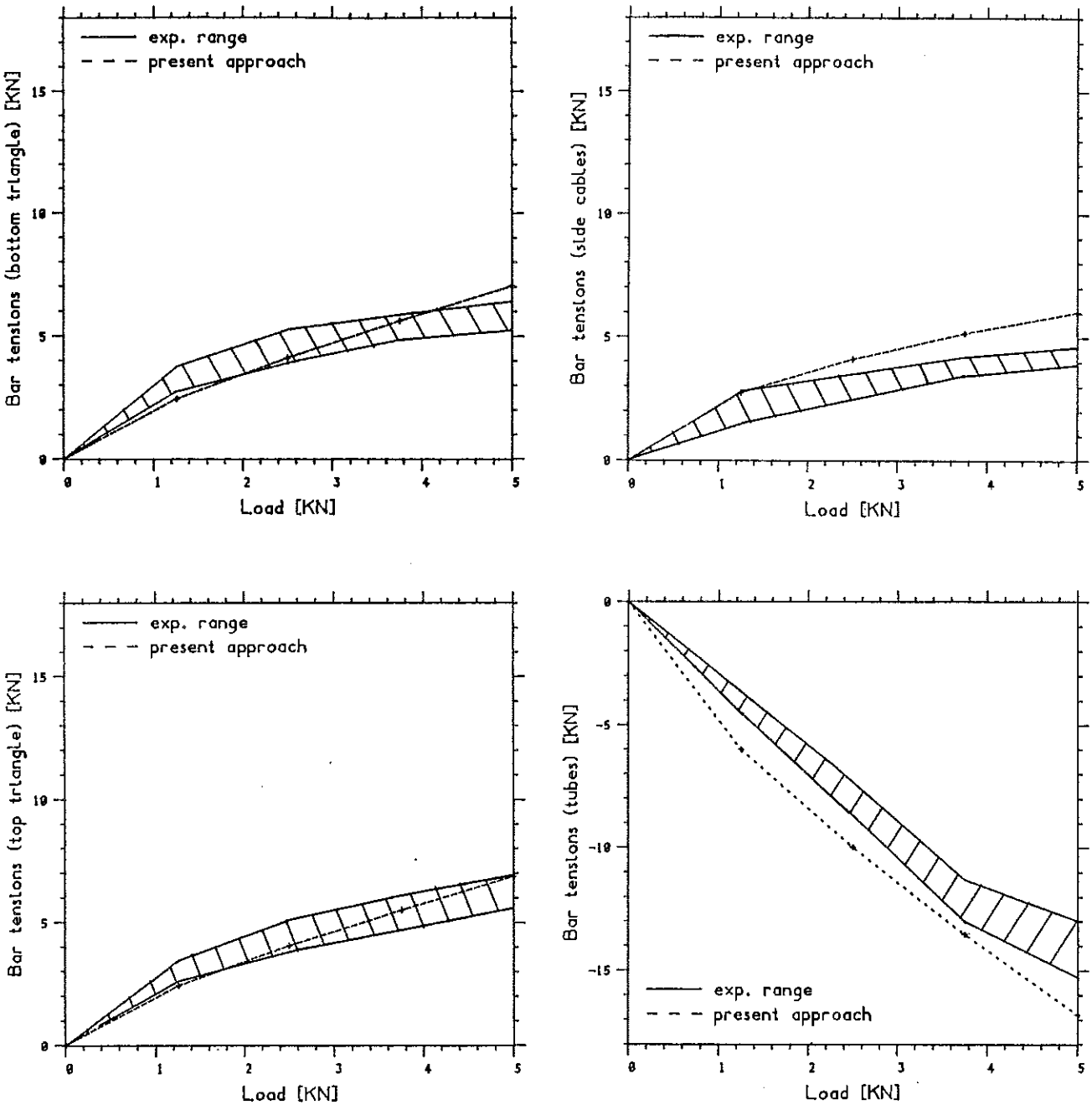

Fig. 6.21 Comparison between experimental and theoretical member tensions of the "Simplex". The experimental results are from Motro (1983).

do not compare as well: all experimental displacements appear to have been substantially overestimated by the theory. Is this because of a fault in the scheme of calculation implemented in MULCA? This point was investigated by including in the comparison a third estimate, from the f.e. approach (in which very small load increments had to be used in order to obtain convergence); it was found that this gave results close to MULCA. There is also an inconsistency in Motro's published data since a comparison of the tensions measured in the side cables - see Fig. 6.21 - with those estimated from the elastic strains due to the 'measured' displacements at the final load showed that the last values were about 30% lower than the bottom value of the experimental range. The present author's view is that an initial (possibly unmeasured) distortion of the model occured during the initial adjustments which, according to Motro's account, were carried out with the top nodes "supported to counteract their selfweight and the weight of the loading device". The consequent distortion might have been large because the size of the nodes, with linear dimensions of about 100mm, certainly made them heavy.

The third test is purely numerical; it consists of a comparison between the response of the cable net of Fig. 6.13 to one of its vectors of product-forces, equal to the first load system considered in Section 6.4, as predicted by MULCA and by the f.e. program mentioned previously. As already noted, this cable net was built and tested, but not under this particular load. In the physical model the breaking load for the wires was found to be about 350N, and therefore the maximum load multiplier of ten which is considered in this numerical test can be still regarded as an 'in service' load condition for the cable net.

Although the largest components of displacement of node 5 (Fig. 6.22) are of the order of 3/100 of the total span, they have been predicted very accurately. But the figure shows that the error on one of the components of displacement of node 6 is rather large. Similarly for the bar tensions (Fig. 6.23): the agreement is rather good for bars 1-4, 9-16 and 21-24 but MULCA leads to an overestimate in all segments belonging to the cables passing through the origin, for which the sag/span ratio is small at the beginning and decreases even further.

It could be argued that these errors contradict the basis of Section 6.4.1, namely that the main effect of a product-force is to increase

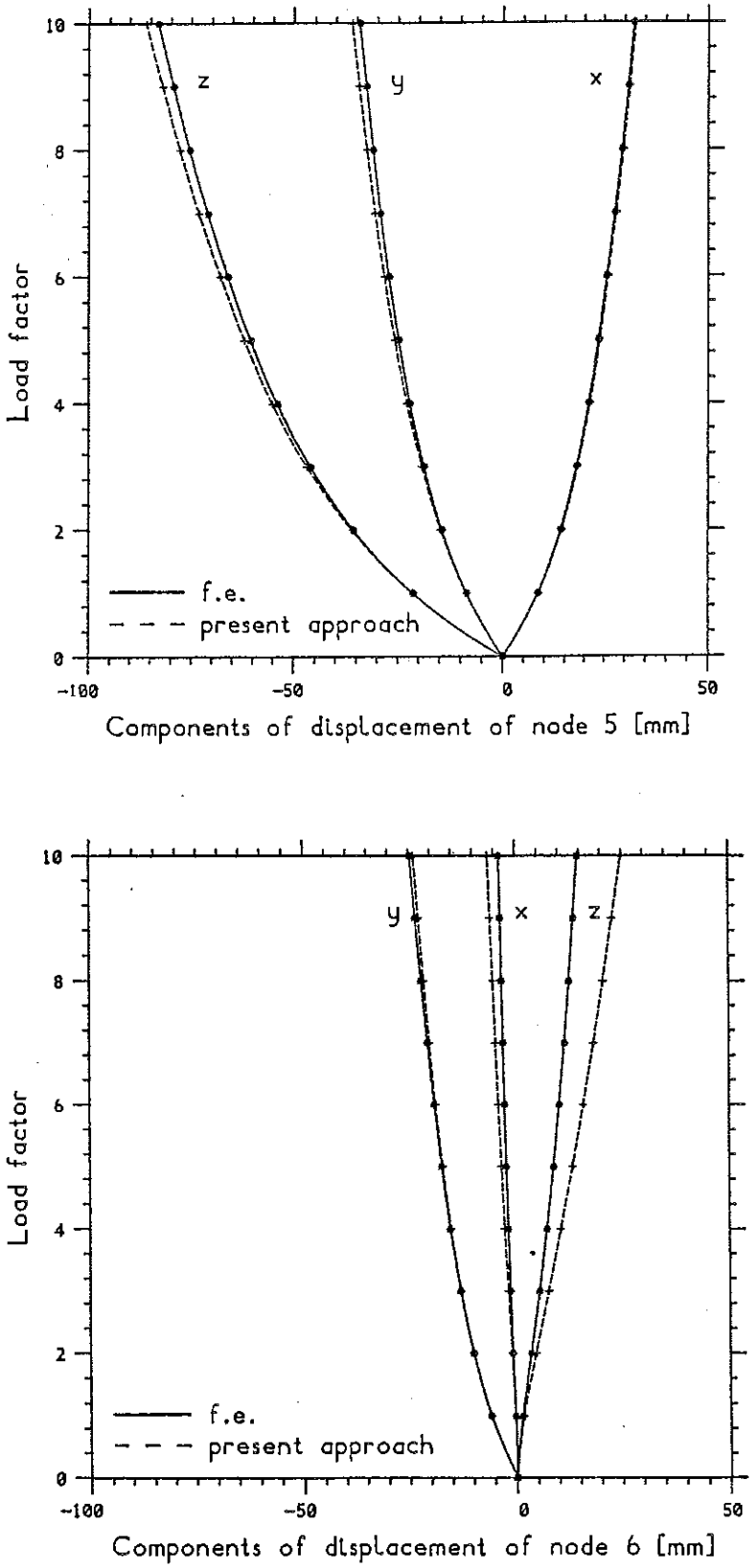

Fig. 6.22 Comparison between two different theoretical estimates of deflections of the cable net shown in Fig. 6.13. The load system consists of the product-forces specified in Section 6.4.

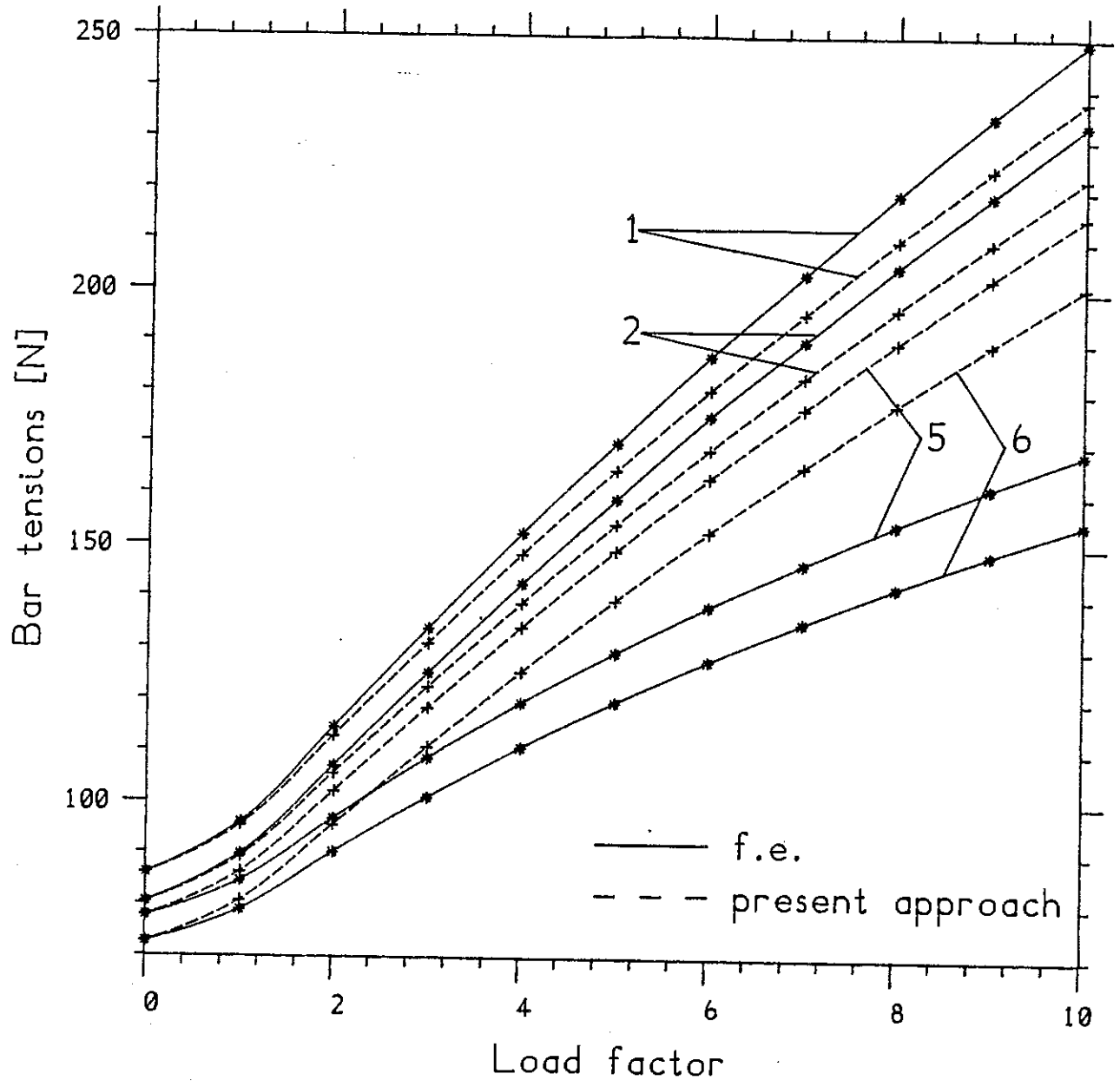

Fig. 6.23 Comparison between two different theoretical estimates of tensions in the cable net shown in Fig. 6.13. See Fig. 6.22. Due to the symmetry of the applied load, the tensions in all of the members can be obtained from this figure.

the level of selfstress without altering the relative values in the different members, which relies on the overall geometry not changing too much. But these are precisely the limitations of the theory which have been violated; and it should be expected that, when the applied loads flatten the net in the middle, this type of side-effects develop.

It can be concluded that the analysis of the response of a kinematically indeterminate framework to a loading system, along the lines of this chapter, is more efficient than the standard formulations based on a 'stiffness' matrix, as noted already; because the present approach does not divide the load into small increments and performs a reduced number of iterations. Another major advantage of the present approach is that it gives correct results (if one neglects the - small - errors discussed above); because it is well equipped for dealing with structural mechanisms, and therefore it never attempts to solve an ill-conditioned system of equations. However, as it is usual when developing a formulation which takes the bar forces as unknowns, instead of the nodal displacements, one has to deal with a more 'articulate' algorithm.

Appendix

The geometrically non-linear finite element program which has provided a 'reference' answer on a number of occasions, and that will be used to find further theoretical comparisons for the experimental results of Chapter 7, is made out of a (small) subset of Fortran subroutines written by T. See and I.M. Kani for the elasto-plastic analysis of three-dimensional structures. Details of the more general versions of the program can be found in See (1983) and Kani, McConnel & See (1984). One special feature of the present version is the possibility for the user to assign a set of bar stresses, due to an initial lack of fit of any member, together with any applied nodal loads. These tensions can be used to define a state of selfstress, in which case zero nodal displacements should occur in consequence of them. In fact this observation is only valid in theory because all formulations based on a stiffness matrix do not cope well with zero displacements, and hence cannot converge unless a small load is applied at the same time. A self-explanatory flow chart of the program is given in Fig. 6.24.

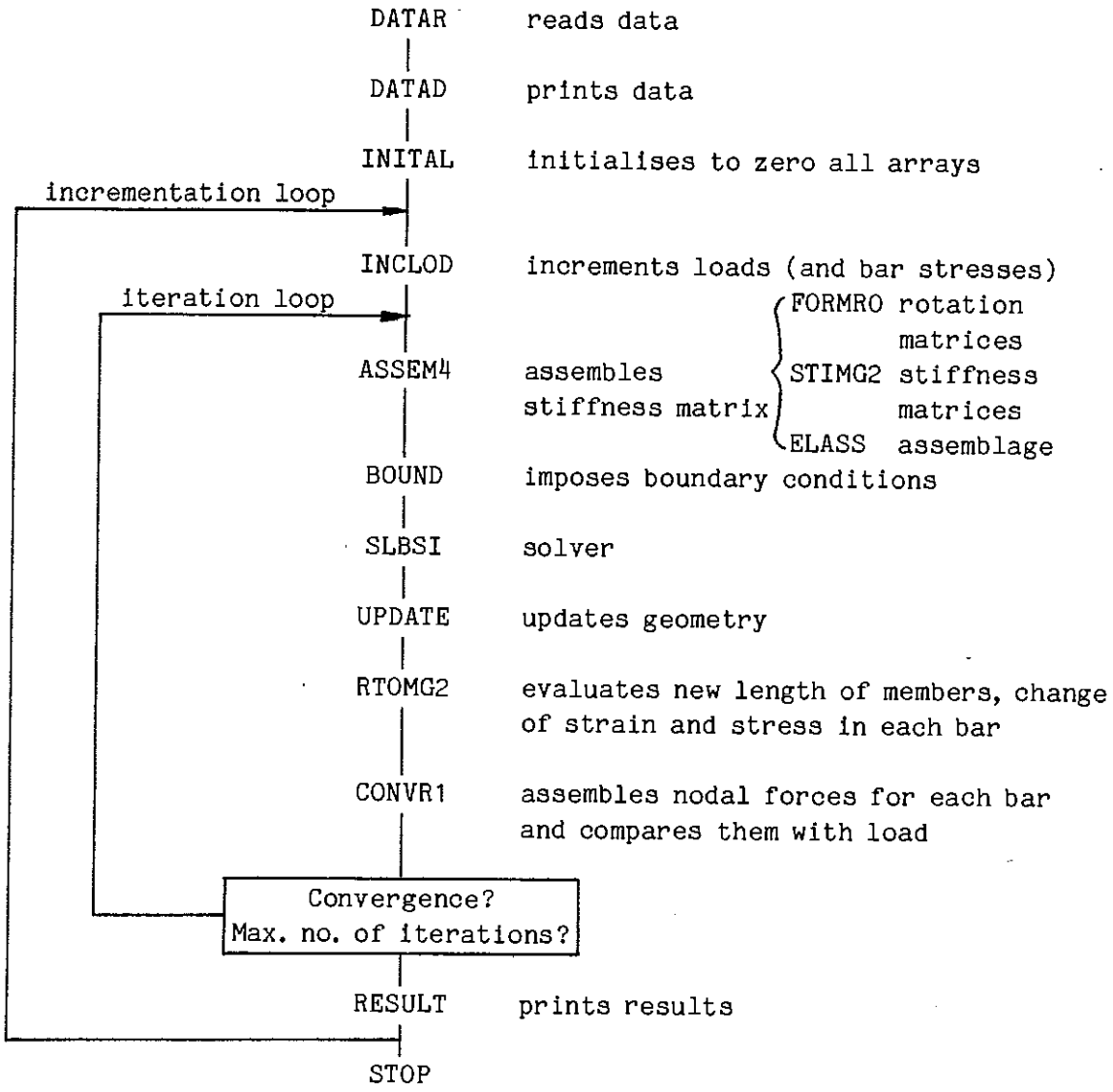

Fig. 6.24 Schematic flow chart of the non-linear finite element program referred to in Chapters 6 and 7.

Two Fortran programs have been written by the present author: SINCA and MULCA. The first one performs precisely the calculations described in Sections 6.2 and 6.3 for any kinematically indeterminate but statically determinate assembly which has been prestressed by an initial ("fitted") load and is then subjected to the action of a live load. The name SINCA comes from the SINgle CAble problems for which the program is intended. MULCA (MULtiple CAbles) deals with pin-jointed assemblies which are kinematically and statically indeterminate, with s=1, and therefore it imposes the condition of geometrical compatibility (6.9) in order to obtain the bar tensions; it also performs both of the non-linear corrections described in Section 6.4. Schematic flow charts of both programs are shown in Fig. 6.25.

Lastly, although no formal comparison of the relative speeds of these programs has been attempted, it emerges from all the computations that the two programs written by the present author are up to five times faster than the f.e. code. In particular, MULCA has been 2-5 times faster in the computations described in Section 7.4; the worst of these results being in connection with the largest of the cable nets loaded by inextensional load conditions. Furthermore, some finite-element computations have 'converged' to the wrong answer - at first ; in which case the correct final configurations were obtained by repeating the calculation with smaller load increments.

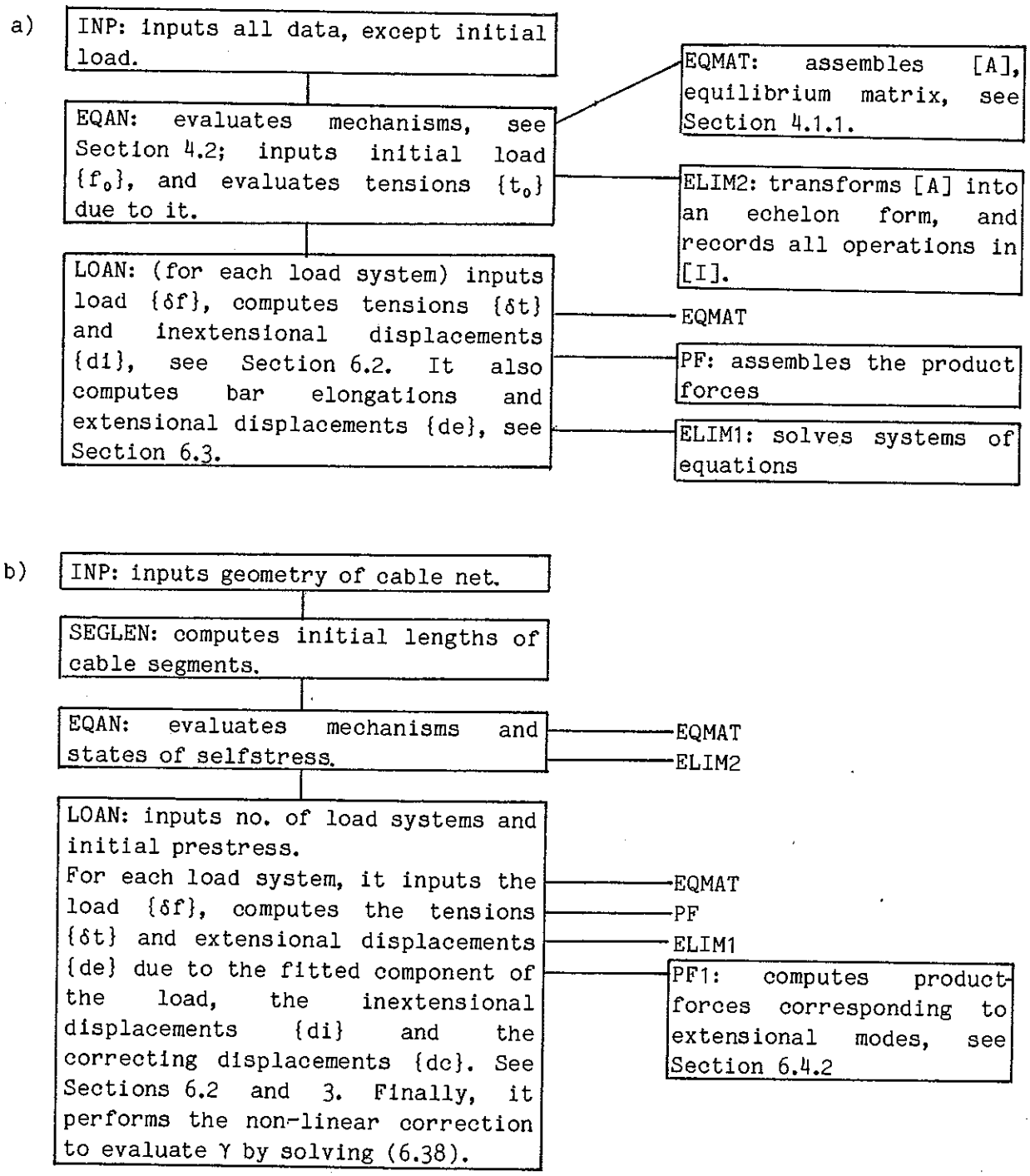

Fig. 6.25 Schematic flow charts of the programs SINCA (a), and MULCA (b), which perform the computations described in Sections 6.2, 6.3 and 6.4. See also the Appendix.

7. Experimental work

A large number of experiments on cable systems has been conducted in the laboratory to build up a reliable set of data against which any numerical estimate based on the theory developed in Chapter 6 could be tested. The background and aims of the investigation will be described in Section 7.1, and the experimental techniques used (or merely attempted) in Section 7.2. The description of the tests and the results obtained, together with comparisons with numerical data from SINCA, MULCA and finite element computations, constitute the remaining part of this chapter.

7.1 Background and aims

Several experimental and theoretical investigations into the behaviour of cable structures have been made in the past. Leaving aside studies conducted earlier than the year 1960, brief accounts of which can be found in Pugsley (1957) and Irvine (1981), the first geometrically non-linear formulations of the analysis of this type of structure were started in the 1960's. The need for a reliable background of experimental knowledge then led to tests on hanging cables and cable trusses[1] some of which have been described by Krishna & Sparks (1968), Buchholdt (1970), Buchholdt & McMillan (1973), and on three-dimensional cable nets by Siev (1967), Krishna & Agarwal (1971).

Once the accuracy of the numerical methods had been demonstrated, most of the subsequent investigators referred to earlier computations instead of performing their own tests. This approach has also been followed, with only a few exceptions, by the present author in Chapter 6. Recent experimental investigations have been concerned with more specific problems, such as assessing the behaviour of a preliminary design of a cable roof for a sports stadium in Iran (Nooshin & Butterworth, 1974) or the influence of boundary deformations on the behaviour of a cable net (Thew, 1982).

When deciding whether the theoretical study described in this dissertation was to be verified against experimentally, rather than merely numerically generated data, it was felt that the novelty of the approach

[1] A cable truss is a plane assembly consisting of two main pretensioned cables which are interconnected by vertical or inclined hangers/struts.

proposed did require convincing evidence: something more convincing than just a comparison with the results of the computations performed with the f.e. program described in the Appendix to Chapter 6. The practical impossibility of obtaining complete results for the investigations performed by other researchers and reported briefly in the literature, which included - for instance - the horizontal components of the nodal displacements; and the hope of accumulating experience on the statical testing of cable systems that could help in a future investigation of their dynamics, were the main reasons for performing the experiments described in this chapter.

The aims of the whole series of experiments were to measure the response of different cable systems (with $s \leq 1$, as in Chapter 6) - made out of thin wire so that unwanted effects such as self-weight, non-linear constitutive relationships of cable strand, bending stiffness, etc. were negligible - under a wide range of loading conditions. For each configuration of the system, the components of nodal displacement and the cable tensions were to be measured to a high degree of accuracy. The only constraints on the physical dimensions of the models were imposed by the availability of space in the laboratory and the dimensions of existing elements of scaffolding, to which all cables and transducers were to be connected.

7.2 Experimental techniques

This section contains the description of the experimental set-up; it also includes details of a novel wire-tension transducer. Finally it describes an unsuccessful attempt to measure the change in the tension carried by a segment of a structural wire by relating it to the change of its electrical resistance.

7.2.1 Wire properties

High tensile steel piano wire of a single cross section ('27 gauge' corresponding to a diameter of 0.42mm) was used for all tests. All the wire came from the same reel and a segment of it was tested in a Hounsfield tensometer; its behaviour was practically linear until the maximum tension of 340N was attained. The wire tensions were well below this value during all the tests. The standard value of $E=210 kN/mm^2$, for the Young's modulus, was found to be acceptable.

7.2.2 Connections

The models for the experiments on hanging cables were built by hanging the required length of wire between two end points at the same level; a small quantity of epoxy glue was used to fix the load hangers and the displacement transducers to the main cable. The cable was connected to the supporting frame by winding heads of the kind used on guitars: they were also handy to adjust the total cable length, see Fig. 7.1a. The same devices were used for the boundary nodes of the cable nets; in this case the internal nodes required a strong connection between the two perpendicular wires and a hanger loop, hence the connection shown in Figs 7.1b, 7.1c and 7.1d. These internal nodes were adjustable so that the lengths of the individual cable segments could be modified when the net was being set up. The mass of each node of this type was less than 20g and was neglected in all calculations.

7.2.3 Supporting frames

Figure 7.2 shows sketches of the supporting frames for the smaller cable net; all the others were similar. The main frame was expected to behave as a rigid foundation for the cables: therefore the maximum deflections of the channel girders were estimated, and bracing elements had to be added for the larger net.

7.2.4 Measurement of nodal displacements

Schlumberger equipment was used because it allowed accurate and rapid collection of results; it consisted of up to fifteen LVDT Sangamo displacement transducers, one Amplifier unit with fifteen channels, one Orion Delta 3630 data logger which printed digitally on thermal paper any reading taken. The displacement transducers had a total travel larger than 100mm and they were calibrated in such a way that the largest non-linearity in their response was ±0.3mm. All readings had been found to be accurately repeatable and therefore it would have been possible to correct any error due to non-linearity; but these errors were neglected. In order to measure the component of displacement in a chosen direction of a given node, a transducer was held fixed to its supporting frame at a distance of about 800mm from the node, parallel to the chosen direction and pointing towards the node. A thin and light rod of 'hypodermic' steel was used to connect the transducer plunger

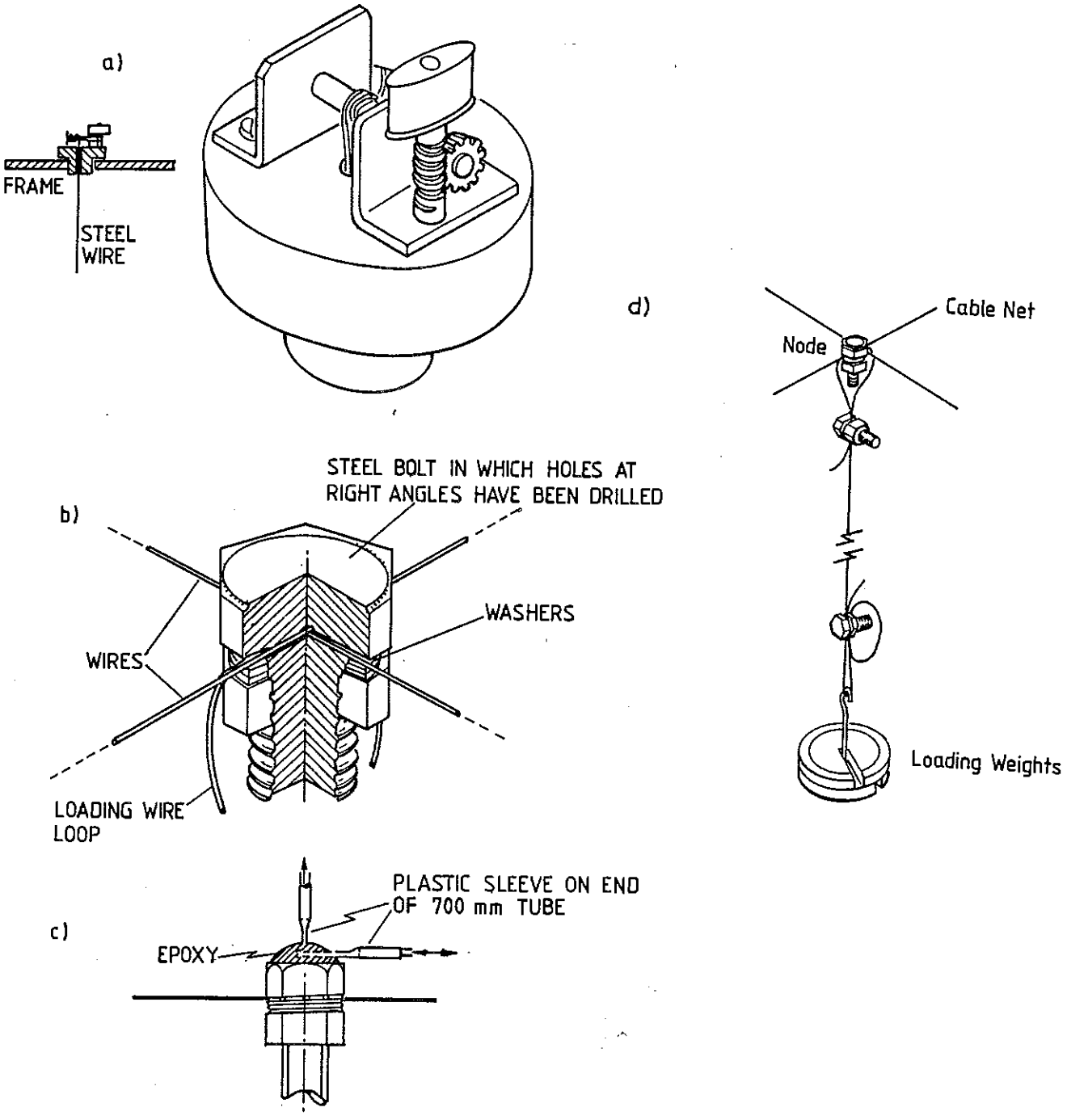

Fig. 7.1 a) Winding head, consisting of a hard plastic (Tufnol) plug which fits into the holes of the channel girders used for the supporting frame; the guitar machine-head is used as a tensioning device.
b) Cut-away view of a joint of a cable net.
c) Connection of displacement transducers to a joint.
d) Loading arrangement to apply vertical forces.

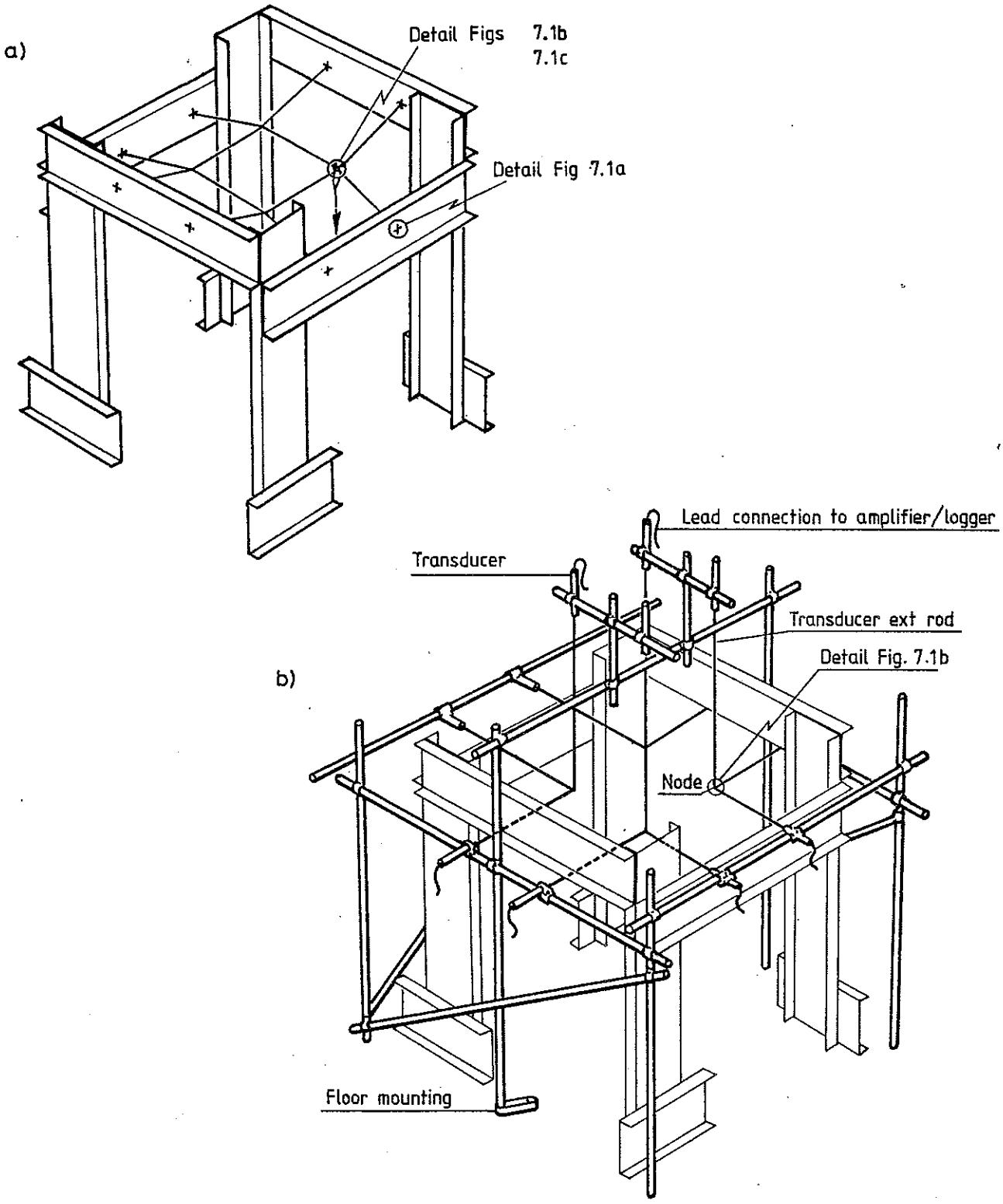

Fig. 7.2 a) Cable net support frame. All main channel girders have dimensions 305×89×1930mm³, with a square grid of bolt holes (not shown here).
b) Support frame for deflection transducers. It is entirely separate from the cable net support frame.
These drawings are not to scale.

to the node; this connection was by means of a heat-shrinkable plastic sleeving, very flexible, to simulate pin-ended conditions. The friction in the transducers was found to be very low: the forces applied on a node by the whole measuring system, which were also neglected, varied in the range 0.03-0.20N according to its direction.

A large nodal displacement perpendicular to the direction in which the transducer of Fig. 7.3 is acting has the consequence of altering its reading. The error ε turns out not to be very significant for most of the experiments conducted, hence all results are uncorrected. As a first approximation, the reader can obtain the error associated with any of the experimental nodal displacements given in this chapter by using the correcting table given in Fig. 7.3, with δ equal to the largest of the two components of displacement in the direction perpendicular to the one of interest.

7.2.5 Measurement of wire tension

A wire tension transducer was designed and built for these experiments. Basically it is of the 'vibrating wire' type already used by Krishna (1968), Nooshin & Butterworth (1974) and Thew (1982), but one important modification has made it more accurate and portable. The starting point is that the fundamental frequency of vibration of any wire in tension depends, leaving constant all other parameters such as its length l and support conditions, on the value t of the tension. For a wire in which the bending stiffness is negligible the theoretical relationship is:

$$f=(1/2l)\sqrt{t/m} \qquad (7.1)$$

where m is the mass/unit length. For the wire used in the experiments, (7.1) would give $t=4.157.10^{-5}\times f^2$[Hz,N].

All the authors mentioned above devised instruments in which an electro-magnet plucked the wire and then the electric signal picked out by the electro-magnet itself was either sent to an oscilloscope or to a frequency counter. For instance Nooshin & Butterworth (1974) measured the period of 100 oscillations after each current pulse had excited the wire. In a recent paper on vibrating wire gauges, which are widely used at present in a number of strain measuring instruments, Ewins (1985) recognized the decaying

amplitude of the vibrating wire as the only limiting factor in their application. One way of making the above system more accurate, but which would involve a rather troublesome trial and error process, requires that the plucking frequency is altered until the wire resonates. This is the observation starting from which a more efficient solution has been developed.

Two electro-magnets have been connected to each other by a simple electric circuit: the first one picks up a signal due to any movement of the wire, this signal is then amplified and sent to the other electro-magnet which plucks the wire at precisely the required frequency. The instrument which has been built following these principles resonates in only a few seconds a gauge length of 100mm, clamped at both sides, of the '27 gauge' wire used for the experiments. In order to put a limit to the amplitude of the induced vibrations, a thermistor has been connected in parallel with the main amplifier. See Fig. 7.4. A frequency counter displays f. The initial idea for the present scheme was suggested by an old Maihak strain transducer which works on a similar principle.

For any measurement, the instrument was held by hand and clamped very gently to each wire segment. Once the wing nuts holding the clamping blocks had been tightened, the instrument was left hanging and the frequency was obtained from the digital display of the counter.

The only source of error of this instrument is the manual skill of its operator (plus, of course, the presence of kinks in the wire) which is likely to lead to larger errors at low tensions. Therefore each measurement was repeated three times; for tensions above 50N the experimental error was always smaller than ±2N. The calibration curve, which was used for converting all the readings into force units, was obtained experimentally; see Fig. 7.5.

The reader can verify that its points are not too distant from the theoretical estimate obtained from (7.1).

An approximate simple way of including the effect of the flexural stiffness and of the clamped ends is to use the formula:

$$f=\frac{1}{2l^2}\sqrt{\frac{5\pi^2 EI+tl^2}{m}} \qquad (7.2)$$

which adds up the stiffness of a wire in tension (without any bending

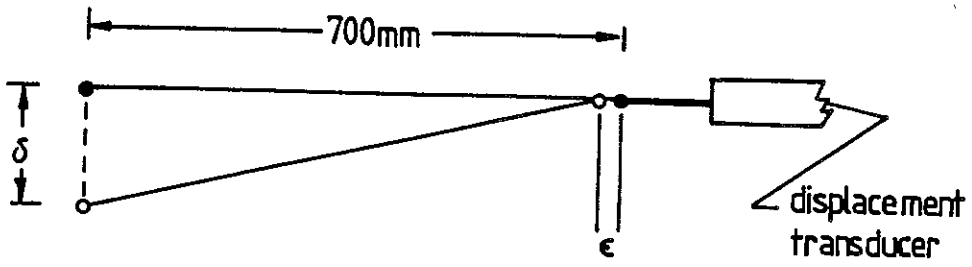

$$\varepsilon = 700(1-\sin \arctan\frac{700}{\delta})$$

δ	10	20	30	40	50	60	70	80	90	100
ε	0.07	0.29	0.64	1.14	1.78	2.56	3.47	4.53	5.71	7.04

Fig. 7.3 Error due to joint displacements in directions perpendicular to a transducer. δ, ε in [mm].

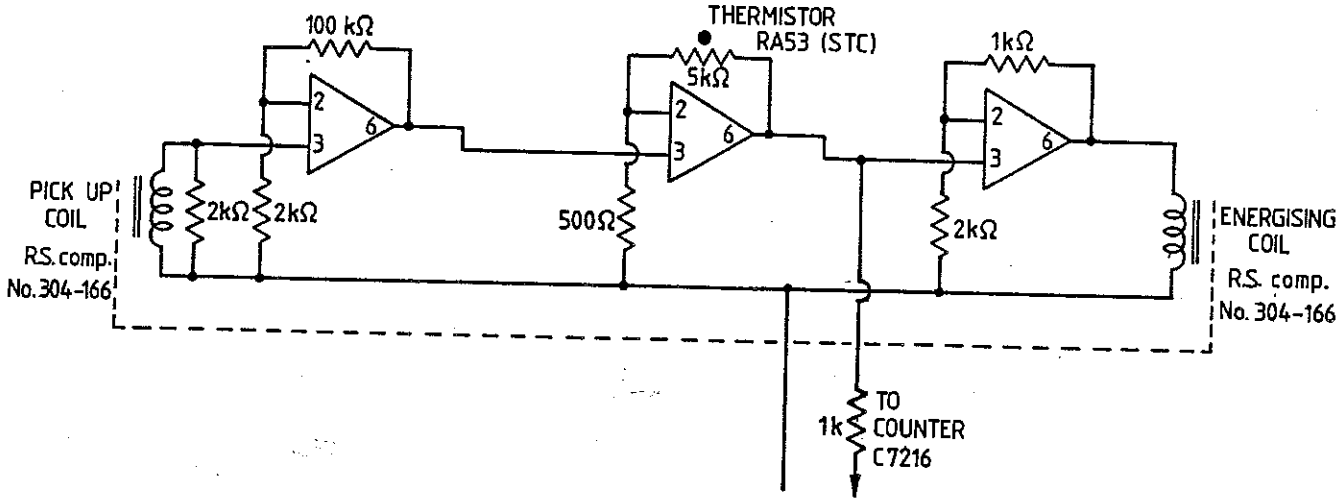

Fig. 7.4 Circuit diagram of wire-tension transducer.

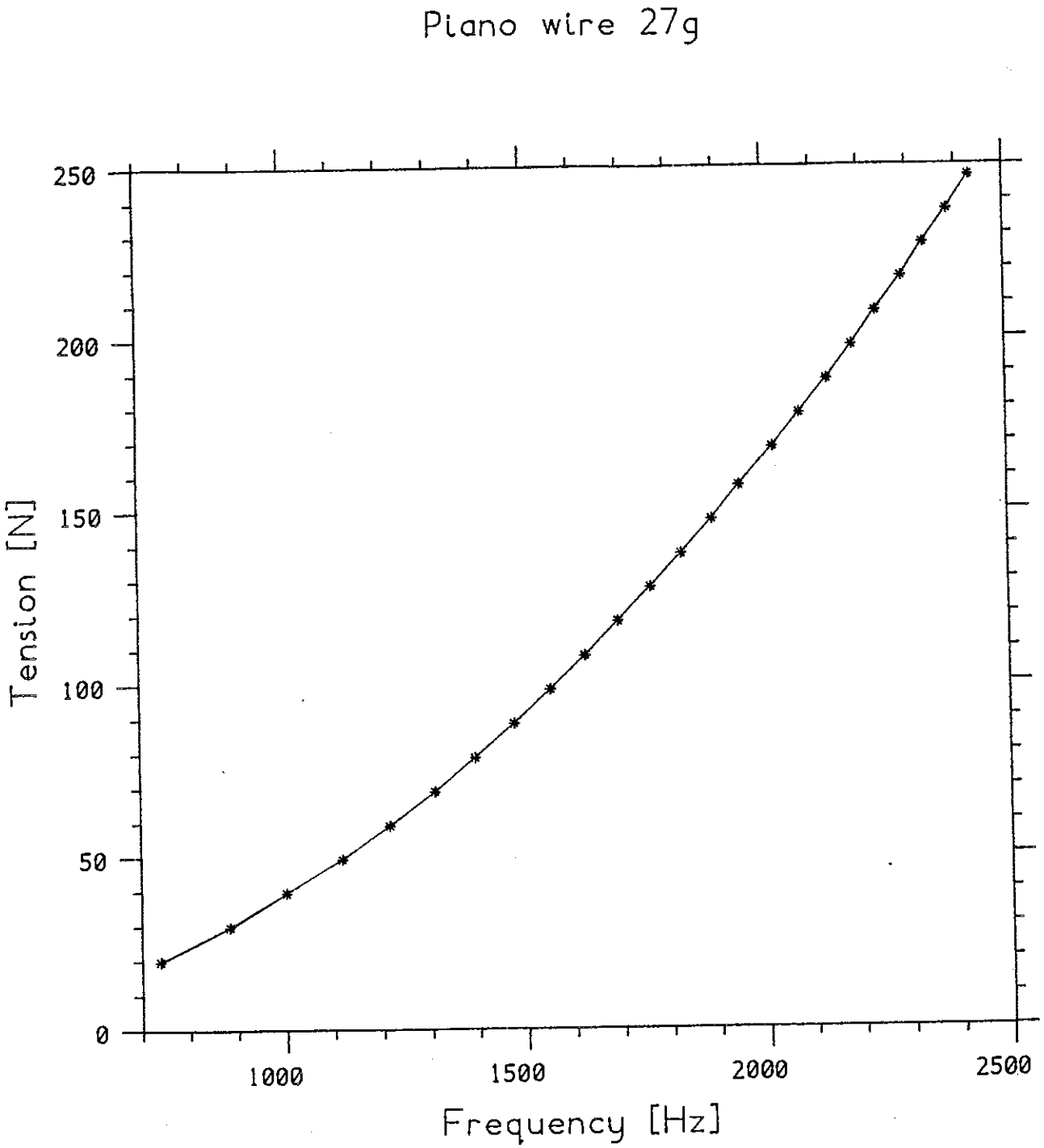

Fig. 7.5 Calibration curve for the wire-tension transducer described in Section 7.2.5. Asterisks indicate experimental points.

stiffness) to that of a fully clamped beam. The hypothesis behind the derivation of (7.2) is that the shapes of the fundamental modes of a wire segment and of a beam of equal length are identical, which is not true. Yet, (7.2) gives in the present case $t=4.157.10^{-5}\times f^2-1.65$ [Hz,N], which is in rather good agreement with the experimental curve shown in Fig. 7.5 (an analytical expression for the experimental curve is given by $t=4.33.10^{-5}\times f^2-3.3$). Estimates which are theoretically sound can be obtained from the approach described by Rayleigh (1894), which has been expanded in a recent paper by Wittrick (1985).

Initially, an attempt was made to measure wire tensions from changes in their electrical resistance. Although this method was referred to by Møllmann (1974), serious difficulties were caused by the mechanical performance of the nickel-chrome wires[2] and by thermocouple effects which caused severe drift of the readings.

7.3 Experiments on hanging cables

The three (initial) configurations of Fig. 7.6 were subjected to the indicated load conditions; initial loads of different values were applied. The figure also gives details on the initial configurations, measured before starting each test; plainly these change by small amounts when the value of the initial load is altered. All of the computer analyses performed were based on these values.

The layout considered in the first test is similar to one of the assemblies studied in Chapter 6. The structural model showed very clearly the existence of a mechanism in which nodes 2 and 3 moved down and up, respectively, along paths inclined at about 45° to the horizontal. By inspection, the corresponding product-forces are directed downwards and upwards, with vertical and horizontal components in the ratio 3/1.

Load condition no. 1 is "fitted". This was confirmed by the experiment, in which all the segment tensions and nodal displacements measured varied linearly with the load. These results are not shown here. A more interesting set of results is obtained from load condition no. 2, which has a large

[2] This material had been chosen because the method can only work if the resistance of the wire gauge is high, and in the present application the gauge length was set to 1m for reasons explained elsewhere.

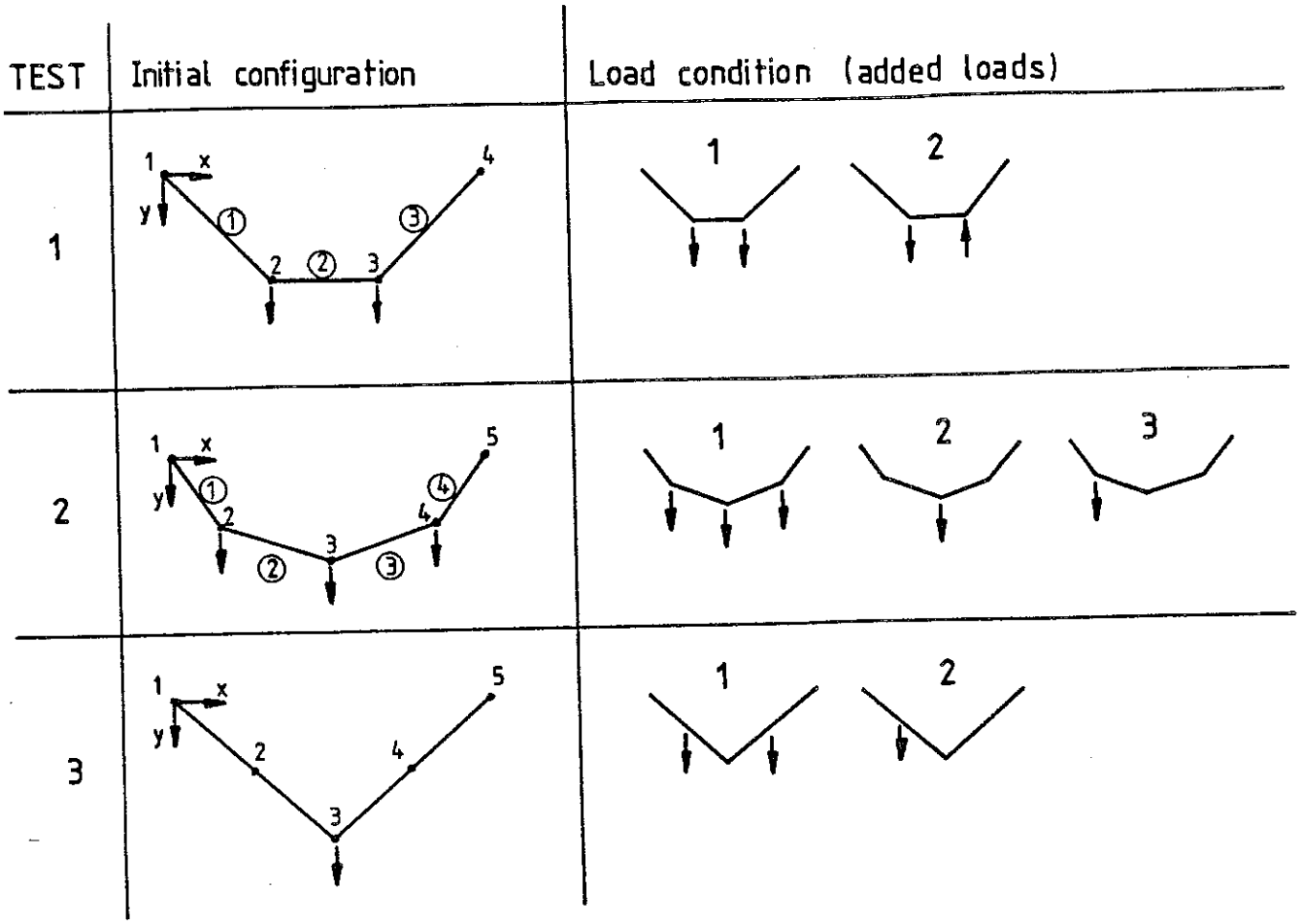

Test no.	Initial load [N]	Node no.	Nodal coordinates [mm] x		y	
1	61.6 (81.6)	1	0.		0.	
		2	989.		1001.	(1005.)
		3	2150.		1001.	(1005.)
		4	3139.		0.	
2	31.6 (51.6)	1	0.		0.	
		2	672.	(669.)	674.	(677.)
		3	1572.		976.	(982.)
		4	2472.	(2475.)	674.	(677.)
		5	3144.		0.	
3	101.7	1	0.		0.	
		2	783.		536.	
		3	1573.		1076.	
		4	2359.		537.	
		5	3142.		0.	

Fig. 7.6 Experiments on hanging cables: cable configurations and load systems for which tests have been made. The table shows the nodal coordinates at the beginnning of each test.
These drawings are not to scale.

non-fitted component. Figures 7.7 and 7.8 show the results obtained for two different levels of initial bar tensions, corresponding to initial loads of 61.6 and 81.6N; here the main feature is that the tension in segment 2 stays constant while the remainder vary linearly in consequence of the "fitted" part of the load. The decomposition of the load condition into its components, sketched in Fig. 7.9, explains why only the tensions in the side wires need vary. The plots of measured nodal displacements vs. added load show that, up to about 10N, nodes 2 and 3 move by equal amounts in the x and y directions following straight lines which correspond to the inextensional mechanism. Only at higher loads do the extensional displacements become visible. In terms of nodal displacements, the only relevant difference between Figs 7.7 and 7.8 is that the actual magnitudes of displacement are larger in the case of smaller initial loads. The theoretical predictions obtained from SINCA are very good.

The second test consisted of symmetrical and non-symmetrical loading of the second cable structure shown in Fig. 7.6. This assembly clearly has two mechanisms: the first of these is most easily visualized by holding node 4 fixed and distorting inextensionally the resulting three-bar linkage as in the first test. The second mechanism is symmetrical to the first one, see Fig. 7.10. This cable behaved as expected when subjected to a uniform increment of all applied loads, load system 1; these results are not shown here. The behaviour under load system 2, see Fig. 7.11, is symmetrical and the tensions vary linearly with the applied load. Similarly, see Figs 7.12 and 7.13 for the response to load system 3.

The third test (see Fig. 7.6) had the objective of testing the theory developed in Chapter 6 in situations where a load is applied to an arbitrary, and previously unloaded, point of a cable. The number of inextensional mechanisms is still two; each mechanism only involves a displacement of either node 2 or 4 in directions perpendicular to the cable. This introduces a further complication because any computed displacement of node 3 is due entirely to the 'extensional component' of displacement {de}. Experimental and theoretical results are given in Figs 7.14 and 7.15. Notice that the graphs of the components of displacement of node 3 (as well as node 4, under load condition 2) have zero initial slope, as expected.

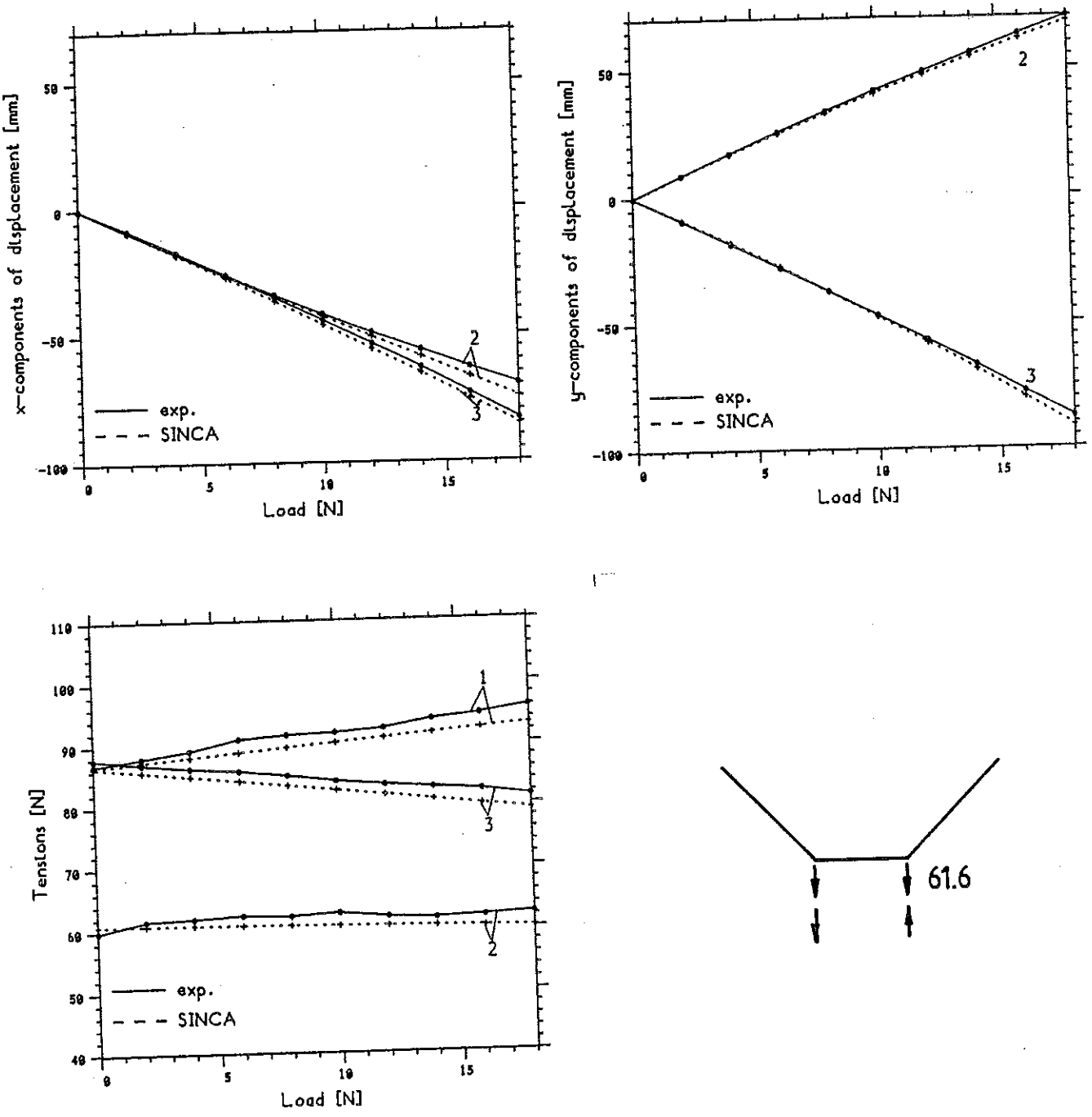

Fig. 7.7 Comparison of experimental and theoretical results of Test 1, load condition no. 2. The loads in the initial configuration are equal to 61.6N.

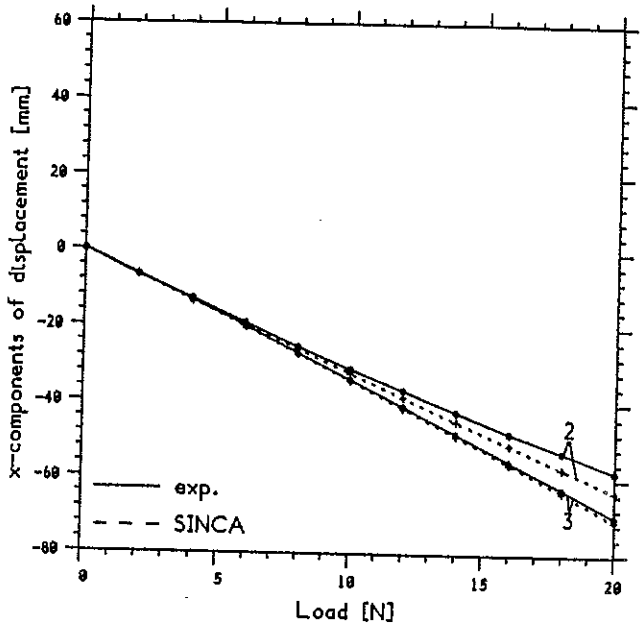

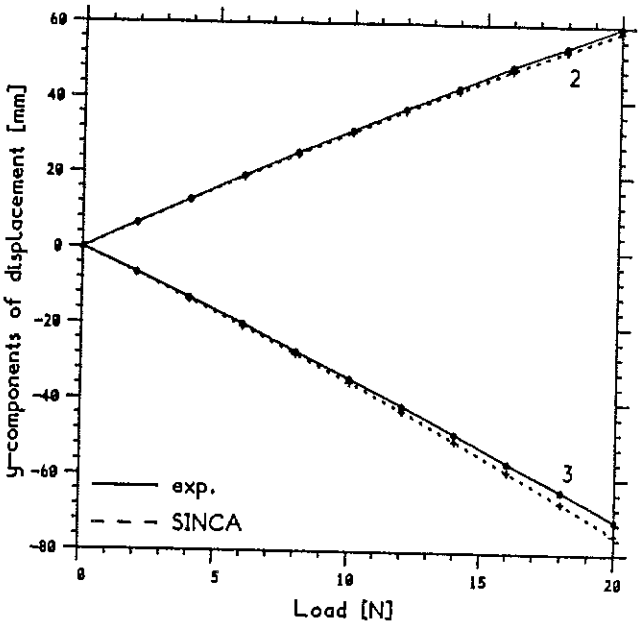

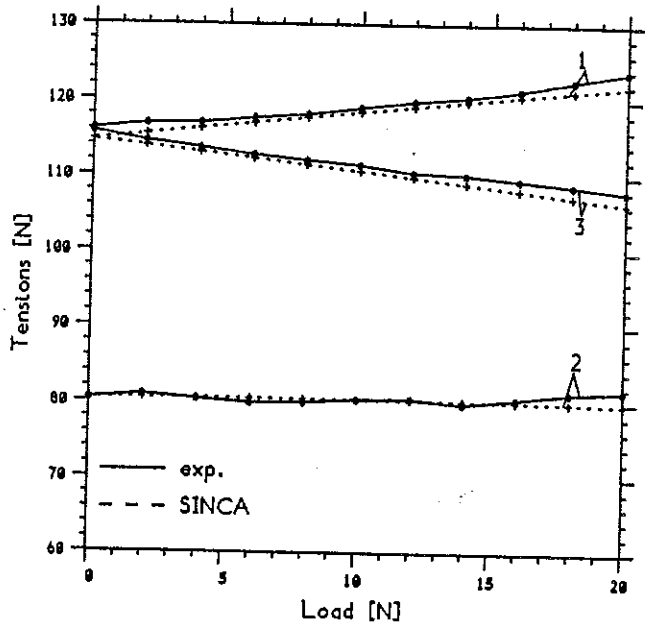

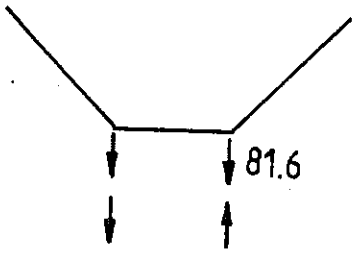

Fig. 7.8 As in Fig. 7.7, but for initial loads of 81.6N.

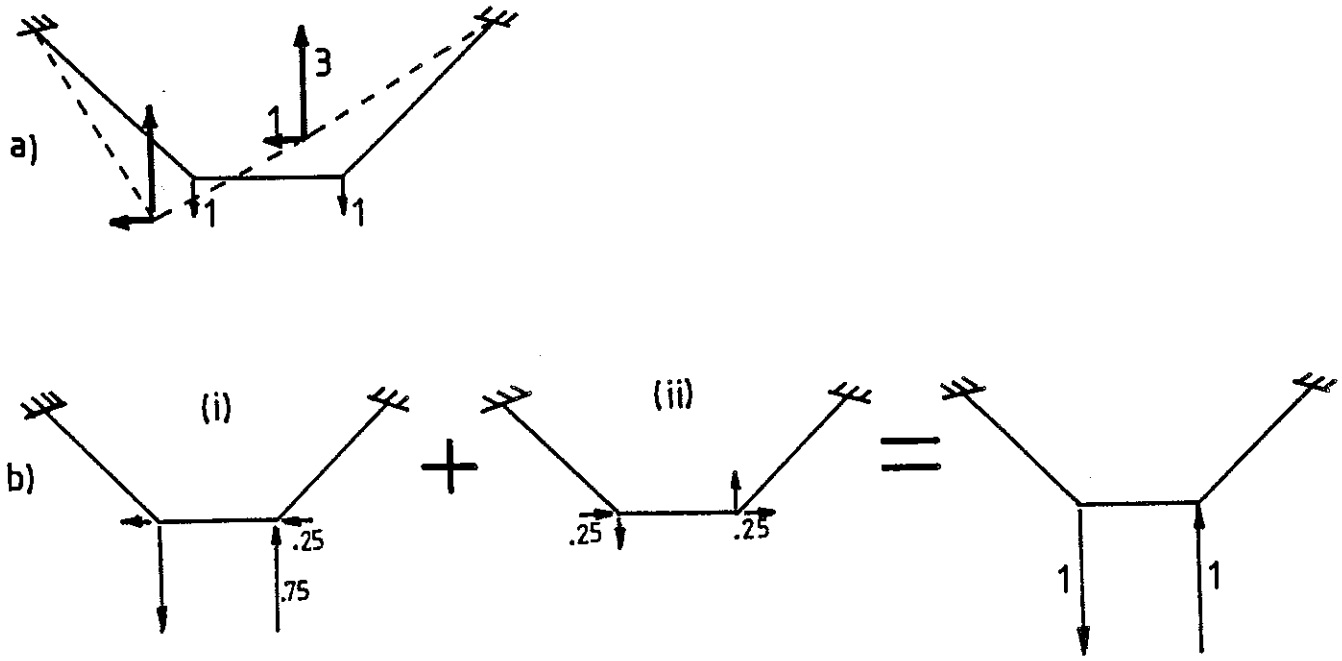

Fig. 7.9 a) Product-forces due to equal initial loads of 1, acting on the structural layout of Test 1 (Fig. 7.6).
b) For the same layout, load condition no. 2 has been decomposed into its inextensional (i) and extensional components (ii). Clearly (i) is proportional to the product-forces in a); and (ii) causes equal and opposite changes of tension in the side wires only.

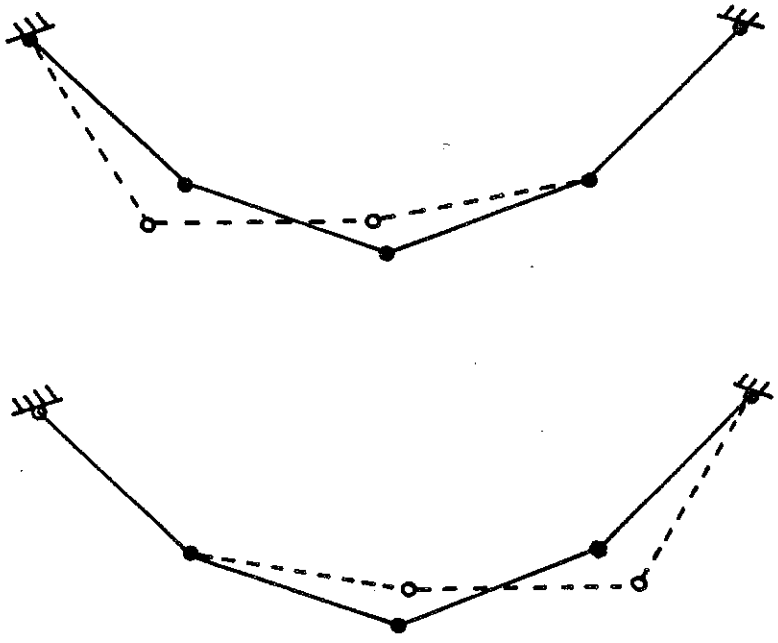

Fig. 7.10 Two independent mechanisms of the hanging cable investigated in Test 2.

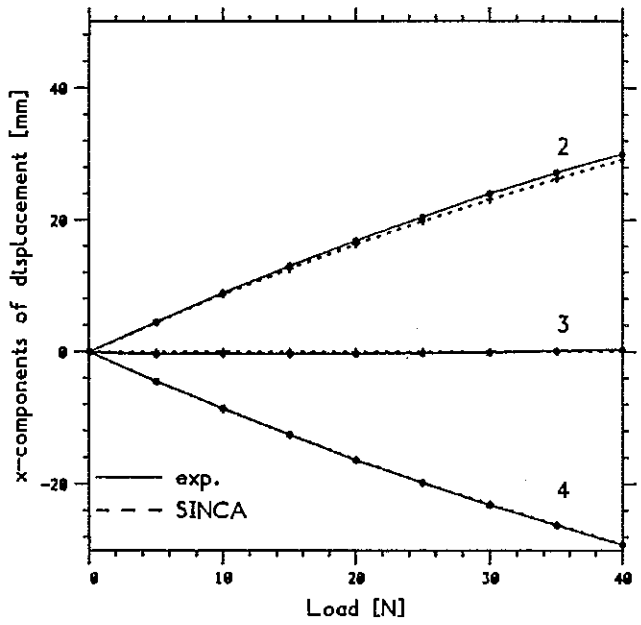

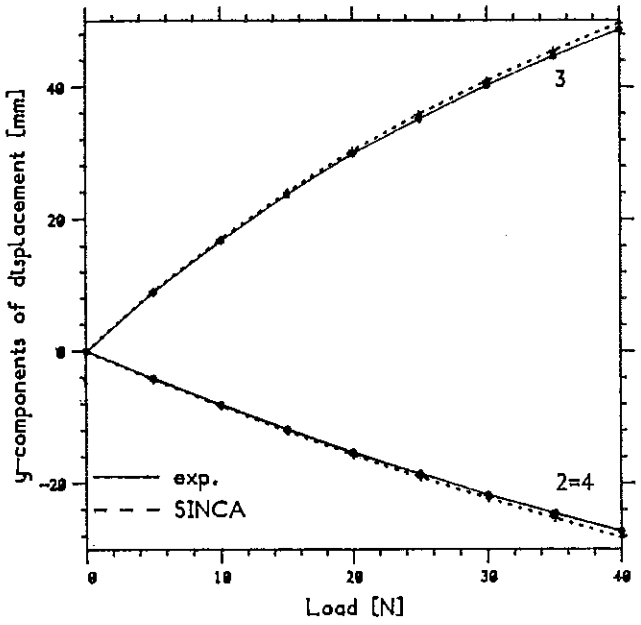

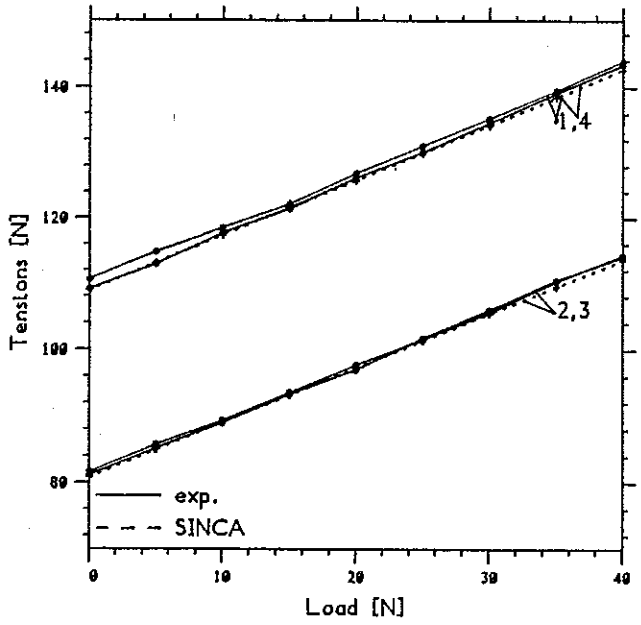

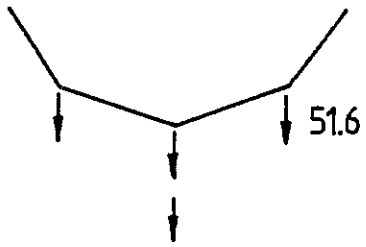

Fig. 7.11 Experimental and theoretical results from Test 2, load condition no. 2. The initial load applied to nodes 2, 3 and 4 was of 51.6N.

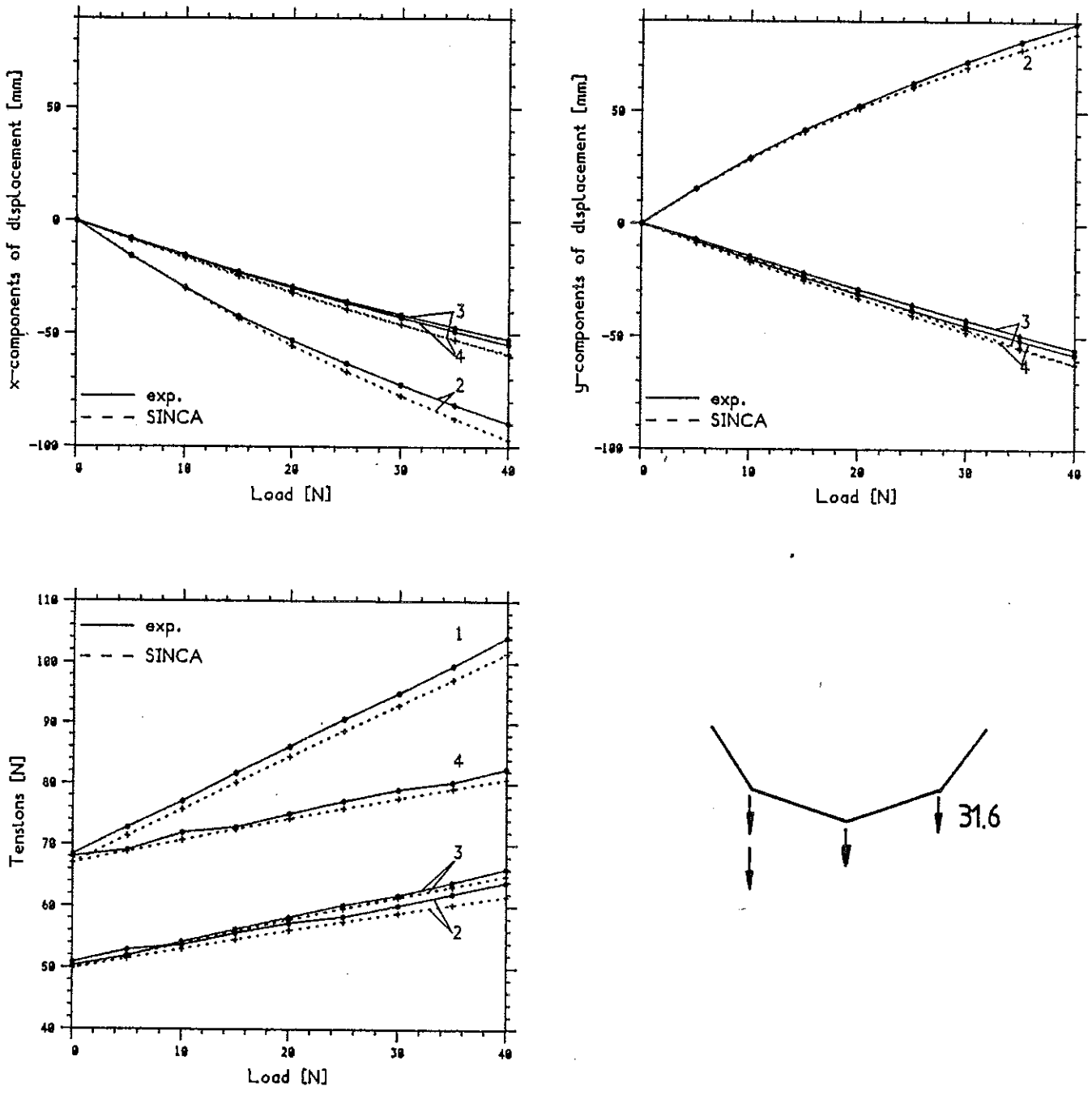

Fig. 7.12 Results from Test 2, load condition no. 3. The initial load applied to nodes 2, 3 and 4 was 31.6N.

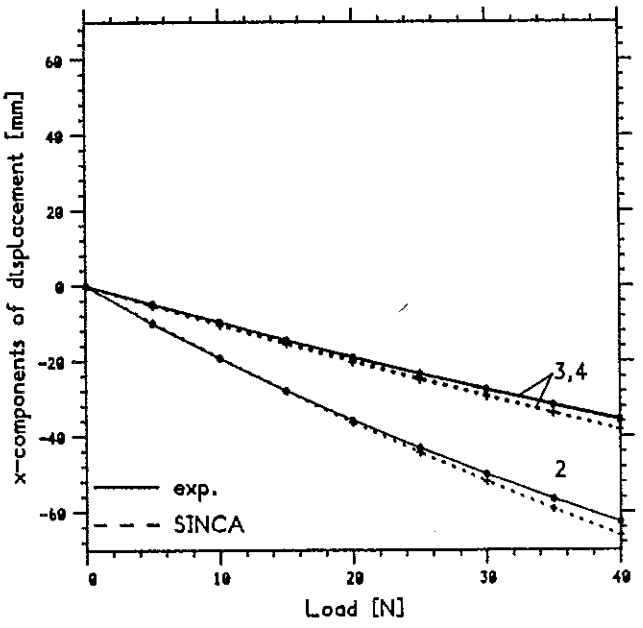

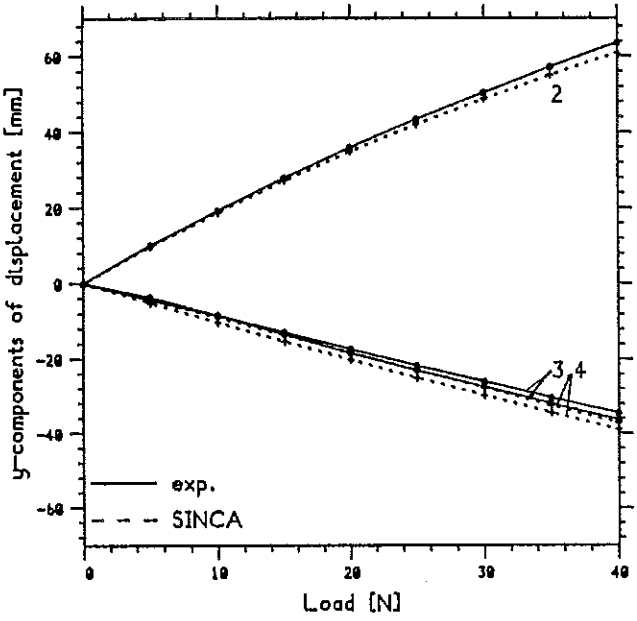

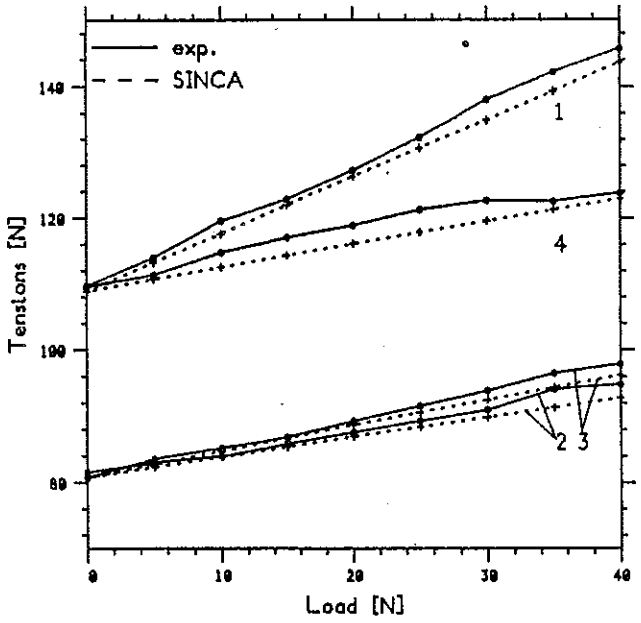

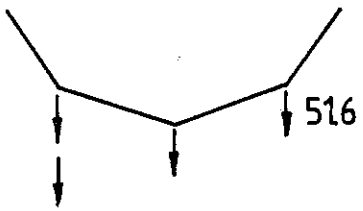

Fig. 7.13 As in Fig. 7.12, but for initial loads of 51.6N.

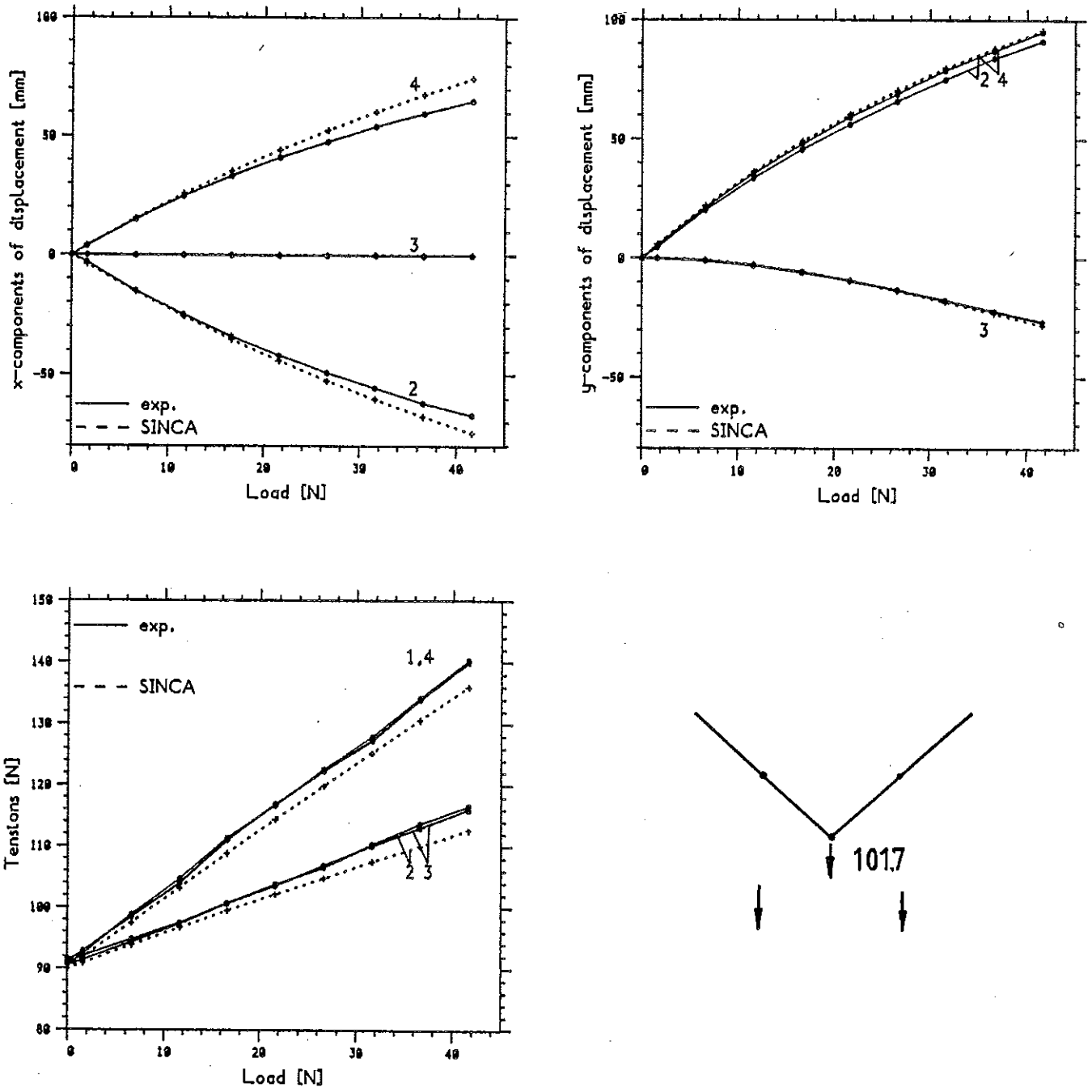

Fig. 7.14 Results from Test 3, load condition no. 1. The initial load was of 101.7N.

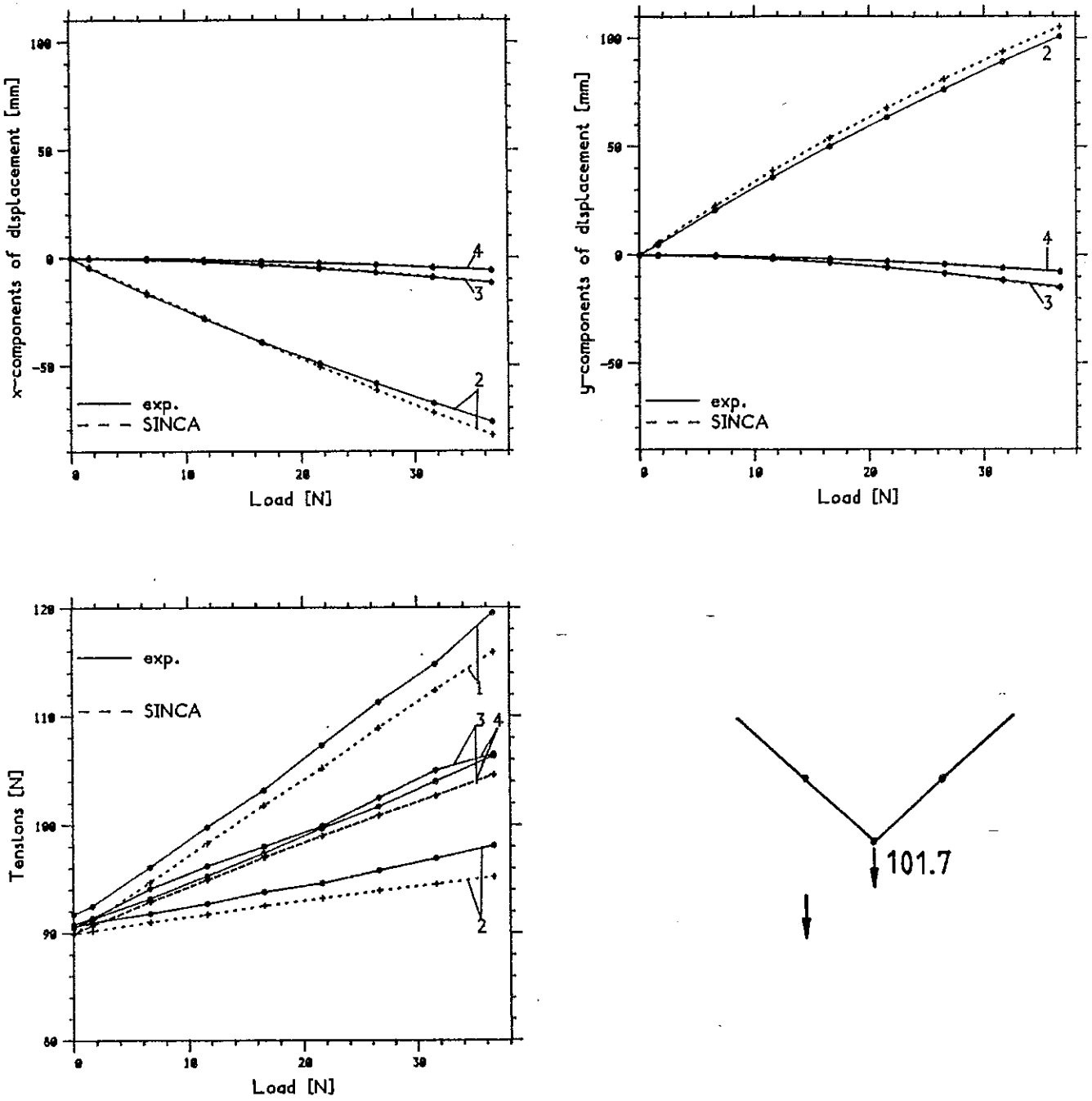

Fig. 7.15 Results from Test 3, load condition no. 2. The initial load was of 101.7N.

7.4 Experiments on cable nets

Tests were conducted on two saddle-shaped cable nets. The layout of the smaller one is sketched in Fig. 7.2a and its nodal coordinates and connectivity are indicated in Fig. 7.16; it consists of two parallel and equal sagging wires - segments 1,2,3 and 4,5,6 of Fig. 7.16 - connected by means of devices as in Fig. 7.1a to the scaffolding described above, and of two similar hogging wires at right angles to them. Initially the horizontal projection of the cable net was to consist of segments of equal length, and the square with vertices in 4,5,9,8 was to be at equal distance from the lower and upper boundaries, as in the framework of Fig. 4.18. But first the horizontal projection had to be modified in order to use the available scaffolding; then an 'error' in the initial setting up of the net was the cause of a difference of 9mm between the vertical coordinates of the lower and upper boundary nodes.[3] The analysis described in Chapter 4 shows that a pin-jointed assembly with the geometry of Fig. 7.16 is statically and kinematically indeterminate, with m=s=1. The state of selfstress is:

$$\{c\ d\ c\ c\ d\ c\ e\ f\ e\ e\ f\ e\}^T$$

where c=1.0275, d=1.00, e=1.0876 and f=1.0616 (the numbering system is indicated in Fig. 7.16). Note that the prestressing tensions in the horizontal segments are no longer equal. The components of displacement associated with the mechanism, which is infinitesimal of first order, are:

$$\{g\ -h\ j\ -g\ -h\ -j\ g\ h\ -j\ -g\ h\ j\}^T$$

where g=1.0616, h=1.00 and j=4.4931.

Once prestressed this assembly has a set of product-forces whose directions resemble the mechanism displacements but do not coincide with

---

[3] A compromise between accurate initial alignment and prestressing had to be reached. The theoretical layout, with x- and y-coordinates as indicated in Fig. 7.16b and a 'perfect' elevation, admits the state of selfstress:

$$\{a\ b\ a\ a\ b\ a\ a\ b\ a\ a\ b\ a\}^T$$

where a=1.0260 and b=1.

them, see Fig. 7.17. The existence of such cases has been noted already.

Two different load conditions were considered: the first one consists of four equal vertical loads directed downwards, and applied in ten increments of 5N each. It is easy to verify that such a system is orthogonal to the mechanism, hence it is a "fitted" loading.

Readings were taken for two levels of initial prestress (≈50N, ≈80N) but only the results relating to the higher pretension will be given here. Figures 7.18 and 7.19 show that the nodal displacements and wire tensions vary more or less linearly, as indeed one would expect after Chapter 6: it is plain from Fig. 7.18 that the horizontal square in the middle of the net translates downwards, and hence all the vertical components of displacement are approximately equal, while elongating its sides by approximately equal amounts; hence x- and y-components of displacement are also approximately equal, in absolute value. The theoretical analysis predicts that the hogging cables become slack at a value of 44N of the applied loads; and in fact Fig. 7.18 shows some 'anomalies' at about this level. The kinks in Fig. 7.18 correspond, effectively, to the transition from the initial cable net into an assembly of two independent sagging wires; the theoretical analysis, which begins to fail because it assumes that all the members can carry tensions of either sign, must be modified accordingly.

The second load condition consisted of equal downward forces acting on two opposite nodes, 5 and 8 in Fig. 7.16, and also applied in ten increments of 5N each. This force system has non-zero "fitted" and non-fitted components, and therefore the response to it involves both of the modes of action described in Chapter 6. The non-linear tightening up of the mechanism due to the increase of the level of selfstress, pointed out in Section 6.4.1, can also be seen clearly in Figs 7.20 and 7.21. Notice that the tensions in the hogging wires remain about constant because the decrease caused by the "fitted" component of the applied load is balanced, within the experimental range, by the non-linear increase.

Numerical estimates based on the f.e. program described previously were obtained for both load conditions; these results are not shown here because, although they tend to be in slightly better agreement with the experimental values that the ones given by MULCA, the difference is not significant.

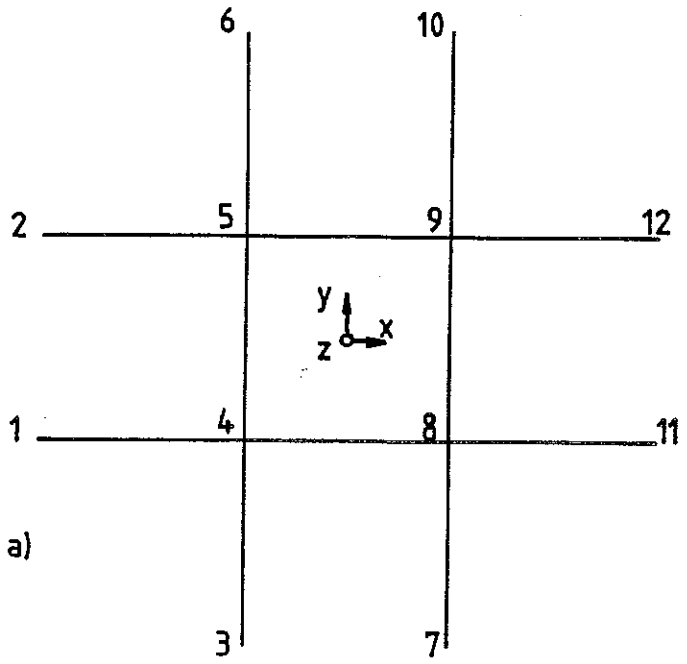

b)

Node no.	x	y	z
1	-961.	-305.	155.
2	-961.	305.	155.
3	-305.	-961.	-146.
4	-305.	-305.	0.
5	-305.	305.	0.
6	-305.	961.	-146.
7	305.	-961.	-146.
8	305.	-305.	0.
9	305.	305.	0.
10	305.	961.	-146.
11	961.	-305.	155.
12	961.	305.	155.

Bar no.	from node	to node	
1	1	4	
2	4	8	
3	8	11	
4	2	5	sagging
5	5	9	
6	9	12	
7	3	4	
8	4	5	
9	5	6	
10	7	8	hogging
11	8	9	
12	9	10	

Fig. 7.16 a) Plan view of the smaller cable net which was tested. The z-axis is upwards.
b) Nodal coordinates and cable segments numbering system. All dimensions are in [mm].

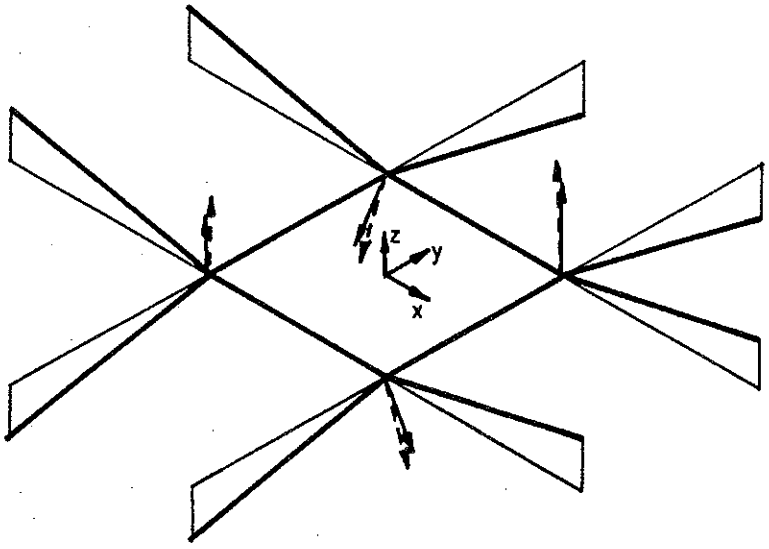

Fig. 7.17 Isometric view of nodal displacements (solid arrows) and product-forces (broken arrows) associated with the infinitesimal mechanism of the cable net of Fig. 7.16.

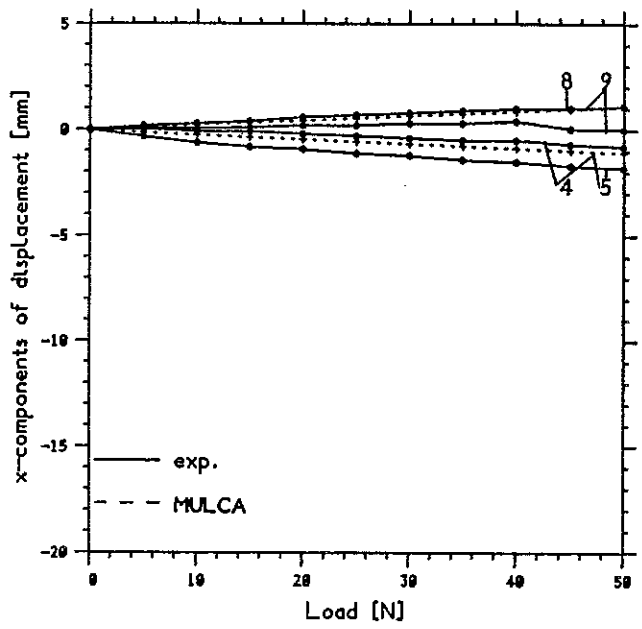

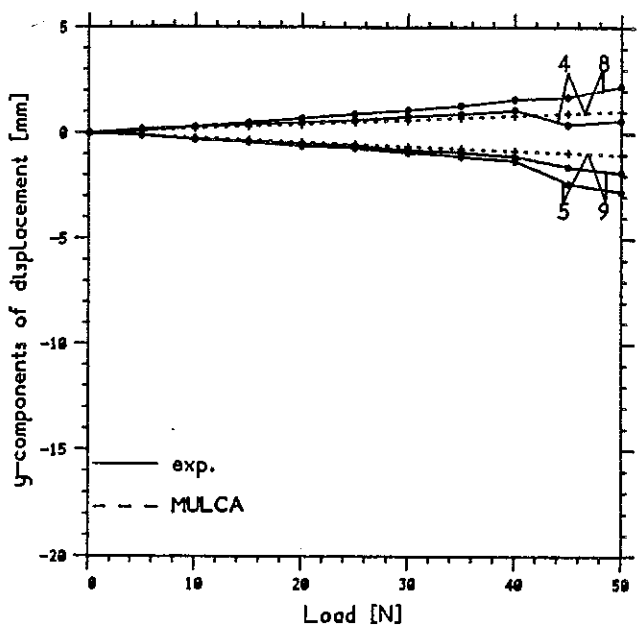

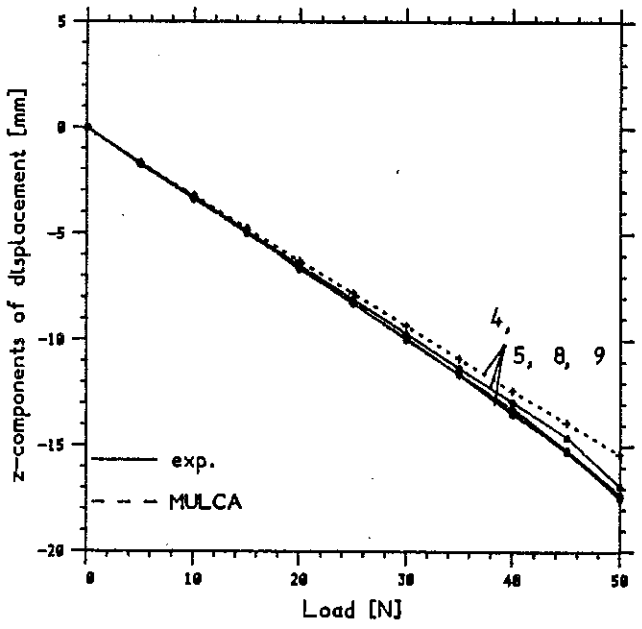

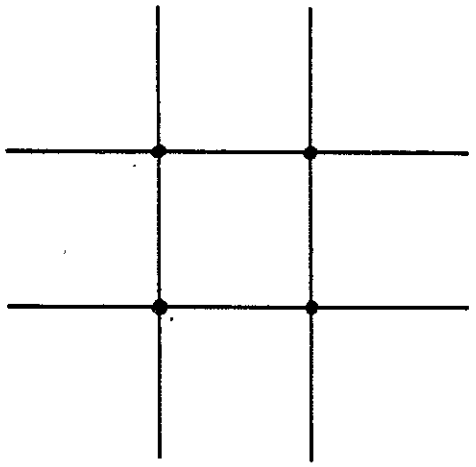

Fig. 7.18 Plots of displacements vs. applied load for the cable net of Fig. 7.16. The load condition, shown in the bottom right corner, consists of equal downward forces on all nodes. The variable 'load' plotted above is the value of each one of these forces.

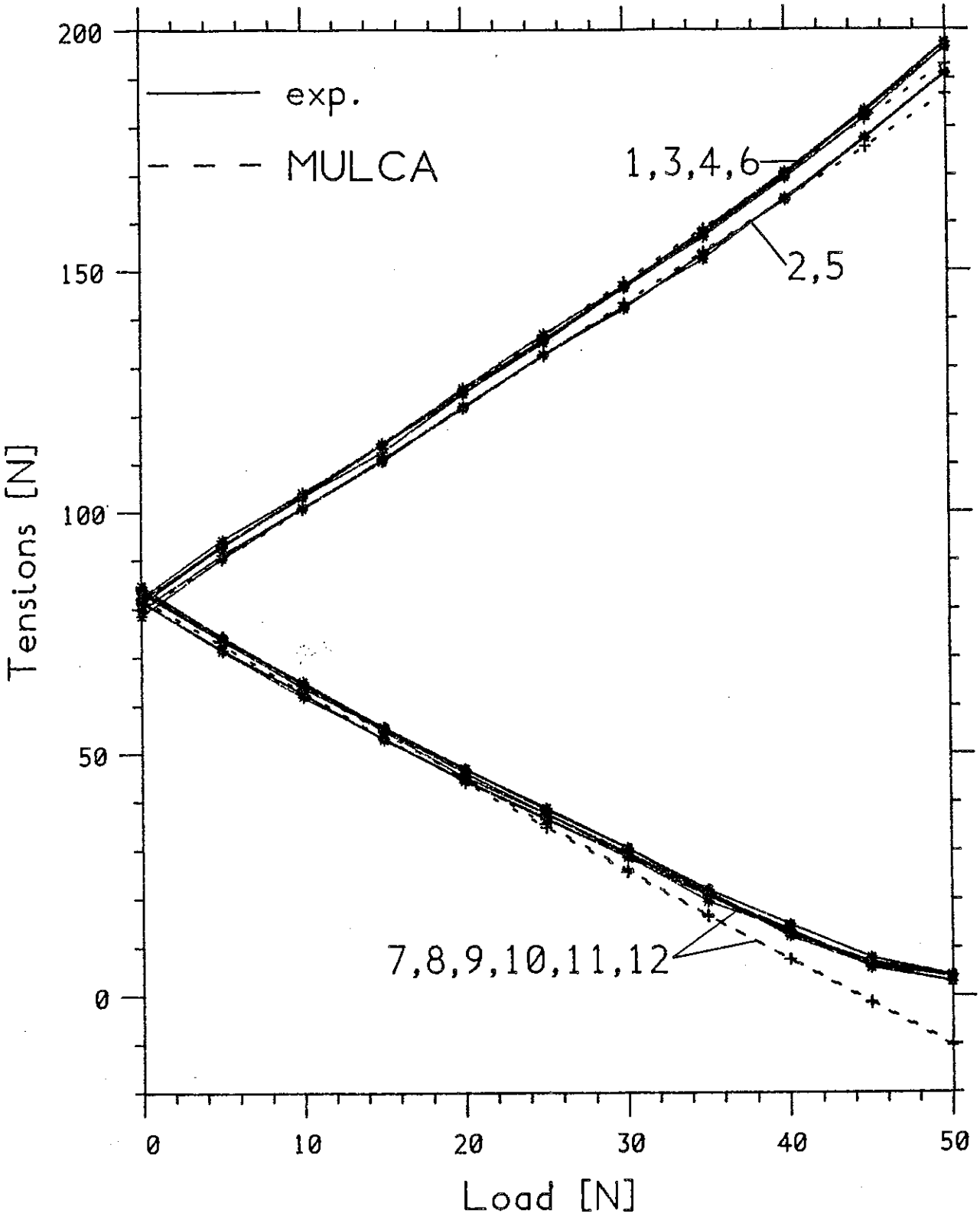

Fig. 7.19 Plots of wire tensions vs. applied load, for the cable net of Fig. 7.16 under uniform vertical load.

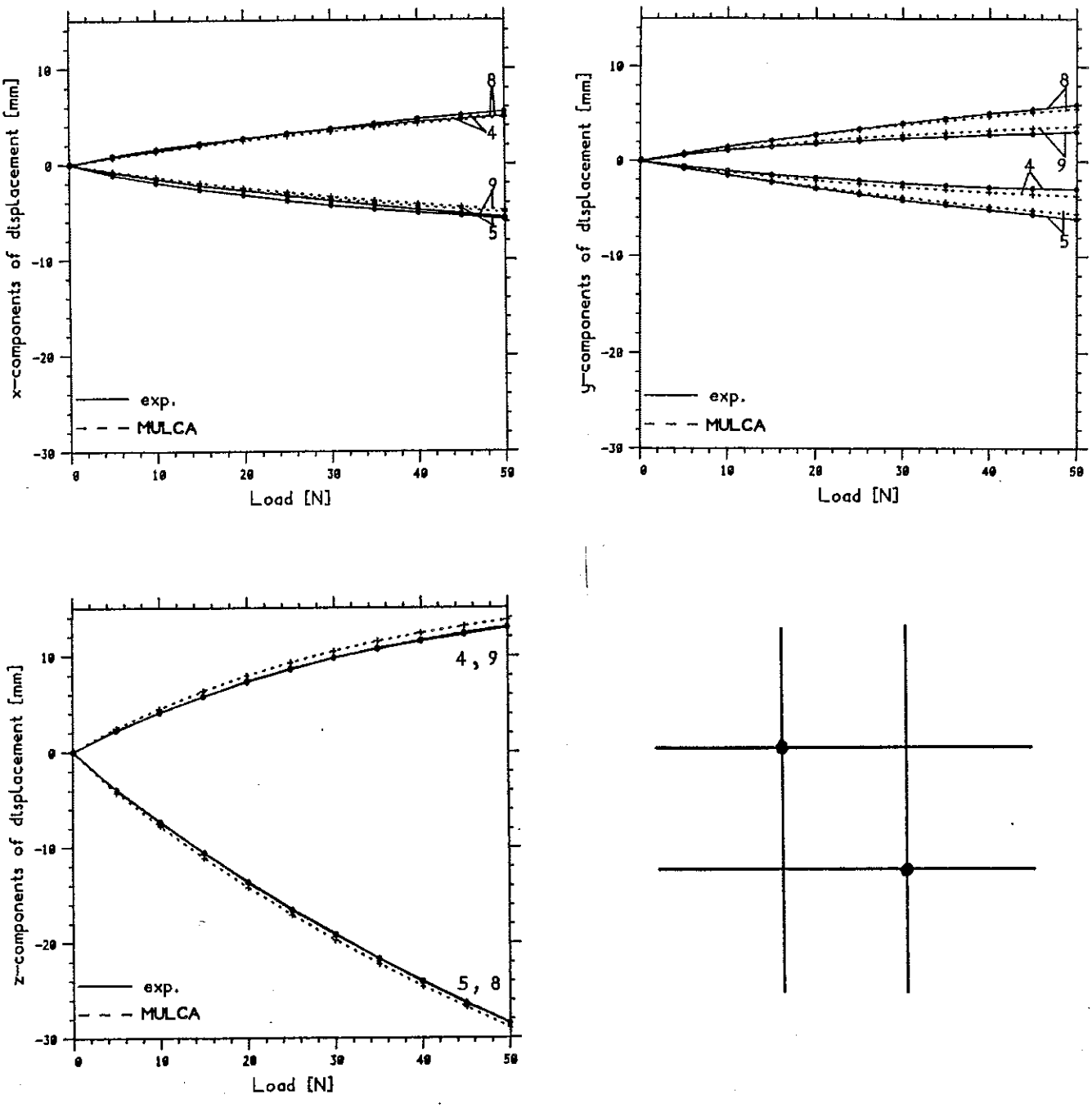

Fig. 7.20 Plots of displacements vs. load for the cable net of Fig. 7.16. The load condition, shown in the bottom right corner, consists of equal downward forces on two diagonally opposite nodes. The variable 'load' plotted here is the value of each one of these forces.

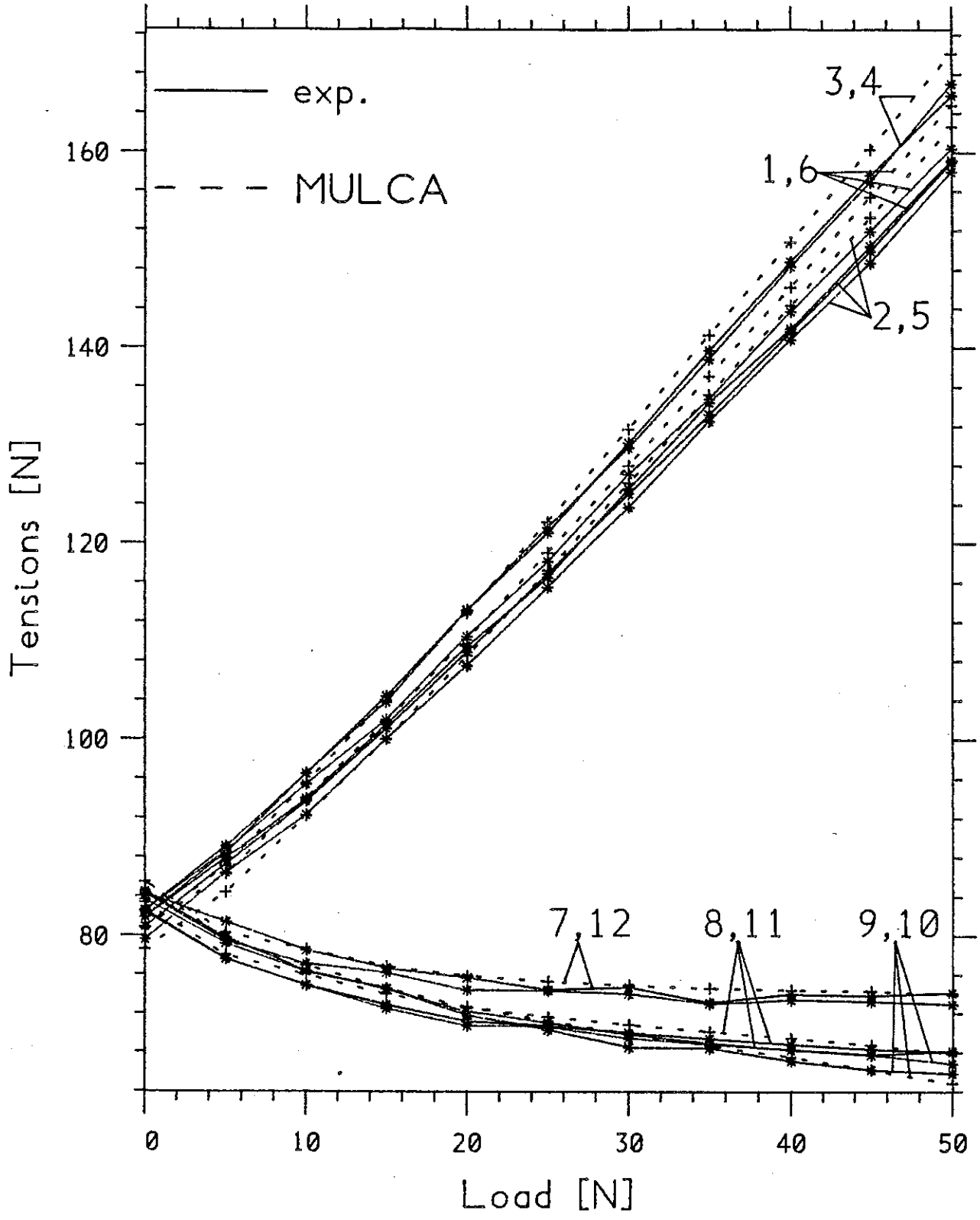

Fig. 7.21 Plot of wire tensions vs. applied load for the cable net of Fig. 7.16, under equal forces applied to diagonally opposite nodes. See also Fig. 7.20.

The larger cable net which was tested, see Fig. 7.22, is made out of three sagging wires of profile approximately parabolic (segments 1-12) and three hogging ones perpendicular to them (13-24). The nodes of the resulting net lie very close to the hyperbolic paraboloidal surface of equation $z=(y^2-x^2)/5955.0$ [mm]. Regarded as an assembly of pin-jointed bars, this structure has n=21, b=24, c=36 and it is found that s=1, m=4; in other words this cable net is a prestressable mechanism like the previous one. This is a feature common to most cable nets built in practice.

The state of selfstress is:

$$\{a\ b\ b\ a\ c\ d\ d\ c\ a\ b\ b\ a\ a\ b\ b\ a\ c\ d\ d\ c\ a\ b\ b\ a\}^T$$

with a=1.00, b=.9356, c=.9042 and d=.8460. Four independent mechanisms have also been produced by means of the usual computer analysis, but they will not be shown here.

The task of setting up this net, by modifying the length of the wire segments by small amounts until the overall geometry was correct and the prestressing tensions were in the expected ratios, gave some puzzling results at first. It was relatively easy to make small adjustments until no error could be measured in the nodal coordinates, yet the tensions were not very accurate and any attempt to modify them altered the global level of pretension rather than only the required values. This 'difficulty' was overcome by leaving the net pretensioned for about 24 hours. This had the beneficial effect of removing small kinks in the wire and hence improving the accuracy of the tensometer described in Section 7.2.5. Only at that stage were the tests begun.

A further confirmation of the correctness of the setting up was obtained from the experimental readings, as there was a rather small scatter - at most 4-5N - of results which, for instance, should have been equal according to a theoretical condition of symmetry.

The three load conditions shown in Fig. 7.23 were considered.

The first one consisted of equal downward forces applied to all the free nodes; a total load of 9×25N was applied in five increments of 5N to each node. This load condition can be obtained as a combination of "fitted loads", hence it causes purely extensional displacements, and tensions varying

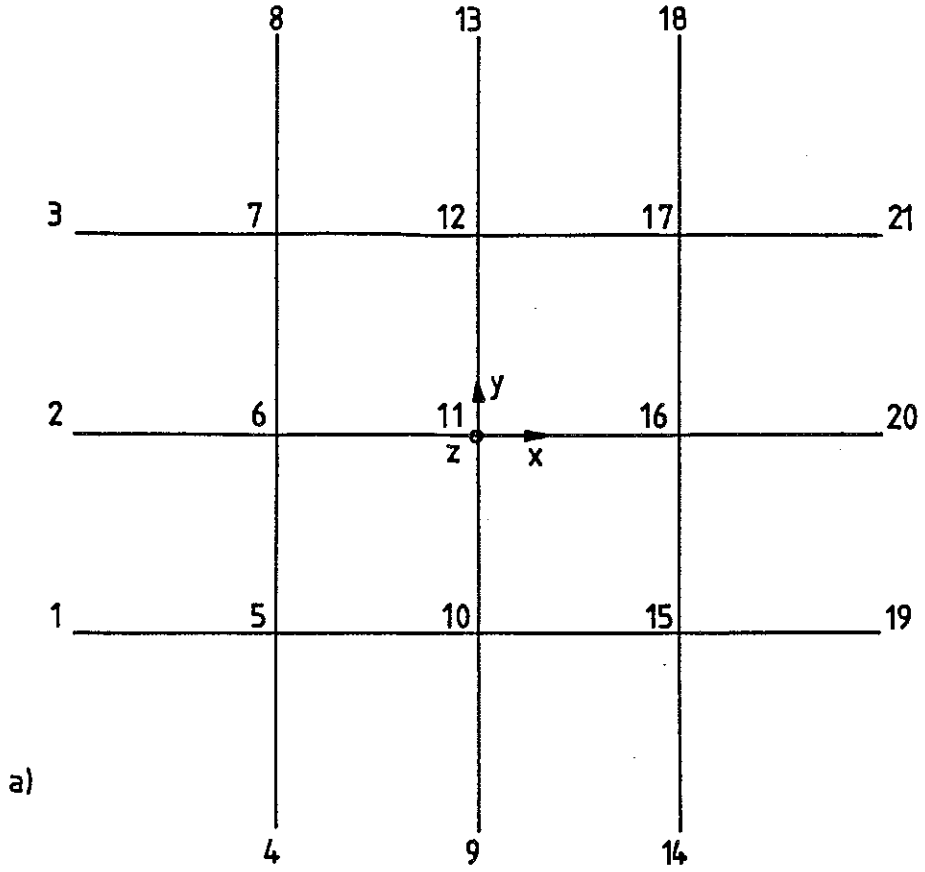

b)

Node no.	x	y	z
1	-1571.	-811.	-304.
2	-1571.	0.	-405.
3	-1571.	811.	-304.
4	-811.	-1571.	304.
5	-811.	-811.	0.
6	-811.	0.	-101.
7	-811.	811.	0.
8	-811.	1571.	304.
9	0.	-1571.	405.
10	0.	-811.	101.
11	0.	0.	0.
12	0.	811.	101.
13	0.	1571.	405.
14	811.	-1571.	304.
15	811.	-811.	0.
16	811.	0.	-101.
17	811.	811.	0.
18	811.	1571.	304.
19	1571.	-811.	-304.
20	1571.	0.	-405.
21	1571.	811.	-304.

Segment no.	from node	to node
1	1	5
2	5	10
3	10	15
4	15	19
5	2	6
6	6	11
7	11	16
8	16	20
9	3	7
10	7	12
11	12	17
12	17	21
13	4	5
14	5	6
15	6	7
16	7	8
17	9	10
18	10	11
19	11	12
20	12	13
21	14	15
22	15	16
23	16	17
24	17	18

Fig. 7.22 a) Plan view of the second cable net described in Section 7.4. The z-axis is upwards.
b) Initial nodal coordinates and connectivity of the cable net shown above. All dimensions are in [mm].

linearly with the load; see Fig. 7.24.

The other two load conditions had significant product-force components: only one corner node was loaded in load condition 2 (Fig. 7.25), and only the central node in load condition 3 (Fig. 7.26). Note that, had the tested structure been 'perfect', it would have had, e.g., $w_5=w_7=w_{15}=w_{17}$ in Fig. 7.24a, $x=-y$ in Fig. 7.25b and $x=y=0$ in Fig. 7.26b.

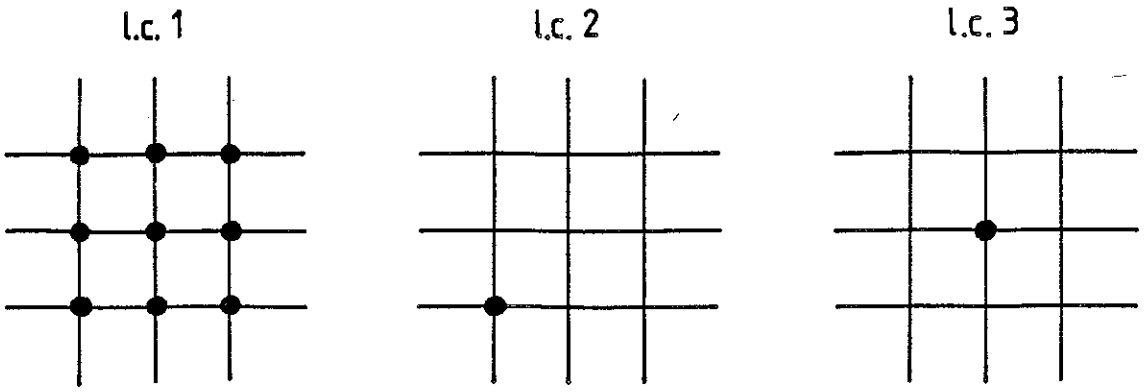

Fig. 7.23 The three load conditions considered for the second experiment described in Section 7.4. All loads are vertical and directed downwards.

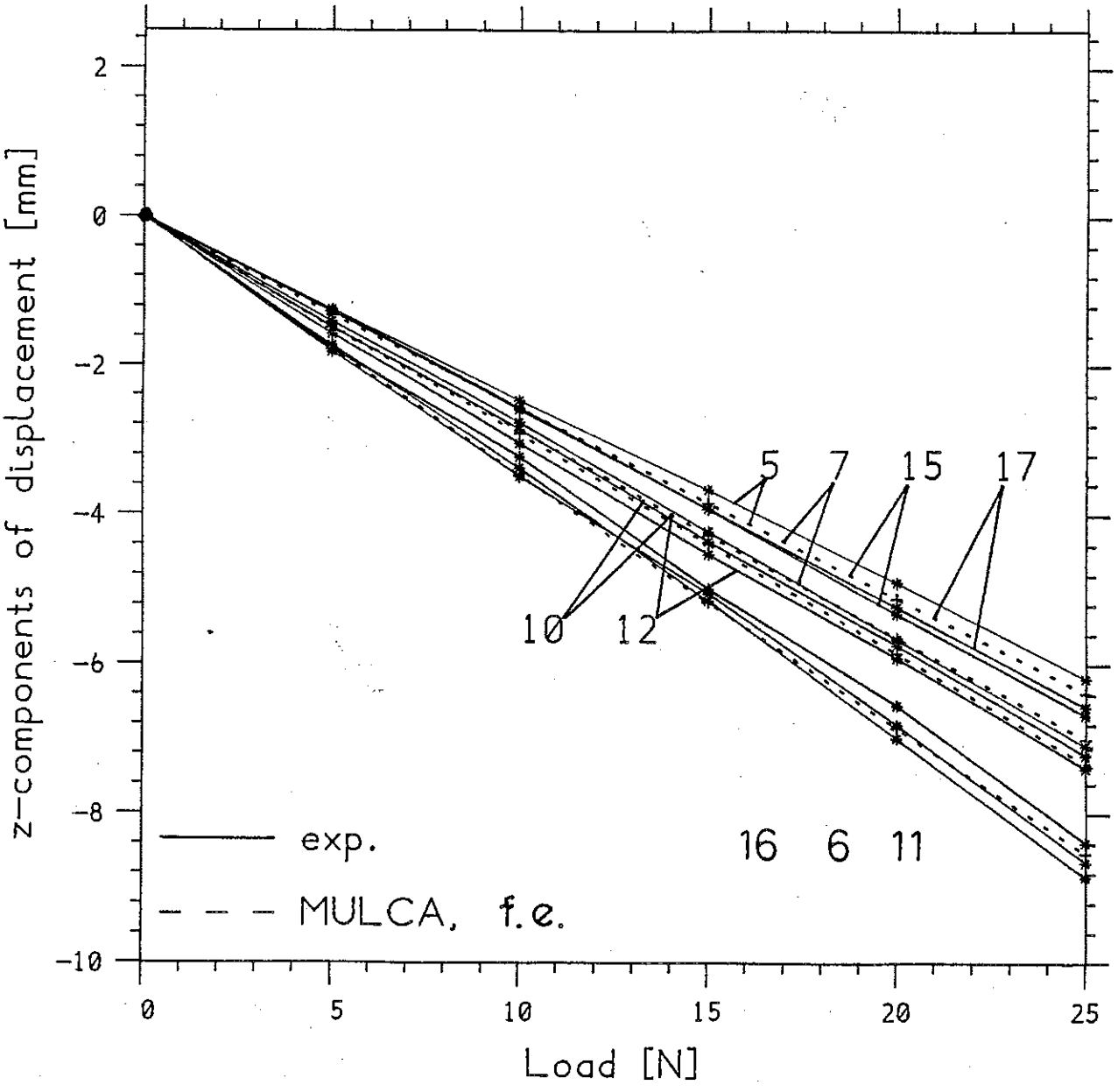

Fig. 7.24a Response of the cable net of Fig. 7.22 to a uniformly distributed load condition, number 1 in Fig. 7.23.

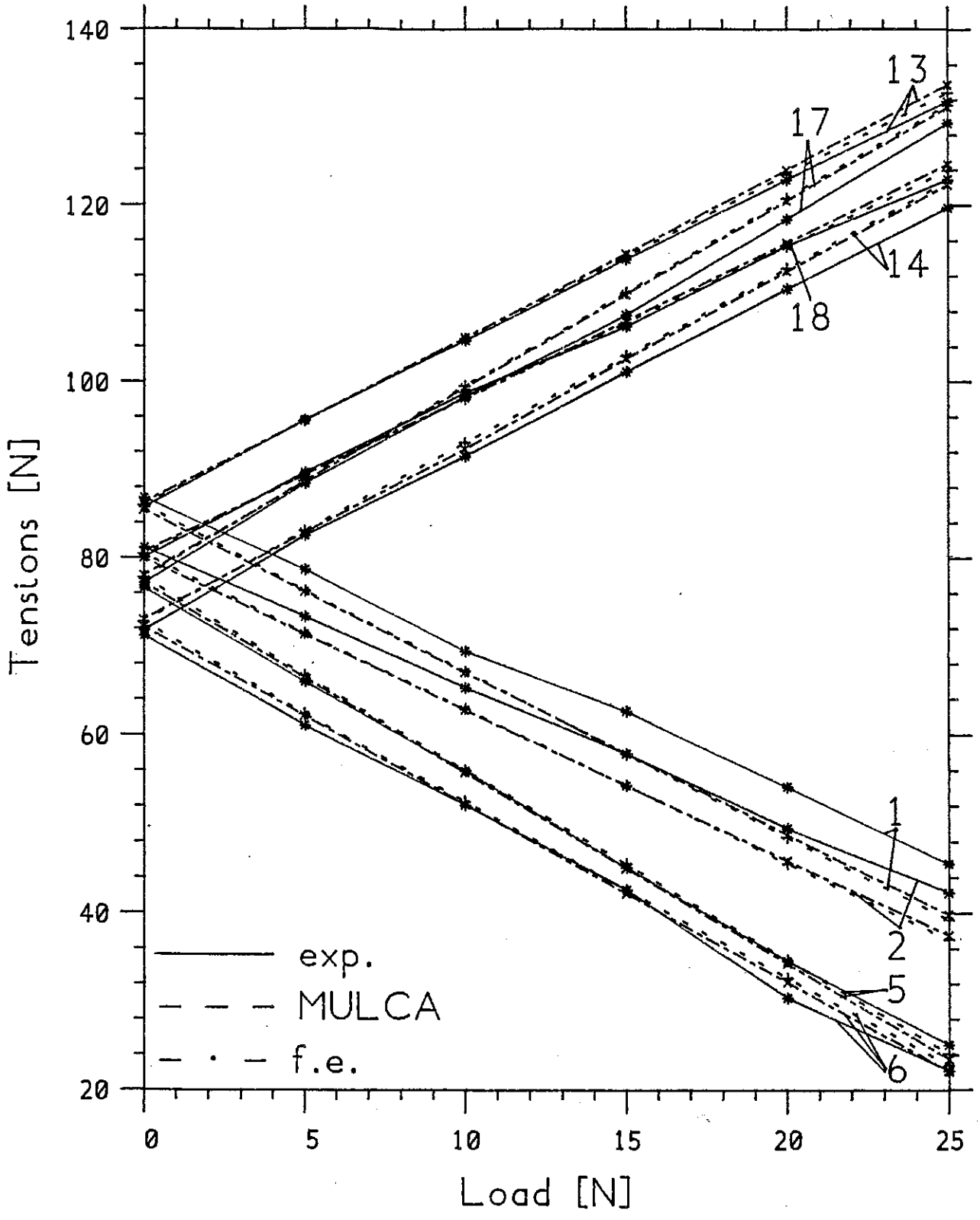
140
120
100
80
60
40
20
0
5
10
15
20
25
Tensions [N]
Load [N]
13
17
14
18
1
2
5
6
exp.
MULCA
f.e.

Fig. 7.24b

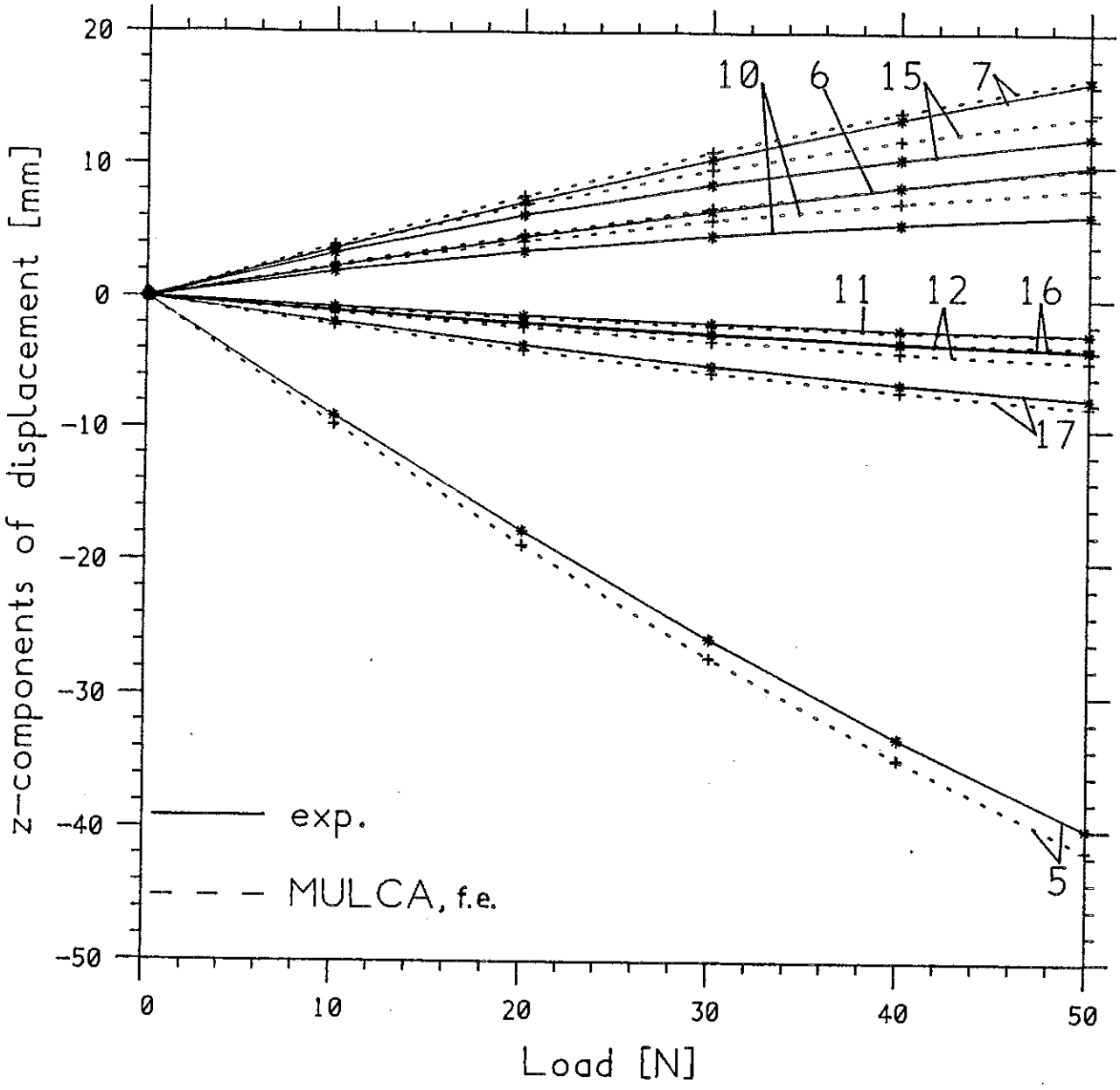

Fig. 7.25a Response of the cable net shown in Fig. 7.22 to a load applied in a corner node, load condition no. 2 of Fig. 7.23. The finite element program gives answers approximately equal to MULCA; the largest discrepancy is of 0.90mm for w_5.

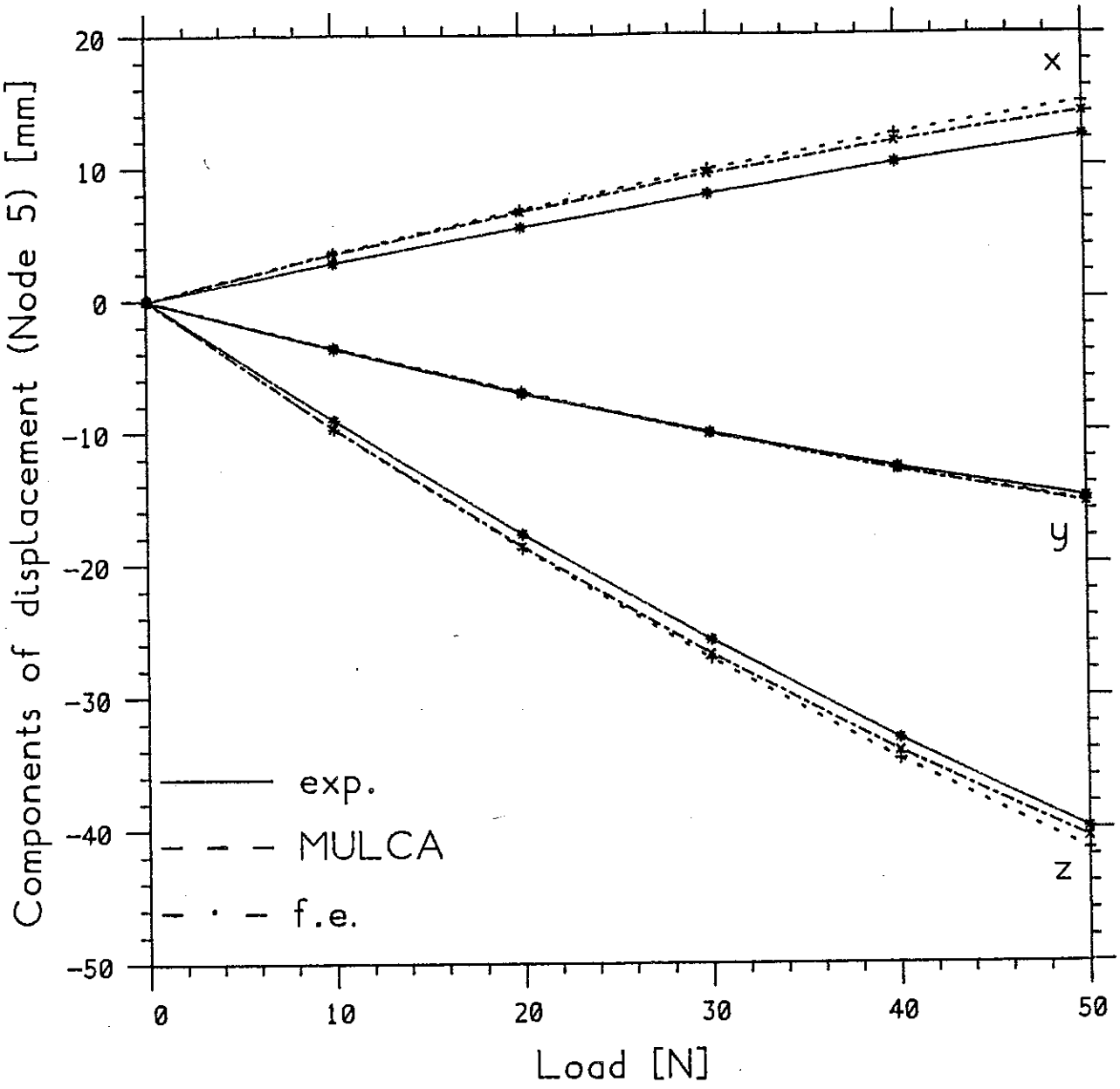

Fig. 7.25b Components of displacement of the loaded node. See Fig. 7.25a. The existence of a (vertical) plane of symmetry inclined at 45° to the x and y axes, explains the (theoretical) equality x=-y.

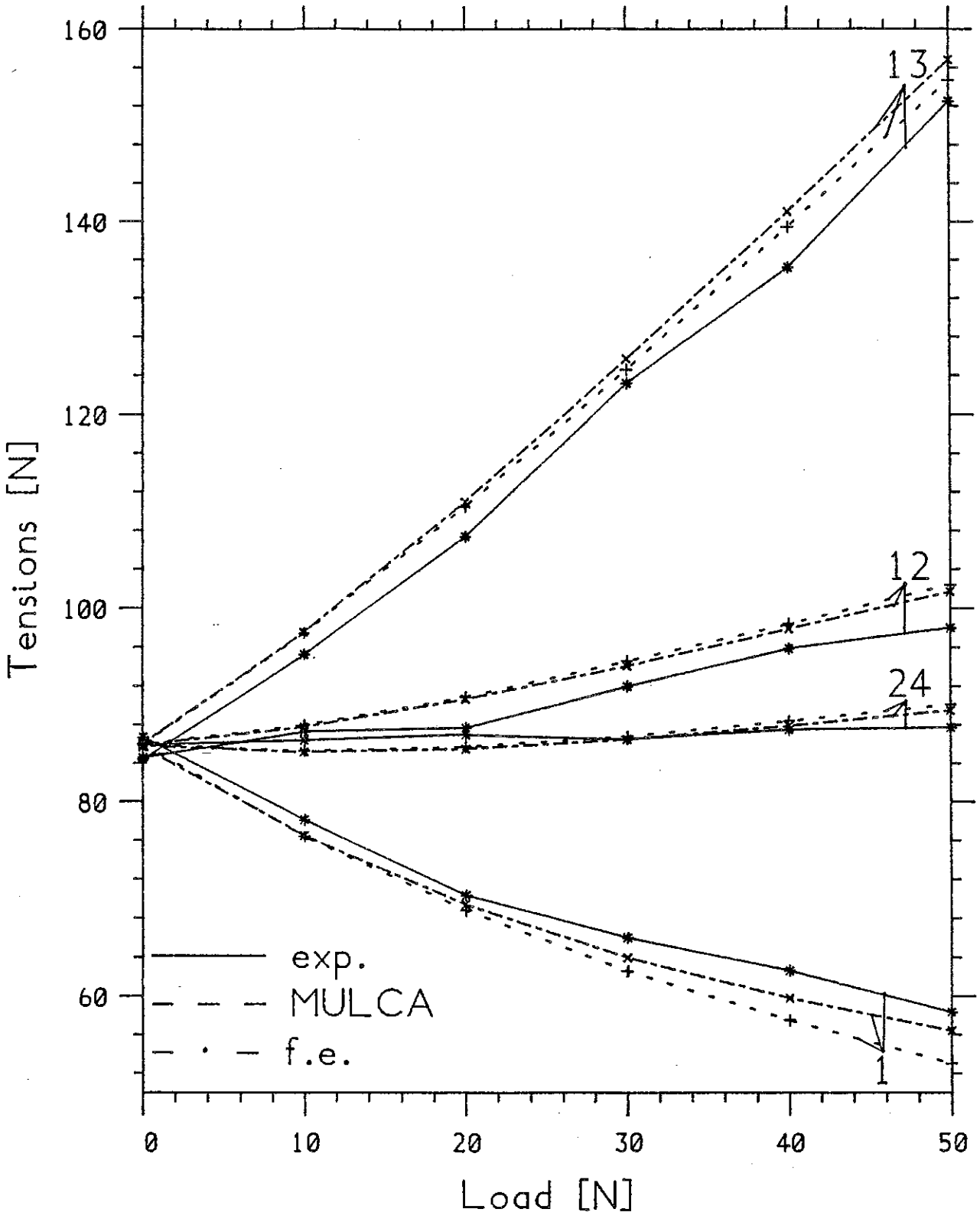

Fig. 7.25c Tensions in the wire segments which belong to the sagging and hogging wires going through the loaded node. See Fig. 7.25a.

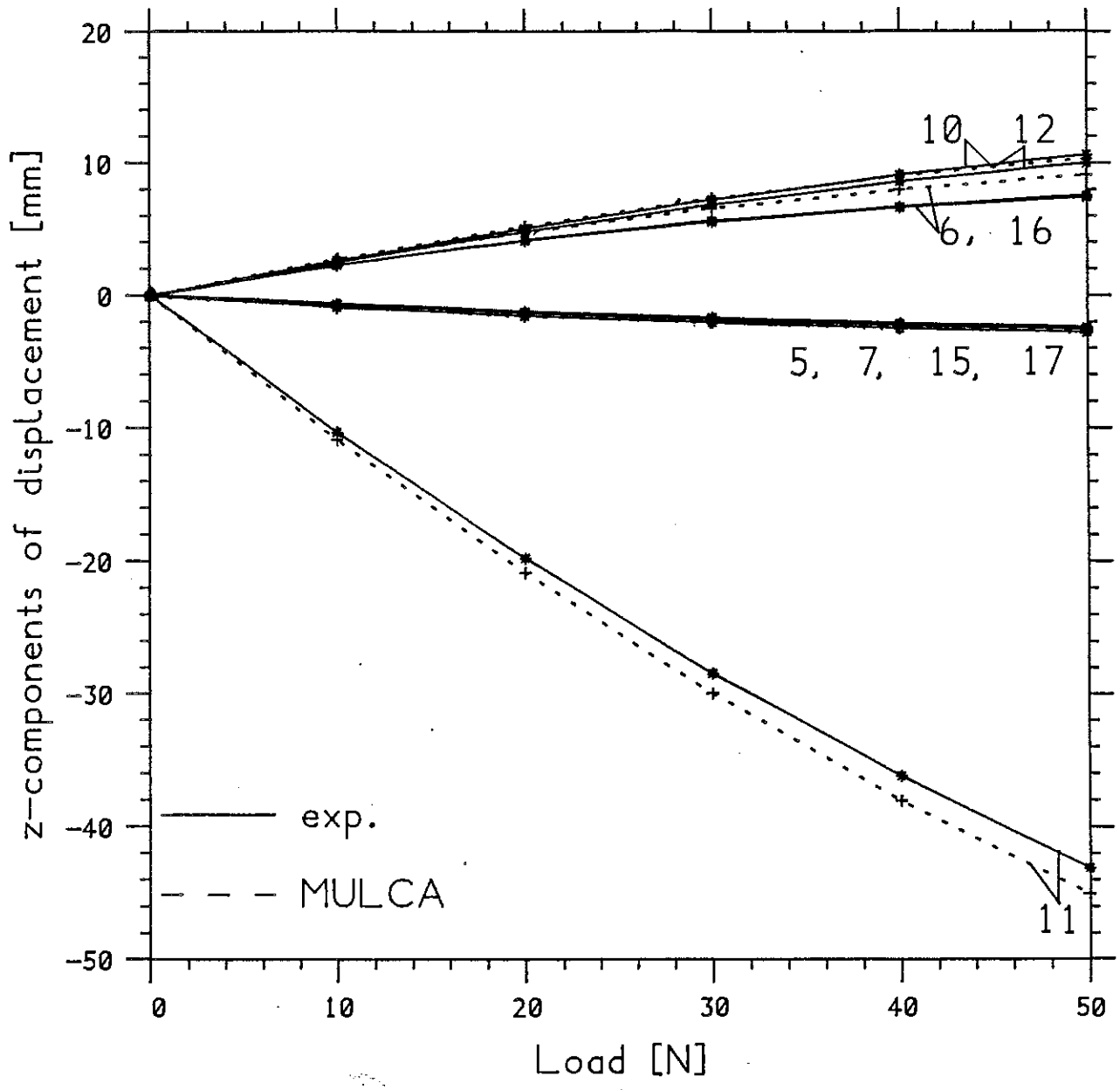

Fig. 7.26a Response of the cable net shown in Fig. 7.22 to a vertical load in the centre, load condition no. 3 of Fig. 7.23.

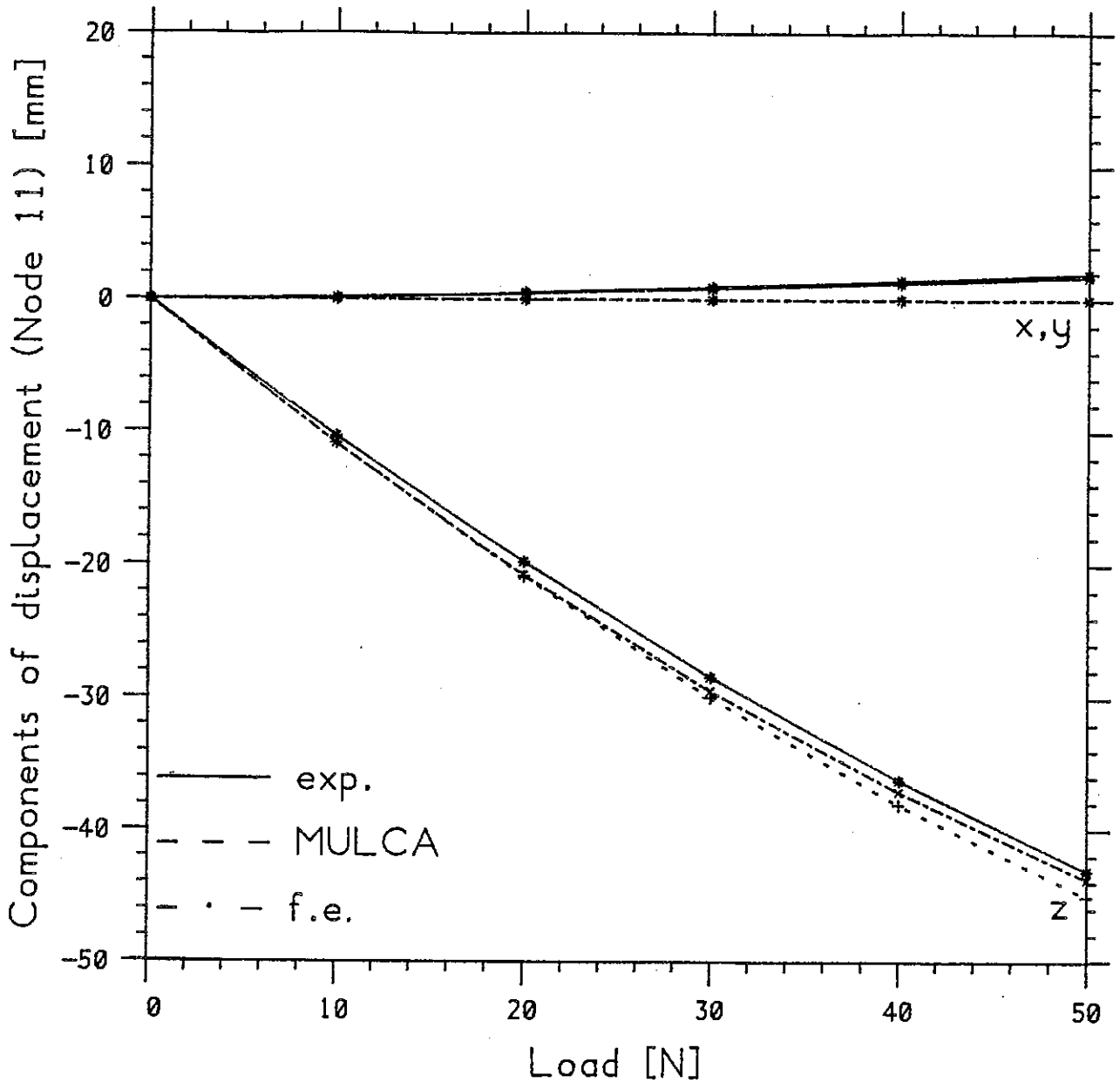

Fig. 7.26b Components of displacement of the loaded node. See Fig. 7.26a.

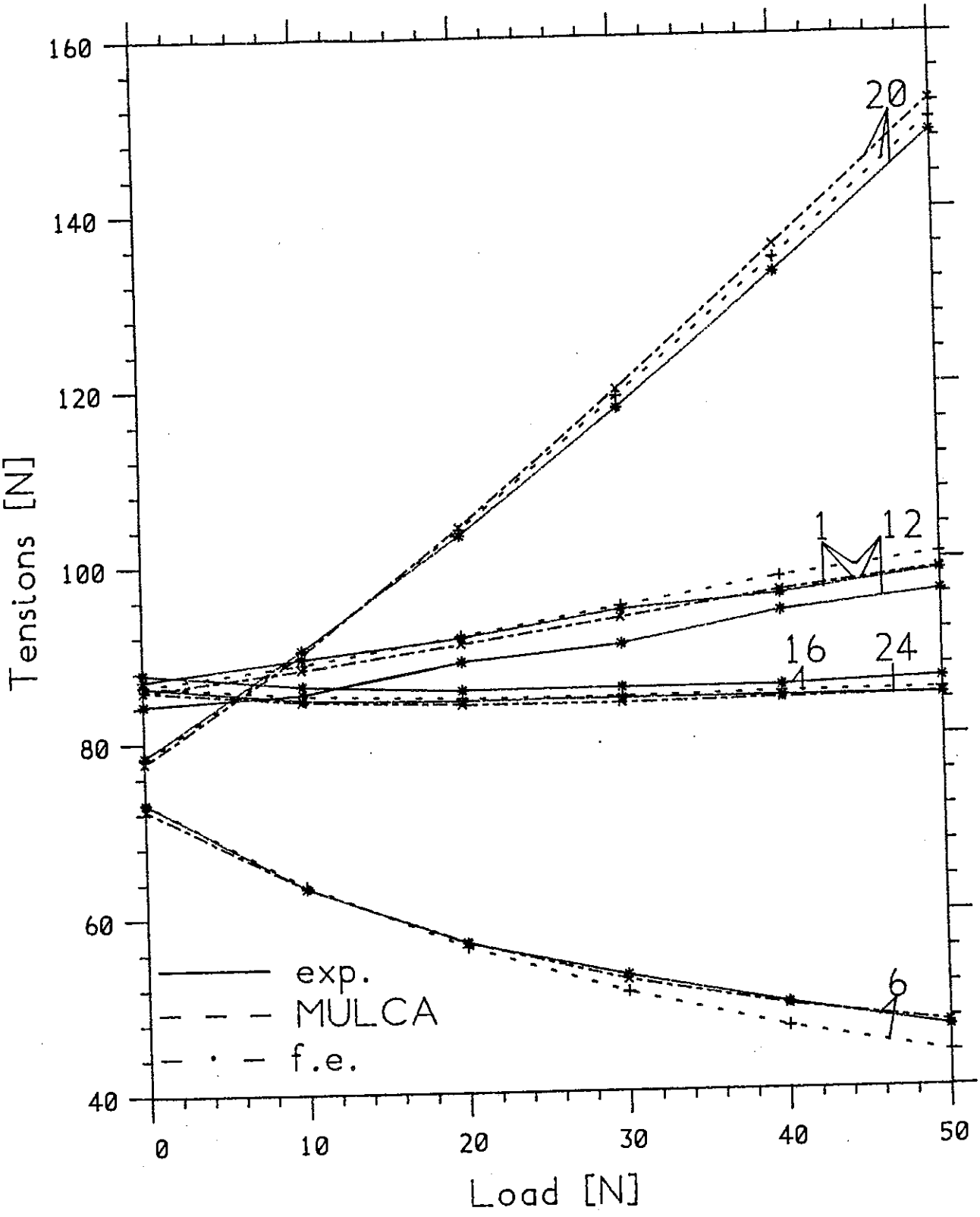

Fig. 7.26c Tensions in some representative wires. See Fig. 7.26a.

8. Conclusion

A comprehensive investigation of the mechanics of pin-jointed assemblies has been conducted.

Trying to find an answer to the fundamental question about a given assembly: is it rigid ? past work on the subject has been revised and summarized, and the results common to independent investigations have been pointed out.

A conceptual framework has been introduced, which relies on the introduction of the four fundamental subspaces of the equilibrium matrix of an assembly. The relevance of computing the bases of these subspaces at the onset of the analysis, in particular of those ones which give statical details of the states of selfstress and kinematical details of the inextensional mechanisms, has been shown. Criteria for the distinction of rigid-body mechanisms, infinitesimal mechanisms of first and higher order, and finite mechanisms have been introduced. All the procedures developed are essentially new; in particular the author is not aware of the existence of any other algorithm for the classification of infinitesimal mechanisms of arbitrary order which refers only to the initial configuration.

The linear and non-linear responses of kinematically indeterminate assemblies have been discussed in simple terms, and the ideas introduced have been exploited to develop efficient algorithms for analysing them, without going through the standard lengthy procedures in which the applied load has to be increased in small steps in order to give good results. The comparison of this new approach to experimental and numerical results has shown its validity and limitations.

Several by—products have emerged from the above investigation: (1) A study of the rigidity of a class of triangulated hyperbolic-paraboloidal surfaces, shown in Fig. 3.1, which have been proved to be rigid and statically determinate if the number of sides is odd. Otherwise they are not rigid, and the number of their infinitesimal mechanisms (of first order) is two less than the number of sides. (2) A simple and general numerical technique to find the initial nodal coordinates (formfinding) of a tensegrity structure. (3) On the experimental side, the main by—product is the construction of a novel instrument for measuring the tension in a steel wire very accurately.

Several points have been left open for further investigation, the most immediate one being the application of the ideas and techniques of Chapters 4 and 6 to more complicated structures, and in particular to problems which are analysed by means of finite elements. This would bring some direct advantages to a structural designer and, possibly, lead to a more widespread use of the force method of analysis.

The application of algorithms based on Chapter 6, for analysing the behaviour of the cable structures built in practice, will require the development of the non-linear correction for assemblies with more than one redundancy; and also the ability to cope with more realistic constitutive relationships than the linear-elastic, for the cable segments.

Lastly, the ideas - given in Section 6.1.2 - for more efficient estimates of lower- and upper-bounds in the hypothesis of rigid-perfectly plastic behaviour need to be developed and tested.

References

Aitken, A.C., (1958), Determinants and Matrices, 9th edition, Edinburgh, Oliver & Boyd.

Argyris, J.H.,(1964), Recent Advances in Matrix Methods of Structural Analysis, Oxford, Pergamon.

Argyris, J.H., and Scharpf, D.W., (1972), Large deflection analysis of prestressed networks, J. Struct. Div. Proc. Am. Soc. Civ. Eng., **98**, ST3, 633-654.

Asimow, L., and Roth, B., (1978), The rigidity of graphs, Trans. Am. Math. Soc., **245**, 279-289.

Asimow, L., and Roth, B., (1979), The rigidity of graphs II, J. Math. Anal. & Appl., **68**, (1), 171-190.

Baker, Lord John, and Heyman, J., (1969), Plastic Design of Frames, 1, Cambridge, C.U.P.

Baldacci, R., Ceradini, G., and Giangreco, E., (1974), Plasticita', Milano, CISIA.

Barnes, M.R., (1975), Applications of dynamic relaxation to the topological design and analysis of cable, membrane and pneumatic structures, in: W.J. Supple, ed., Proc. 2nd Int. Conf. Space Struct., Guildford, Univ. of Surrey, 211-219.

Barnes, M.R., (1984), Form-finding, analysis and patterning of tension structures, in: Nooshin, H., ed., Proc. 3rd Int. Conf. Space Struct., London, Elsevier Appl. Sci. Publ., 730-736.

Baron, F., and Venkatesan, M.S., (1971), Nonlinear analysis of cable and truss structures, J. Struct. Div. Proc. Am. Soc. Civ. Eng., **97**, ST2, 679-710.

Bennet, G.T., (1911), Deformable Octahedra, Proc. London Math. Soc., series 2, **10**, 309-343.

Besseling, J.F., (1978), The force method and its application in plasticity problems, Computers & Structures, **8**, 323-330.

Besseling, J.F., (1979), Finite element methods, in: Besseling, J.F., and Van der Heijden, A.M.A., eds, Trends in Solid Mechanics, Noordoff Int. Publ., 53-78.

Besseling, J.F., (1981), Applicatiecursus Eindige Elementen Methode, T. H. Delft, Afdeling Werktingbowwkunde.

Bolker, E.D., and Roth, B., (1980), When is a bipartite graph a rigid framework?, Pac. J. Math., **90**, (1), 27-44.

Bricard, M.R., (1897), Memoire sur la theorie de l'octahedre articule', J. Math. Pure Appl., **3**, 113-148.

Buchholdt, H.A., (1970), Pretensioned cable girders, Proc. Inst. Civ. Eng., 45,

453-469.

Buchholdt, H.A., Davies, M., and Hussey, M.J.L, (1968), The analysis of cable nets, J. Inst. Maths. Appl., 4, 339-358.

Buchholdt, H.A., and McMillan, B.R., (1973), A non-linear vector method for the analysis of vertically and laterally loaded cables and cable assemblies, Proc. Inst. Civ. Eng., Part 2, 55, 211-228.

Calladine, C.R., (1977), The static-geometric analogy in the equations of thin shell structures, Math. Proc. Cambridge Phil. Soc., 82, 335-351.

Calladine, C.R., (1978), Buckminster Fuller's 'Tensegrity' structures and Clerk Maxwell's rules for the construction of stiff frames, Int. J. Solids Struct., 14, 161-172.

Calladine, C.R., (1982), Modal stiffnesses of a pretensioned cable net, Int. J. Solids Struct., 18, (10), 829-846.

Calladine, C.R., (1983), Discussion of "Tensegric shell behaviour", by Vilnay, O., and Soh, S.S., J. Struct. Eng., 109, (12), 2946-2948.

Cauchy, A.L., (1813), Deuxieme memoire sur les polygones et les polyedres, J. Ecole Polytechnique, 16 , 87-98.

Charlton, T.M., (1982), A History of Theory of Structures in the Nineteenth Century, Cambridge, C.U.P.

Connelly, R., (1980), The rigidity of certain cabled frameworks and the second-order rigidity of arbitrarily triangulated convex surfaces, Adv. Math., 37, 272-299.

Connelly, R., (1982), Rigidity and energy, Invent. Math., 66, 11-33.

Connelly, R., Conjectures and open questions in rigidity, preprint.

Crapo, H., (1979), Structural rigidity, Struct. Topology, 1, 26-45.

Crapo, H., (1982), The octahedral/tetrahedral truss, Struct. Topology, 6, 52-61.

Day, A.S., (1965), An introduction to dynamic relaxation, Engineer, 219, 218-221.

Day, A.S., and Bunce, J., (1969), The analysis of hanging roofs, Arup Journal, 30-31.

Den Hartog, J.P., (1952), Advanced Strength of Materials, New York, Mcgraw-Hill.

Domaszewski, M., and Borkowski, A., (1979), On automatic selection of redundancies, Computers & Structures, 10, 577-582.

Domaszewski, M., and Borkowski, A., (1984), Generalized inverses in elastic-plastic analysis of structures, J. Struct. Mech., 12, (2), 219-244.

Ewins, A.J., (1985), Microcomputer systems for logging vibrating wire gauges, Strain, 21, (2), 79-80.

Fiorenza, R., and Greco, D., (1978), Lezioni di Analisi Matematica, 2, part 2, Napoli, Liguori.

Flügge, W., (1973), Stresses in Shells, 2nd edition, Heidelberg, Springer-Verlag.

Föppl, A., (1892), Das Fachwerk im Raume, Leipzig.

Föppl, A., (1912), Vorlesungen über Technische Mechanik, 2, Leipzig and Berlin, Teubner.

Fuller, R.B., (1975), Synergetics, 2nd edition, New York, Macmillan.

Goldberg, M., (1978), Unstable polyhedral structures, Math. Mag., 51, (3), 165-170.

Heyman, J., (1974), Beams and Framed Structures, 2nd edition, Oxford, Pergamon.

Heyman, J., (1975), Overcomplete mechanisms of plastic collapse, J. Optimization Theory Appl., 15, (1), 27-35.

Hoff, N.J., and Fernandez-Sintes, J., (1980), Kinematically unstable space frameworks, in: Nemat-Nasser, S., ed., Mechanics Today, 5, Oxford, Pergamon, 95-111.

Irvine, H.M., (1981), Cable Structures, Cambridge, MIT Press.

Kani, I.M., McConnel, R.E., and See, T., (1984), The analysis and testing of a single layer, shallow braced dome, in: Nooshin, H., ed., Proc. 3rd Int. Conf. Space Struct., London, Elsevier Appl. Sci. Publ., 613-618.

Kenner, H., (1976), Geodesic Maths and how to use it, Berkeley, Univ. of California Press.

Koiter, W.T., (1984), On Tarnai's conjecture with reference to both statically and kinematically indeterminate structures, Lab. Report no. 788, Laboratory for Engineering Mechanics, Univ. Technol. Delft.

Kötter, E., (1912), Uber die Möglichkeit, n Punkte in der Ebene oder im Raume durch weniger als 2n-3 oder 3n-6 Stäbe von ganz unveränderlicher Länge unverschieblich miteinander zu verbinden, in: Festschrift Heinrich Müller-Breslau, Leipzig, A. Kröner, 61-80.

Krishna, P., (1968), Experiments on the wire model of a suspended cable structure, J. Inst. Eng. (India), 68, CI3, 870-878.

Krishna, P., and Agarwal, T.P., (1971), Study of suspended roof model, J. Struct. Div. Proc. Am. Soc. Civ. Eng., 97, ST6, 1671–1684.

Krishna, P., and Sparkes, S.R., (1968), Analysis of pretensioned cable systems,

Proc. Inst. Civ. Eng., 39, 103-109.

Kuznetsov, E.N., (1973), Mekhanica Tverdogo Tela, in Russian, Izv. AN SSSR, 8, (2), 108-112. Problems in the statics of variable systems, Russian Mechanics of Solids, Allerton Press.

Kuznetsov, E.N., (1975), Statical-kinematic analysis of spatial systems, in: Supple, W.J., ed., Proc. 2nd Int. Conf. Space Struct., Univ. Surrey, Guildford, 123-127.

Kuznetsov, E.N., (1979), Statical-kinematic analysis and limit equilibrium of systems with unilateral constraints, Int. J. Solids Struct., 15, 761-767.

Laman, G., (1970), On graphs and rigidity of plane skeletal structures, J. Eng. Math., 4, (4), 331-340.

Levi-Civita, T., and Amaldi, U., (1949), Lezioni di Meccanica Razionale, 1, Bologna, Zanichelli.

Livesley, R.K., (1967), The selection of redundant forces in structures, with an application to the collapse analysis of frameworks, Proc. Roy. Soc., series A, 301, 493-505.

Livesley, R.K., (1973), Linear Programming in Structural Analysis and Design, in: Gallagher, R.H., and Zienkiewicz, O.C., editors, Optimum Structural Design, London, Wiley, 79-108.

Livesley, R.K., (1975), Matrix Methods of Structural Analysis, 2nd edition, Oxford, Pergamon.

Luenberger, D.G., (1984), Linear and Nonlinear Programming, 2nd edition, Reading (MA), Addison-Wesley.

McGuire, W., and Gallagher, R.H., (1979), Matrix Structural Analysis, Chichester, Wiley.

Makowski, Z.S., (1966), A survey of recent three-dimensional structures, Archit. Des., London.

Makowski, Z.S., (1981), Space structures in Mexico: a review of their recent developments, Build. Specif., (10), 21-25.

Marks, R.W., (1960), The Dymaxion World of Buckminster Fuller, New York, Reinhold.

Maxwell, J.C., (1864), On the calculation of the equilibrium and stiffness of frames, London, Edinburgh, Dublin Philos. Mag. J. Sci., 27, 4th series, 294-299.

Michalos, J., and Birnstiel, C., (1960), Movements of a cable due to changes in loading, J. Struct. Div. Proc. Am. Soc. Civ. Eng., 86, ST12, 23-38.

Möbius, A.F., (1837), Lehrbuch der Statik, Leipzig, Göschen, 2, 63-128.

Mohr, O.C., (1874), Beitrag zur Theorie des Fachwerkes, Z. Architekten- und Ingenieur-Vereins zu Hannover, 20, 509; 21, 17.

Mohr, O., (1885), Beitrag zur Theorie des Fachwerkes, Der Civilingenieur, 31, 289-310.

Møllmann, H., (1974), Analysis of Hanging Roofs by means of the Displacement Method, Lyngby, Polyteknisk Forlag.

Morris, J.Ll., (1983), Computational Methods in Elementary Numerical Analysis, Chichester, Wiley.

Motro, R., (1983), Formes et Forces dans les Systemes Constructifs cas des Systemes Reticules Spatiaux Autocontraints, 2 vols., Thesis, Acad. Montpellier, Univ. Sci. Tech. Languedoc.

Motro, R., (1984), Forms and forces in tensegrity systems, in: Nooshin, H., ed., Proc. 3rd Int. Conf. Space Struct., London, Elsevier Appl. Sci. Publ., 283-288.

NAG, (1984), Numerical Algorithms Group, Fortran Library Manual, Mark 11, Vol.3.

Neal, B.G., (1964), Structural Theorems and their Applications, Oxford, Pergamon.

Nooshin, H., and Butterworth, J.W., (1974), Experimental study of a prestressed cable roof, International Conference on Tension Structures, London.

Oravas, G.AE., and McLean, L., (1966), Historical development of energetical principles in elastomechanics, 2 parts, Appl. Mech. Rev., 19, 8 and 11, 647-658 and 919-933.

Parkes, E.W., (1974), Braced Frameworks, 2nd edition, Oxford, Pergamon.

Pellegrino, S., (1983), Analysis of kinematically indeterminate structures with examples, first year report, CUED.

Pellegrino, S., and Calladine, C.R., (1984), Two-step matrix analysis of prestressed cable nets, in: Nooshin, H., ed., Proc. 3rd Int. Conf. Space Struct., London, Elsevier Appl. Sci. Publ., 744-749.

Pellegrino, S., and Calladine, C.R., (1986), Matrix analysis of statically and kinematically indeterminate frameworks, to appear in: Int. J. Solids Struct.

Pestel, E.C., and Leckie, F.A., (1963), Matrix Methods in Elastomechanics, New York, McGraw-Hill.

Pollaczek-Geiringer, H., (1927), Uber die Gliederung ebener Fachwerke, Z. Angew. Math. Mech., 7, (1), 59-72.

Pollaczek-Geiringer, H., (1932), Zur Gliederungstheorie räumlicher Fachwerke, Z. Angew. Math. Mech., 12, (6), 369-376.

Przemieniecki, J.S., (1968), Theory of Matrix Structural Analysis, New York, McGraw-Hill.

Pugsley, Sir Alfred, (1957), The Theory of Suspension Bridges, London, Arnold.

Rabinovich, I.M., (1962), Mgnovenno-zhestkie sistemy, ikh svoistva i osnovy rascheta (Instantaneously rigid systems: their properties and principles of computation), Visiachie pokrytiia, Gosstroiizdat.

Rayleigh, J.W.S., (1894), The Theory of Sound, 1. Dover edition (1945).

Robinson, J.S., (1966), Structural Matrix Analysis for the Engineer, New York, Wiley.

Roth, B., (1980), Questions on the rigidity of structures, Struct. Topology, 4, 67-71.

Roth, B., (1981), Rigid and flexible frameworks, Am. Math. Mon., 88, (1), 6-21.

Roth, B., and Whiteley, W., (1981), Tensegrity frameworks, Trans. Am. Math. Soc., 265, (2), 419-446.

See, T., (1983), Large Displacement Elastic Buckling of Space Structures, Ph.D. Thesis, Univ. Cambridge.

Siev, A., (1967), Prestressed suspended roofs bounded by main cables, Int. Assoc. Bridge Struct. Eng., 27, 171-186.

Southwell, R.V., (1920), Primary stress determination in space frames, Engineering, 109 , 165-168.

Strang, G., (1980), Linear Algebra and its Applications, 2nd edition, London, Academic Press.

Szabo', J., (1973), The equation of state-change of structures, Period. Polytech. Mech. Eng., 17, (1), 55-71.

Szabo', J., and Kollar, L., (1984), Structural Design of Cable-Suspended Roofs, Chichester, Ellis Horwood.

Tarnai, T., (1980a), Simultaneous static and kinematic indeterminacy of space trusses with cyclic symmetry, Int. J. Solids Struct., 16, 347-359.

Tarnai, T., (1980b), Problems concerning spherical polyhedra and structural rigidity, Struct. Topology, 4, 61-66.

Tarnai, T., (1984a), Comments on Koiter's classification of infinitesimal mechanisms, manuscript.

Tarnai, T., (1984b), Infinitesimal mechanisms and stiffening effects of prestress, manuscript.

Tarnai, T., (1986), Finite mechanisms and the octagon of Ely Cathedral, to

appear in: Struct. Topology.

Thew, R., (1982), The geometrical Non-linear Response of some Pre-tensioned Cable Structures, Ph.D. Thesis, Univ. Nottingham.

Thompson, J.M.T., and Hunt, G.W., (1973), A General Theory of Elastic Stability, London, Wiley.

Thompson, J.M.T., and Hunt, G.W., (1984), Elastic Instability Phenomena, Chichester, Wiley.

Timoshenko, S.P., (1953), History of Strength of Materials, New York, McGraw-Hill.

Timoshenko, S.P., and Young, D.H., (1965), Theory of Structures, 2nd edition, New York, McGraw-Hill.

Vilnay, O., (1981), Determinate tensegric shells, J. Struct. Div. Proc. Am. Soc. Civ. Eng., **107**, ST10, 2029-2033.

Vilnay, O., and Soh, S.S., (1982), Tensegric shell behaviour, J. Struct. Div. Proc. Am. Soc. Civ. Eng., **108**, ST8, 1831-1845.

Vilnay, O., (1984), Discussion of "Modal stiffnesses of a pretensioned cable net", by Calladine, C.R., Int. J. Solids Struct., 20, (4), 411-413.

Webster, R.L., (1980), On the static analysis of structures with strong geometric nonlinearity, Computers & Structures, **11**, 137-145.

Wegner, B., (1984), On the projective invariance of shaky structures in Euclidean Space, Acta Mech., 53, 163-171.

Whiteley, W., (1979), Motions of bipartite frameworks, Struct. Topology, 3, 62-63.

Whiteley, W., (1982), Motions of trusses and bipartite frameworks, Struct. Topology, 7, 61-68.

Wittrick, W.H., (1985), On the vibration of stretched strings with clamped ends and non-zero flexural rigidity, preprint.

Wunderlich, W., (1965), Starre, kippende, wackelige und bewegliche Achtflache, Elem. Math., 20, (2), 25-32.

Wunderlich, W., (1976), On deformable nine-bar linkages with six triple joints, Indagationes Math., 38, (3), 257-262.

Wunderlich, W., (1982), Projective invariance of shaky structures, Acta Mech., **42**, 171-181.